

Click and Cut: Enzymatic production of chemical nuclease triplex-forming oligonucleotide hybrids with gene-editing applications

Bríonna McGorman M.Sc.

Ph.D. Thesis

Assoc. Prof. Andrew Kellett

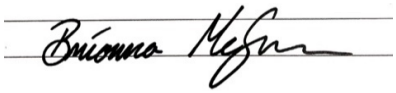
School of Chemical Sciences

Dublin City University

January 2022

Declaration

I hereby certify that this material, which I now submit for assessment on the programme of study leading to the award of Doctor of Philosophy is entirely my own work, and that I have exercised reasonable care to ensure that the work is original, and does not to the best of my knowledge breach any law of copyright, and has not been taken from the work of others save and to the extent that such work has been cited and acknowledged within the text of my work.

Signed:  ID No.: 16213161 Date: 12th January 2022

Acknowledgement

I would like to express my sincere gratitude to my supervisor Assoc. Prof. Andrew Kellett, without his enthusiasm and encouragement I would not have undertaken this PhD project. His support and guidance throughout my PhD has helped me develop into the scientist I am today. He may have almost driven me insane with his constant changes in colour scheme and figure preferences, but without all those changes my research would not have been given the justice it deserves. It has been a privilege to work in his research group.

I would also like to thank my colleagues, both past and present, in the Kellett research group. As a geneticist joining a chemistry lab I was apprehensive of how I would fit-in, but thanks to the warm welcome I received and the respect you all had for the knowledge and skills I brought, I have not once felt out of place. I would particularly like to acknowledge Sinéad O'Carroll and Joseph Hennessy, my PhD experience would not have been the same without them. Sinéad, I do not know how I would of survived the PhD without you, you cheered me up on the darkest days and celebrated with me at any opportunity, with you I have made a friend for life.

I would also like to express my thanks to the technical staff in the NRF and School of Chemical Sciences. No request was ever too much. I also need to acknowledge the technical staff in the School of Biotechnology, they have allowed me access to their equipment and instruments whenever I needed.

Finally, I would like to express the largest thank-you to my parents. Without their understanding, help and support it would not have been possible for me to undertake and succeed in this chapter of my life. Having parents who fully understood the hard work and commitment required to achieve a PhD has been invaluable to me.

Scientific Output

Publications:

Zuin Fantoni N., McGorman B., Molphy Z., Singleton, D., Walsh, S., El-Sagheer, A. H., McKee, V., Brown, T. and Kellett, A. Development of Gene-Targeted Polypyridyl Triplex-Forming Oligonucleotide Hybrids. *ChemBioChem* 2020 doi.org/10.1002/cbic.202000408

Hennessy J., McGorman B., Molphy Z., Singleton D., Brown T. and Kellett A. A click chemistry approach to targeted DNA crosslinking with *cis*-platinum(II) modified triplex forming oligonucleotides. *Angewandte Chemie* 2021 doi.org/10.1002/anie.202110455

Manuscript under review:

McGorman B., Zuin Fantoni N., O'Carroll S., Ziemele A., El-Sagheer A. H., Brown T. and Kellett A. Enzymatic synthesis of chemical nuclease triplex-forming oligonucleotides with gene-editing applications. (Chapter 5)

Manuscripts in preparation:

McGorman B., O'Carroll S., Zuin Fantoni N., Brown T. and Kellett A. Multiple nucleotide incorporation primer extension: A method for the enzymatic synthesis of therapeutic oligonucleotides. (Chapter 6)

Gomez Gonzalez, J., McGorman B., Kellett A. and Vazquez Lopez M. Copper-binding helicates that target DNA three-way junctions.

Awards:

Best postgraduate presentation, IBICS-4. 27th November 2020.

Runner-up for postgraduate poster, DCU annual chemistry research day 2019.

Best postgraduate flash talk, DCU annual chemistry research day 2018.

2018 Irish Research Council Government of Ireland Postgraduate Scholar GOIPG/2018/1427.

Scientific talks:

McGorman B., Zuin Fantoni N., Brown T. and Kellett A. Click and Cut: Enzymatic production of targeted DNA scissors. IS3NA-IRT Virtual Symposium. 27th August 2021.

McGorman B., Zuin Fantoni N., Brown T. and Kellett A. Click and Cut: Enzymatic production of targeted DNA scissors. Royal Society of Chemistry's Nucleic Acids Forum. 9th July 2021.

McGorman B. and Kellett A. Click and Cut: Enzymatic production of molecularly targeted DNA scissors. IBICS-4. 27th November 2020.

McGorman B. and Kellett A. Click and Cut: Enzymatic production of molecularly targeted DNA scissors. DCU annual chemistry research day. 5th June 2020.

McGorman B. and Kellett A. Flash Talk: Next generation antisense therapeutics. 70th Irish Universities Chemistry Research colloquium. Queen's University, Belfast. 21st-22nd June 2018.

McGorman B. and Kellett A. Flash Talk: Next generation antisense therapeutics. DCU annual chemistry research day. Dublin City University. 4th May 2018.

Posters:

McGorman B. and Kellett A. 2020. Enzymatic synthesis and qPCR analysis of AMN-TFO hybrids. SFI Science Summit, 5th-6th November 2020.

McGorman B., Zuin Fantoni N. and Kellett A. Enzymatic synthesis and qPCR analysis of AMN-TFO hybrids. 1st Metals in Medicine workshop. Chimie ParisTech, Paris, France. 14th-15th November 2019.

McGorman B., Zuin Fantoni N., Brown T. and Kellett A. Development of new qPCR methodology to probe gene knockdown. 15th RSC Nucleic Acids forum. Royal Society of Chemistry, Burlington House, London. 12th July 2019.

McGorman B., Zuin Fantoni N. and Kellett A. Next generation antisense therapeutics. RSC Organic division Ireland regional meeting. University College Dublin. 7th June 2019.

McGorman B., Zuin Fantoni N. and Kellett A. Next generation antisense therapeutics. 71st Irish Universities Chemistry Research colloquium. Technological University Dublin, Aungier Street and Royal College of Surgeons, Dublin. 20th-21st June 2019.

McGorman B., Zuin Fantoni N. and Kellett A. Next generation antisense therapeutics. DCU annual chemistry research day. Dublin City University. 10th May 2019.

Table of Contents

Acknowledgement ..... *i*
Scientific Output ..... *ii*
List of Abbreviations ..... *xvi*
Abstract ..... *xix*
Chapter 1 ..... *1*
Introduction *1*
1.1 Antisense and antigene therapeutics **2**
1.2 Triplex forming oligonucleotides **4**
1.3 Gene-editing systems **6**
1.3.1 Enzymatic nucleases 6
1.3.2 Targeted chemical nucleases 9
1.4 Click chemistry **11**
1.5 Synthesis of oligonucleotides **14**
1.6 Enzymatic synthesis **18**
References **23**
Chapter 2 ..... *29*
Project Rationale *29*
References **33**
Chapter 3 ..... *34*
Molecular methods for the analysis of gene-targeted metallodrug-hybrids *34*
3.1 Molecular methods **35**
3.1.1 Gel electrophoresis 35
3.1.2 Thermal Melting 36
3.1.3 Real-time quantitative PCR 38
3.2 Polyacrylamide gel electrophoresis for the analysis of sequence specific damage **41**
3.2.1 PAGE triplex analysis 41
3.2.2 PAGE analysis of AMN-TFO hybrids 43
3.2.3 PAGE analysis of Pt(II)-TFO hybrids 48
3.2.4 PAGE analysis for three way junction binding helicates 49
3.3 Fluorescent thermal melting **51**
3.4 qPCR analysis of DNA damage **52**
3.5 Conclusion **57**
3.6 Experimental **58**
3.6.1 General information 58
3.6.2 Amplification of TFO target and *off*-target dsDNA 58
3.6.3 PAGE analysis of TPMA-TFO hybrids 58
3.6.4 DPA-TFO PAGE 59
3.6.5 ROS scavengers 59
3.6.6 Platinum-TFO PAGE 59
3.6.7 Three Way Junction PAGE 60
3.6.8 Fluorescent melting 60
3.6.9 qPCR analysis of catalytic activity of Cu-TPMA-TFO hybrids 61
3.6.10 qPCR analysis of target and *off*-target damage induced by DPA-TFOs 61
3.6.11 qPCR with ROS scavengers 62
References **63**
Chapter 4 ..... *66*
Enzymatic synthesis of modified oligonucleotides *66*
4.1 Introduction **67**

4.2 Library preparation of modified dNTPs 67
4.3 Enzymatic synthesis of TFO 70
4.3.1 Incorporation of C8-alkyne-dNTPs 70
4.3.2 Incorporation of $dN^{TPMA}TPs$ 72
4.3.3 Incorporation of $dN^{DPA}TPs$ 74
4.4 Streptavidin Beads 77
4.5 Conclusion 78
4.6 Experimental 79
4.6.1 General information 79
4.6.2 Triplex forming oligonucleotide 79
4.6.3 Click chemistry with short oligonucleotides 79
4.6.4 Click Chemistry with dNTPs 80
4.6.5 SNI-PEX for PAGE 80
4.6.6 SNI-PEX for TFO synthesis 81
4.6.7 Streptavidin-biotin magneto-separation of TFO 82
References 83
Chapter 5 85
Enzymatic synthesis of chemical nuclease triplex-forming oligonucleotides with gene-editing applications 85
5.1 Abstract 86
5.2 Introduction 86
5.3 Results and Discussion 89
5.3.1 Synthesis of $4N_3$-Benzyl-DPA. 89
5.3.2 Enzymatic synthesis of DPA-TFO hybrids. 89
5.3.3 Thermal melting analysis. 92
5.3.4 Targeted oxidative cleavage by DPA-TFO hybrids. 93
5.3.5 Mechanistic studies 94
5.3.6 Quantification of DNA damage by qPCR. 95
5.3.7 Targeted damage of supercoiled plasmid DNA 97
5.3.8 Cleavage resolution experiments. 99
5.4 Conclusion 99
5.5 Experimental 101
5.5.1 General information 101
5.5.2 Synthesis of N-4-azidobenzyl-N-di-(2-picolyl)amine ($4N_3$-Benzyl-DPA) 101
5.5.3 Solid-phase synthesis of DPA-TFO 103
5.5.4 Enzymatic synthesis of DPA-TFO 104
5.5.5 Denaturing PAGE to visualise single nucleotide incorporation 105
5.5.6 Amplification of TFO target and *off*-target 105
5.5.7 Fluorescent thermal melting 106
5.5.8 Triplex formation 106
5.5.9 DPA-TFO hybrids PAGE 106
5.5.10 ROS scavengers 107
5.5.11 qPCR analysis of catalytic activity with target and off-target 107
5.5.12 Plasmid Studies 108
5.5.13 Sequencing 108
References 110
Chapter 6 114
Multiple nucleotide incorporation-primer extension: A method for the enzymatic synthesis of therapeutic oligonucleotides 114
6.1 Abstract 115
6.2 Introduction 115
6.3 Design of MNI-PEX 116
6.4 Application of MNI-PEX for the synthesis of TPMA-TO-TFO 119
6.5 Conclusion 125

6.6 Experimental 126
6.6.1 General information 126
6.6.2 Click chemistry for the production of modified dNTPs 126
6.6.3 MNI-PEX for PAGE analysis 126
6.6.4 Denaturing PAGE 127
6.6.5 MNI-PEX for synthesis of TPMA-TO-TFO 127
6.6.6 Streptavidin bead isolation of TPMA-TO-TFO 128
6.6.7 Analysis of TPMA-TO-TFO 128
References 129
Chapter 7 131
Conclusion and Future Work 131
7.1 Conclusion 132
7.2 Future work 133
7.2.1 MNI-PEX 133
7.2.2 NEAR for primer synthesis 134
7.2.3 Analysis of TFO hybrids within a cellular system 135
7.2.4 Alternative genetic targets 135
References 137
Appendix A ..... A-I
A.1 PAGE analysis ..... A-I
A.1.1 Triplex PAGE ..... A-I
A.1.2 AMN-TFO hybrids ..... A-II
A.1.3 Pt(II)-TFO hybrids ..... A-II
A.2 qPCR controls ..... A-IV
Appendix B ..... B-I
B.1 Incorporation of modified dNTPs ..... B-I
B.1.1 SNI-PEX – $dN^{TPMA}TPs$ ..... B-I
B.1.2 SNI-PEX - $dN^{DPA}TPs$ ..... B-II
Appendix C ..... C-I
C.1 Synthesis of $4N_3$-benzyl-DPA ..... C-I
C.2 'Click' reaction yields ..... C-VII
C.3 Mass Spectrometry Data of the Oligonucleotides ..... C-VIII
C.4 Mass Spectrometry Data of the DPA-dU^{DPA} triphosphate ..... C-IX
C.5 Enzymatic synthesis of DPA-TFO ..... C-X
C.6 Analysis of DPA-TFO ..... C-XV
C.7 Sequencing data ..... C-XXIII
C.7.1 Control Forward ..... C-XXIII
C.7.2 Cu-DPA Forward ..... C-XXIII
C.7.3 DPQ-Cu-DPA-TFO ..... C-XXIV
C.7.4 DPPZ-Cu-DPA-TFO Forward ..... C-XXV
C.7.5 Control Reverse ..... C-XXV
C.7.6 Cu-DPA-TFO Reverse ..... C-XXVI
C.7.7 DPQ-Cu-DPA-TFO Reverse ..... C-XXVI
C.7.8 DPPZ-Cu-DPA-TFO Reverse ..... C-XXVII
Appendix D ..... D-II
D.1 Previous modified-dNTPs incorporated during SNI-PEX ..... D-II
D.2 MNI-PEX of TFO with TPMA and TO modifications ..... D-II

Table of Figures

Figure 1: *Antisense and antigene therapeutics* ***A.*** *Proteins are produced in the body by processes known as transcription and translation. An RNA polymerase transcribes the gene sequence into mRNA. This mRNA is transported to the ribosome where it is translated into protein.* ***B.*** *Antisense therapeutics inhibit protein synthesis by sequestering the mRNA and preventing it from entering the ribosome.* ***C.*** *Antigene oligonucleotides instead bind directly to dsDNA and prevent the RNA polymerase from accessing the gene sequence.* ***D.*** *A DNA polymerase unwinds dsDNA and simultaneously synthesises the complementary sequence for both DNA strands, thereby replicating the DNA sequence.* ***E.*** *Combining the sequence selectivity of an antigene TFO with a DNA damaging agent prevents both DNA replication and mRNA transcription. Figure produced using BioRender graphics and is based on information in reference 23. ..... 3*

Figure 2: A. *Structure of triple helix with parallel TFO (purple) binding in the major groove of Watson-Crick duplex DNA (modified from PDB 1D3X).* ***B.*** *Parallel and anti-parallel TFO binding motif.* ***C.*** *Triplets formed through Hoogsteen and reverse-Hoogsteen hydrogen bonds for parallel and anti-parallel triplexes, respectively. 6*

Figure 3: A*. Two ZFNs recognise their triplet target sequence, anneal to complementary DNA strands, the FokI domains dimerise and cleavage occurs.* ***B.*** *TALENS operate by a similar mechanism but the TALE proteins offer single-base recognition. Again, two TALENs hybridise with the target sequence and cleavage occurs through FokI dimerisation.* ***C.*** *The traditional CRISPR/Cas system with crRNA and tracrRNA.* ***D.*** *sgRNA CRISPR/Cas system enables recognition of the target and delivery of the Cas nuclease with a single looped RNA. This figure was produced using BioRender graphics. 9*

Figure 4: A. *Structure of traditional sequence-specific hybrid systems, where a triplex forming oligonucleotide (purple) has been coupled to an EDTA, Phen or Platinum (green) moiety, either through a peptide linker (black) or by direct attachment to the nucleobase.* ***B.*** *Hybrid systems synthesised through click chemistry. The metallodrug can be attached to either the phosphate backbone or nucleobase. 11*

Figure 5: A. *The copper catalysed azide-alkyne cycloaddition (CuAAC) enables an azide and an alkyne to be "clicked" in the presence of a copper(I) catalyst to generate a 1,4, functionalised 1,2,3 triazole.* ***B.*** *Strain-promoted click chemistry uses a cyclooctyne (e.g. BCN), with high ring-strain, to trigger the click reaction. This removes the need for a copper(I) catalyst. 13*

Figure 6: *Solid-phase synthesis schematic showing the steps in each cycle of oligonucleotide synthesis. 16*

Figure 7: A. *The polymerase chain reaction (PCR) can exponentially amplify a double-stranded DNA sequence of interest.* ***B.*** *Primer extension (PEX) is a relatively simple method for the synthesis of a strand of DNA containing modified dNTPs. If a natural dNTP is replaced by its modified derivative the modified dNTP will be incorporated at all complementary positions.* ***C.*** *Single-nucleotide incorporation (SNI) PEX allows for a single modified nucleotide to be incorporated at a specific position in a DNA sequence.* ***D.*** *The nicking enzyme amplification reaction (NEAR) allows for the linear amplification of a short single-stranded DNA sequence. 21*

Figure 8: *Gel electrophoresis systems where the negatively charged DNA moves from the cathode (black) towards the anode (red).* ***A.*** *Agarose gel electrophoresis is run in horizontal tanks and is typically used for the analysis of long DNA fragments.* ***B.*** *Polyacrylamide gel electrophoresis (PAGE) runs vertically, and can separate short DNA fragments based on their molecular weight. Figure was produced using BioRender graphics. 36*

Figure 9: *Example of data collected from absorbance and fluorescence T_M of triplex DNA. The fluorescence signal (green) decreases as the DNA melts. Conversely, the absorbance signal (purple) increases as the concentration of single-stranded DNA rises. The triplex and duplex melt are highlighted in blue and red, respectively. 38*

Figure 10: A. *SYBR green I is a non-specific fluorescent dye that binds to dsDNA. The fluorescence signal emitted is quantified during qPCR.* ***B.*** *TaqMan probes are short sequences of ssDNA that bind to a specific DNA sequence. When the probe is intact the quencher is in close proximity to the fluorophore and no fluorescence is detected. During PCR Taq DNA polymerase degrades the probe strand enabling the fluorescent signal to be quantified. 39*

Figure 11: *Optimisation of native Tris-acetate (50 mM) PAGE with NaCl (0-150 mM) and $MgCl_2$ (2-5 mM). Lane 1: Target duplex (57 bp). Lane 2-4: Triplex with 10, 25 and 50 equivalents of TFO*

*(32 nt) to duplex respectively. The running position of TFO and target duplex was known due to the presence of TFO and target dsDNA controls (appendix **Figure A - 1**). 42*
***Figure 12:** Target (grey) and off-target (blue) duplexes incubated with 25 equivalents of TFO were analysed by Tris-acetate PAGE (20%). Lane 1: 57 bp target duplex. Lane 2: 40 bp off-target duplex. Lanes 3-5: Triplex with 10, 25 and 50 equivalents of TFO to duplex. 43*
***Figure 13: A.** 20% native PAGE analysis of TPMA-TFO(I) incubated with target and off-target DNA duplexes in the presence of increasing concentrations of Na-L-ascorbate (25-500 equivalents to TFO). Lane 1: TPMA-TFO(I). Lane 2: Target duplex (57 bp). Lane 3: Off-target duplex (40 bp). Lane 4: TPMA-TFO(I) forming triple helical DNA with target duplex. Lane 5: TFO does not hybridise with off-target duplex. Lanes 6-10: TPMA-TFO(I) incubated with target and off-target duplexes and increasing concentrations of Na-L-ascorbate (25-500 eq.). **B.** $5N_3$-TPMA. **C.** Octadiynyl-dU modification included in TFO sequence. 44*
***Figure 14:** DNA damage resulting from incubation with free Cu-TPMA and free TFO was analysed by 20% native PAGE. Lane 1: Alkyne TFO. Lane 2: Target duplex (57 bp). Lane 3: Off-target duplex (40 bp). Lane 4: TFO incubated with target duplex, and triplex DNA can be visualised. Lane 5: TFO does not hybridise with off-target duplex. Lanes 6-10: Cu-TPMA and alkyne-TFO incubated with target and off-target duplexes and increasing concentrations of Na-L-ascorbate (25-500 eq.).....45*
***Figure 15:** Structure of Cu($5N_3$-TPMA),[32] Cu($6N_3$-TPMA)[32] and Cu($4N_3$-benzyl-DPA)[33,34]. $5N_3$-TPMA and $6N_3$-TPMA have three pyridyl groups, they differ only in the position of the azide group. $4N_3$-benzyl-DPA is a less sterically hindered caging ligand and contains two pyridyl groups[33]..45*
***Figure 16: A.** Tris-acetate native PAGE (20%) analysis of damage inflicted by DPA-TFO hybrid. Lane 1: DPA-TFO. Lane 2: Target duplex (57 bp). Lane 3: Off-target duplex (40 bp). Lane 4: Triple helical DNA forms when DPA-TFO is incubated with target duplex. Lane 5: TFO does not hybridise with off-target duplex. Lanes 6-13: Cu-DPA-TFO incubated with target and off-target duplex and increasing concentrations of Na-L-ascorbate. **B.** $4N_3$-benzyl-DPA. **C.** Internal octadiynyl-dU modification. 46*
***Figure 17:** Analysis of the cleavage profile of free Cu-DPA and free TFO. Lane 1: Alkyne-TFO. Lane 2: 57 bp target duplex. Lane 3: 40 bp off-target duplex. Lane 4: Alkyne-TFO and target duplex hybridise to form triple helical DNA. Lane 5: TFO does not bind with off-target duplex. Lanes 6-13: Free Cu-DPA and alkyne-TFO incubated with target and off-target dsDNA in the presence of increasing concentrations of Na-L-ascorbate (0-1000 eq.). 47*
***Figure 18:** 20% native PAGE showing the impact of ROS scavengers on the activity of the Cu-DPA-TFO hybrid. Lane 1: DPA-TFO. Lane 2: Target duplex. Lanes 3-6: Cu-DPA-TFO with target duplex and 0, 50, 500 and 2000 equivalents of Na-L-ascorbate, respectively. Control contains no ROS scavenger.....48*
***Figure 19: A.** Azido-platinum complexes that were clicked to TFOs. **B.** Alkyne base and phosphate modifications included in the TFO sequences. **C.** TFO sequence showing the position of the modified base (purple). **D.** PAGE analysis of carboplatin-TFO2 incubated with target and off-target duplexes at 37 ºC for 2 hours (top), 24 hours (middle) and 48 hours (bottom). Lane 1: Alkyne TFO. Lane 2: Carboplatin-TFO. Lane 3: Target duplex. Lane 4: Off-target duplex. Lane 5: 50 equivalents of alkyne TFO with target and off-target duplexes, triplex has formed. Lanes 6-10: 2.5, 5, 10, 15 and 50 equivalents of carboplatin-TFO with target and off-target duplexes, intensity of the triplex band increases as incubation time increases, which suggests that platinum has crosslinked with the target duplex thereby stabilising the triplex.....49*
***Figure 20:** Preliminary PAGE analysis of Cu(II)-LLD helicate in the presence of the 3WJ and a dsDNA control. Lane 1: 3WJ. Lane 2: dsDNA control. Lane 3: 3WJ and dsDNA with LLD, no Cu, no Na-L-ascorbate. Lane 4: 3WJ and dsDNA with LLD, no Na-L-ascorbate. Lanes 5 – 8: 3WJ and dsDNA with 1, 2.5, 5 and 10 equivalents Cu(II)-LLD helicate, respectively, and 10 equivalents Na-L-ascorbate (i.e. Lane 7 = 1:5:50, 3WJ:Helicate:Na-L-ascorbate). The Cu(II)-LLD helicate selectively binds to the 3WJ and oxidative cleavage occurs.....50*
***Figure 21:** 20% native PAGE showing the cleavage profile of the Cu-LLD helicate in the presence of ROS scavengers. Lanes 1-4: Control (no scavenger). Lanes 5-8: Top: D-Mannitol, Bottom: Tiron. Lanes 9-12: Top: L-Methionine. Bottom: L-Histidine. Lanes 1,5,9: 3WJ control. Lanes 2,6,10: 5 equivalents Cu-LLD helicate. Lanes 3,7,11: 7.5 equivalents Cu-LLD helicate. Lanes 4,8,12: 10 equivalents Cu-LLD helicate. 51*
***Figure 22:** Left: Biphasic melting profile of a 32 nucleotide alkyne-modified TFO and its 57 bp target duplex. Right: First negative derivative is calculated and two peaks are observed. Triplex T_M = 44.0 °C and duplex T_M = 86.2 °C. 52*

Figure 23: A. *Schematic of qPCR with intact dsDNA using SYBR green as the fluorescent reporter.* ***B.*** *Inhibition of DNA amplification due to DNA damage resulting from incubation with an AMN-TFO hybrid.* ***C.*** *Sequence of TFO, showing position of modification, and target duplex to be amplified by qPCR.* ***D.*** *Damage resulting from incubation with 25 equivalents of copper-bound TPMA-TFO hybrid was analysed by comparing the threshold cycle (C_T) of target (6 hour) and control (0 hour) samples (target C_T – control C_T) to give ΔC_T. ΔC_T was normalised to a non-treated control ($\Delta\Delta C_T$), and the data was plotted as linear values ($2^{-\Delta\Delta CT}$). DNA polymerase graphic was produced in BioRender. 54*
Figure 24: A*. Schematic of qPCR for target dsDNA. The DPA-TFO hybrid selectively cleaves and inhibits DNA amplification.* ***B.*** *The TFO does not hybridise with the off-target duplex, thereby no damage is inflicted and amplification can occur.* ***C.*** *The fold change of intact DNA concentration ($2^{-\Delta\Delta CT}$) is plotted for the target (green) and off-target (purple) duplexes.* ***D.*** *Damage post-incubation with free Cu-DPA and free TFO was quantified, again the target and off-target are shown in green and purple, respectively. DNA polymerase graphic was adapted from BioRender. 56*
Figure 25: *Fold change of intact DNA in the presence of the tiron. 57*
Figure 26: A. *20% native PAGE analysis of products following click reaction with a single-stranded oligonucleotide (16 bases) with $3N_3$-7-hydroxycoumarin. Lane 1: Control ssDNA where no azide was present for the click reaction, Lanes 2, 3 and 4: 3, 6 and 24 hour click reactions, respectively. The shift upwards in the gel shows there was an increase in molecular weight, which is indicative of a successful click reaction.* ***B.*** *When $3N_3$-7-hydroxycoumarin is clicked to a C8-alkyne-dUTP the fluorescence intensity significantly increases when exposed to UV light. 69*
Figure 27: A. *Natural thymidine base and uracil bases bearing alkyne, TPMA and DPA modifications.* ***B.*** *Library of natural and modified cytidine bases (triphosphates not shown for clarity). 69*
Figure 28: A. *A template (black), complementary to the desired TFO sequence, and a short primer (purple), which will form the beginning of the TFO, are annealed. A modified dUTP (red) is then incorporated by a DNA polymerase (blue) immediately 3′ of the primer. The remainder of the sequence is then synthesised with natural dNTPs (dark blue).* ***B.*** *For an oligonucleotide to behave as a TFO it must be single stranded, therefore the template and newly synthesised DNA sequence must be separated. Streptavidin coated magnetic particles bind to the biotin-tag on the template, and then through the use of a magnet and a denaturation step the TFO can be isolated. DNA polymerase graphic was adapted from BioRender. 71*
Figure 29*: A. 20% denaturing PAGE: Lanes 1-3: SNI-PEX. Lane 1: Full length TFO with a single dU^aTP. Lane 2: positive control, TFO with all natural dNTPs. Lane 3: Negative control, SNI-PEX reaction in the absence of dTTPs and dUTPs, no full-length TFO is observed, which shows that Vent (exo-) has high base complementarity. Lanes 4-6: SNI, with no PEX. Lane 4: Primer with a single dU^aTP incorporated. Lane 5: Positive control, primer and single dTTP. Lane 6: Negative control, primer with no dNTP incorporated. Lane 7: Primer. Lane 8: Template. By comparing lanes 4, 5 and 6 the incorporation of a single dNTP can be visualised; as dU^aTPs were the only substrate available to the DNA polymerase, the increase in molecular weight visualised in lane 4 represents the addition of a single dU^aTP base to the primer.* ***B.*** *Structure of dTTP and C8-alkyne dUTP (dU^aTP) (triphosphates not shown for clarity).* ***C.*** *Sequences for DNA fragments labelled in the gel (image* ***A****). 72*
Figure 30*: 20% denaturing PAGE analysis of products from SNI-PEX with five DNA polymerases. Pwo and Taq DNA polymerases are not suitable due to the degradation pattern observed. Vent (exo-), Therminator and Sequenase DNA polymerases were capable of incorporating a $dU^{TPMA}TP$, however Vent (exo-) and Therminator incorporated multiple bases, while excess non-reacted primer remained in the Sequenase samples. 73*
Figure 31: A. *Incorporation of a single modified nucleotide at the desired position in the TFO sequence.* ***B.*** *An additional two uridine nucleotide triphosphates are incorporated. These are non-templated as they will not form Watson-Crick bonds with the guanine bases on the complementary strand.* ***C.*** *PAGE analysis showing templated (incorporation 1) and two non-templated (incorporations 2 and 3) incorporation of $dU^{DPA}TP$. 75*
Figure 32*: Denaturing PAGE (20%) analysis of SNI-PEX products. Lanes 1-5: Primer 1 (12 nt) and dUTP incorporation. Lanes 6-10: Primer 2 (10 nt) and dCTP incorporation. Lanes 1, 6: Incorporation of $dN^{TPMA}TP$. Lanes 2, 7: SNI-PEX with $dN^{DPA}TP$. Lanes 3, 8: Incorporation of dN^aTP. Lanes 4, 9: Primer with natural dTTP or dCTP. Lanes 5, 10: Negative control, no incorporation has occurred. 76*

Figure 33: *Enzymatic synthesis concept for the DPA-5mC-TFO hybrid and proceeding steps for targeted DNA cleavage: i.) DNA polymerase synthesises DPA-TFO; ii.) Cu(II) coordinates to the DPA ligand; iii.) Cu(II)-DPA-TFO recognises target duplex; iv.) TFO hybridises to duplex forming triple helical DNA; and v.) Na-L-ascorbate activates the AMN to trigger DNA cleavage. 87*
Figure 34: A. *Synthesis of 4N_3-benzyl-DPA* ***B.*** *Scheme of click reaction between C8-alkyne-dUTP and 4N_3-benzyl-DPA to form a DPA-dUTP (dU^{DPA}TP).* ***C.*** *Sequence of SPS DPA-TFO1, SNI-PEX DPA-TFO2 and SNI-PEX DPA-5mC-TFO3, where M = 5mC.* ***D.*** *Template (black)—complementary to the desired TFO sequence—and a short primer (purple)—that will form the start of the TFO—are annealed. dU^{DPA}TP (red) is then incorporated by a DNA polymerase (blue) immediately 3′ of the primer. The remainder of the sequence is then synthesised with natural dNTPs (dark blue). For an oligonucleotide to behave as a TFO it must be single stranded, therefore the template and newly synthesised TFO sequence must be separated. Streptavidin coated magnetic particles bind to the biotin-tag on the template, then using a magnet and a denaturation step the TFO can be isolated. 90*
Figure 35: A. *20% denaturing PAGE analysis of SNI-PEX products, showing incorporation of Lane 1: dU^{DPA}TP. Lane 2: dU^{a}TP. Lane 3: dTTP, and Lane 4: no incorporation.* ***B.*** *20% native PAGE showing targeted cleavage by the enzymatically synthesised Cu-DPA-TFO2. Lane 1: TFO (32 nt). Lane 2: Target duplex (57 bp). Lane 3: Off-target duplex (40 bp). Lane 4: TFO and target duplex hybridise to form triplex. Lane 5: TFO does not bind with off-target duplex. Lane 6-15: Target and off-target duplexes incubated with Cu-DPA-TFO2 (25 eq.) and 0-1000 eq. Na-L-ascorbate. TFO2 only binds with its target sequence inflicting DNA damage, while off-target remains relatively intact. The same cleavage profile was observed for the SPS TFO1 (appendix* ***Figure C - 23****). 94*
Figure 36: A. *The DPA-TFO hybrid damaged its dsDNA target, therefore amplification of this sequence was inhibited. No fluorescence was detected.* ***B.*** *The off-target duplex was not damaged by the hybrid and thereby successful cycles of PCR were completed. SYBR green fluorescence was detected.* ***C.*** *Damage inflicted upon the target and off-target duplexes during incubation with SPS Cu-DPA-TFO1 (25 eq.) or SNI-PEX Cu-DPA-TFO2 (25 eq.) was analysed by comparing the threshold cycle (C_T) of experiment (15 h) and reference (0 h) samples (experiment C_T – reference C_T) to give ΔC_T. ΔC_T for each sample was normalised to a non-treated control ($\Delta\Delta C_T$) and plotted as a linear value ($2^{-\Delta\Delta CT}$) of fold change in intact DNA. A significant difference is observed between the target and off-target for TFO1 and 2, while no significant difference is observed between SPS TFO 1 and SNI-PEX TFO2. * = p = < 0.05, significant ** = p < 0.01, very significant. *** = p < 0.001, extremely significant. 96*
Figure 37: A. *DPA-TFO hybrid incubated with target (GFP) and off-target (pUC19) plasmid DNA.* ***B.*** *1% agarose gel electrophoresis. Lane 1: Supercoiled (SC) GFP (6389 bp). Lane 2: GFP linearised by EcoRI. Lane 3: Supercoiled (SC) pUC19 (2686 bp). Lane 4: pUC19 treated with EcoRI. Lane 5: SC GFP control. Lane 6: SC pUC19 control. Lane 7-15: GFP and pUC19 with 25 equivalents of Cu-DPA-TFO2 and 25-2000 equivalents of Na-L-ascorbate. The DPA-TFO hybrid can distinguish between the GFP and pUC19 plasmids, it cleaves a single strand of the GFP plasmid, resulting in the formation of open-circular (OC) DNA.* ***C.*** *Molecular structures of Cu-DPA (left), DPQ-Cu-DPA (middle) and DPPZ-Cu-DPA (right), along with cartoon illustration of sequencing cleavage studies involving the enzymatic DPA-TFO hybrid.* ***D.*** *Cu-DPA-TFO2 cuts a single strand of DNA target within 20 bases of the Cu-DPA modification site (top), DPQ-Cu-DPA-TFO2 nicks the target sequence < 10 bases from the modification site (middle), and DPPZ-Cu-DPA-TFO2 inflicts a single strand break < 2 bases from the modified dNTP (bottom). 98*
Figure 38: *Library of modified dUTPs (****A.****) and dCTPs (****B.****) that could be generated by nucleic acid click chemistry. 117*
Figure 39: *MNI-PEX is performed without any wash/purification steps. All reaction components are sequentially added to the same solution.* ***A.*** *Primer A (purple) was annealed to the biotinylated template (black) and a dUTP bearing modification A (red) was incorporated immediately 3′ of primer A.* ***B.*** *Primer B (green) was added and a dCTP bearing modification B (orange) was incorporated.* ***C.*** *The remainder of the TFO sequence was synthesised with natural dNTPs (blue).* ***D.*** *The 'nick' (*) between the dUTP (red) and primer B (green) was ligated using T4 ligase (pink).* ***E.*** *The newly synthesised DNA strand was then isolated using streptavidin magnetic particles and a magneto-denaturation step. 120*
Figure 40: *20% denaturing polyacrylamide gel electrophoresis (PAGE) showing the incorporation of dU^{TPMA}TPs by five DNA polymerases. 122*
Figure 41: *20% denaturing PAGE analysis of SNI-PEX with dC^{TO}TPs. Left: DNA stained with SYBR gold and visualised by UV fluorescence. Right: Thiazole orange fluorescence visualised*

under UV fluorescence prior to staining with SYBR gold. Lane 1: 30 min. Lane 2: 45 min. Lane 3: 60 min. Lane 4: $dU^{a}TP$ control. There is a large concentration of unreacted primer remaining in lanes 1, 2 and 3, due to the TO intercalating with the primer-template dsDNA rather than being incorporated by Vent (exo-) DNA polymerase..... 123
Figure 42: *20% denaturing PAGE showing incorporation of modified dNTPs during MNI-PEX. Each lane contains template DNA. Lane 1: Primer A. Lane 2: Primer A + $dU^{TPMA}TP$. Lane 3: Primer B. Lane 4: Primer B + $dC^{TO}TP$. Lane 5: Primer A + $dU^{TPMA}TP$ + primer B. Lane 6: Primer A + $dU^{TPMA}TP$ + primer B + $dC^{TO}TP$. The presence of TO can be visualised prior to staining with SYBR gold (appendix* ***Figure D - 2****)..... 124*
Figure 43: *20% native PAGE showing the ability of the TPMA-TO-TFO to hybridise with its genetic target. Lane 1: TPMA-TO-TFO. Lane 2: 57 bp target duplex. Lane 3-5: TPMA-TO-TFO (10, 25 and 50 eq., respectively) forming triplex DNA with a target duplex..... 124*
Figure 44: *Possible expansions of the MNI-PEX protocol, includes alternative backbones and a wider variety of modifications. LNA = locked nucleic acid. PS = phosphorothioate. 134*

Appendix A

Figure A - 1: *20% native Tris-acetate PAGE analysis of triplex formation. Lane 1: TFO (32 nt). Lane 2: Target duplex (57 bp). Lane 3-6: Triplex formation; TFO incubated with target duplex at 10, 25, 50 and 100 equivalents to duplex, respectively. Ultra-low molecular weight double-stranded DNA ladder shown in outside lanes. .....A-I*
Figure A - 2: A. *20% native PAGE showing the DNA damage resulting from incubation with TPMA-TFO(II). Lane 1: TPMA-TFO(II). Lane 2: 57 bp target duplex. Lane 3: Off-target duplex (40 bp). Lane 4: TPMA-TFO hybridised with target duplex to form triplex DNA. Lane 5: TFO does not bind with off-target duplex. Lanes 6-10: TPMA-TFO(II) incubated with target and off-target duplexes and increasing concentrations of Na-L-ascorbate (25-500 eq.).* ***B.*** *$6N_3$-TPMA.* ***C.*** *Octadiynyl-dU modification included in TFO sequence.....A-II*
Figure A - 3: *20% native Tris-acetate PAGE analysis of cisplatin-TFO3 hybrid. Lane 1: Alkyne TFO. Lane 2: Pt-TFO. Lane 3: Target duplex. Lane 4: Off-target duplex. Lane 5: Alkyne TFO and duplexes. Lanes 6-10: 2.5, 5, 10, 25 and 50 equivalents of Pt-TFO to duplex. TFO was incubated with duplex for 2 (**A.**), 24 (**B.**) or 48 (**C.**) hours. * = TFO, ** = Off-target duplex, *** = Target duplex, **** = Triplex. .....A-II*
Figure A - 4: *Native PAGE (20%) analysis of carboplatin-TFO3 hybrid. Lane 1: Alkyne TFO. Lane 2: Pt-TFO. Lane 3: Target duplex. Lane 4: Off-target duplex. Lane 5: Alkyne TFO and duplexes. Lanes 6-10: 2.5, 5, 10, 25 and 50 equivalents of Pt-TFO to duplex. TFO was incubated with duplex for 2 (**A.**), 24 (**B.**) or 48 (**C.**) hours. * = TFO, ** = Off-target duplex, *** = Target duplex, **** = Triplex.....A-III*
Figure A - 5: *20% Tris-acetate PAGE analysis of oxaliplatin-TFO3 hybrid. Lane 1: Alkyne TFO. Lane 2: Pt-TFO. Lane 3: Target duplex. Lane 4: Off-target duplex. Lane 5: Alkyne TFO and duplexes. Lanes 6-10: 2.5, 5, 10, 25 and 50 equivalents of Pt-TFO to duplex. TFO was incubated with duplex for 2 (**A.**), 24 (**B.**) or 48 (**C.**) hours. * = TFO, ** = Off-target duplex, *** = Target duplex, **** = Triplex. .....A-III*
Figure A - 6: *Control qPCR experiment performed with 25 equivalents of $Cu(ClO_4)_2$ to duplex DNA and increasing equivalents of Na-L-ascorbate. No significant DNA damage was observed. ..... A-IV*

Appendix B

Figure B - 1: *Incorporation of $dU^{TPMA}TP$ with various concentration of Sequenase DNA polymerase, incubated at 37 ºC for 60 min. Lane 1: 2.5 U sequenase. Lane 2: 2.5 U sequenase + $MgSO_4$. Lane 3: 5 U sequenase. Lane 4: 5 U sequenase + $MgSO_4$. Lane 5: 7.5 U sequenase. Lane 6: 7.5 U sequenase + $MgSO_4$. Lane 7: Incorporation of $dU^{a}TP$ with 2.5 U sequenase. Lane 8: Primer control. In all lanes sequenase DNA polymerase incorporated multiple dUTPs, the second (and third) of which are non-templated. Therefore sequenase DNA polymerase was not suitable for the incorporation of $dU^{TPMA}TPs$.....B-I*
Figure B - 2: *Vent (exo-) DNA polymerase incorporation of $dU^{DPA}TP$. Lane 1: 2 U Vent (exo-) DNA polymerase incubated for 5 min. Lane 2: 2 U Vent (exo-) DNA polymerase and $MgSO_4$*

incubated for 5 min. Lane 3: 1 U Vent (exo-) DNA polymerase incubated for 5 min. Lane 4: 1 U Vent (exo-) DNA polymerase and $MgSO_4$ incubated for 5 min. A second (non-templated) $dU^{DPA}TP$ is incorporated by Vent (exo-) DNA polymerase but after 5 min of incubation no incorporation of a third $dU^{DPA}TP$ is observed. ..... *B-II*
Figure B - 3: *Incorporation of $dU^{DPA}TP$ by Vent (exo-) DNA polymerase at 37 ºC. Lane 1-4: Incubation time of 5, 15, 30 and 60 min, respectively. A maximum of two $dU^{DPA}TP$s (the first templated and the second non-templated) are incorporated at 37 ºC.* ..... *B-II*

Appendix C

Figure C - 1: *Schematic for the synthesis of $4N_3$-benzyl-DPA.* ..... *C-I*
Figure C - 2: *^{1}H-NMR spectrum of N-4-nitrobenzyl-N-di-(2-picolyl)amine (1).* ..... *C-I*
Figure C - 3: *^{13}C-NMR spectrum of N-4-nitrobenzyl-N-di-(2-picolyl)amine (1).* ..... *C-II*
Figure C - 4: *^{1}H-^{1}H COSY spectrum of N-4-nitrobenzyl-N-di-(2-picolyl)amine (1).* ..... *C-II*
Figure C - 5: *^{1}H-13C HSQC spectrum of N-4-nitrobenzyl-N-di-(2-picolyl)amine (1).* ..... *C-III*
Figure C - 6: *^{1}H-NMR spectrum of N-4-amminobenzyl-N-di-(2-picolyl)amine (2).* ..... *C-III*
Figure C - 7: *^{13}C-NMR spectrum of N-4-amminobenzyl-N-di-(2-picolyl)amine (2).* ..... *C-IV*
Figure C - 8: *^{1}H-^{1}H COSY spectrum of N-4-amminobenzyl-N-di-(2-picolyl)amine (2).* ..... *C-IV*
Figure C - 9: *^{1}H-^{1}^{3}C HSQC spectrum of N-4-amminobenzyl-N-di-(2-picolyl)amine (2).* ..... *C-V*
Figure C - 10: *^{1}H-NMR spectrum of N-4-azidobenzyl-N-di-(2-picolyl)amine (3).* ..... *C-V*
Figure C - 11: *^{13}C-NMR spectrum of N-4-azidobenzyl-N-di-(2-picolyl)amine (3).* ..... *C-VI*
Figure C - 12: *^{1}H-^{1}H COSY spectrum of N-4-azidobenzyl-N-di-(2-picolyl)amine (3).* ..... *C-VI*
Figure C - 13: *^{1}H-^{13}C HSQC spectrum of N-4-azidobenzyl-N-di-(2-picolyl)amine (3* ..... *C-VII*
Figure C - 14: A. *UPLC-MS chromatograms of pure DPA-TFO. SPS DPA-TFO1 was produced in yields according to* ***Table C - 1*** *and mass was confirmed according to* ***Table C - 2*** *UPLC x-axis = time (min) and y-axis = UV absorbance at 260nm.* ***B.*** *Deconvoluted (MaxEnt) mass spectrum of SPS DPA-TFO1.* ..... *C-VIII*
Figure C - 15: *UPLC-MS chromatograms of $dU^{DPA}TP$.* ..... *C-IX*
Figure C - 16: *ESI-mass spectrum of DPA-$dU^{DPA}TP$ [M+Cu^{2+}].* ..... *C-X*
Figure C - 17: A. *Incorporation of a single modified nucleotide at the desired position in the TFO sequence.* ***B.*** *An additional two uridine nucleotide triphosphates are incorporated. These are non-templated as they will not form Watson-Crick bonds with the guanine bases on the complementary strand.* ***C.*** *20% denaturing PAGE analysis of incorporation by Therminator DNA polymerase. There is one templated (incorporation 1) and two non-templated (incorporation 2 and 3) incorporations of $dU^{DPA}TP$.* ..... *C-XI*
Figure C - 18: *20% denaturing PAGE showing the incorporation of $dU^{DPA}TP$ by Vent (exo-) DNA polymerase. Lane 1-4: Incubation time 5, 10, 15 and 20 min, respectively. A maximum of two $dU^{DPA}TP$s (the first templated and the second non-templated) are incorporated.* ..... *C-XI*
Figure C - 19: A. *ESI-mass spectrum of DPA-TFO2 [M + Cu^{2+}],* ***B.*** *ESI-mass spectrum of DPA-5mC-TFO3 [M + Cu^{2+}].* ..... *C-XIII*
Figure C - 20: *Mass spectroscopy (**A.**) and HPLC (**B.**) trace of PEX DPA-TFO2 spiked with non-modified TFO. DPA-TFO2 was spiked with 0, 10, 25, 50 or 75% non-modified TFO to determine the amount of non-modified TFO present in the PEX DPA-TFO2 sample.* ***A.*** *5.27/5.28 = non-modified TFO. 5.54 = DPA-TFO.* ***B.*** *5.17/5.19/5.20 = non-modified TFO. 5.42/5.44/5.45 = DPA-TFO.* ..... *C-XIV*
Figure C - 21: A. *Plot of fluorescence readings taken during thermal melting.* ***B.*** *First negative derivative of fluorescence measurements.* ..... *C-XV*
Figure C - 22: *TFO (purple) hybridises with target duplex (grey) to form triplex, while off-target (blue) remains in duplex state. Lane 1: 57 bp target duplex. Lane 2: Off-target duplex. Lanes 3-5: Triplex with 10, 25 and 50 equivalents of TFO to duplex.* ..... *C-XVI*
Figure C - 23: *20% native PAGE showing the targeted DNA damage inflicted by SPS Cu-DPA-TFO1. Lane 1: TFO (32 nt). Lane 2: Target duplex (57 bp). Lane 3: Off-target duplex (40 bp). Lane 4: TFO and target duplex hybridise to form triplex. Lane 5: TFO does not bind with off-target duplex. Lane 6-15: Target and off-target duplexes incubated with Cu-DPA-TFO (25 eq.) and 0-1000 equivalents of Na-L-ascorbate. TFO only binds with its target sequence inflicting DNA damage, while off-target remains relatively intact.* ..... *C-XVI*
Figure C - 24: *20% native PAGE displaying DNA damage caused by free Cu-DPA and free-alkyne-TFO. Lane 1: Alkyne TFO (32 nt). Lane 2: Target duplex (57 bp). Lane 3: Off-target duplex (40 bp). Lane 4: Alkyne-TFO and target duplex hybridise to form triplex. Lane 5: Alkyne-TFO does not bind with off-target duplex. Lane 6-15: Target and off-target duplexes incubated with free*

Cu(II)-DPA and free alkyne-TFO (25 eq.) and 0-1000 equivalents of Na-L-ascorbate. No significant DNA damage is observed for either DNA duplex. .....C-XVII
Figure C - 25: *20% native PAGE showing impact ROS have on activity of Cu-DPA-TFO. Lane 1: TFO. Lane 2: Target duplex. Lane 3-6: Cu-DPA-TFO incubated with target duplex and ROS scavenger and 0, 50, 500 or 2000 equivalents of Na-L-ascorbate. Control contains no scavenger species. .....C-XVII*
Figure C - 26: *Target and off-target DNA duplexes were incubated with free Cu-DPA and free alkyne-modified TFO. The fold change in intact DNA concentration was plotted. No significant damage has occurred to either DNA duplex. .....C-XVIII*
Figure C - 27: *qPCR was performed to quantify the DNA damage that occurred to the target duplex in the presence of Cu-DPA-TFO and the ROS species tiron. No significant damage was observed. This confirms that the DNA damage inflicted by the DPA-TFO hybrid is responsible for inhibiting DNA amplification during PCR. .....C-XVIII*
Figure C - 28: *Agarose (1%) gel electrophoretic analysis of the damage inflicted upon target and off-target supercoiled DNA plasmids by SPS Cu-DPA-TFO1. Lane 1: Supercoiled (SC) GFP (6389 bp). Lane 2: Supercoiled (SC) pUC19 (2686 bp). Lane 3-11: GFP and pUC19 with 25 equivalents of Cu-DPA-TFO1 and 25-2000 equivalents of Na-L-ascorbate. .....C-XIX*
Figure C – 29: *1% agarose gel analysis of enzymatically synthesised TFO3. Lane 1: Supercoiled (SC) GFP (6389 bp). Lane 2: Supercoiled (SC) pUC19 (2686 bp). Lane 3-11: GFP and pUC19 with 25 equivalents of Cu-DPA-5mC-TFO3 and 25-2000 equivalents of Na-L-ascorbate. ....C-XX*
Figure C - 30: *1% agarose gel displaying the sequence specific damage inflicted by the enzymatically synthesised Cu-DPA-TFO2 and Cu-DPA-5mC-TFO3. Left: Lane 1: Supercoiled (SC) GFP (6389 bp). Lane 2: Supercoiled (SC) pUC19 (2686 bp). Lane 3-5: GFP and pUC19 with 25 equivalents of Cu-DPA-TFO2 and 50, 500 or 2000 equivalents of Na-L-ascorbate. Right: Lane 1: Supercoiled (SC) GFP (6389 bp). Lane 2: Supercoiled (SC) pUC19 (2686 bp). Lane 3-5: GFP and pUC19 with 25 equivalents of Cu-DPA-TFO2 and 50, 500 or 2000 equivalents of Na-L-ascorbate.....C-XXI*
Figure C - 31: *1% agarose gel showing targeted DNA cleavage for Cu-DPA-TFO with designer intercalators, DPQ and DPPZ. Lane 1: Supercoiled (SC) GFP (6389 bp). Lane 2: GFP linearised (L) with EcoRI. Lane 3: Supercoiled (SC) pUC19 (2686 bp). Lane 4: pUC19 linearised (L) with EcoRI. Lane 5: GFP control. Lane 6: pUC19 control. Lane 7-9: GFP and pUC19 with 25 equivalents of DPQ-Cu-DPA-TFO and 50, 500 or 2000 equivalents of Na-L-ascorbate. Lane 10: GFP control. Lane 11: pUC19 control. Lanes 12-14: GFP and pUC19 with 25 eq. DPPZ-Cu-DPA-TFO and 50,500 or 2000 equivalents of Na-L-ascorbate. .....C-XXII*

Appendix D

Figure D - 1: *Modified dNTPs previously incorporated by a DNA polymerase during SNI-PEX. Left: Peptide crosslinking agent. Middle: Fluorophore: Right: Artificial metallo-nuclease. ..... D-II*
Figure D - 2: *20% denaturing PAGE analysis of MNI-PEX products. Left: SYBR gold stain. Right: Thiazole orange fluorescence. A single $d^{UTPMA}TP$ and a $dC^{TO}TP$ have been incorporated at the desired sequence positions..... D-III*

Table of Tables

Table 1: *Concentration of azide and alkyne for CuAAC. 80*
Table 2: *SNI-PEX primer and template sequences. Phos = phosphate, Bio = Biotin 81*
Table 3*: Incubation time and temperature for functionalised-dNTPs 81*
Table 4: *Concentration of azide and alkyne for CuAAC. 126*

Appendix C

Table C - 1: *Experimental yields of DPA-TFO1 after 'click' reaction, desalting and HPLC purification; int-dU[a] = internal-octadiynyl-deoxyuridine; 4N$_3$-DPA = N-4-azidobenzyl-N-di-(2-picolyl)amine. ..... C-VII*
Table C - 2: *Oligonucleotide sequences, modifications and dC content. Calculated and found m/z; (a) = + 63 m/z caused by the ligand scavenging Cu(II) from the UPLC column in the analysis. int-dU[a] = internal-octadiynyl-deoxyuridine; 4N$_3$-DPA = N-4-azidobenzyl-N-di-(2-picolyl)amine.. C-VIII*
Table C - 3: *Sequence of SNI-PEX primers, template and TFOs. M = 5-methyl-cytosine. ..... C-X*
Table C - 4: *Yield for enzymatically synthesised DPA-TFO hybrids. M = 5-methyl-cytosine. ... XII*
Table C - 5: *Oligonucleotide sequence and modifications. Calculated and found m/z; (a) = + 63 m/z caused by the ligand scavenging Cu(II) from the UPLC column in the analysis. M = 5-methyl-cytosine ..... C-XII*
Table C - 6: *Triplex melting temperature for TFO1, TFO 2 and TFO3. ..... C-XV*

List of Abbreviations

3WJ	three-way junction
5mC	5-methylcytosine
A	adenine
AAC	azide-alkyne cycloaddition
AMN	artificial metallo-nuclease
bp	base pair
C	cytosine
C^+	protonated cytosine
Cas	CRISPR associated
CRISPR	clustered regularly interspaced short palindromic repeat
crRNA	CRISPR RNA
C_T	threshold cycle
Cu-Phen	copper(II) bis-1,10-phenanthroline
CuAAC	copper catalysed azide-alkyne cycloaddition
dATP	adenine triphosphate
dC^aTP	C8-alkyne dCTP
$dC^{DPA}TP$	DPA-dTP
$dC^{TO}TP$	TO-dCTP
dCTP	cytidine triphosphate
$dC^{TPMA}TP$	TPMA-dCTP
dGTP	guanine triphosphate
DMSO	dimethyl sulfoxide
DNA	deoxyribonucleic acid
dNTPs	deoxyribonucleotide triphosphates

DPA	*di*-(2-picolyl)amine
dsDNA	double stranded DNA
dTTP	thymidine thiophosphate
$dU^{a}TP$	C8-alkyne dUTP
$dU^{DPA}TP$	DPA-dUTP
$dU^{TO}TP$	TO-dUTP
dUTP	uridine triphosphate
$dU^{TPMA}TP$	TPMA-dUTP
EDTA	ethylenediaminetetraacetic acid
EdU	5-ethyl-2′-deoxyuridine
EMSA	electrophoretic mobility shift assay
eq.	equivalents
FRET	fluorescence resonance energy transfer
G	guanine
GFP	green fluorescent protein
HPLC	high performance liquid chromatography
L	linear
MNI-PEX	multiple nucleotide incorporation - primer extension
mRNA	messenger RNA
NEAR	nicking enzyme amplification reaction
nt	nucleotide
OC	open circular
PAGE	polyacrylamide gel electrophoresis
PCR	polymerase chain reaction
PEX	primer extension
Phen	1,10-phenanthroline

qPCR	quantitative PCR
RNA	ribonucleic acid
ROS	reactive oxygen species
SC	supercoiled
sgRNA	single-guide RNA
SNI-PEX	single nucleotide incorporation-primer extension
SPAAC	stain-promoted azide-alkyne cycloaddition
SPS	solid-phase synthesis
T	thymidine
TAE	tris-acetate-EDTA
TALEN	transcription activator-like effector nuclease
TBE	tris-borate-EDTA
TBTA	tris-[(1-benzyl-1*H*-1,2,3-triazol-4-yl)methyl]-amine
TdT	terminal deoxytransferase
TFO	triplex forming oligonucleotide
THPTA	tris(3-hydroxypropyltriazolylmethyl)amine
T_M	melting temperature
TO	thiazole orange
TPMA	tris-(2-picolyl)amine
tracrRNA	trans-activating CRISPR RNA
U	uracil
V	volt
ZFN	zinc finger nuclease
ΔC_T	change in threshold cycle

Abstract

Click and Cut: Enzymatic production of chemical nuclease triplex-forming oligonucleotide hybrids with gene-editing applications

Bríonna McGorman. M.Sc.

Triplex forming oligonucleotides (TFOs) are short strands of nucleotides that can hybridise to duplex DNA and form triple helical structures. As triplex formation is sequence selective, there is significant interest in applying this technology for antigene therapy. In this work, primer extension (PEX) protocols were designed and utilised to enzymatically synthesise TFOs bearing artificial metallo-nucleases (AMNs). Initially, single nucleotide incorporation–primer extension (SNI-PEX) was employed to generate TFOs bearing a single modification. This was then expanded to the novel multiple nucleotide incorporation–primer extension (MNI-PEX) protocol, which enabled multiple different modified bases to be incorporated at specific sites in the TFO sequence. Click chemistry was employed to generate a library of functionalised nucleotides, which were then enzymatically incorporated into the TFO strand by a DNA polymerase. These AMN-TFO hybrids can recognise and damage specific DNA sequences, and therefore are capable of targeting a gene of interest. Real-time PCR (qPCR) and polyacrylamide gel electrophoresis (PAGE) protocols were then developed to analyse and compare the activity of these sequence-selective hybrids. PAGE was employed to visualise the sequence specificity of the TFO-drug hybrids and to identify 'on' and 'off' targeting effects. Next, the DNA damaging capabilities of three distinct TFO-hybrids, each bearing a unique AMN ligand ($5N_3$-TPMA, $6N_3$-TPMA and $4N_3$-benzyl-DPA), were quantified by a specifically developed qPCR protocol. Here, target DNA post treatment with the AMN-TFO hybrid, was amplified in the presence of SYBR Green I and the resulting fluorescent signal was compared to that of the untreated controls. Results show the AMN-TFOs can discriminate between target and *off*-target DNA, and differences in the DNA damaging capabilities of each AMN ligand were recorded. These results indicate that TFO-drug hybrids may have the ability to overcome problems associated with non-molecularly targeted DNA damaging agents, and represent a new class of gene knockout agent.

Chapter 1

Introduction

1.1 Antisense and antigene therapeutics

Targeted therapeutics are drugs with specific biological targets, usually genes or proteins that are involved with a disease phenotype. These therapies are capable of recognising their target, and binding with it under physiological conditions. Antisense gene therapy is a gene silencing technique that involves short single strands of DNA (oligonucleotides) complementary to the messenger RNA (mRNA) of the disease causing gene. The oligonucleotide enters the cell, hybridises to the mRNA and silences the gene, thereby inhibiting protein production, preventing the disease phenotype, and/or causing death of the diseased cell. Traditionally, the main focus of antisense therapeutics was to prevent gene expression by sequestering mRNA (**Figure 1**). However, focus has expanded to anti-gene strategies, one of which involves the modification of oligonucleotides to facilitate their binding to double stranded (dsDNA) targets through the formation of triple helical DNA.[1] These triplex forming oligonucleotides (TFOs) when bound to the double helix make the promoter of the disease causing gene inaccessible to the RNA polymerase and pre-initiation complex, and thereby inhibits transcription[2] and prevents synthesis of the undesired protein (**Figure 1**). TFOs can therefore be considered an elegant drug design choice as they can block the synthesis of specific proteins by direct inhibition of genomic DNA. Although TFOs themselves can block mRNA synthesis they do not permanently impact DNA, and thus do not prevent DNA replication (**Figure 1**). Therefore it would be beneficial if a TFO could be modified to permanently alter DNA and prevent cell replication. This can be achieved by tethering a DNA damaging moiety, such as a chemical nuclease,[3-6] or a crosslinking agent,[7, 8] to an antigene oligonucleotide, thereby essentially using the TFO as a delivery vector for the DNA damaging agent. These TFO hybrids are capable of delivering the chemical nuclease to the correct DNA sequence, thereby selectively blocking mRNA synthesis and preventing DNA replication (**Figure 1**).

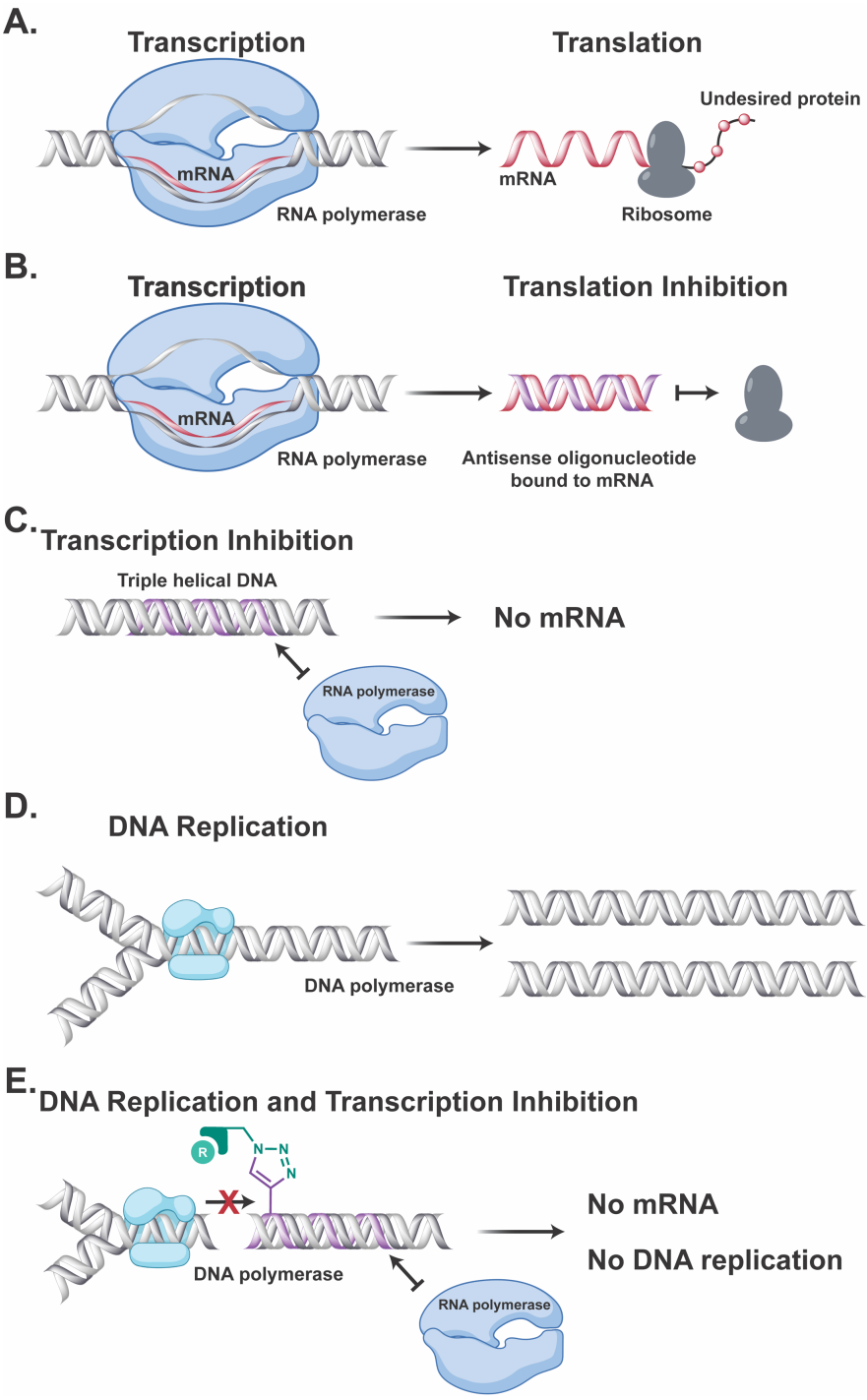


Figure 1: Antisense and antigene therapeutics **A.** Proteins are produced in the body by processes known as transcription and translation. An RNA polymerase transcribes the gene sequence into mRNA. This mRNA is transported to the ribosome where it is translated into protein. **B.** Antisense therapeutics inhibit protein synthesis by sequestering the mRNA and preventing it from entering the ribosome. **C.** Antigene oligonucleotides instead bind directly to dsDNA and prevent the RNA polymerase from accessing the gene sequence. **D.** A DNA polymerase unwinds dsDNA and simultaneously synthesises the complementary sequence for both DNA strands, thereby replicating the DNA sequence. **E.** Combining the sequence selectivity of an antigene TFO with a DNA damaging agent prevents both DNA replication and mRNA transcription. Figure produced using BioRender graphics and is based on information in reference 23.

1.2 Triplex forming oligonucleotides

TFOs are short single-strands of DNA that can bind to dsDNA and form triple helical structures.[9] They are typically 10-30 nucleotides in length and bind to double helical DNA at regions which have runs of purines (adenines, A, and guanines, G) on one strand, and pyrimidines (cytosines, C, and thymines, T) on the complementary strand. TFOs can be poly-pyrimidine—and bind parallel to the DNA duplex—or poly-purine—and bind either parallel or anti-parallel—but they always bind to the purine-rich strand of the dsDNA target.[10, 11]

A TFO binds within the major groove of the DNA duplex in a sequence specific manner, where it is stabilised by two Hoogsteen (or reverse-Hoogsteen) hydrogen bonds.[9] In purine rich TFOs these bonds form between A and the AT Watson-Crick pair, while G binds to the GC pair, forming A-AT and G-GC triplets.[12, 13] Similarly in pyrimidine TFOs, the T binds to AT, but the C bases must be protonated at N3 to form two Hoogsteen bonds with the GC base pair, thereby the binding motif for pyrimidine TFOs is T-AT and C^+-GC (**Figure 2**).[1, 14] Both triplex motifs are capable of recognising and binding to their corresponding duplex sequence, but pyrimidine TFOs—which bind parallel to the target duplex—are isomorphic (*i.e.* if the C1' atoms of the Watson-Crick base pairs are superimposed, the positions of the C1' atoms of the TFO are almost identical), which minimises backbone distortion.[11, 15] Additionally, purine TFOs are often capable of self-association into structures such as G-quadruplexes and GA-duplexes, thereby triplex formation is in competition with this self-association, which reduces the concentration of TFO available to bind with its target.[11] Therefore, pyrimidine-rich TFOs are more commonly used, but they require acidic conditions to protonate the C bases in the TFO strand. This requirement initially limited their functionality as they struggled to form triplexes under physiological conditions, but many modifications (to the base, sugar and phosphate backbone) that increase the binding stability of CT-rich TFOs have since been reported to enable binding at physiological pH.[11]

The introduction of a methyl group to the C5 position of cytosine is one of the simplest modifications. The 5-methylcytosine (5mC) base reduces the pH dependence of pyrimidine TFOs as it has a higher pK_a, disrupts the surrounding

water structure, enables greater base stacking and/or has hydrophobic interactions in the major groove.[11] Many intercalators have also been employed to aid in triplex stabilisation[16-20] and recent efforts have focused on thiazole orange (TO)—a fluorogenic intercalator—tethered to poly-pyrimidine TFOs as a adjuvant to stabilise triple helical DNA under physiological conditions.[19] It was reported that the incorporation of a single thiazole orange derivative at the 5-position of thymine can increase triplex stability by ~23 ºC (pH 5.8) with the addition of a second, and third thiazole orange modification increasing triplex melting temperatures above 78 ºC.[19] It was also reported that under physiological conditions (pH 7) that when three bases were modified with thiazole orange the triplex was stabilised by >26 ºC.[19] Walsh *et al.*[19] also combined the intercalation abilities of thiazole orange with methylcytosine bases, this achieved triplex melting temperature >70 ºC at neutral pH. More recently, TFOs bearing 6-amino-5-nitropyridin-2-one (Z) bases were reported.[21] This modification is an uncharged C-glycoside mimic of a protonated cytosine, with an electron withdrawing group attached at the 5-position.[22, 23] This Z nucleobase has a pK_a of ~7.8, which enables formation of the Z-GC triplet at neutral pH. Rusling *et al.*[21] reported a 13 nucleotide TFO, where all the natural cytidines were replaced with the Z base. This Z-TFO sequence was capable of forming stable triplex DNA between pH 5 and pH 9 (T_M = 78.1 °C and 76.5 °C, respectively).[21] Thereby, the inclusion of this Z nucleobase in a poly-pyrimidine TFO alleviates the pH dependency and enables triplex formation across a wide pH range. Therefore, through the use of a combination of triplex stabilising agents and/or modified bases, pyrimidine TFOs can form stable triple helical structures under physiological conditions.

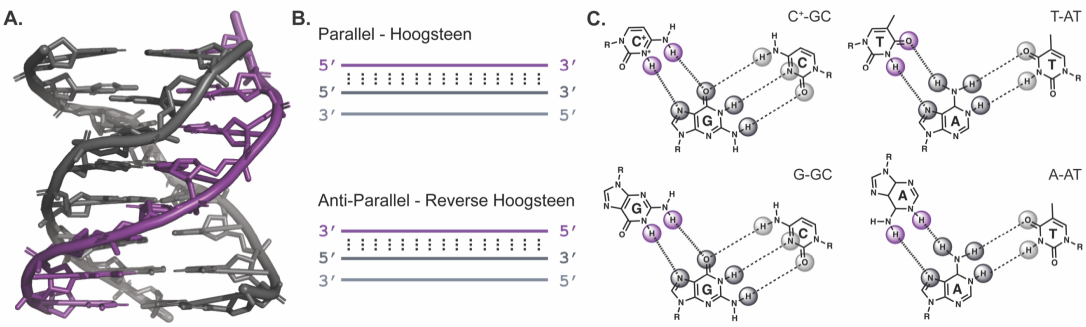


Figure 2: A. Structure of triple helix with parallel TFO (purple) binding in the major groove of Watson-Crick duplex DNA (modified from PDB 1D3X). **B.** Parallel and anti-parallel TFO binding motif. **C.** Triplets formed through Hoogsteen and reverse-Hoogsteen hydrogen bonds for parallel and anti-parallel triplexes, respectively.

1.3 Gene-editing systems

1.3.1 Enzymatic nucleases

Nucleases are enzymes that can cleave the phosphodiester bonds between the nucleotides of nucleic acids, which makes then a useful tool for DNA engineering. However, nucleases typically have a recognition site of 4 bp, which prevents them from being used for genome manipulation in higher organisms.[24] Much research has been performed to develop methods by which nucleases can be adapted for use as genome-editing tools, and technologies such as zinc-finger nucleases (ZFNs), transcription activator-like effector nucleases (TALENs) and clustered regularly interspaced short palindromic repeats (CRISPR) have been developed.[25-28]

1.3.1.1 Zinc-finger nucleases

The Cys_2-His_2 zinc-finger domain is one of the most common DNA binding motifs in eukaryotes.[25] Each zinc finger consists of approximately 30 amino acids in a highly conserved $\beta\beta\alpha$ configuration. Amino acids on the surface of the α-helix are capable of recognising 3 bp of DNA for sequence specific binding. However, 3 bp was not sufficient for genome-editing applications, so it was necessary to develop unnatural arrays that contained three or more zinc-fingers.[25] This enabled DNA sequences of 9-18 bp to be recognised. As 18 bp is sufficient to

confer specificity within 68 billion bp of DNA, these unnatural arrays allowed specific sequences in the human genome to be targeted for the first time.[26] Zinc-fingers have been developed to recognise the 64 possible triplets, and these can be linked together to target any combination of DNA triplets.[25] The cleavage domain of zinc finger-nucleases (ZFNs) comes from *Fok*I, which is tethered to the DNA binding zinc-fingers, and consequently is delivered to the target DNA sequence. Two ZFNs anneal to complementary DNA strands, the *Fok*I domains dimerise, and targeted DNA cleavage occurs (**Figure 3A**).[27] Despite their complex design and triplet limitations, ZFNs were employed in the first gene-edited cell therapy clinical trial. ZFNs were used to disrupt the HIV co-receptor gene *CCR5* in the $CD4^+$ T-cells of HIV patients, and thereby block the HIV-CCR5 interaction (NCT00842634).[29] This clinical trial paved the way for future ZFN and gene-editing trials, and is currently the most advanced clinical genome editing system.[30]

1.3.1.2 Transcription activator-like effector nucleases

Transcription activator-like effector nucleases (TALENs) were introduced as an advancement to ZFNs. Transcription activator-like effectors (TALEs) are a class of proteins from the plant pathogenic bacteria genus *Xanthomonas*. They consist of a DNA-binding domain composed of 33-35 amino acids, with residue 12 and 13 being responsible for DNA base recognition.[27] Each TALE binds with a specific DNA base, and consequently series of TALEs can be linked together to target any DNA sequence.[25, 27] Like ZFNs, TALENs use the *Fok*I cleavage domain, and consequently two TALEN units must hybridise with complementary DNA sequences, and the *Fok*I domains must dimerise for cleavage to occur (**Figure 3B**).[27] The single-base recognition of the TALENs gives them greater sequence flexibility than ZFNs, but they are still limited by their complex design. However, TALENs have also entered clinical trials, where they are employed to knockout the TCRα and the CD52 genes of T-cells for the treatment of acute lymphoblastic leukaemia (NCT02808442).[30] Preliminary data from this study has been positive and consequently has led to TALEN gene-editing trials for the treatment of other blood cancers.

1.3.1.3 Clustered regularly interspaced short palindromic repeats (CRISPR) and CRISPR-associated (Cas) proteins

Clustered regularly interspaced short palindromic repeats (CRISPR) and CRISPR associated (Cas) proteins are now considered the gold-standard for gene-editing, but they originated as an adaptive immune response in bacteria and archaea to protect them from invading viruses, bacteriophages and plasmids. Fragments of DNA from the attacking species—protospacers—are incorporated into the host genome at the CRISPR locus between CRISPR RNA (crRNA) repeats.[28, 31] When Cas proteins are expressed, the CRISPR locus is transcribed into pre-crRNA that is then cleaved and processed into mature crRNA. This mature crRNA contains a target sequence for the invading species and the crRNA repeat sequence is recognised by the Cas proteins. A non-coding RNA, known as trans-activating CRISPR RNA (tracrRNA) is also required. It is critical for crRNA processing, Cas9 binding and the Cas-mediated cleavage of the target sequence.[31] A protospacer adjacent motif (PAM) sequence must also be present adjacent to the crRNA binding site. This sequence is recognised by the Cas nuclease and enables cleavage at the target site. This requirement is important as it protects the CRISPR/Cas system from self-cleavage.[28, 31]

This immune CRISPR/Cas system was adapted to be a gene-editing tool, with the 2020 Nobel prize in Chemistry being awarded to Emmanuelle Charpentier and Jennifer Doudna for its development.[31] A crRNA sequence (17-20 nt) complementary to the genetic target is designed, it then hybridises with tracrRNA, which serves as a scaffold between the crRNA and the Cas nuclease (typically Cas9). This mechanism delivers Cas9 to the target DNA sequence, and if the PAM site is present, cleavage occurs[31] (**Figure 3C**). More recently, crRNA and tracrRNA have been combined into a single molecule known as single-guide RNA (sgRNA)[27]. This is a looped RNA structure that contains the crRNA target recognition and the tracrRNA domains (**Figure 3D**), thereby simplifying the design of CRISPR/Cas9 gene-editing systems, and cementing their position as the gold-standard for genome-editing technology. CRISPR/Cas9 has also moved towards clinical trials, with the first CRISPR trial involving the use of T-cells for the treatment of non-small cell lung cancer (NCT02793856).[30] This trial used CRISPR/Cas9 to knockout the programmed cell death-1 (PD-1) gene—an

immune checkpoint inhibitor—in T-cells, with the aim of preventing cancer cells evading the patient's natural immune response. CRISPR has since been employed for the treatment of other diseases, with clinical trials for HIV, β-thalassemia and sickle cell disease underway.[30]

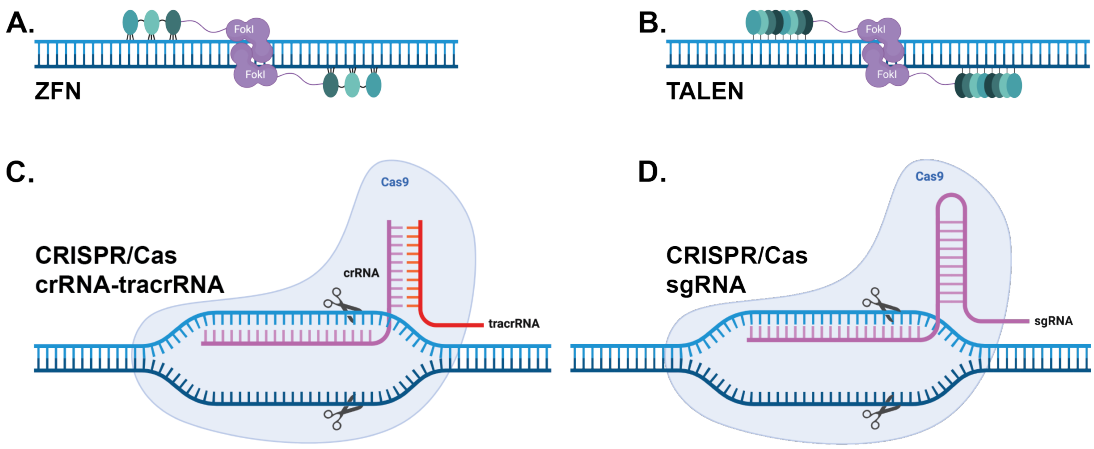


Figure 3: A. Two ZFNs recognise their triplet target sequence, anneal to complementary DNA strands, the *Fok*I domains dimerise and cleavage occurs. **B.** TALENS operate by a similar mechanism but the TALE proteins offer single-base recognition. Again, two TALENs hybridise with the target sequence and cleavage occurs through *Fok*I dimerisation. **C.** The traditional CRISPR/Cas system with crRNA and tracrRNA. **D.** sgRNA CRISPR/Cas system enables recognition of the target and delivery of the Cas nuclease with a single looped RNA. This figure was produced using BioRender graphics.

1.3.2 Targeted chemical nucleases

Chemical nucleases have also been developed, these are small inorganic molecules that can cleave, or nick DNA. However, many have no sequence selectivity, and consequently extensive research has been performed to develop a mechanism by which chemical nucleases can be directed to cleave a specific DNA sequence.

Artificial metallo-nucleases (AMNs) were first reported by Sigman *et al.*[32] in 1979, when it was reported that $[Cu(1,10\text{-phenantroline})_2]^{2+}$ (Cu-Phen) could semi-intercalate and oxidise DNA from the minor groove in the presence of a reductant, such as ascorbate.[32, 33] This led to the development of a variety of AMNs including: bis-chelate Cu^{2+} phenanthroline-phenazine complexes[34, 35] and polypyridyl copper-binding AMN architectures.[36, 37] However, none of these

chemical nucleases were capable of damaging a specific target. Extensive research has been performed to develop a mechanism by which AMNs can be directed to a desired DNA sequence.[38-43] Initial research into sequence specific targeting focused on the covalent linkage of Fe-EDTA or Cu-Phen complexes to distamycin derivatives,[39, 44, 45] but this involved complex protocols, so research shifted towards the use of oligonucleotides as sequence specific targeting vectors. Dervan *et al.,*[46] Sigman *et al.*[47, 48] and Hélène *et al.*[42, 49] reported the attachment of Fe-EDTA and Cu-Phen to oligonucleotides in the 1980s (**Figure 4**). These metallodrug-hybrids showed great promise as targeted therapeutics, but as nucleic acid chemistry was in its infancy, the complicated, and labour-intensive protocols required to synthesise these complexes ultimately resulted in a lack of further development.

In recent years, research into the tethering of metallodrugs to oligonucleotides has re-surfaced. For example, in 2012 Paul Miller reported a family of platinum-derivatised homopyrimidine TFOs, which consisted of 2′-*O*-methyl-5-methyluridine, 2′-*O*-methyl-5-methylcytidine and a single 3′-N7-*trans*-chlorodiamine platinum(II)-deoxyguanosine[7] (**Figure 4**). These TFOs were capable of binding to their target sequence, while the transplatin moiety cross-linked DNA, thereby preventing DNA replication at a specific site. The attachment of copper AMNs to TFOs has also been revisited. Short oligonucleotides containing modified nucleosides are now commercially available and the discovery of click chemistry[50] has simplified the attachment of chemical nucleases to the oligonucleotide strand. DNA bearing alkyne modified bases can be ‘clicked’ to azide modified AMNs through fast and reliable click chemistry protocols. Clip-phenanthroline TFOs that are capable of cleaving double-stranded DNA in a sequence specific manner have recently been reported by the Hocek group,[5] and TFOs ‘clicked’ to polypyridyl copper-binding AMNs,[3, 6] copper-phenanthrene derivatives,[4] and *cis*-platinum(II) molecules[8] (**Figure 4**) have been synthesised and published by the Kellett group and collaborators.

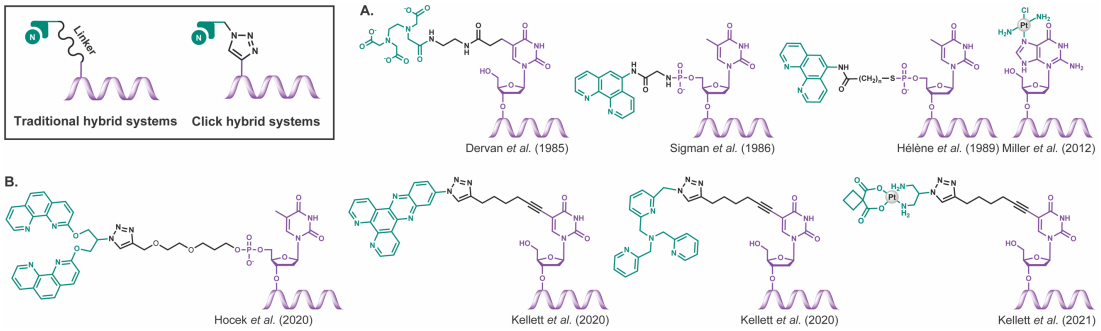


Figure 4: A. Structure of traditional sequence-specific hybrid systems, where a triplex forming oligonucleotide (purple) has been coupled to an EDTA, Phen or Platinum (green) moiety, either through a peptide linker (black) or by direct attachment to the nucleobase. **B.** Hybrid systems synthesised through click chemistry. The metallodrug can be attached to either the phosphate backbone or nucleobase.

1.4 Click chemistry

Click chemistry is a group of reactions that are fast and simple to perform, are versatile and regiospecific, give high product yields and do not require complex purification. There are a number of reactions that satisfy these criteria but the Cu(I)-catalysed Huisgen 1,3-dipolar cycloaddition of azides and terminal alkynes to form 1,2,3-triazoles[51, 52] has become the most popular click chemistry reaction. The classic Huisgen cycloaddition[53] required high temperatures (~100 °C) and long reaction times, but the use of a copper catalyst enables the azide-alkyne cycloaddition (AAC) to be performed at room temperature, in both aqueous media and organic solvents, over a wide range of pH values (pH 5 – 12). The presence of copper also increases the reaction kinetics 10^7 times.[51, 52] Additionally, the Cu(I)-catalysed azide-alkyne cycloaddition (CuAAC) is regiospecific, with only 1,4 functionalised 1,2,3-triazole products obtained (**Figure 5A**), compared with the mixture of regioisomers[53] obtained for the uncatalysed reaction. The 'click' product from the CuAAC is also non-toxic and stable, these features along with the small size of the reaction components, their stability in complex environments (azides and alkynes have no biological target), and the ease with which azide and alkyne functional groups can be incorporated into a wide range of substrates[54] justifies CuAAC being at the forefront of click chemistry.

The active form of the copper(I) catalyst must be generated before the CuAAC click reaction can commence. One of the most common techniques employed for this task is the reduction of Cu(II) salts, such as $CuSO_4 \bullet 5H_2O$, *in situ* to form Cu(I). Sodium-*L*-ascorbate is the most commonly used reducing agent, and it is typically present in a 3- to 10-fold excess.[51] This reduction can be performed in water which means moieties bearing hydroxyl and amide groups do not require protection.[50] A disadvantage of this method is that the reducing agent may cause Cu(II) to be reduced to Cu(0), but this can be prevented through the use of optimised equivalents of reducing agent and catalyst, and/or by adding a copper-chelator, such as THPTA (*tris*-(hydroxyoropyltriazolmethyl)-amine) or TBTA (*tris*-(benzyltriazolylmethyl)-amine).[55] A second method to introduce the Cu(I) catalyst to the click reaction, is the direct addition of a Cu(I) salt, for example CuBr, to the reaction solution.[51] This method does not require a reducing agent, but a deoxygenated atmosphere and an organic solvent are necessary, which means protecting groups may be required. This method is therefore slow and unreliable in comparison to the use of Cu(II) salts.

Click chemistry reactions can also occur in the absence of a catalyst if the alkyne is incorporated into an eight-membered ring, forming a cyclooctyne.[56] The large bond angle deformation (~160º versus 180º in linear alkynes) causes 18 kcal/mol of ring-strain compared with 0.2 kcal/mol for linear alkynes. This additional energy leads to a dramatic acceleration, compared with the traditional Huisgen cycloaddition, and enables the azide-alkyne cycloaddition to be performed under physiological conditions in the absence of a copper catalyst.[56] This strain-promoted azide-alkyne cycloaddition (SPAAC) (**Figure 5B**) has a wide-variety of bioorthogonal applications, including chemical reporting, fluorescent tagging and it has drug delivery applications where the copper requirement had prevented the use of the CuAAC reaction.

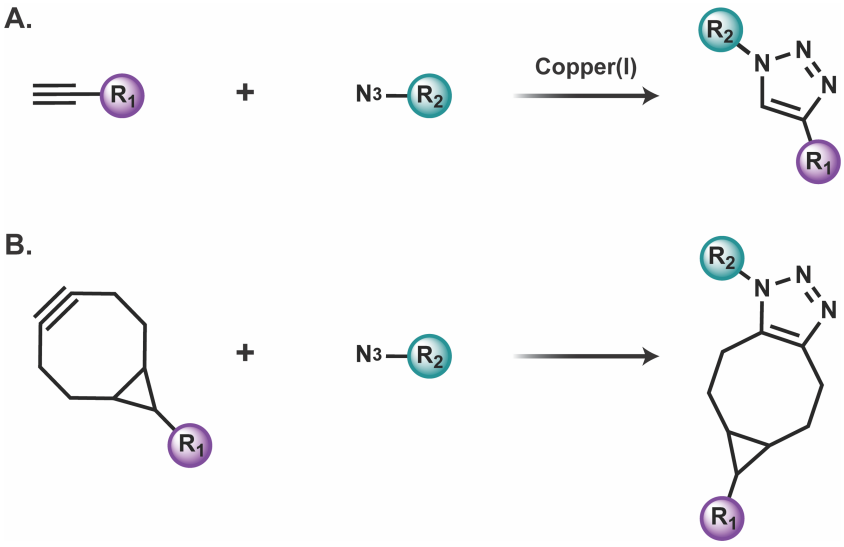


Figure 5: A. The copper catalysed azide-alkyne cycloaddition (CuAAC) enables an azide and an alkyne to be "clicked" in the presence of a copper(I) catalyst to generate a 1,4, functionalised 1,2,3 triazole. **B.** Strain-promoted click chemistry uses a cyclooctyne (*e.g.* BCN), with high ring-strain, to trigger the click reaction. This removes the need for a copper(I) catalyst.

There are many applications of click chemistry. Originally it was reported as a method for the rapid synthesis of complex molecules from a library of 'building blocks' through the generation of carbon-heteroatom links (C-X-C).[50] However it has also been employed for fluorescent labelling,[57, 58] oligonucleotide synthesis,[59] drug delivery[5] and as a molecular probing technique.[60] In 2006 the Carell group reported the first use of click chemistry for the post-synthetic functionalisation of DNA.[57] Here, the suitability of the CuAAC reaction for nucleic acid click chemistry was investigated. A variety of short DNA sequences, with various numbers of alkyne-modified nucleosides, were chemically synthesised for this task. The compatibility of these oligonucleotides with a variety of click conditions was studied; strand breaks were observed when a click reaction with excess azide, Cu(I) and an alkyne modified oligonucleotide were performed. This suggested that the CuAAC method was not suitable for the high-density functionalisation of DNA. But the addition of a Cu(I)-stabilising ligand, such as THPTA, to the reaction mixture yielded full conversion of the alkyne-modified nucleosides to their triazole products with no apparent degradation.[57] This showed that CuAAC click chemistry reaction could be employed for the simple and rapid functionalisation of DNA sequences. This click functionalisation

technique has also been employed for the labelling of DNA within cells. 5-Ethynyl-2′-deoxyuridine (EdU) bases are incorporated into DNA during the S-phase of the cell cycle. Then these alkyne groups can be clicked to azide modified fluorophores and the DNA can be visualised by techniques such as flow cytometry and fluorescence microscopy.[60]

1.5 Synthesis of oligonucleotides

Nucleic acids bearing modifications have been extensively studied since the 1950s, with various clinical applications being reported including antiviral and anti-tumour therapeutics.[61] The majority of modified nucleic acids are chemically synthesised through solid-phase synthesis, the mostly widely used method of which is classic phosphoramidite synthesis on a solid support. The phosphoramidite method was originally reported in 1981 by Marvin Caruthers[62] and was further developed by the same laboratory to be performed on an automated instrument.[63] This method has since become the technique of choice for solid-phase synthesis of oligonucleotides. The phosphoramidite method is a multi-step process that synthesises DNA in the 3′ to 5′ direction (the opposite of DNA synthesis during DNA replication), adding one nucleotide per synthesis cycle[62] (**Figure 6**). Oligonucleotide synthesis begins with the first nucleoside pre-attached to the resin of the column,[64] there are four columns, A, G, C and T, depending on the nucleoside desired at the 3′ end of the sequence. This solid-support bound nucleotide has a 5′-DMT (4,4′-dimethoxytrityl), which prevents polymerisation of the nucleotide during resin functionalisation.[64] This protecting group must be removed, through a process known as detritylation, before oligonucleotide synthesis can begin.

Phosphoramidite synthesis begins with the addition of a large excess of the next nucleoside phosphoramidite monomer required for the desired sequence. The diisopropylamino group of the phosphoramidite is protonated by the activator (tetrazole), thereby becoming a good leaving group. This group is then displaced by the 5′-hydroxyl group of the solid-support bound nucleoside, forming a phosphorus-oxygen bond and creating a support-bound phosphite triester[62-64] (**Figure 6**). However, not all of the resin-bound phosphoramidite will

have reacted, so to avoid the synthesis of truncated oligonucleotides, these phosphoramidites must be prevented from partaking in next synthesis cycle. Therefore, step 2 is capping the unreacted 5′ hydroxyl groups. A premixed solution of acetic anhydride and *N*-methylimidazole (NMI) (dissolved in tetrahydrofuran and a small concentration of pyridine) are added to the synthesis column. The alcohol group is acetylated, which renders it inert for subsequent synthesis cycles[62, 63] (**Figure 6**). Step 3 is the oxidation of the P(III) in the phosphite-triester to a P(V), as P(III) is unstable in acid and therefore would not survive the next round of detritylation. This step is achieved using iodine in the presence of water and pyridine[62, 63] (**Figure 6**). The final step in the phosphoramidite synthesis method is another detritylation step, this prepares the nucleosides for the next synthesis cycle. Again, the DMT protecting group is removed from the 5′-end of the resin bound DNA chain, so that the hydroxyl group can react with the next nucleoside phosphoramidite.[62, 63] The cycle is repeated until the desired oligonucleotide chain length has been achieved.

The oligonucleotide must then be cleaved from the solid support.[64] Various different linkers can be used between the first nucleoside and the resin, but the most common is a succinyl linker as it can be cleaved using concentrated ammonium hydroxide within 1 hour at room temperature.[64] Finally, the oligonucleotide that is dissolved in concentrated ammonium hydroxide, is heated to remove the protecting group from the heterocyclic bases and phosphates. The solution is then removed by evaporation and the oligonucleotide is ready for purification.[63, 64]

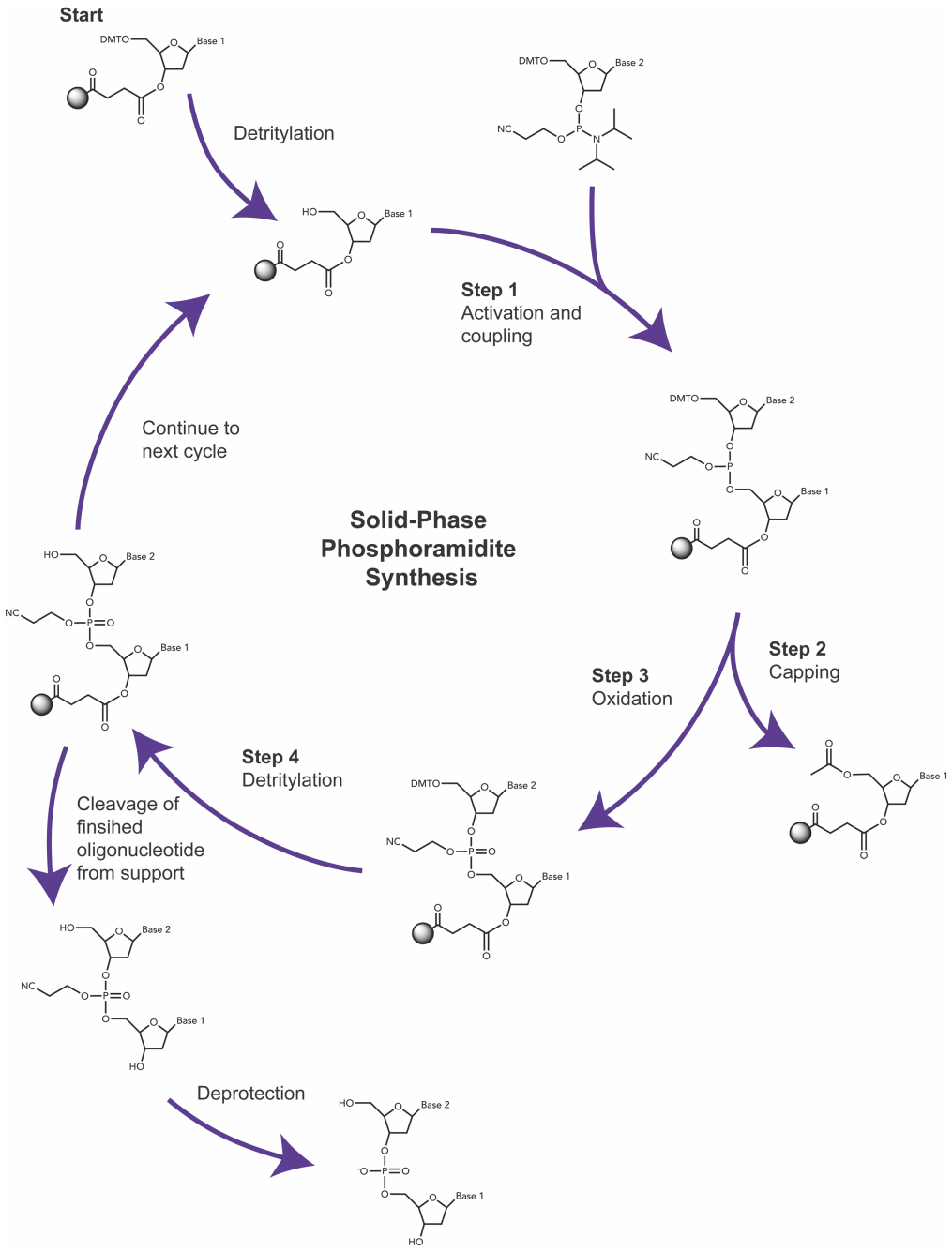


Figure 6: Solid-phase synthesis schematic showing the steps in each cycle of oligonucleotide synthesis.

Oligonucleotides post-phosphoramidite synthesis must be purified to remove any impurities, such as truncated products and reaction components. This is typically achieved through chromatography. Chromatography is the separation of the components of a mixture by differential adsorption onto an adsorbent surface (stationary phase), the components are then eluted by a

solvent, or a mix of solvents (mobile phase), and collected. Gel filtration is the simplest purification method, it separates components by size and therefore is only suitable for the removal of cleaved protecting groups and short truncated nucleic acids. It does not remove impurities that are of similar size to the desired product and therefore is only recommended for very short (<20 bases) non-modified oligonucleotides.[62] High-performance liquid chromatography (HPLC) is a more efficient method for the purification of oligonucleotides and it enables the separation of sequences of similar lengths. Reverse-phase HPLC separates oligonucleotides and contaminants by their hydrophobicity. The reaction mixture is loaded onto a column that consists of hydrocarbon chains bound to a silica support, and is washed with aqueous ammonium acetate. This forces the oligonucleotides to bind to the reverse-phase column. Gradients of acetonitrile in ammonium acetate are added to the column. The hydrophobicity of the column increases as the concentration of acetonitrile rises, and therefore, the molecules with the a greater degree of hydrophobicity elute more slowly, allowing for the separation of the components in the reaction mixture.[63] However, reverse-phase HPLC is not suitable for the separation of longer nucleic acid sequences as it becomes increasing more difficult to separate similar sequences as the length of the nucleotide chain increases. A third purification method is anion-exchange HPLC. This method separates oligonucleotides based on their charge. Oligonucleotides are polyanions and the particular negative charge of a sequence is dependent on the number of phosphodiester groups in the molecule. The stationary phase for anion-exchange HPLC is a cationic tertiary amine. The anionic oligonucleotide interacts with the cationic stationary phase, and thereby reaction components are separated as the ionic strength of the mobile phase increases, which weakens the interaction between the DNA and the stationary phase. Shorter oligonucleotides are eluted first as they are less anionic than longer sequences.[65] Anion-exchange HPLC is suitable for nucleic acids between 5 and 50 bases in length.

Although the coupling efficiency is high for each cycle of phosphoramidite synthesis, the overall yield of oligonucleotide synthesis can be greatly affected by even a small drop in efficiency.[66] For example: with a coupling efficiency of 95% the yield for a 10 base sequence is 38.7%, which decreases to 13.5% for

20 bases and >0.01% for 200 bases. Even with a coupling efficiency of 97% the overall yield for 10, 20 and 200 bases is 76%, 56.1% and 0.2%, respectively.[66] However, when the coupling efficiency is increased to 99.5%, the yield for 10 and 20 bases is 95.6% and 90.9%, respectively, but the yield is still low for longer sequences, with a 200 nucleotide sequence having a yield of 36.9%.[66] Therefore, solid-phase phosphoramidite synthesis as a process is not efficient, and there is a high concentration of reagents required for a small concentration of the finished product. It is also not suitable for the synthesis of longer DNA sequences,[59] and so its main functionality is in the synthesis of short nucleic acid fragments.

Although solid-phase nucleic acid synthesis is a robust and scalable method for the synthesis of short oligonucleotides, the process becomes more complex when DNA bearing a modification is desired. The phosphoramidite method is not compatible with modifications that are susceptible to oxidation or are reactive with nucleophiles.[61] However, phosphoramidites bearing various base modifications, including methylcytosine,[67] *trans*-platin,[68, 69] and alkynes[57, 58, 70] have been synthesised, and oligonucleotides bearing alkynes, among other modifications, are now commercially available. But, solid-phase synthesis is still a multi-step process that requires specialised equipment, and the products must undergo complex purification steps to achieve relatively low yields of the final product. An alternative method for the generation of modified oligonucleotides is enzymatic synthesis using DNA polymerases and modified deoxyribonucleotide triphosphates (dNTPs).

1.6 Enzymatic synthesis

The first report of the enzymatic synthesis of DNA using modified dNTPs was published in 1981 by Langer *et al.*,[71] wherein the ability of several DNA polymerases to incorporate C5-biotin-modified dUTPs was reported.[71] Since then the incorporation of a variety of modifications by various different DNA polymerases has been published.[72-77] The best substrates for enzymatic synthesis are C5-modified pyrimidines or C7-modified 7-deazapurines as these allow the modification to sit in the major groove, and thus do not inhibit the formation of double helical DNA.[76] The use of C5-modified pyrimidines, in

particular uracil, is the most common due to the difficult synthesis required for 7-deazapurines.[61]

The enzymatic synthesis of DNA is routinely performed in molecular biology but the incorporation of modified dNTPs is a more challenging task. The polymerase chain reaction (PCR)[78] is one of the most widely used enzymatic protocols, as it enables the exponential amplification of a DNA sequence of interest. Template DNA along with forward and reverse primers (flanking the sequence to be amplified) are incubated in cycles (20 – 40) of denaturation, annealing and extension in the presence of a thermostable DNA polymerase (most commonly *Taq* DNA polymerase) and dNTPs (**Figure 7A**). Theoretically, each PCR cycle doubles the number of amplicons present and therefore the resulting dsDNA concentration is 2^n (n = number of cycles) times that originally added to the PCR mix.[78] PCR can also be performed with modified dNTPs but this can be challenging as the polymerase must be able to incorporate the modified nucleotide into the sequence, and also read those modified-dNTPs correctly for the next round of amplification. PCR is typically used for the generation of long DNA sequences (>100 bp) with the minimum length being 36 bp as PCR primers are typically 18-22 nt and it is recommended that they do not have overlapping regions to avoid primer-dimer formation.

Primer extension (PEX) is another method of enzymatic synthesis, and it can be used for the generation of shorter (<100 bp) DNA fragments. PEX is a relatively straight forward protocol as it does not amplify DNA. Therefore template and primer are incubated with a DNA polymerase and dNTPs at a constant temperature. The template and primer anneal and the DNA polymerase extends the primer using dNTPs (**Figure 7B**).[79] Due to the relative simplicity of PEX it is an excellent tool for analysing the ability of DNA polymerases to recognise a modified dNTP as substrate. If one natural dNTP is replaced by its modified analogue in a PEX reaction the DNA polymerase should incorporate the modified dNTP at every complementary position. The products are analysed by polyacrylamide gel electrophoresis (PAGE) and compared to positive (all natural dNTPs) and negative (absence of one natural dNTP) controls. If the modified dNTP is substrate for the DNA polymerase a full length product (similar to positive

control) will be visualised, whereas truncated products will be observed if the DNA polymerase cannot recognise the modified nucleotide as substrate.

PCR and PEX both produce double stranded products, but for an oligonucleotide to act as an antisense or antigene therapeutic it must be single stranded. However, if one strand of a dsDNA product bears a biotin tag, the strands can be separated and a single stranded oligonucleotide can be isolated. If PEX is performed with a biotinylated template, the strands can be separated using streptavidin coated magnetic particles and a denaturation magneto-separation step.[80] Unfortunately this technique is not applicable to PCR products. To separate the strands resulting from PCR, one of the primers would need to be biotinylated, but there are also challenges in separating the DNA strands. The melting temperature of DNA sequences >100 bp is higher than the denaturation temperature of the streptavidin-biotin bond, therefore streptavidin-biotin magneto-separation is not suitable.

Another method for the synthesis of short single stranded oligonucleotides (<15 nt) is the nicking enzyme amplification reaction (NEAR). This requires a template and primer that contain the recognition sequence of nicking endonuclease. Similar to PEX, the template and primer are annealed and the primer is extended with dNTPs by a DNA polymerase. Next the nicking enzyme is added, this cleaves the DNA at the recognition site and the newly synthesised stretch of DNA falls off the template due to its low melting temperature. These steps are repeated, which results in linear amplification of the newly synthesised section (**Figure 7D**). If a suitable DNA polymerase is chosen NEAR can also be performed with modified dNTPs, and therefore it is a useful method for the generation of modified primers[81] that can then be used in the other enzymatic protocols described.

However, none of the above mentioned methods allow for the synthesis of an oligonucleotide with a single modification at a specific position. In 2013 the Hocek group reported a solution to this problem.[82] This new protocol involved two steps: i.) the incorporation of a single modified nucleotide immediately 3′ of the primer; and ii.) extension of the primer-modified dNTP sequence with natural dNTPs (**Figure 7C**). This single nucleotide incorporation-primer extension (SNI-PEX) protocol followed by streptavidin-biotin magneto-separation is therefore an

alternative to solid-phase synthesis of DNA oligonucleotides and can be used for the synthesis of antisense/antigene therapeutics. But this SNI-PEX method only allows for the inclusion of a single modified base in a DNA sequence, which limits its functionality as multiple specific modifications are often required in antisense/antigene oligonucleotides.

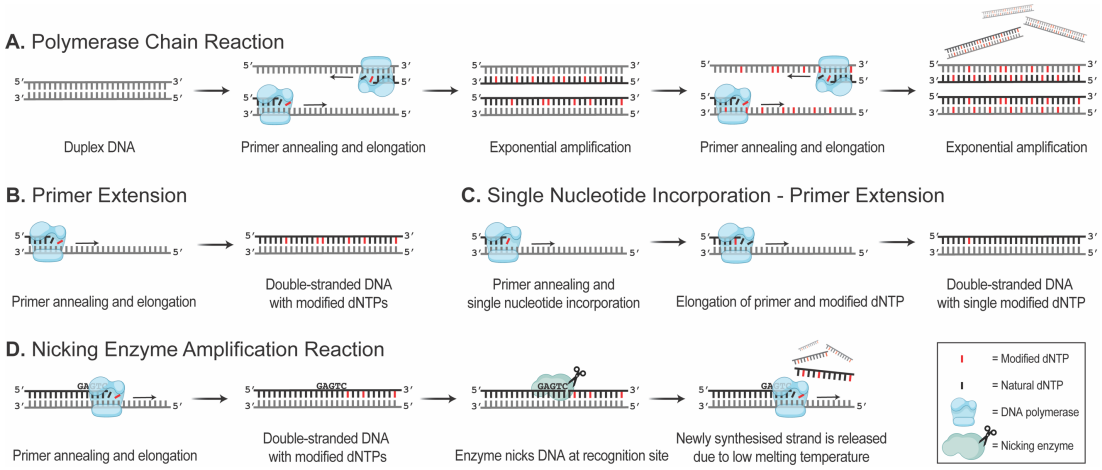


Figure 7: A. The polymerase chain reaction (PCR) can exponentially amplify a double-stranded DNA sequence of interest. **B.** Primer extension (PEX) is a relatively simple method for the synthesis of a strand of DNA containing modified dNTPs. If a natural dNTP is replaced by its modified derivative the modified dNTP will be incorporated at all complementary positions. **C.** Single-nucleotide incorporation (SNI) PEX allows for a single modified nucleotide to be incorporated at a specific position in a DNA sequence. **D.** The nicking enzyme amplification reaction (NEAR) allows for the linear amplification of a short single-stranded DNA sequence.

However, all of the above methods of enzymatic synthesis require a DNA template that is produced through solid-phase synthesis, or isolated from a biological source (*e.g.* plasmid DNA). PCR can be performed on biological DNA to amplify a sequence of interest, but it still requires primers that are typically produced by solid-phase synthesis. Terminal deoxynucleotidyl transferase (TdT) offers a potential solution to this. TdT is a DNA polymerase that can synthesise DNA in a template-independent fashion.[83, 84] However, as there is no template TdT randomly incorporates dNTPs, and consequently is not applicable for the synthesis of a specific DNA sequence. Much research has been performed to investigate a mechanism by which TdT could be employed as an alternative to phosphoramidite synthesis, and multiple companies have been founded that now

synthesise DNA using TdT.[85] However, the synthesis of a specific oligonucleotide sequence using TdT is not a simple process, it is performed in a stepwise manner similar to SPS where a single dNTP is added, protected and deprotected per synthesis cycle.[86] This requires specialised equipment, and thereby makes TdT synthesis inaccessible to the majority of research laboratories.

References

1. Moser, H. E.; Dervan, P. B., Sequence-specific cleavage of double helical DNA by triple helix formation. *Science* **1987,** *238* (4827), 645-50.
2. Hacia, J. G.; Dervan, P. B.; Wold, B. J., Inhibition of Klenow Fragment DNA-Polymerase on Double-Helical Templates by Oligonucleotide-Directed Triple-Helix Formation. *Biochem.* **1994,** *33* (20), 6192-6200.
3. Zuin Fantoni, N.; McGorman, B.; Molphy, Z.; Singleton, D.; Walsh, S.; El-Sagheer, A. H.; McKee, V.; Brown, T.; Kellett, A., Development of Gene-Targeted Polypyridyl Triplex-Forming Oligonucleotide Hybrids. *ChemBioChem* **2020,** *21* (24), 3563-3574.
4. Lauria, T.; Slator, C.; McKee, V.; Müller, M.; Stazzoni, S.; Crisp, A. L.; Carell, T.; Kellett, A., A Click Chemistry Approach to Developing Molecularly Targeted DNA Scissors. *Chem. Eur. J.* **2020**.
5. Panattoni, A.; El-Sagheer, A. H.; Brown, T.; Kellett, A.; Hocek, M., Oxidative DNA Cleavage with Clip-Phenanthroline Triplex-Forming Oligonucleotide Hybrids. *ChemBioChem* **2020,** *21* (7), 991-1000.
6. McGorman, B.; Zuin Fantoni, N.; O'Carroll, S.; Ziemele, A.; El-Sagheer, A. H.; Brown, T.; Kellett, A., Enzymatic synthesis of chemical nucelase triple-forming oligonucleotides with gene-editing applications. *Manuscript under review*.
7. Graham, M. K.; Miller, P. S., Inhibition of transcription by platinated triplex-forming oligonucleotides. *J Biol Inorg Chem* **2012,** *17* (8), 1197-208.
8. Hennessy, J.; McGorman, B.; Molphy, Z.; Farrell, N. P.; Singleton, D.; Brown, T.; Kellett, A., A Click Chemistry Approach to Targeted DNA Crosslinking with cis-Platinum(II) Modified Triplex Forming Oligonucleotides. *Angew. Chem. Int. Ed.* **2021,** *60*.
9. Felsenfeld, G.; Davies, D.; Rich, A., Formation of a three stranded polynucleotide molecule-annotated. *J. Am. Chem. Soc.* **1957,** *79* (8), 2023-2024.
10. Knauert, M. P.; Glazer, P. M., Triplex forming oligonucleotides: sequence-specific tools for gene targeting. *Hum Mol Genet* **2001,** *10* (20), 2243-51.
11. Fox, K. R.; Brown, T.; Rusling, D. A., Chapter 1. DNA Recognition by Parallel Triplex Formation. In *DNA - targeting molecules as therapeutic agents*, Waring, M. J., Ed. Royal Society of Chemistry: 2018; pp 1-32.
12. Beal, P. A.; Dervan, P. B., Second structural motif recognition of DNA by oligonucleptide-directed triple-helix formation. *Science* **1991,** *251*, 1360-1363.
13. Durland, R. H.; Kessler, D. J.; Gunnell, S.; Duvic, M.; Pettitt, B. M.; Hogan, M. E., Binding of triple helix forming oligonucleotides to sites in gene promoters. *Biochem.* **1991,** *30* (38), 9246-55.
14. Le Doan, T.; Perrouault, L.; Praseuth, D.; Habhoub, N.; Decout, J. L.; Thuong, N. T.; Lhomme, J.; Helene, C., Sequence-specific recognition, photocrosslinking and cleavage of the DNA double helix by an oligo-[alpha]-thymidylate covalently linked to an azidoproflavine derivative. *Nucleic Acids Res* **1987,** *15* (19), 7749-60.
15. Thenmalarchelvi, R.; Yathindra, N., New insights into DNA triplexes: residual twist and radial difference as measures of base triplet non-isomorphism and their implication to sequence-dependent non-uniform DNA triplex. *Nucleic Acids Res* **2005,** *33* (1), 43-55.

16. Bevers, S.; Schutte, S.; McLaughlin, L. W., Naphthalene- and Perylene-Based Linkers for the Stabilization of Hairpin Triplexes. **2000,** *122* (25), 5905-5915.
17. Sun, J. S.; Francois, J. C.; Montenay-Garestier, T.; Saison-Behmoaras, T.; Roig, V.; Thuong, N. T.; Helene, C., Sequence-specific intercalating agents: intercalation at specific sequences on duplex DNA via major groove recognition by oligonucleotide-intercalator conjugates. *Proc. Natl. Acad. Sci.* **1989,** *86* (23), 9198-9202.
18. Wilson, W. D.; Tanious, F. A.; Mizan, S.; Yao, S.; Kiselyov, A. S.; Zon, G.; Strekowski, L., DNA triple-helix specific intercalators as antigene enhancers: Unfused aromatic cations. *Biochem.* **1993,** *32*, 10614-10621.
19. Walsh, S.; El-Sagheer, A. H.; Brown, T., Fluorogenic thiazole orange TOTFO probes stabilise parallel DNA triplexes at pH 7 and above. *Chem Sci* **2018,** *9* (39), 7681-7687.
20. Zhou, B.-W.; Puga, E.; Sun, J.-S.; Garestier, T.; Helene, C., Stable Triple Helixes Formed by Acridine-Containing Oligonucleotides with Oligopurine Tracts of DNA Interrupted by One or Two Pyrimidines. *J. Am. Chem. Soc.* **1995,** *117* (42), 10425-10428.
21. Rusling, D. A., Triplex-forming properties and enzymatic incorporation of a base-modified nucleotide capable of duplex DNA recognition at neutral pH. *Nucleic Acids Res.* **2021,** *49* (13), 7256-7266.
22. Yang, Z.; Hutter, D.; Sheng, P.; Sismour, A. M.; Benner, S. A., Artificially expanded genetic information system: a new base pair with an alternative hydrogen bonding pattern. *Nucleic Acids Res.* **2006,** *34* (21), 6095-6101.
23. Hutter, D.; Benner, S. A., Expanding the Genetic Alphabet: Non-Epimerizing Nucleoside with the pyDDA Hydrogen-Bonding Pattern. *The Journal of Organic Chemistry* **2003,** *68* (25), 9839-9842.
24. Aiba, Y.; Sumaoka, J.; Komiyama, M., Artificial DNA cutters for DNA manipulation and genome engineering. *Chem. Soc. Rev.* **2011,** *40* (12), 5657.
25. Gaj, T.; Gersbach, C. A.; Barbas, C. F., ZFN, TALEN, and CRISPR/Cas-based methods for genome engineering. *Trends in Biotechnology* **2013,** *31* (7), 397-405.
26. Beerli, R. R.; Segal, D. J.; Dreier, B.; Barbas, C. F., Toward controlling gene expression at will: Specific regulation of the erbB-2/HER-2 promoter by using polydactyl zinc finger proteins constructed from modular building blocks. *Proc Natl Acad Sci U S A* **1998,** *95* (25), 14628-14633.
27. Zuin Fantoni, N.; Brown, T.; Kellett, A., DNA-targeted metallodrugs: an untapped source of artificial gene editing technology. *ChemBioChem* **2021**.
28. Wang, H.; La Russa, M.; Qi, L. S., CRISPR/Cas9 in Genome Editing and Beyond. *Annual Review of Biochemistry* **2016,** *85* (1), 227-264.
29. Tebas, P.; Stein, D.; Tang, W. W.; Frank, I.; Wang, S. Q.; Lee, G.; Spratt, S. K.; Surosky, R. T.; Giedlin, M. A.; Nichol, G.; Holmes, M. C.; Gregory, P. D.; Ando, D. G.; Kalos, M.; Collman, R. G.; Binder-Scholl, G.; Plesa, G.; Hwang, W.-T.; Levine, B. L.; June, C. H., Gene Editing ofCCR5in Autologous CD4 T Cells of Persons Infected with HIV. *New England Journal of Medicine* **2014,** *370* (10), 901-910.
30. Ashmore-Harris, C.; Fruhwirth, G. O., The clinical potential of gene editing as a tool to engineer cell-based therapeutics. *Clinical and Translational Medicine* **2020,** *9* (1).

31. Jinek, M.; Chylinski, K.; Fonfara, I.; Hauer, M.; Doudna, J. A.; Charpentier, E., A Programmable Dual-RNA-Guided DNA Endonuclease in Adaptive Bacterial Immunity. *Science* **2012,** *337* (6096), 816-821.
32. Sigman, D. S.; Graham, D. R.; D'Aurora, V.; Stern, A. M., Oxygen dependent cleavage of DNA by the 1,10-Phenanthroline cuprous complex. *J. Biol. Chem.* **1979,** *254*, 12269-12272.
33. Sigman, D. S., Nuclease activity of 1,10-phenanthroline-copper ion. *Acc. Chem. Res.* **1986,** *19* (6), 180-186.
34. Molphy, Z.; Prisecaru, A.; Slator, C.; Barron, N.; McCann, M.; Colleran, J.; Chandran, D.; Gathergood, N.; Kellett, A., Copper phenanthrene oxidative chemical nucleases. *Inorg. Chem.* **2014,** *53* (10), 5392-404.
35. Molphy, Z.; Slator, C.; Chatgilialoglu, C.; Kellett, A., DNA oxidation profiles of copper phenanthrene chemical nucleases. *Front. Chem.* **2015,** *3*, 28.
36. Zuin Fantoni, N.; Molphy, Z.; O'Carroll, S.; Menounou, G.; Mitrikas, G.; Krokidis, M.; Chatgilialoglu, C.; Colleran, J.; Banasiak, A.; Clynes, M.; Roche, S.; Kelly, S.; McKee, V.; Kellett, A., Polypyridyl-Based Copper Phenanthrene Complexes: Combining Stability with Enhanced DNA Recognition. *Chem. Eur. J.* **2020**.
37. Zuin Fantoni, N.; Molphy, Z.; Slator, C.; Menounou, G.; Toniolo, G.; Mitrikas, G.; McKee, V.; Chatgilialoglu, C.; Kellett, A., Polypyridyl-Based Copper Phenanthrene Complexes: A New Type of Stabilized Artificial Chemical Nuclease. *Chem. Eur. J.* **2019,** *25* (1), 221-237.
38. Bales, B. C.; Kodama, T.; Weledji, Y. N.; Pitie, M.; Meunier, B.; Greenberg, M. M., Mechanistic studies on DNA damage by minor groove binding copper-phenanthroline conjugates. *Nucleic Acids Res.* **2005,** *33* (16), 5371-9.
39. Pitie, M.; Burrows, C. J.; Meunier, B., Mechanisms of DNA cleavage by copper complexes of 3-clip-phen and of its conjugate with a distamycin analogue. *Nucleic Acids Res.* **2000,** *28* (24), 4856-64.
40. Pitié, M.; Van Horn, J. D.; Brion, D.; Burrows, C. J.; Meunier, B., Targeting the DNA Cleavage Activity of Copper Phenanthroline and Clip-Phen to A·T Tracts via Linkage to a Poly-N-methylpyrrole. *Bioconjug. Chem.* **2000,** *11* (6), 892-900.
41. Sigman, D. S.; Bruice, T. W.; Mazumder, A.; Sutton, C. L., Targeted chemical nucleases. *Acc. Chem. Res.* **1993,** *26* (3), 98-104.
42. Francois, J. C.; Saison-Behmoaras, T.; Barbier, C.; Chassignol, M.; Thuong, N. T.; Helene, C., Sequence-specific recognition and cleavage of duplex DNA via triple-helix formation by oligonucleotides covalently linked to a phenanthroline-copper chelate. *Proc. Natl. Acad. Sci.* **1989,** *86* (24), 9702-9706.
43. Kane, S. A.; Hecht, S. M.; Sun, J.-S.; Garestier, T.; Helene, C., Specific cleavage of a DNA triple helix by FeII.bleomycin. *Biochem.* **1995,** *34* (51), 16715-16724.
44. Shultz, P. G.; Taylor, J. S.; Dervan, P. B., Design synthesis of a sequence-specific DNA cleaving molecule. (Distamycin-EDTA)iron(II). **1982,** *104* (24), 6861-6863.
45. Schultz, P. G.; Dervan, P. B., Sequence-specific double-strand cleavage of DNA by penta-N-methylpyrrolecarboxamide-EDTA X Fe(II). **1983,** *80* (22), 6834-6837.
46. Dreyer, G. B.; Dervan, P. B., Sequence-specific cleavage of single-stranded DNA: oligodeoxynucleotide-EDTA X Fe(II). *Proc. Natl. Acad. Sci.* **1985,** *82* (4), 968-972.

47. Chen, C. H.; Sigman, D. S., Nuclease activity of 1,10-phenanthroline-copper: sequence-specific targeting. **1986,** *83* (19), 7147-7151.
48. Chen, C. H. B.; Sigman, D. S., Sequence-specific scission of RNA by 1,10-phenanthroline-copper linked to deoxyoligonucleotides. **1988,** *110* (19), 6570-6572.
49. Francois, J. C.; Saison-Behmoaras, T.; Helene, C., Sequence-specific recognition of the major groove of DNA by oligodeoxynucleotides via triple helix formation. Footprinting studies. *Nucleic Acids Res* **1988,** *16* (24), 11431-40.
50. Kolb, H. C.; Finn, M. G.; Sharpless, K. B., Click Chemistry: Diverse Chemical Function from a Few Good Reactions. *Angew. Chem. Int. Ed.* **2001,** *40*, 2004-2021.
51. Rostovtsev, V. V.; Green, L. G.; Fokin, V. V.; Sharpless, K. B., A stepwise Huisgen cycloaddition process: Copper (I)-catalysed regioselective "ligation" of azides and terminal alkynes. *Angew. Chem. Int. Ed.* **2002,** *41* (14).
52. Tornøe, C. W.; Christensen, C.; Meldal, M., Peptidotriazoles on Solid Phase: [1,2,3]-Triazoles by Regiospecific Copper(I)-Catalyzed 1,3-Dipolar Cycloadditions of Terminal Alkynes to Azides. *J. Org. Chem.* **2002,** *67* (9), 3057-3064.
53. Huisgen, R., 1,3-Dipolar Cycloadditions: Past and Future. *Angew Chem Int Ed Engl* **1963,** *2* (10), 565-632.
54. Debets, M. F.; Van Der Doelen, C. W. J.; Rutjes, F. P. J. T.; Van Delft, F. L., Azide: A Unique Dipole for Metal-Free Bioorthogonal Ligations. *ChemBioChem* **2010,** *11* (9), 1168-1184.
55. Bock, V. D.; Hiemstra, H.; Van Maarseveen, J. H., CuI-Catalyzed Alkyne-Azide "Click" Cycloadditions from a Mechanistic and Synthetic Perspective. *European Journal of Organic Chemistry* **2006,** *2006* (1), 51-68.
56. Agard, N. J.; Prescher, J. A.; Bertozzi, C. R., A Strain-Promoted [3 + 2] Azide−Alkyne Cycloaddition for Covalent Modification of Biomolecules in Living Systems. *J. Am. Chem. Soc.* **2004,** *126* (46), 15046-15047.
57. Gierlich, J.; Burley, G.; Gramlich, P. M.; Hammond, D. M.; Carell, T., Click chemistry as a reliable method for the high density functionalisation of alkyne modified DNA. *Organic Letters* **2006,** *8* (17), 3639-3642.
58. Seela, f.; Sirivolu, V. R.; Chittepu, P., Modification od DNA with Octadiynyl Side Chains: Synthesis, Base Pairing, and Formation of Fluorescent Coumarin Dye Conjugates of Four Nucleobases by the Alkyne-Azide "Click" Reaction. *Bioconjug. Chem.* **2008,** *19*, 211-224.
59. El-Sagheer, A. H.; Brown, T., Click Nucleic Acid Ligation: Applications in Biology and Nanotechnology. *Acc. Chem. Res.* **2012,** *45* (8), 1258-1267.
60. Buck, S. B.; Bradford, J.; Gee, K. R.; Agnew, B. J.; Clarke, S. T.; Salic, A., Detection of S-phase cell cycle progression using 5-ethynyl-2′-deoxyuridine incorporation with click chemistry, an alternative to using 5-bromo-2′-deoxyuridine antibodies. *BioTechniques* **2008,** *44* (7), 927-929.
61. Hocek, M., Synthesis of base-modified 2'-deoxyribonucleoside triphosphates and their use in enzymatic synthesis of modified DNA for applications in bioanalysis and chemical biology. *J. Org. Chem.* **2014,** *79* (21), 9914-21.
62. Beaucage, S. L.; Caruthers, M. H., Deoxynucleoside phosphoramidites—A new class of key intermediates for deoxypolynucleotide synthesis. *Tetrahedron Lett.* **1981,** *22* (20), 1859-1862.

63. Caruthers, M., Gene synthesis machines: DNA chemistry and its uses. *Science* **1985,** *230* (4723), 281-285.
64. Caruthers, M. H., Chemical synthesis of DNA and DNA analogs. *Acc. Chem. Res.* **1991,** *24* (9), 278-284.
65. Edelson, E. H.; Lawless, J. G., Ion-exchange separation of nucleic acid constituents by high-performance liquid chromatography. *Journal of Chromatography* **1979,** *174*, 409-419.
66. Hecker, K. H.; Rill, R. L., Error analysis of chemically synthesised polynucleotides. *Biotechniques* **1998,** *24*, 256-260.
67. Lee, J. S.; Woodsworth, M. L.; Latimer, L. J. P.; Morgan, A. R., Poly(pyrimidine) poly(purine) synthetic DNAs containing 5-methylcytosine form stable triplexes at neutral pH. **1984,** *12* (16), 6603-6614.
68. Cech, D.; Schliepe, J.; Berghoff, U.; Lippert, B., Automated Solid Phase Synthesis of Platinated Oligonucleotides via Nucleoside Phosphonates. *Angewandte Chemie International Edition in English* **1996,** *35* (6), 646-648.
69. Schmidt, K. S.; Filippov, D. V.; Meeuwenoord, N. J.; van der Marel, G. A.; van Boom, J. H.; Lippert, B.; Reedijk, J., Solid-Phase Synthesis of a Monofunctional trans-a2 Pt(II) Complex Tethered to a Single-Stranded Oligonucleotide. *Angew Chem Int Ed Engl* **2000,** *39* (2), 375-377.
70. Panattoni, A.; Pohl, R.; Hocek, M., Flexible Alkyne-Linked Thymidine Phosphoramidites and Triphosphates for Chemical or Polymerase Synthesis and Fast Postsynthetic DNA Functionalization through Copper-Catalyzed Alkyne-Azide 1,3-Dipolar Cycloaddition. *Org Lett* **2018,** *20* (13), 3962-3965.
71. Langer, P. R.; Waldrop, A. A.; Ward, D. C., Enzymatic synthesis of biotin-labeled polynucleotides: novel nucleic acid affinity probes. *Proc. Natl. Acad. Sci.* **1981,** *78* (11), 6633-7.
72. Latham, J. A.; Johnson, R.; Toole, J. J., The application of a modified nucleotide in aptamer selection: novel thrombin aptamers containing 5-(1-pentynyl)-2'-deoxyuridine. *Nucleic Acids Res* **1994,** *22* (14), 2817-22.
73. Sawai, H.; Ozaki, A. N.; Satoh, F.; Ohbayashi, T.; Masud, M. M.; Ozaki, H., Expansion of structural and functional diversities of DNA using new 5-substituted deoxyuridine derivatives by PCR with superthermophilic KOD Dash DNA polymerase. *Chem. Comm.* **2001,** (24), 2604-2605.
74. Sawai, H.; Nagashima, J.; Kuwahara, M.; Kitagata, R.; Tamura, T.; Matsui, I., Differences in substrate specificity of C5 substituted or C5 unsubstituted pyrimidine nucleotides by DNA polymerases from thermophilic bacteria archae and phages. *Chemistry and Biodiversity* **2007,** *4*, 1979-1995.
75. Held, H. A.; Benner, S. A., Challenging artificial genetic systems: thymidine analogs with 5-position sulfur functionality. *Nucleic Acids Res* **2002,** *30* (17), 3857-69.
76. Jager, S.; Rasched, G.; Kornreich-Leshem, H.; Engeser, M.; Thum, O.; Famulok, M., A versatile toolbox for variable DNA functionalization at high density. *J Am Chem Soc* **2005,** *127* (43), 15071-82.
77. Hocek, M.; Fojta, M., Cross-coupling reactions of nucleoside triphosphates followed by polymerase incorporation. Construction and applications of base-functionalized nucleic acids. *Org Biomol Chem* **2008,** *6* (13), 2233-41.
78. Mullis, K.; Faloona, F.; Scharf, S.; Saiki, R.; Horn, G.; Erlich, H., Specific enzymatic amplification of DNA in vitro: the polymerase chain reaction. *Cold Spring Harb Symp Quant Biol* **1986,** *51 Pt 1* (0), 263-73.

79. Carey, M. F.; Peterson, C. L.; Smale, S. T., The primer extension assay. *Cold Spring Harb Protoc* **2013,** *2013* (2), 164-73.
80. Brazdilova, P.; Vrabel, M.; Pohl, R.; Pivonkova, H.; Havran, L.; Hocek, M.; Fojta, M., Ferrocenylethynyl derivatives of nucleoside triphosphates: synthesis, incorporation, electrochemistry, and bioanalytical applications. *Chemistry* **2007,** *13* (34), 9527-33.
81. Menova, P.; Hocek, M., Preparation of short cytosine-modified oligonucleotides by nicking enzyme amplification reaction. *Chem Commun (Camb)* **2012,** *48* (55), 6921-3.
82. Menova, P.; Cahova, H.; Plucnara, M.; Havran, L.; Fojta, M.; Hocek, M., Polymerase synthesis of oligonucleotides containing a single chemically modified nucleobase for site-specific redox labelling. *Chem. Comm.* **2013,** *49* (41), 4652-4.
83. Hiatt, A. C.; Rose, F. Enzyme catalysed template-independent creation of hosphodiester bonds using protected nucelotides. 1998.
84. Michelson, A. M.; Orkin, S. H., Charachterisation of the homopolymer tailing reaction catalyzed by terminal deoxynucleotidyl transferase. *The Journal of Biological Chemistry* **1982,** *257* (25), 14773-14782.
85. Eisenstein, M., Enzymatic DNA synthesis enters new phase. *Nat. Biotech.* **2020,** *38* (10), 1113-1115.
86. Palluk, S.; Arlow, D. H.; De Rond, T.; Barthel, S.; Kang, J. S.; Bector, R.; Baghdassarian, H. M.; Truong, A. N.; Kim, P. W.; Singh, A. K.; Hillson, N. J.; Keasling, J. D., De novo DNA synthesis using polymerase-nucleotide conjugates. *Nat. Biotech.* **2018,** *36* (7), 645-650.

Chapter 2

Project Rationale

Antisense and antigene therapeutics are capable of recognising a nucleic acid sequence of interest and inhibiting protein production but they do not permanently alter the DNA/RNA sequence. By combining the sequence selectivity of an antigene therapeutic with a DNA damaging agent, such as a metallodrug, the gene can be irreversibly damaged and prevent DNA replication. Triplex forming oligonucleotides (TFOs) are antigene nucleic acids that bind directly to the DNA double helix, and form relatively stable triple helical structures.[1] TFOs have successfully been tethered to a variety of DNA damaging agents by both traditional conjugation methods,[2-6] and more recently through nucleic acid click chemistry.[7-10] The advent of click chemistry for the functionalisation of oligonucleotides[11] has allowed for the rejuvenation of antigene therapeutics, as molecules that are incompatible with the chemical synthesis of DNA can now be attached to oligonucleotides through a 'click' reaction. However, the solid-phase synthesis of oligonucleotides is an intricate process that requires specialised equipment, complex purification steps and produces hazardous waste. Therefore, in this project alternative enzymatic methods for the synthesis of modified oligonucleotides were devised and optimised. These protocols are a step towards the development of new technologies for the synthesis of modified DNA.

As the field of targeted metallodrug hybrids is in its infancy there are limited number of protocols available for the analysis of targeted DNA damage. Therefore the first objective of this project was the development of new protocols for the detection and quantification of sequence selective DNA damage. Polyacrylamide gel electrophoresis (PAGE) conditions that enable visualisation of triple helical DNA were identified and optimised to allow routine analysis of target and *off*-target DNA damage to be performed. Although gel electrophoresis was suitable for visualisation of the targeted DNA damage inflicted by metallo-drug-TFO hybrids, it did not accurately quantify the damage that had occurred. Therefore, a real-time quantitative PCR (qPCR) protocol that enabled quantification of the DNA damage inflicted upon target and *off*-target sequences was developed. A relative quantification method was selected as it allowed the concentration of intact DNA in a sample to be directly compared to that of a non-

treated control, and thereby the extent of DNA damage that has occurred could be calculated.

The second objective of this project was to develop an alternative enzymatic protocol for the synthesis of oligonucleotides bearing large modifications. This began with the production of a library of click-functionalised nucleotide triphosphates (dNTPs). Alkyne-functionalised dNTPs are commercially available, and through the CuAAC reaction they were conjugated to drug complexes, and fluorophores. These modified dNTPs were then ready to be incorporated into the oligonucleotide sequence by a DNA polymerase. The method of enzymatic synthesis chosen was an expansion of primer extension, thereby it was performed using instruments found in the majority of molecular biology laboratories, and alleviated the need for complicated purification protocols. The single nucleotide incorporation–primer extension (SNI-PEX)[12] method of enzymatic synthesis enables an oligonucleotide bearing a modification at only the desired sequence position to be synthesised. The oligonucleotide of interest was then isolated through a relatively simple streptavidin-biotin magneto-separation step. Thus, an oligonucleotide with a modification at a specific position was synthesised and purified from all reaction components without the need for specialised equipment, making the synthesis of modified single-stranded DNA more accessible.

The molecular methods for detecting targeted DNA damage and the SNI-PEX protocol reported were then combined for the synthesis and analysis of an artificial metallo-nuclease (AMN) TFO hybrid. The *di*-(2-picoyl)amine (DPA)-TFO was produced through nucleic acid click chemistry and SNI-PEX, and its activity was compared to its SPS and post-synthetic functionalised counterpart. This confirmed that SNI-PEX was a viable method for modified oligonucleotide synthesis.

Since the SNI-PEX protocol enables only one modified nucleotide to be incorporated into a DNA sequence, the potential of this method for producing heavily modified oligonucleotides is limited. Consequently, the final aim of this project was to expand the SNI-PEX protocol to enable multiple different modified bases to be incorporated at distinct positions in the oligonucleotide sequence. This novel protocol, named multiple nucleotide incorporation–primer extension

(MNI-PEX), enables both a DNA damaging metallo-drug and a TFO stabilising agent, such as a DNA intercalator, to be enzymatically incorporated at specific positions in the TFO sequence. MNI-PEX therefore has the potential to extend enzymatic synthesis and increase the accessibility of modified oligonucleotides.

References

1. Helene, C., Control of gene expression by triplex-forming-oligonucleotides. The antigene strategy. *Anticancer Drug Des* **1991,** *6* (6), 569-84.
2. Dreyer, G. B.; Dervan, P. B., Sequence-specific cleavage of single-stranded DNA: oligodeoxynucleotide-EDTA X Fe(II). *Proc. Natl. Acad. Sci.* **1985,** *82* (4), 968-972.
3. Chen, C. H.; Sigman, D. S., Nuclease activity of 1,10-phenanthroline-copper: sequence-specific targeting. **1986,** *83* (19), 7147-7151.
4. Francois, J. C.; Saison-Behmoaras, T.; Helene, C., Sequence-specific recognition of the major groove of DNA by oligodeoxynucleotides via triple helix formation. Footprinting studies. *Nucleic Acids Res* **1988,** *16* (24), 11431-40.
5. Francois, J. C.; Saison-Behmoaras, T.; Barbier, C.; Chassignol, M.; Thuong, N. T.; Helene, C., Sequence-specific recognition and cleavage of duplex DNA via triple-helix formation by oligonucleotides covalently linked to a phenanthroline-copper chelate. *Proc. Natl. Acad. Sci.* **1989,** *86* (24), 9702-9706.
6. Graham, M. K.; Miller, P. S., Inhibition of transcription by platinated triplex-forming oligonucleotides. *J Biol Inorg Chem* **2012,** *17* (8), 1197-208.
7. Lauria, T.; Slator, C.; McKee, V.; Müller, M.; Stazzoni, S.; Crisp, A. L.; Carell, T.; Kellett, A., A Click Chemistry Approach to Developing Molecularly Targeted DNA Scissors. *Chem. Eur. J.* **2020**.
8. Panattoni, A.; El-Sagheer, A. H.; Brown, T.; Kellett, A.; Hocek, M., Oxidative DNA Cleavage with Clip-Phenanthroline Triplex-Forming Oligonucleotide Hybrids. *ChemBioChem* **2020,** *21* (7), 991-1000.
9. Zuin Fantoni, N.; McGorman, B.; Molphy, Z.; Singleton, D.; Walsh, S.; El-Sagheer, A. H.; McKee, V.; Brown, T.; Kellett, A., Development of Gene-Targeted Polypyridyl Triplex-Forming Oligonucleotide Hybrids. *Chembiochem* **2020,** *21*, 3563-3574.
10. Hennessy, J.; McGorman, B.; Molphy, Z.; Farrell, N. P.; Singleton, D.; Brown, T.; Kellett, A., A Click Chemistry Approach to Targeted DNA Crosslinking with cis-Platinum(II) Modified Triplex Forming Oligonucleotides. *Angew. Chem. Int. Ed.* **2021,** *60*.
11. Gierlich, J.; Burley, G.; Gramlich, P. M.; Hammond, D. M.; Carell, T., Click chemistry as a reliable method for the high density functionalisation of alkyne modified DNA. *Organic Letters* **2006,** *8* (17), 3639-3642.
12. Menova, P.; Cahova, H.; Plucnara, M.; Havran, L.; Fojta, M.; Hocek, M., Polymerase synthesis of oligonucleotides containing a single chemically modified nucleobase for site-specific redox labelling. *Chem. Comm.* **2013,** *49* (41), 4652-4.

Chapter 3

Molecular methods for the analysis of gene-targeted metallodrug-hybrids

3.1 Molecular methods

The analysis of metallodrugs and their ability to bind with DNA is not a new phenomenon, and there are many molecular methods available for the analysis of non-covalent drug-DNA interactions. These include absorbance and fluorescence techniques, such as thermal melting, circular dichroism and competitive displacement assays, as well as electrophoretic methods and amplification inhibition assays.[1, 2] However, the techniques available for the study of metallodrug-oligonucleotide hybrids is limited,[3-8] with no previous reports of the analysis of target specific DNA damage. Consequently, there is a need to develop a range of molecular methods for the analysis of sequence selective DNA binding, and the damage inflicted by target therapeutics. Within this chapter polyacrylamide gel electrophoresis, fluorescent thermal melting and real-time quantitative PCR assays will be developed for the identification and analysis of target specific metallodrug-hybrids.

3.1.1 Gel electrophoresis

Gel electrophoresis is a molecular biology technique for the analysis of nucleic acids (and proteins). There are two main types of gel electrophoresis; horizontal agarose gel electrophoresis and vertical polyacrylamide gel electrophoresis (PAGE), but both forms operate under the same principle. A DNA sample is loaded onto the gel and is pulled through the porous gel matrix by an electrical current, due to its inherent negative charge DNA moves from the cathode towards the anode (**Figure 8**). The higher the molecular weight of the DNA fragment the slower it will move through the gel, thereby separating DNA fragments by size. Agarose gels are typically used for the visualisation of long DNA sequences (>100 bp) whereas PAGE is employed for short DNA fragments and can be optimised to enable visualisation of single nucleotide differences in sequence length (**Figure 8**).

Gel electrophoresis can also be employed to study the DNA binding properties of a compound of interest. When a drug compound binds to DNA the total molecular weight of the complex increases and thereby the migration of DNA in a gel matrix will be altered. This electrophoretic mobility shift assay (EMSA)[9,

[10] is therefore a relatively simple method to determine if a compound of interest binds to DNA. The principle behind EMSA can be used to visualise triple helical DNA; when a TFO binds to dsDNA the molecular weight of the complex increases and thus the triplex will migrate slower through the gel. However as non-modified pyrimidine TFOs require a slightly acidic pH to form triplexes, the gel conditions for this EMSA type assay deviate from standard PAGE conditions.

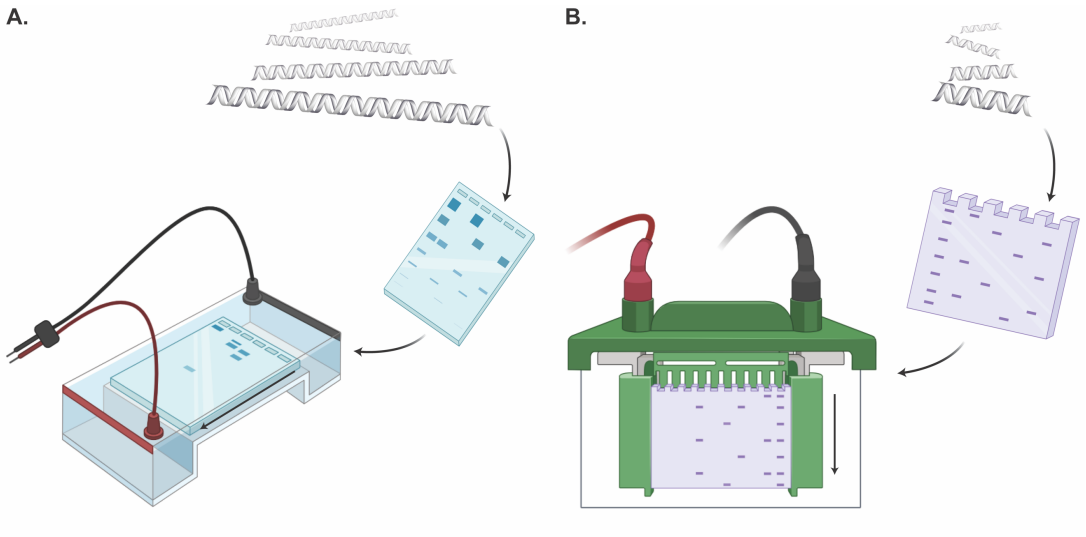


Figure 8: Gel electrophoresis systems where the negatively charged DNA moves from the cathode (black) towards the anode (red). **A.** Agarose gel electrophoresis is run in horizontal tanks and is typically used for the analysis of long DNA fragments. **B.** Polyacrylamide gel electrophoresis (PAGE) runs vertically, and can separate short DNA fragments based on their molecular weight. Figure was produced using BioRender graphics.

3.1.2 Thermal Melting

The melting temperature of a DNA sample corresponds to the equilibrium temperature at which half the DNA is helical and half is single stranded.[1, 11] Thermal melting (T_M) can be determined through absorbance or fluorescence spectroscopy. Nucleic acids display their highest absorbance at 260 nm, which increases as DNA is denatured to its single strands.[11] Therefore, the T_M of double, or triple, helical DNA can be determined by monitoring the absorbance at 260 nm. Fluorescence melting is an alternative method that relies on fluorophores for detection. The fluorophores used can be DNA binding dyes, such

as SYBR green, or FRET (fluorescence resonance energy transfer) probes. SYBR green I is a sequence independent fluorescent dye that binds to duplex, triplex and quadruplex DNA,[12, 13] but is released when DNA is denatured to single strands. Therefore, SYBR green fluorescence can be measured to determine the T_M of a DNA complex.[12] FRET probes can also be used to monitor the T_M of DNA. Labelling a DNA structure of interest with donor and acceptor fluorophores allows a change in fluorescence to be detected as the DNA is denatured. When the DNA is complexed, emission from the acceptor fluorophore is detected, but as it melts the acceptor fluorescence decreases and the donor fluorescence increases. This continues until all the DNA is single stranded and only the donor fluorescence can be detected.

Absorbance and fluorescence T_M both have their advantages. Absorbance measurements are performed with a UV spectrophotometer and do not require any additives to be included with the DNA sample. However, absorbance T_M typically requires large volumes of DNA (0.1 mL), and melting experiments are performed over a long time period (12-90 °C, 0.5 °C/min, 2 min hold). Fluorescence measurements require a fluorophore, but typically lower concentrations of DNA are needed for accurate detection. Fluorescence T_M can be performed using a fluorescence spectrophotometer or a real-time PCR apparatus, which is advantageous as the T_M of 96 (or 384) samples can be monitored simultaneously. Fluorescence T_M is typically performed in 20 μL with measurements between 20 and 99 °C being recorded in under 30 minutes. This combined with the multi-well format of real-time PCR instruments, enables the rapid analysis of a large number of samples. The T_M of triple helical DNA can be determined using absorbance or fluorescence measurements, and typically a biphasic melting profile is recorded (**Figure 9**).

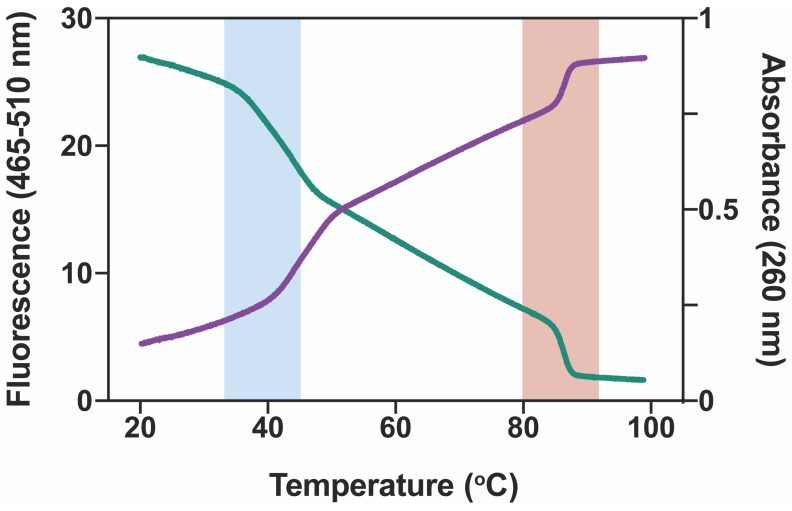


Figure 9: Example of data collected from absorbance and fluorescence T_M of triplex DNA. The fluorescence signal (green) decreases as the DNA melts. Conversely, the absorbance signal (purple) increases as the concentration of single-stranded DNA rises. The triplex and duplex melt are highlighted in blue and red, respectively.

3.1.3 Real-time quantitative PCR

PCR employs a thermostable DNA polymerase to exponentially amplify a DNA sequence of interest, which enables small quantities of DNA to be amplified to concentrations that can be more easily studied.[14] Real-time PCR or quantitative PCR (qPCR) is a variation on this amplification process in which the concentration of DNA is monitored after each cycle, through the use of a fluorescent reporter. The fluorescent signal detected is directly proportional to the number of PCR amplicons generated. The fluorescent reporters used are typically either dsDNA-binding dyes, such as SYBR green, or dyes attached to PCR probes that hybridise with a specific sequence, such as 5′ hydrolysis probes (*e.g.* TaqMan probes).

SYBR green I is a non-specific fluorescent dye whose fluorescence increases by 20 to 100-fold upon binding to dsDNA, thereby as the concentration of dsDNA increases during PCR the fluorescent signal increases correspondingly (**Figure 10A**). The TaqMan assay is sequence specific and relies on the 5′-3′ exonuclease activity of *Taq* DNA polymerase. TaqMan probe strands are a short oligonucleotides with a 5′ fluorescent reporter dye and a 3′ quencher dye. The

reporter and quencher dyes must be a FRET (fluorescence resonance energy transfer) pair so that light emitted by the reporter is absorbed by the quencher. Therefore, no fluorescent signal is observed when the probe strand is intact. However, during PCR *Taq* DNA polymerase hydrolyses the probe, separating the reporter and quencher, enabling the fluorescent signal of the reporter to be detected (**Figure 10B**). The fluorescent signal observed is proportional to the amount of PCR products present in the sample, and therefore enables quantification of a specific dsDNA sequence.

qPCR has also been employed for the detection and quantification of an RNA sequence of interest. Reverse-transcription qPCR (RT-qPCR) begins with RNA-dependent DNA polymerase, known as reverse transcriptase, transcribing the RNA sequence into double-stranded complementary DNA (cDNA).[15] This cDNA can then partake in normal cycles of PCR, with SYBR green or TaqMan detection.

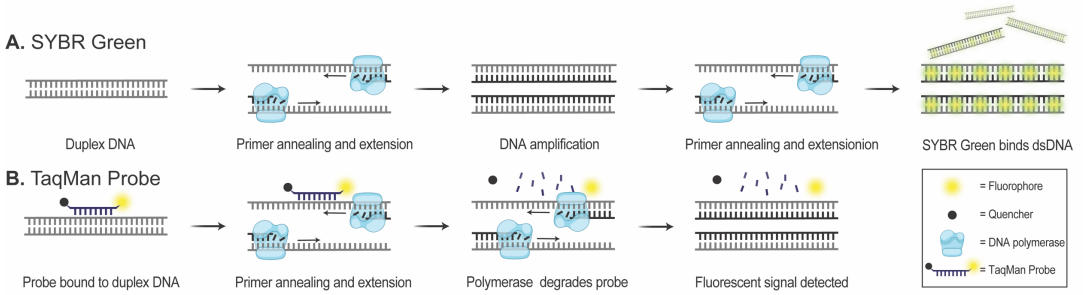


Figure 10: A. SYBR green I is a non-specific fluorescent dye that binds to dsDNA. The fluorescence signal emitted is quantified during qPCR. **B.** TaqMan probes are short sequences of ssDNA that bind to a specific DNA sequence. When the probe is intact the quencher is in close proximity to the fluorophore and no fluorescence is detected. During PCR *Taq* DNA polymerase degrades the probe strand enabling the fluorescent signal to be quantified.

qPCR reactions are typically characterised by the PCR cycle where the target amplification is first detected, this is referred to as the threshold cycle (C_T). The C_T occurs when the target fluorescence signal is significantly different from the baseline signal for that reaction, usually this is when the fluorescent signal reaches 10 times the standard deviation of the baseline fluorescence.[16] The

numerical C_T value is inversely related to the concentration of DNA in the sample, thereby the lower the C_T value the higher the initial amount of DNA.[17]

PCR has been used to analyse drug-DNA interactions for many decades, with early research from Hartley *et al.*[18, 19] paving the way for the current real-time qPCR assays. The ability of qPCR to detect and analyse minute concentrations of DNA and RNA, has made it is an indispensable tool for research, forensic and clinical analysis of nucleic concentration, DNA integrity analysis, diagnostics, and for the determination of patient drug responses.[20-29] A sophisticated high throughput assay, termed 'qPCR-Block' was reported by van Kan *et al*.[26] for the quantification of melphalan-induced DNA damage in peripheral blood mononuclear cells.[26] This assay is used to determine a patients' response to an alkylating therapeutic (*e.g.* melphalan, cisplatin or carboplatin) prior to administration of the treatment. PCR amplification of the *p*53 gene, which is mutated in 50% of human malignancies,[30] was found to be inversely proportional to the treatment concentration of the anticancer drugs being examined. Therefore this assay can determine which patients will respond to a particular alkylating cancer therapeutic.[24, 26] qPCR has also been used to analyse the DNA damage that occurs under a variety of CuAAC click chemistry conditions.[29] This study showed that qPCR can be employed to detect oxidative lesions, as the DNA polymerase cannot read-through this damaged site and therefore amplification does not occur.[29]

A qPCR protocol based on this principle—that a DNA polymerase cannot bypass DNA lesions—will be developed for the analysis of the DNA damage inflicted by the metallodrug-TFO hybrids that have been synthesised. The development of this qPCR protocol will enable the DNA damage resulting from incubation with the hybrids to be quantified, and the sequence specificity of the metallodrug-TFOs to be determined.

3.2 Polyacrylamide gel electrophoresis for the analysis of sequence specific damage

3.2.1 PAGE triplex analysis

In gel electrophoresis the most commonly used buffers are TBE (Tris-Borate-EDTA) pH 8.3, and TAE (Tris-Acetate-EDTA) pH 8.3, with TBE often employed for polyacrylamide gel electrophoresis. However, basic pH is not suitable for the visualisation of triple helical DNA and EDTA, a sequestering agent, present in TBE may interact with the copper of the AMN-TFO hybrids. Therefore, alternative buffers such as HEPES and MOPS were investigated before Tris-acetate buffer at pH 6.1 was identified. Tris-acetate was chosen as the pH could easily be reduced to ~pH 6 through the addition of a small concentration of acetic acid. This slightly acidic buffer aided with stabilisation of triple helical DNA, but the presence of NaCl and $MgCl_2$ salts have a greater impact on triplex stability. Various concentrations of these salts were tested: NaCl (0 – 200 mM) and $MgCl_2$ (0-5 mM). The addition of $MgCl_2$ (5 mM) to the gel mixture helped to stabilise the triplex but it resulted in curved bands and a 'frowning' effect. The presence of NaCl did not negatively impact how the gel ran but it was not as efficient at stabilising the triple helix. Therefore, multiple combinations of $MgCl_2$ and NaCl were tested (**Figure 11**). It was found that when the NaCl concentration was high (150 mM), the $MgCl_2$ could not effectively stabilise the triplex, thus the NaCl concentration needed to be reduced, while the $MgCl_2$ concentration was varied between 2 mM and 5 mM. The most suitable buffer conditions were found to be 50 mM Tris-acetate, pH 6.1, with 75 mM NaCl and 5 mM $MgCl_2$.

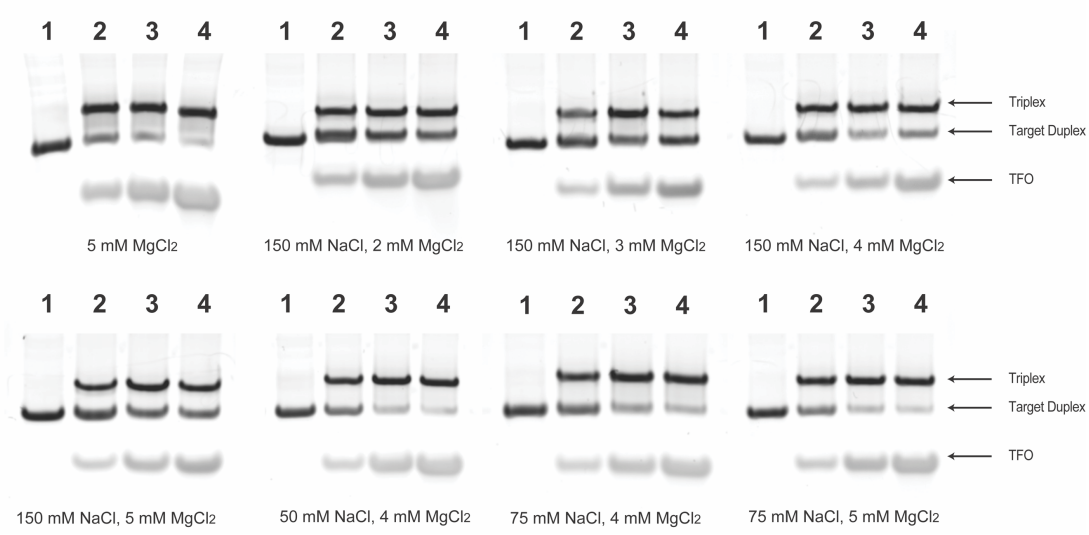


Figure 11: Optimisation of native Tris-acetate (50 mM) PAGE with NaCl (0-150 mM) and $MgCl_2$ (2-5 mM). Lane 1: Target duplex (57 bp). Lane 2-4: Triplex with 10, 25 and 50 equivalents of TFO (32 nt) to duplex respectively. The running position of TFO and target duplex was known due to the presence of TFO and target dsDNA controls (appendix **Figure A - 1**).

Once the conditions for triplex visualisation were optimised it was important to ensure the TFO would only bind to the correct duplex target. Various equivalents of TFO were incubated with 'target' and '*off*-target' dsDNA (*i.e.* GFP sequence containing the TFO recognition sequence, and a sequence from pUC19 lacking the TFO binding site, respectively, see section 3.6.2). The samples were then analysed by PAGE and it was observed that the TFO only formed a triplex with its GFP target, while the pUC19 *off*-target duplex did not show any mobility shift in the gel matrix (**Figure 12**). Therefore these conditions are suitable for visualisation of a TFO hybridising to its target sequence and should also be suitable for analysis of target and *off*-target DNA damage.

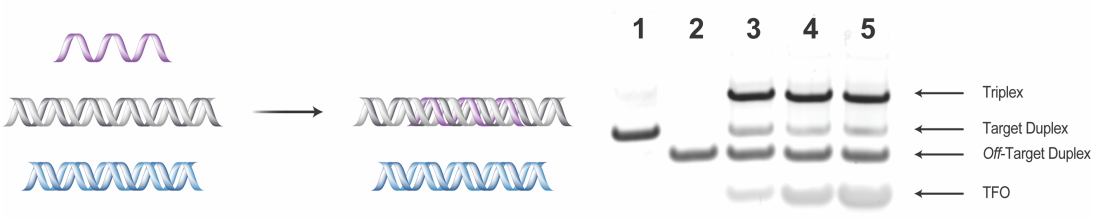


Figure 12: Target (grey) and *off*-target (blue) duplexes incubated with 25 equivalents of TFO were analysed by Tris-acetate PAGE (20%). Lane 1: 57 bp target duplex. Lane 2: 40 bp *off*-target duplex. Lanes 3-5: Triplex with 10, 25 and 50 equivalents of TFO to duplex.

3.2.2 PAGE analysis of AMN-TFO hybrids

3.2.2.1 TPMA-TFO hybrids

In collaboration with group member Dr Nicolò Zuin Fantoni (NZF), the sequence selectivity and DNA damaging capabilities of a family of artificial metallo-nuclease (AMN) TFO hybrids was analysed. *Tris*-(2-pyridylmethyl)amine (TPMA)[31] was the AMN selected for this study as it was shown to be capable of stabilising the copper centre, and binding with DNA.[31] In this work, two TPMA derivatives with azide modifications were synthesised by NZF—$5N_3$-TPMA (I) and $6N_3$-TPMA (II) (**Figure 15**)—and they were attached to alkyne-modified TFOs through a copper-catalysed azide-alkyne cycloaddition (CuAAC). TPMA-TFO(I) and TPMA-TFO(II) were produced with $5N_3$-TPMA and $6N_3$-TPMA, respectively. PAGE analysis was performed, using the conditions developed above, to determine the ability of these TPMA-TFO hybrids to bind with and damage a DNA sequence of interest. Each TPMA-TFO was incubated with $Cu(ClO_4)_2$, to allow copper coordinate with the TPMA ligand. The Cu-TPMA-TFO was then incubated with target and *off*-target DNA duplexes in the presence of increasing concentrations of Na-*L*-ascorbate at 37 °C for 6 hours. The resulting DNA damage was visualised by PAGE (TPMA-TFO(I); **Figure 13**. TPMA-TFO(II); appendix **Figure A - 2**). It was shown that the TPMA-TFO hybrids could discriminate between the target and *off*-target sequences with significant differences in DNA damage observed (72% versus 24%, for the target and *off*-target, respectively, at 25 equivalents TPMA-TFO(I):Duplex and 100 equivalents of Na-*L*-ascorbate:TFO).

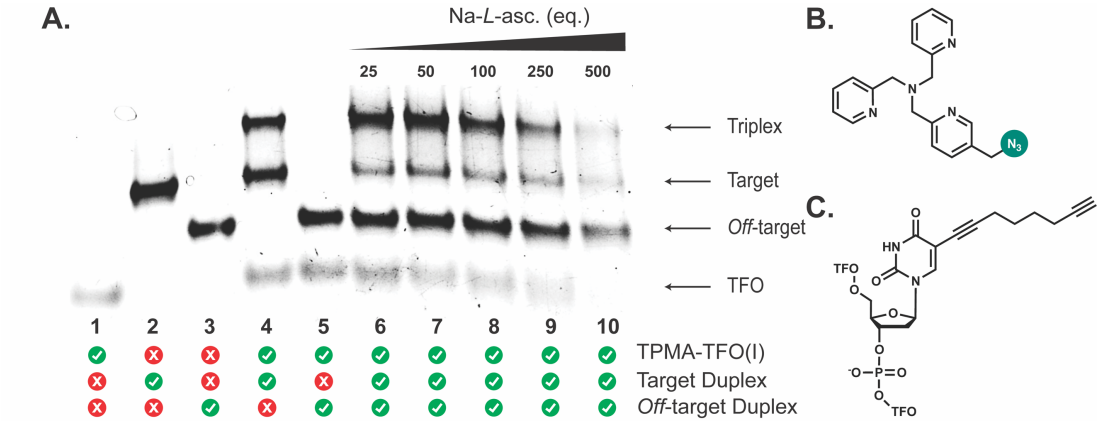


Figure 13: A. 20% native PAGE analysis of TPMA-TFO(I) incubated with target and *off*-target DNA duplexes in the presence of increasing concentrations of Na-*L*-ascorbate (25-500 equivalents to TFO). Lane 1: TPMA-TFO(I). Lane 2: Target duplex (57 bp). Lane 3: *Off*-target duplex (40 bp). Lane 4: TPMA-TFO(I) forming triple helical DNA with target duplex. Lane 5: TFO does not hybridise with *off*-target duplex. Lanes 6-10: TPMA-TFO(I) incubated with target and *off*-target duplexes and increasing concentrations of Na-*L*-ascorbate (25-500 eq.). **B.** $5N_3$-TPMA. **C.** Octadiynyl-dU modification included in TFO sequence.

To ensure this sequence specific damage was due to the TPMA-TFO hybrids, free Cu-TPMA and free alkyne-modified TFO were incubated with target and *off*-target duplexes in the presence of increasing equivalents of reductant, and the products were analysed by native PAGE (**Figure 14**). No significant DNA damage was observed on either the target or *off*-target sequence (**Figure 14**). Upon comparison of the damage inflicted by the TPMA-TFO hybrid (**Figure 13**) and free Cu-TPMA (**Figure 14**) it was noted that in addition to sequence selectivity, the TPMA-TFO hybrids demonstrated higher DNA damaging propensity compared to the free nuclease. This shows that attachment of an AMN to a TFO delivery vector increases the nuclease activity. This method formed a fundamental part of the analysis of this class of TFO hybrid and was published in ChemBioChem.[32]

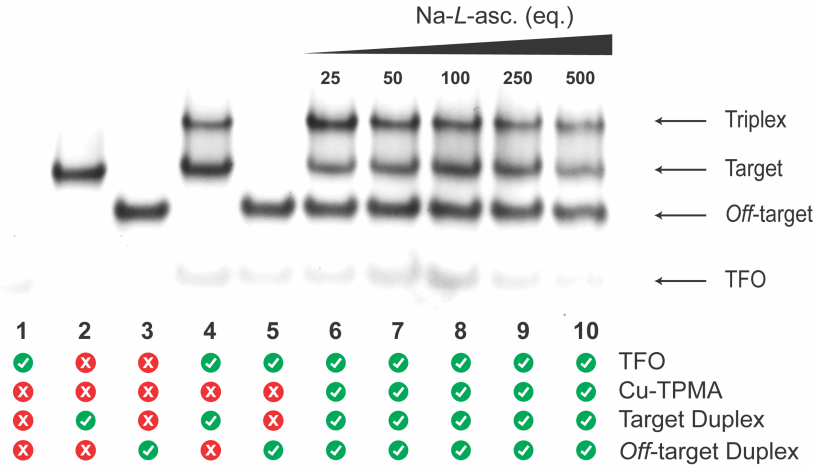


Figure 14: DNA damage resulting from incubation with free Cu-TPMA and free TFO was analysed by 20% native PAGE. Lane 1: Alkyne TFO. Lane 2: Target duplex (57 bp). Lane 3: *Off*-target duplex (40 bp). Lane 4: TFO incubated with target duplex, and triplex DNA can be visualised. Lane 5: TFO does not hybridise with *off*-target duplex. Lanes 6-10: Cu-TPMA and alkyne-TFO incubated with target and *off*-target duplexes and increasing concentrations of Na-*L*-ascorbate (25-500 eq.).

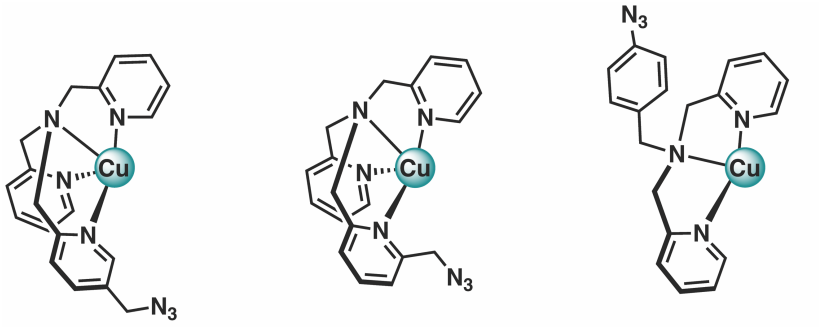


Figure 15: Structure of Cu(5N_3-TPMA),[32] Cu(6N_3-TPMA)[32] and Cu(4N_3-benzyl-DPA)[33,34]. 5N_3-TPMA and 6N_3-TPMA have three pyridyl groups, they differ only in the position of the azide group. 4N_3-benzyl-DPA is a less sterically hindered caging ligand and contains two pyridyl groups[33].

3.2.2.2 DPA-TFO hybrids

A second generation of AMN-TFO hybrid was also studied. It was found that *di*-(2-picoyl)amine (DPA)[33] is a less sterically hindered copper caging ligand with higher DNA binding affinity than TPMA.[33] Therefore, there was interest in developing second generation DPA-TFO hybrids. 4N_3-benzyl-DPA (**Figure 15**) was synthesised by NZF and 'clicked' to an internally modified octadiynyl-dU

modified TFO. The ability of this DPA-TFO to hybridise with and cleave a target DNA sequence was investigated. The DPA-TFO was incubated with $Cu(ClO_4)_2$ to allow Cu(II) coordinate with the DPA ligand. The Cu(II)-DPA-TFO hybrid was then incubated with target and *off*-target duplexes and Na-*L*-ascorbate at 37 °C for 15 hours, and the products were analysed by PAGE (**Figure 16**). Similar to the TPMA-TFO hybrids, the DPA-TFO was capable of recognising its dsDNA target and inflicting DNA cleavage. However, in this work, the DPA-TFO required a longer period of incubation compared with its TPMA counterpart—15 versus 6 hours. This is unsurprising as when the DNA cleavage abilities of the free Cu-bound ligands were tested,[31, 33] lower concentrations of TPMA were required to inflict DNA damage on pUC19 plasmid DNA. Studies involving DPA-TFO hybrids have been expanded upon in Chapter 5.[34]

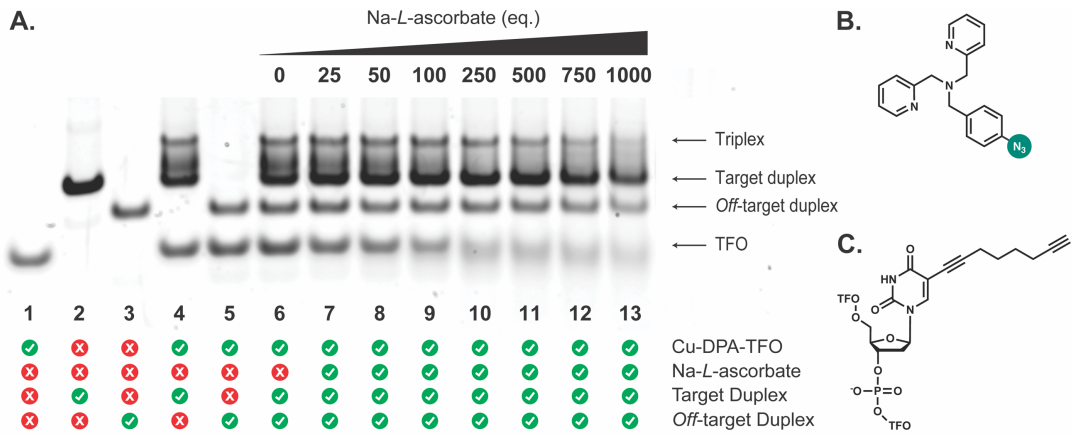


Figure 16: A. Tris-acetate native PAGE (20%) analysis of damage inflicted by DPA-TFO hybrid. Lane 1: DPA-TFO. Lane 2: Target duplex (57 bp). Lane 3: *Off*-target duplex (40 bp). Lane 4: Triple helical DNA forms when DPA-TFO is incubated with target duplex. Lane 5: TFO does not hybridise with *off*-target duplex. Lanes 6-13: Cu-DPA-TFO incubated with target and *off*-target duplex and increasing concentrations of Na-*L*-ascorbate. **B.** $4N_3$-benzyl-DPA. **C.** Internal octadiynyl-dU modification.

To confirm the DPA-TFO hybrid was responsible for the sequence specific cleavage, free Cu-DPA and free TFO were incubated with target duplex, *off*-target duplex, and Na-*L*-ascorbate. The resulting DNA damage was visualised by PAGE (**Figure 17**). No significant damage was inflicted upon either dsDNA

sequence, thereby confirming that the DPA-TFO hybrid is responsible for the targeted DNA damage.

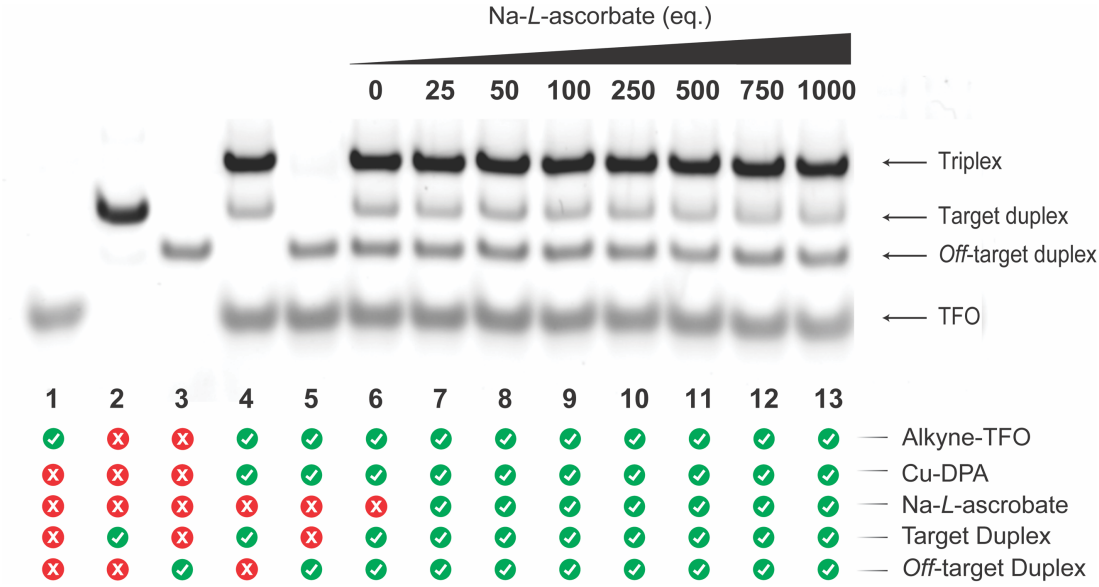


Figure 17: Analysis of the cleavage profile of free Cu-DPA and free TFO. Lane 1: Alkyne-TFO. Lane 2: 57 bp target duplex. Lane 3: 40 bp *off*-target duplex. Lane 4: Alkyne-TFO and target duplex hybridise to form triple helical DNA. Lane 5: TFO does not bind with *off*-target duplex. Lanes 6-13: Free Cu-DPA and alkyne-TFO incubated with target and *off*-target dsDNA in the presence of increasing concentrations of Na-*L*-ascorbate (0-1000 eq.).

3.2.2.3 Mechanistic studies for DPA-TFO hybrids

Studies with reactive oxygen species (ROS) scavengers were performed to investigate the mechanism of action of the Cu-DPA-TFO hybrid. Each scavenger captures a specific ROS and thereby prevents it from partaking in the DNA damage mechanism. Cu-DPA-TFO was incubated with target duplex and Na-*L*-ascorbate and a ROS scavenger—L-histidine (singlet oxygen; $^1O_2$), D-mannitol (hydroxyl radical, $^{\bullet}OH$), L-methionine (hydroxyl radical; OH, hypochlorous acid; HOCl, and hydrogen peroxide; H_2O_2) or tiron (superoxide; $O_2^{\bullet-}$)[1]—and the resulting DNA cleavage was analysed by PAGE. Tiron completely inhibited DNA damage, which indicates that cleavage primarily occurs through a superoxide mediated pathway (**Figure 18**). Incubation with L-histidine and L-methionine resulted in low levels of cleavage inhibition (**Figure 18**), and it was observed that D-mannitol has no impact (**Figure 18**). This method revealed that $^1O_2$, H_2O_2 and HOCl contribute only a minor role in the cleavage pathway.

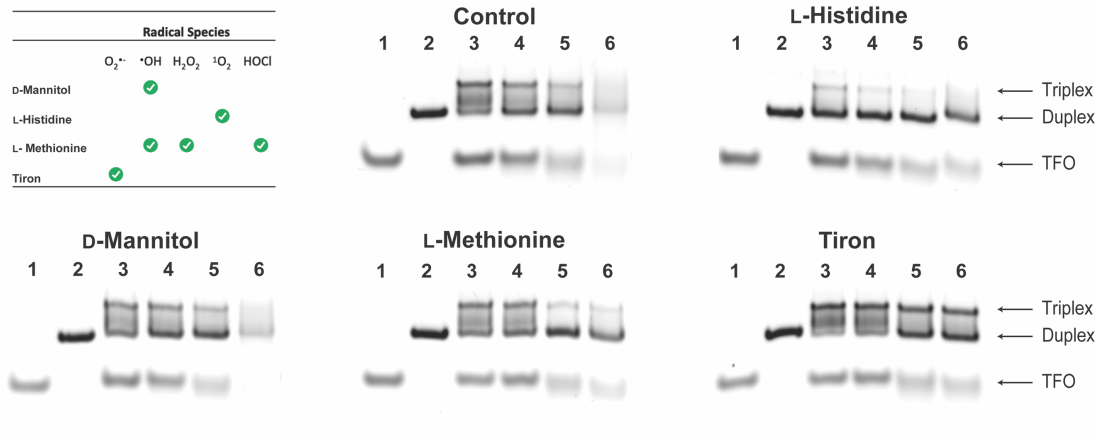


Figure 18: 20% native PAGE showing the impact of ROS scavengers on the activity of the Cu-DPA-TFO hybrid. Lane 1: DPA-TFO. Lane 2: Target duplex. Lanes 3-6: Cu-DPA-TFO with target duplex and 0, 50, 500 and 2000 equivalents of Na-*L*-ascorbate, respectively. Control contains no ROS scavenger.

3.2.3 PAGE analysis of Pt(II)-TFO hybrids

Although PAGE methods were successfully designed to identify Cu(II)-TFO interactions, it was of interest to extend this methodology to crosslinking hybrid systems. As such, PAGE analysis was performed on *cis*-platinum(II)-TFO hybrids (**Figure 19**), synthesised by group member Joseph Hennessy. These hybrids contain cisplatin, carboplatin, and oxaliplatin chemotypes and were generated using nucleic acid click chemistry methodology. These Pt(II)-TFOs form triple helical structures, which directs the Pt(II)-crosslinks to the desired DNA sequence. The Tris-acetate PAGE conditions identified were also suitable for the analysis of the sequence specificity of Pt(II)-TFO hybrids. Target and *off*-target duplexes (1 pmol) were incubated with cisplatin-, carboplatin-, and oxaliplatin-TFO hybrids (2.5 to 50 equivalents) at 37 °C for 2, 24 and 48 hours. The intensity of the triplex band increased at the longer incubation times (**Figure 19**, appendix **Figure A - 3, Figure A - 4, Figure A - 5**), which suggests the presence of Pt(II)-crosslinks. This was confirmed through the addition of sodium cyanide to the triplex samples followed by PAGE analysis to investigate if the triplex intensity has reverted. The results from this method were recently published in Angewandte Chemie.[35]

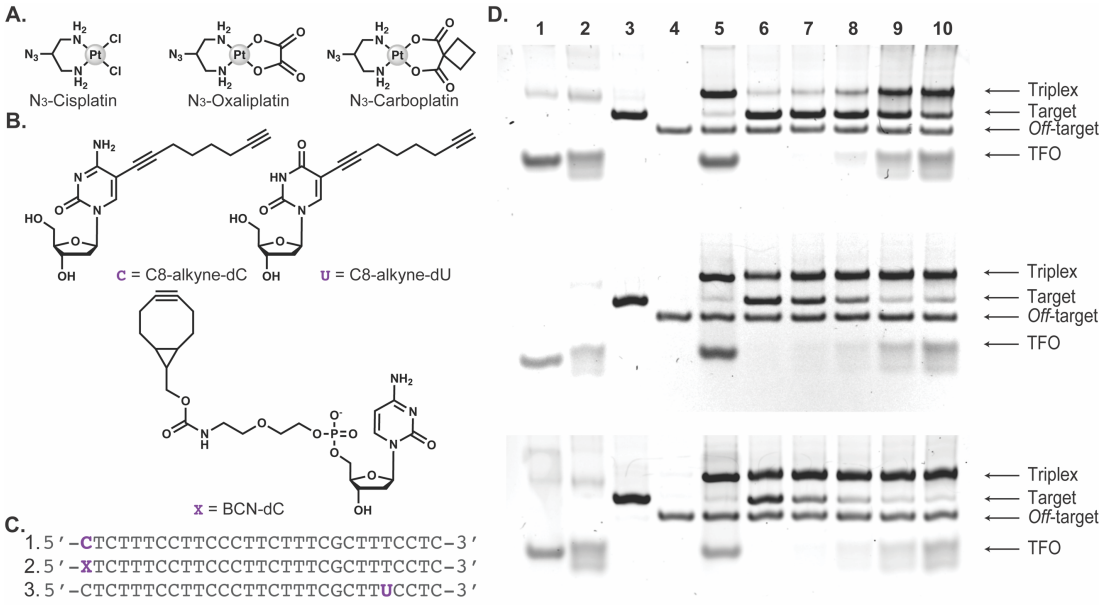


Figure 19: A. Azido-platinum complexes that were clicked to TFOs. **B.** Alkyne base and phosphate modifications included in the TFO sequences. **C.** TFO sequence showing the position of the modified base (purple). **D.** PAGE analysis of carboplatin-TFO2 incubated with target and *off*-target duplexes at 37 ºC for 2 hours (top), 24 hours (middle) and 48 hours (bottom). Lane 1: Alkyne TFO. Lane 2: Carboplatin-TFO. Lane 3: Target duplex. Lane 4: *Off*-target duplex. Lane 5: 50 equivalents of alkyne TFO with target and *off*-target duplexes, triplex has formed. Lanes 6-10: 2.5, 5, 10, 15 and 50 equivalents of carboplatin-TFO with target and *off*-target duplexes, intensity of the triplex band increases as incubation time increases, which suggests that platinum has crosslinked with the target duplex thereby stabilising the triplex.

3.2.4 PAGE analysis for three way junction binding helicates

In collaboration with Prof. Miguel Vázquez López of the Universidade de Santiago de Compostela, Spain, PAGE analysis for the binding of a Cu(II)-LLD helicate to DNA three way junctions (3WJs) was performed. 3WJs consist of three DNA strands that are partially complementary to each other. There are both RNA and DNA 3WJs. In RNA, 3WJs are involved in biological functions, such as splicing and translation, while DNA 3WJs are formed transiently during DNA replication (replication fork).[36] The Vázquez López group have synthesised novel artificial peptide ligands, that fold into chiral and discrete supramolecular helicates in the presence of labile metal ions such as Cu(II), Fe(II) and Co(II),[37] and these can selectively bind with DNA 3WJs. Conditions similar to that used for the analysis of triplex formation (*i.e.* Tris-acetate PAGE at pH 6.1) were suitable for the 3WJ. These PAGE conditions enabled visualisation of the 3WJ in the absence of

helicate, and the DNA damage that the Cu-helicate inflicts in the presence of Na-*L*-ascorbate (**Figure 20**). It was observed that the Cu-LLD helicate was capable of discriminating between a DNA 3WJ and a dsDNA control.

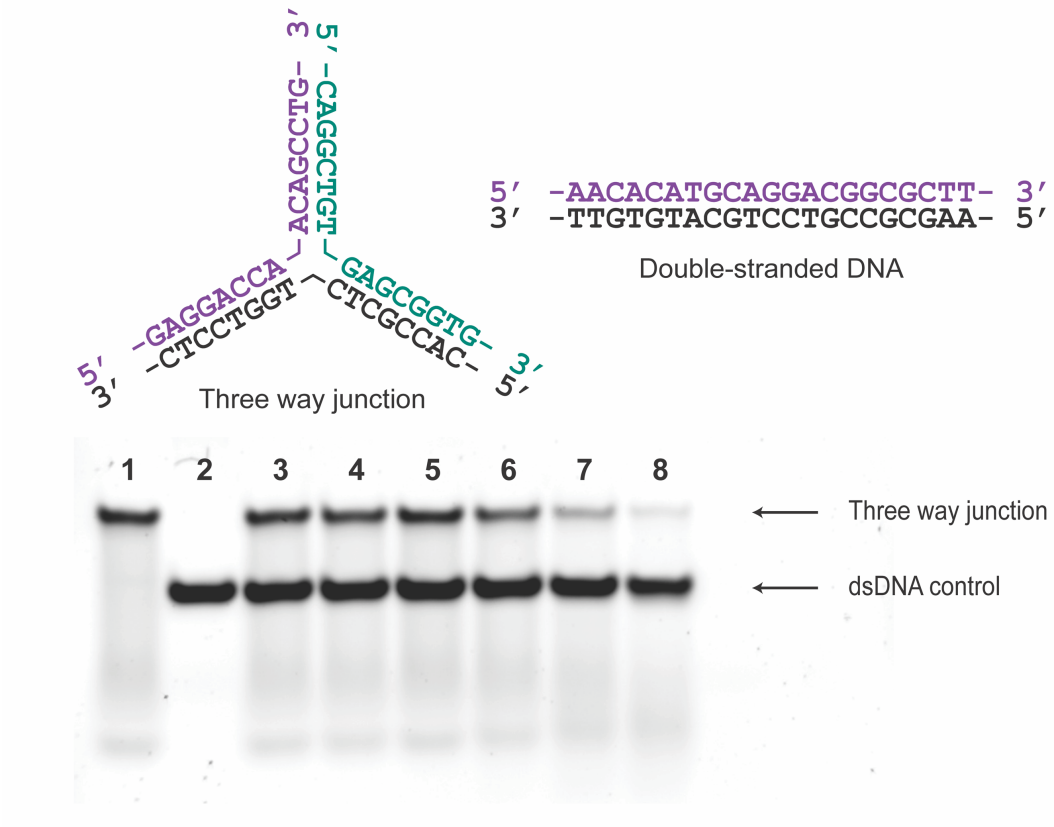


Figure 20: Preliminary PAGE analysis of Cu(II)-LLD helicate in the presence of the 3WJ and a dsDNA control. Lane 1: 3WJ. Lane 2: dsDNA control. Lane 3: 3WJ and dsDNA with LLD, no Cu, no Na-*L*-ascorbate. Lane 4: 3WJ and dsDNA with LLD, no Na-*L*-ascorbate. Lanes 5 – 8: 3WJ and dsDNA with 1, 2.5, 5 and 10 equivalents Cu(II)-LLD helicate, respectively, and 10 equivalents Na-*L*-ascorbate (*i.e.* Lane 7 = 1:5:50, 3WJ:Helicate:Na-*L*-ascorbate). The Cu(II)-LLD helicate selectively binds to the 3WJ and oxidative cleavage occurs.

The mechanism of action for the Cu-LLD helicate was then determined using ROS scavengers. Here, 3WJ DNA was incubated with the Cu(II)-LLD helicate, Na-*L*-ascorbate and a ROS scavenger (L-histidine, D-mannitol, L-methionine or tiron) at 37 °C for 24 hours. The resulting 3WJ cleavage profile was visualised by PAGE (**Figure 21**). The presence of tiron and L-histidine significantly impacted the activity of the helicate, indicating that superoxide ($O_2^{\bullet-}$)

and singlet oxygen ($^1O_2$) play the largest role in Cu-LLD-helicate DNA cleavage. A publication containing this method is in preparation.

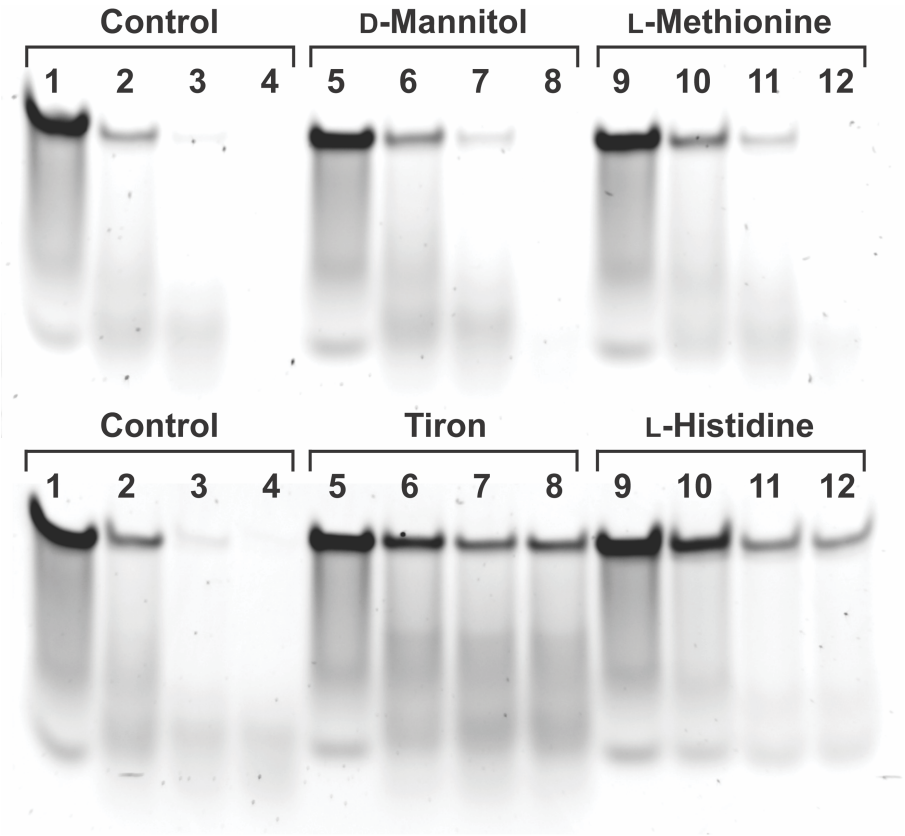


Figure 21: 20% native PAGE showing the cleavage profile of the Cu-LLD helicate in the presence of ROS scavengers. Lanes 1-4: Control (no scavenger). Lanes 5-8: Top: D-Mannitol, Bottom: Tiron. Lanes 9-12: Top: L-Methionine. Bottom: L-Histidine. Lanes 1,5,9: 3WJ control. Lanes 2,6,10: 5 equivalents Cu-LLD helicate. Lanes 3,7,11: 7.5 equivalents Cu-LLD helicate. Lanes 4,8,12: 10 equivalents Cu-LLD helicate.

3.3 Fluorescent thermal melting

A fluorescence thermal melting (T_M) method was designed to determine the melting temperature of a 32-nucleotide TFO and its 57 bp duplex target. SYBR green I was selected as the fluorophore of choice as it enabled both triplex and duplex melting to be visualised within a single sample.[13] Here, the TFO and target dsDNA were incubated at 37 °C for 15 hours to allow for formation of triple helical DNA. SYBR green was added and using a LightCycler 480 II (section 3.6.8) the

sample was heated to 99 °C with 10 fluorescence (465-510 nm) measurements being recorded per °C. A plot of temperature versus fluorescence was obtained (**Figure 22**) and the first negative derivative was calculated, resulting in the melting temperature being obtained as a peak (**Figure 22**). This fluorescence melting protocol was widely employed for the analysis of DPA-TFO hybrids reported in Chapter 5.[34]

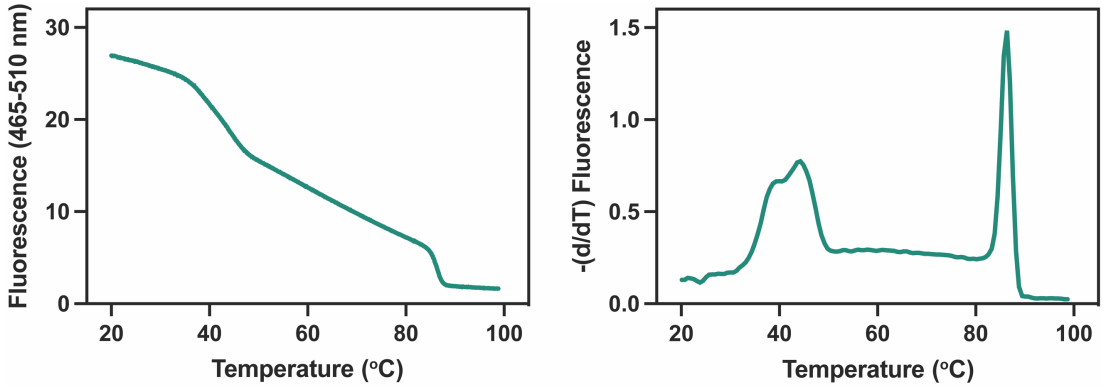


Figure 22: Left: Biphasic melting profile of a 32 nucleotide alkyne-modified TFO and its 57 bp target duplex. Right: First negative derivative is calculated and two peaks are observed. Triplex T_M = 44.0 °C and duplex T_M = 86.2 °C.

3.4 qPCR analysis of DNA damage

Although it was shown that TFO-metallodrug hybrids can identify and bind to their target dsDNA sequence though PAGE and T_M analysis, these methods do not enable the damage inflicted to be accurately quantified. Therefore a qPCR protocol was developed to analyse the DNA damage resulting from incubation with an AMN-TFO hybrid (**Figure 23**). This assay was designed to be applicable for the analysis of a variety of DNA damage profiles, and to be easily adaptable for different DNA targets. SYBR green I was selected as the fluorescent reporter, as it can bind to any intact dsDNA sequence and the fluorescence intensity increases as the concentration of dsDNA rises, *i.e.* as successful PCR cycles are completed. The more DNA damage the hybrid inflicts, the lower the fluorescent signal detected.

For this assay to be successful the concentration of starting DNA must fall within a particular range: too much DNA and the C_T will be reached too quickly meaning small changes in DNA concentration will not be detected; too little DNA and the C_T will move into the range of the negative controls, thereby rendering the values obsolete. For this reason it is vital to run positive (dsDNA of a known concentration) and negative (no template, just primers) controls. To determine the optimum concentration range, for the 113 bp amplicon of GFP, multiple standard curves of 1 in 10 dilutions were analysed with different concentrations of DNA being tested as the top standard. It was decided that a $1:20^5$ dilution of 0.625 pmol of GFP was the most suitable, as it gave a C_T value of ~20 cycles. Additionally, to perform relative quantification analysis appropriate reference and control samples were required. Typically the reference samples are a house keeping gene from the same cell,[17] but in this situation the DNA has not been derived from a cell line so an alternative was required. It was decided that the most suitable reference was samples that had been incubated for 0 hours. The reference DNA was treated exactly as that in the samples except it had not been subjected to incubation with the DNA damaging agent. A non-treated control duplex was chosen as the positive control and a sample lacking the dsDNA template (*i.e.* just primers) was selected as the negative control.

Internally modified TPMA-TFO hybrids, TFO bound to $5N_3$-TPMA (I) and $6N_3$-TPMA (II) (**Figure 23C**), synthesised by NZF were selected for this study as they displayed excellent sequence selectivity during preliminary gel electrophoretic experiments. A 113 bp amplicon from the GFP gene (0.625 pmol, section 3.6.9), which contains the recognition sequence for the TFO, was incubated with a Cu(II)-bound TPMA-TFO hybrid (25 eq., 15.625 pmol) and Na-*L*-ascorbate (0-2000 eq., 0-31.25 nmol) at 37 °C for 6 hours. The resulting product was then analysed by the qPCR protocol developed. The DNA target sequence is amplified by *Taq* DNA polymerase, while the relative concentration is monitored through SYBR green I fluorescence. The initial concentration of intact duplex DNA is directly proportional to the C_T value. Therefore the C_T value for each sample can be compared to determine the extent of DNA cleavage that had occurred. The TFO that inflicts the most DNA damage will have the highest C_T value.

qPCR was also performed on free Cu-TPMA and free alkyne-modified TFO. In this instance no significant damage is observed until 250 equivalents of reductant are present (fold change at 250 eq. Na-*L*-ascorbate = 0.58). However, DNA damage was detected for Cu(II)-bound TPMA-TFO hybrids even in the absence of reductant (fold change for 0 eq. Na-*L*-ascorbate = 0.54 for both TPMA-TFO(I) and TPMA-TFO(II)) and in the presence of ascorbate—a reductant natively present in biological systems—the target duplex was ablated. The TPMA-TFOs display similar cleavage profiles, while attenuated cleavage by the non-clicked Cu(II)-TPMA complex with alkyne-TFO was observed (**Figure 23**). This shows that the TPMA-TFO hybrids not only allow for sequence recognition, but also increase the cleavage abilities of the Cu(II)-bound ligands. Results from this method were published in ChemBioChem.[32]

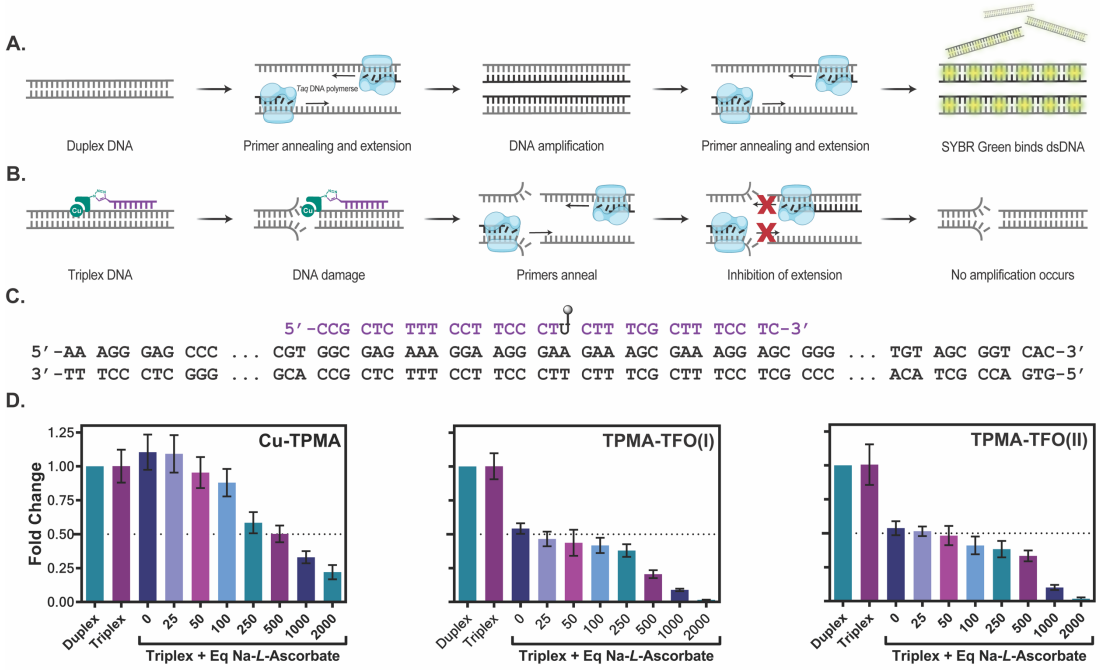


Figure 23: A. Schematic of qPCR with intact dsDNA using SYBR green as the fluorescent reporter. **B.** Inhibition of DNA amplification due to DNA damage resulting from incubation with an AMN-TFO hybrid. **C.** Sequence of TFO, showing position of modification, and target duplex to be amplified by qPCR. **D.** Damage resulting from incubation with 25 equivalents of copper-bound TPMA-TFO hybrid was analysed by comparing the threshold cycle (C_T) of target (6 hour) and control (0 hour) samples (target C_T – control C_T) to give ΔC_T. ΔC_T was normalised to a non-treated control ($\Delta\Delta C_T$), and the data was plotted as linear values ($2^{-\Delta\Delta CT}$). DNA polymerase graphic was produced in BioRender.

The aim of metallo-drug-TFO hybrids is to selectively damage a DNA sequence of interest, so it was important that the qPCR protocol was expanded to quantify the damage inflicted upon both target and *off*-target sequences. This task required significant planning and optimisation as many factors needed to be considered: i.) The 113 bp primers (forward: 5′-AAAGGGAGCCCCCGATTTAG-3′ and reverse: 5′-GTGACCGCTACACTTGCCA-3′) used to amplify the target duplex could not have a binding site within the *off*-target sequence, and vice versa; ii.) the *off*-target duplex must not contain the TFO recognition site (*i.e.* 5′-GGCGAGAAAGGAAGGGAAGAAAGCGAAAGGAG-3′); iii.) the target and *off*-target primers must have the same annealing temperature to allow qPCR with both amplicons be performed simultaneously; iv.) the target and *off*-target amplicons must have similar amplification efficiencies to allow for an accurate comparison, and v.) ideally, both amplicons would be of a similar length, which allows free nuclease controls to be accurately evaluated. A 116 bp region of the pUC19 plasmid was found to satisfy these criteria. In a similar manner to the sequence selective PAGE experiments, the Cu(II)-DPA-TFO was incubated with target (113 bp GFP) and *off*-target (116 bp pUC19) duplexes in the presence of increasing equivalents of Na-*L*-ascorbate. After 15 hours the reaction was quenched with EDTA and the samples were diluted to a concentration suitable for qPCR analysis. Each sample was amplified in the presence of both the target, GFP, and *off*-target, pUC19, primers, and the C_T for each sample was recorded. The DPA-TFO hybrid binds with the target duplex, inflicts DNA damage and prevents DNA amplification (**Figure 24A**). Hybridisation does not occur with the *off*-target dsDNA and therefore it does not undergo DNA cleavage (**Figure 24B**). The change in C_T for the target and *off*-target samples was calculated and normalised to the corresponding non-treated control. The fold change of intact DNA concentration was plotted (**Figure 24C**). The damage inflicted by free Cu-DPA and free TFO was also evaluated (**Figure 24D**), and it was noted that no significant damage occurs in the presence of free nuclease. This confirms the results visualised by gel electrophoresis; attachment of DPA to a TFO delivery vector allows for sequence specific damage and increases the DNA damaging propensity of the nuclease.

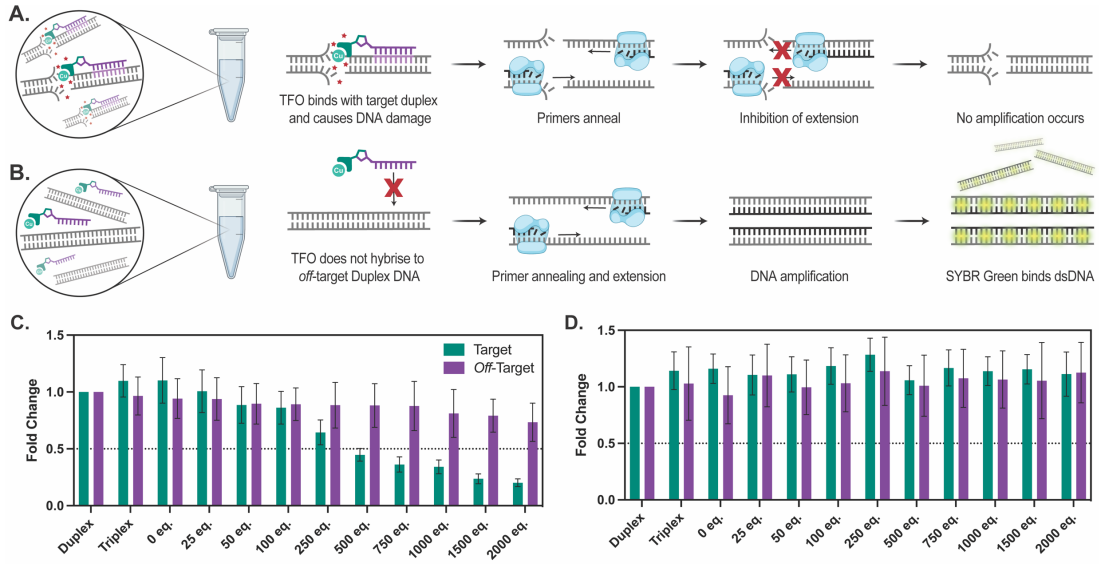


Figure 24: A. Schematic of qPCR for target dsDNA. The DPA-TFO hybrid selectively cleaves and inhibits DNA amplification. **B.** The TFO does not hybridise with the *off*-target duplex, thereby no damage is inflicted and amplification can occur. **C.** The fold change of intact DNA concentration ($2^{-\Delta\Delta CT}$) is plotted for the target (green) and *off*-target (purple) duplexes. **D.** Damage post-incubation with free Cu-DPA and free TFO was quantified, again the target and *off*-target are shown in green and purple, respectively. DNA polymerase graphic was adapted from BioRender.

To ensure the amplification inhibition was due to cleavage by the DPA-TFO, the qPCR experiment was repeated with samples incubated in the presence of a ROS scavenger. If damage inflicted by the DPA-TFO is responsible for the change in C_T, then it will be impeded by the inclusion of a scavenger during the preceding incubation. But, if another factor—such as the conditions or presence of the TFO—is responsible, amplification will continue to be impeded in the presence of an appropriate ROS scavenger. From PAGE analysis it was known that tiron prevents DNA cleavage by the Cu-DPA-TFO, as damage occurs primarily through the formation of copper-superoxo ($Cu\text{-}O_2^{\bullet-}$) adducts. Therefore, Cu-DPA-TFO, target duplex (113 bp GFP), Na-*L*-ascorbate and tiron were incubated at 37 °C for 15 hours, and the resulting amplification inhibition was determined (**Figure 25**). The presence of tiron PCR amplification of the target sequence could proceed, thereby confirming that the Cu-DPA-TFO was responsible for the sequence selective cleavage.

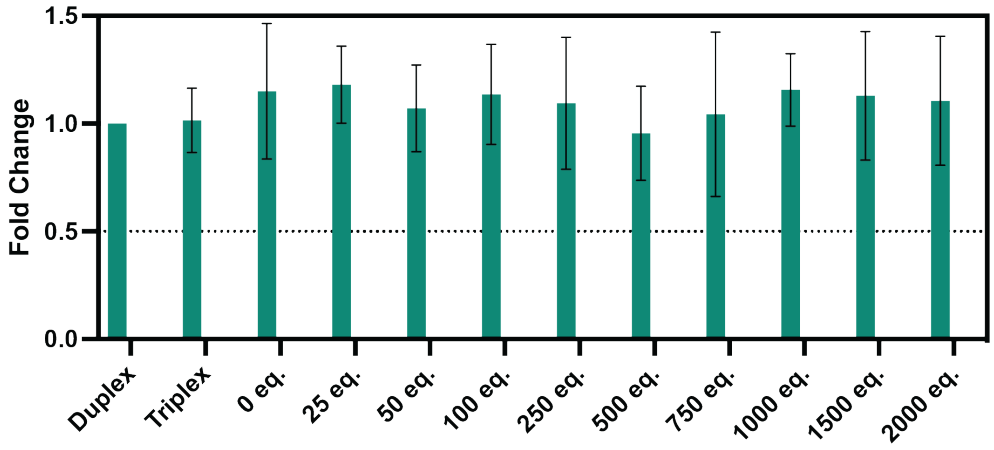


Figure 25: Fold change of intact DNA in the presence of the tiron.

3.5 Conclusion

As the field of targeted metallodrugs is in its infancy there was a need to develop protocols for analysis of sequence specific damage. Polyacrylamide gel electrophoretic conditions that enabled the visualisation of triplex formation and targeted DNA cleavage were identified and optimised. These were then applied to investigate the DNA binding profile of AMN-TFO hybrids, Pt(II)-TFOs and three-way junction binding helicates. A fluorescent thermal melting method, using SYBR green I fluorescence, was developed for the analysis of triple helical DNA, and real-time PCR was employed for the quantification of DNA damage. The qPCR protocol reported is the first example of a method that can accurately quantify the DNA damage inflicted by AMN-TFOs on both target and *off*-target genetic sequences. The molecular methods reported are an expansion of those previously used within the field of metallodrug-DNA interactions, but this is the first report of methodology for the visualisation and accurate quantification of sequence specific DNA damage. The molecular methods developed here will be invaluable as research into the field of therapeutic oligonucleotides expands.

3.6 Experimental

3.6.1 General information

PAGE gels were cast using a SureCast™ gel casting system (Invitrogen) and SureCast™ acrylamide solution (Invitrogen), and run in an Invitrogen mini gel tank. A Bio-Rad basic Power Pac™ was used for PAGE gel electrophoresis. All gels were imaged using a Syngene G:Box 9 mini gel documentation system. PCR was performed using a Mastercycler® nexus (Eppendorf). Real-time PCR (qPCR) and fluorescence thermal melting were performed on a Roche LightCycler® 480 II using SYBR green I master mix (Roche).

Raw gel images are available to download on Google drive: https://drive.google.com/drive/folders/1tu199tKFWnem-pHC3Suwn_c1pU1_YWMs?usp=sharing

3.6.2 Amplification of TFO target and *off*-target dsDNA

A 57 bp amplicon containing the TFO recognition sequence (pCSanDI-HYG plasmid; forward: 5′-AAGCCGGCGAACGTGGCGG-3′ and reverse: 5′-CCTAGCGCCCGCTCCTTTCG -3′), and a 40 bp amplicon lacking the TFO target sequence (pUC19, NEB; forward: 5′-TGACTCCCCGTCGTGTAGAT-3′ and reverse: 5′-AGCCCTCCCGTATCGTAGTT-3′) were generated by PCR (MyTaq Red DNA polymerase, Bioline) and purified into 6 μL of nuclease-free water using membrane spin columns (Monarch PCR & DNA clean-up kit, NEB).

3.6.3 PAGE analysis of TPMA-TFO hybrids

Each TPMA-TFO ($5N_3$-TPMA or $6N_3$-TPMA) hybrid (15.625 pmol) was incubated with 1 equivalent of $Cu(ClO_4)_2$ for 15 min at room temperature, to allow Cu(II) coordinate within the polypyridyl ligand. This copper-bound TPMA-TFO hybrid (15.625 pmol), with increasing concentrations of Na-*L*-ascorbate (25-500 eq.), was then incubated with a target duplex (57 bp fragment of GFP, 0.625 pmol) and an *off*-target duplex (40 bp fragment of pUC19, 0.625 pmol) in phosphate buffer (10 mM PO_4^{3-}, 150 mM NaCl, 2 mM $MgCl_2$, pH 6.1) at 37 °C for 6 hours.

The reaction was quenched with loading dye (6X, 10 mM Tris-HCl, pH 7.6, 0.03% bromophenol blue, 0.03% xylene cyanol FF, 60% glycerol, 60 mM EDTA, Invitrogen) and stored at 4 °C overnight. The entire solution was loaded onto a 20% native PAGE gel (50 mM Tris-acetate, 75 mM NaCl, 5 mM $MgCl_2$, pH 6.1) and was run at 70 V for 240 min, before being post-stained with SYBR gold (1X, Invitrogen).

3.6.4 DPA-TFO PAGE

DPA-TFO hybrid was incubated with $Cu(ClO_4)_2$ to allow copper coordinate within the polypyridyl ligand. In a final volume of 6 μL, Cu(II)-DPA-TFO (15.625 pmol), target duplex (57 bp fragment of GFP, 0.625 pmol), *off*-target duplex (40 bp fragment of pUC19, 0.625 pmol) and Na-*L*-ascorbate (0-1000 eq.) were incubated in phosphate buffer (10 mM PO_4^{3-}, 150 mM NaCl, 2 mM $MgCl_2$, pH 6.1) at 37 °C for 15 hours. Loading dye (6X, 10 mM Tris-HCl, pH 7.6, 0.03% bromophenol blue, 0.03% xylene cyanol FF, 60% glycerol, 60 mM EDTA, Invitrogen) was added to quench the reaction and entire sample was loaded onto a 20% native Tris-acetate PAGE gel (50 mM Tris-acetate, 75 mM NaCl, 5 mM $MgCl_2$, pH 6.1) and was run at 70 V for 240 min. The gel was post-stained with SYBR gold (1X, Invitrogen).

3.6.5 ROS scavengers

Samples were prepared as described above, however the *off*-target sequence was excluded, and a reactive oxygen species (ROS) scavenger (50 nmol); L-histidine, D-mannitol, L-methionine or 4,5-dihydroxy-1,3-benzendisulfonic acid (tiron) was added prior to incubation at 37 °C for 15 hours. The DNA damage inflicted was analysed by 20% native PAGE.

3.6.6 Platinum-TFO PAGE

In a total volume of 5 μL, the target duplex sequence (57 bp fragment of GFP, 1 pmol) and *off*-target duplex (40 bp fragment of pUC19, 1 pmol) were incubated in reaction buffer (10 mM PO_4^{3-}, 150 mM NaCl, 2 mM $MgCl_2$, pH 6.1) with the

Pt(II)-TFO (29 nt, 2.5 to 50 pmol) at 37 °C for 2, 24 or 48 hours. Loading dye (6X, 10 mM Tris-HCl, pH 7.6, 0.03% bromophenol blue, 0.03% xylene cyanol FF, 60% glycerol, 60 mM EDTA) was added to the sample and the entire volume was loaded onto a 20% native PAGE gel (50 mM Tris-acetate, 75 mM NaCl, 5 mM $MgCl_2$, pH 6.1). Gel was run at 70 V for 240 min and post-stained with SYBR gold.

3.6.7 Three Way Junction PAGE

3.6.7.1 Targeted DNA damage

The three stands that comprise the 3WJ were annealed prior to the cleavage studies to ensure the correct confirmation was adopted. Equal concentrations of each strand were mixed in HEPES buffer (40 mM HEPES, 750 mM NaCl, 50 mM $MgCl_2$, pH 7) and heated to 95 °C before being cooled in 5 °C increments to 4 °C. The annealed 3WJ (5 pmol), and an *off*-target DNA duplex (5 pmol), were then incubated at 37 °C for 24 hours with copper-bound LLD-helicate (1, 2.5, 5, 7.5, 10 or 25 equivalents) and Na-*L*-ascorbate (10 eq. to LLD). The reaction was quenched with loading dye (6X, 10 mM Tris-HCl, pH 7.6, 0.03% bromophenol blue, 0.03% xylene cyanol FF, 60% glycerol, 60 mM EDTA) and loaded onto a 20% native PAGE gel (50 mM Tris-acetate, 75 mM NaCl, 5 mM $MgCl_2$, pH 6.1). The gel was run at 70 V for 240 min, and post-stained with SYBR gold.

3.6.7.2 ROS scavengers

3WJ binding Cu-LLD helicate samples were prepared as previously described, but the dsDNA *off*-target was replaced with a ROS scavenger (50 nmol); L-histidine, D-mannitol, L-methionine or tiron, and incubated at 37 °C for 24 hours. Products were analysed by 20% Tris-acetate PAGE (50 mM Tris-acetate, 75 mM NaCl, 5 mM $MgCl_2$, pH 6.1).

3.6.8 Fluorescent melting

TFO (25 pmol) and 57 bp target duplex (5 pmol) were incubated in phosphate buffer (10 mM PO_4^{3-}, 150 mM NaCl, 2 mM $MgCl_2$, pH 6.1) at 37 ºC for 15 hours.

SYBR green I (1 μL, Roche) was added to each sample and the melting profile for the triplex was analysed on a LightCycler® 480 II (Roche). Samples were heated to 99 ºC with 10 fluorescence measurements recorded per ºC. A plot of sample temperature versus fluorescence was obtained and the first negative derivative of the sample was calculated to obtain the T_M.

3.6.9 qPCR analysis of catalytic activity of Cu-TPMA-TFO hybrids

Real-time PCR quantification was performed on a Roche LightCycler® 480 II using SYBR green I detection. Stock solutions of AMN-TFOs and target duplexes were initially prepared in nuclease-free water and further dilutions prepared in the reaction buffer (10 mM PO_4^{3-}, 150 mM NaCl, 2 mM $MgCl_2$, pH 6). A 113 bp amplicon containing the TFO sequence was generated using a set of primers designed on the pCSanDI-HYG plasmid, which contains the GFP gene (forward: 5′-AAAGGGAGCCCCCGATTTAG-3′ and reverse: 5′-GTGACCGCTACACTTGCCA-3′). In a total volume of 12 μL, the target DNA duplex sequence (113 bp, 1.25 pmol) was exposed to each test drug (31.25 pmol of either TPMA-TFO(I), TPMA-TFO(II) or a 1:1 mixture of free Cu-TPMA and alkyne-TFO) in the presence of increasing equivalents of Na-*L*-ascorbate. At t = 0 hours, 6 μL of each reaction volume was removed and quenched with EDTA (90 nmol), these were the reference samples. The remaining 6 μL was incubated at 37 °C for t = 6 hours (experimental) prior to addition of EDTA. Reference and experimental samples were diluted (1:20^5) and analysed by qPCR over 45 PCR cycles. The changes in C_T (threshold cycle) between target and reference sample (target C_T – reference C_T) were calculated (ΔC_T) and normalised to a non-treated control ($\Delta\Delta C_T$). $\Delta\Delta C_T$ were plotted as linear values $2^{-\Delta\Delta CT}$.

3.6.10 qPCR analysis of target and *off*-target damage induced by DPA-TFOs

qPCR quantification was using SYBR green I fluorescence. A 113 bp amplicon containing the TFO recognition sequence (pCSanDI-HYG plasmid; forward: 5′-AAAGGGAGCCCCCGATTTAG-3′ and reverse: 5′-GTGACCGCTACACTTGCCA-3′), and a 116 bp amplicon lacking the TFO target sequence (pUC19, NEB; forward:

5′-TCCGGTCCCAACGATCAAG-3′ and reverse: 5′-AGTGATAACACTGCGGCCAA-3′) were generated by PCR (MyTaq Red DNA polymerase, Bioline) and purified using membrane spin columns (Monarch PCR & DNA clean-up kit, NEB). In a total volume of 12 μL (10 mM PO_4^{3-}, 150 mM NaCl, 2 mM $MgCl_2$, pH 6), the target duplex (113 bp, 1.25 pmol) and *off*-target sequence (116 bp, 1.25 pmol) were exposed to Cu-DPA-TFO or a 1:1 mixture of free Cu-DPA and free TFO (31.25 pmol) in the presence of increasing equivalents of Na-*L*-ascorbate (0-2000 eq.). At t = 0 hours, 6 μL of each reaction volume was quenched with EDTA (60 nmol) and kept as the reference samples. The remaining 6 μL was incubated at 37 °C for t = 15 hours (experiment) prior to addition of EDTA. Diluted ($1:40^5$) reference and experiment samples were analysed by qPCR over 45 PCR cycles. The changes in C_T (threshold cycle) between experiment and reference samples (experiment C_T – reference C_T) were calculated (ΔC_T). ΔC_T was then normalised to a non-treated control (ΔC_T sample - ΔC_T control = $\Delta\Delta C_T$), and this was plotted as a linear value $2^{-\Delta\Delta CT}$.

3.6.11 qPCR with ROS scavengers

Samples were prepared as described above, however the *off*-target DNA was excluded, and a reactive oxygen species (ROS) scavenger, tiron (50 nmol) was added prior to incubation at 37 °C for 15 hours. The DNA damage inflicted was diluted ($1:40^5$) and analysed by qPCR. $2^{-\Delta\Delta CT}$ values were calculated and plotted.

References

1. Kellett, A.; Molphy, Z.; Slator, C.; McKee, V.; Farrell, N. P., Molecular methods for assessment of non-covalent metallodrug-DNA interactions. *Chem. Soc. Rev.* **2019,** *48* (4), 971-988.
2. Liu, Y. W.; Wilson, D., *Drug-DNA Interaction Protocols*. 2 ed.; Humana Pres: 2010; Vol. 613.
3. Hacia, J. G.; Dervan, P. B.; Wold, B. J., Inhibition of Klenow Fragment DNA-Polymerase on Double-Helical Templates by Oligonucleotide-Directed Triple-Helix Formation. *Biochem.* **1994,** *33* (20), 6192-6200.
4. Plum, G. E.; Park, Y. W.; Singleton, S. F.; Dervan, P. B.; Breslauer, K. J., Thermodynamic Characterization of the Stability and the Melting Behavior of a DNA Triplex - a Spectroscopic and Calorimetric Study. *Proceedings of the National Academy of Sciences of the United States of America* **1990,** *87* (23), 9436-9440.
5. Graham, M. K.; Miller, P. S., Inhibition of transcription by platinated triplex-forming oligonucleotides. *J Biol Inorg Chem* **2012,** *17* (8), 1197-208.
6. Orson, F. M.; Thomas, D. W.; McShan, W. M.; Kessler, D. J.; Hogan, M. E., Oligonucleotide inhibition of IL2R alpha mRNA transcription by promoter region collinear triplex formation in lymphocytes. *Nucleic Acids Res* **1991,** *19* (12), 3435-41.
7. Helene, C., Control of gene expression by triplex-forming-oligonucleotides. The antigene strategy. *Anticancer Drug Des* **1991,** *6* (6), 569-84.
8. Sigman, D. S.; Bruice, T. W.; Mazumder, A.; Sutton, C. L., Targeted chemical nucleases. *Acc. Chem. Res.* **1993,** *26* (3), 98-104.
9. Fried, M.; Crothers, D. M., Equilibria and kinetics of lac repressor-operator interactions by polyacrylamide gel electrophoresis. *Nucleic Acids Res.* **1981,** *9* (23), 6505-6525.
10. Garner, M. M.; Revzin, A., A gel electrophoresis method for quantifying the binding of proteins to specific DNA regions: application to components of the Escherichia coli lactose operon regulatory system. *Nucleic Acids Res.* **1981,** *9* (13), 3047-3060.
11. Guedin, A.; Lacroix, L.; Mergny, J. L., Thermal melting studies of ligand DNA interactions. In *DNA-Drug Interaction Protocols*, Fox, K. R., Ed. Humana Press: Methods in Molecular Biology, 2010; pp 25-35.
12. Darby, R. A. J.; Sollogoub, M.; McKeen, C.; Brown, L.; Risitano, A.; Brown, N.; Barton, C.; Brown, T.; Fox, K. R., High throughput measurement of duplex, triplex and quadruplex melting curves using molecular beacons and a LightCycler. *Nucleic Acids Res.* **2002,** *30* (9), 39e-39.
13. Trantakis, I. A.; Fakis, M.; Tragoulias, S. S.; Christopoulos, T. K.; Persephonis, P.; Giannetas, V.; Ioannou, P., Ultrafast fluorescence dynamics of Sybr Green I/DNA complexes. *Chemical Physics Letters* **2010,** *485* (1-3), 187-190.
14. Mullis, K.; Faloona, F.; Scharf, S.; Saiki, R.; Horn, G.; Erlich, H., Specific enzymatic amplification of DNA in vitro: the polymerase chain reaction. *Cold Spring Harb Symp Quant Biol* **1986,** *51 Pt 1* (0), 263-73.
15. Krebs, J. E.; Goldstein, E. S.; Kilpatrick, S. T., Methods in Molecular Biology and Genetic Engineering. In *Lewin's Genes XI*, 11 ed.; Johnson, M., Ed. Jones & Barlett: 2011.

16. Wong, M. L.; Medrano, J. F., Real time PCR for mRNA quantification. *BioTechniques* **2005,** *39* (1), 75-85.
17. Schmittgen, T. D.; Livak, K. J., Analyzing real-time PCR data by the comparative C(T) method. *Nat Protoc* **2008,** *3* (6), 1101-8.
18. Grimaldi, K. A.; Hartley, J. A., PCR-based methods for detecting DNA damage and its repair at the subgene and single nucleotide levels in cells. In *Drug-DNA interaction protocols*, Fox, K. R., Ed. Humana Press: Methods in Molecular Biology, 1997; Vol. 90.
19. Grimaldi, K. A.; McAdam, S. R.; Souhami, R. L.; Hartley, J. A., DNA damage by anti-cancer agents resolved at the nucleotide level of a single copy gene: evidence for a novel binding site for cisplatin in cells. *Nucleic Acids Res.* **1994,** *22* (12), 2311-2317.
20. Cho, E.; Buick, J. K.; Williams, A.; Chen, R. X.; Li, H. H.; Corton, J. C.; Fornace, A. J.; Aubrecht, J.; Yauk, C. L., Assessment of the performance of the TGx-DDI biomarker to detect DNA damage-inducing agents using quantitative RT-PCR in TK6 cells. *Environmental and Molecular Mutagenesis* **2019,** *60* (2), 122-133.
21. Graham, M. K.; Brown, T. R.; Miller, P. S., Targeting the human androgen receptor gene with platinated triplex-forming oligonucleotides. *Biochem.* **2015,** *54* (13), 2270-82.
22. Hunter, S. E.; Jung, D.; Di Giulio, R. T.; Meyer, J. N., The QPCR assay for analysis of mitochondrial DNA damage, repair, and relative copy number. *Methods* **2010,** *51* (4), 444-451.
23. Movassaghi, S.; Jafari, S.; Falahati, K.; Ataei, M.; Sanati, M. H.; Jadali, Z., Quantification of mitochondrial DNA damage and copy number in circulating blood of patients with systemic sclerosis by a qPCR-based assay. *An Bras Dermatol* **2020,** *95* (3), 314-319.
24. Stefanou, D. T.; Episkopou, H.; Kyrtopoulos, S. A.; Bamias, A.; Gkotzamanidou, M.; Bamia, C.; Liakou, C.; Bekyrou, M.; Sfikakis, P. P.; Dimopoulos, M.-A.; Souliotis, V. L., Development and validation of a PCR-based assay for the selection of patients more likely to benefit from therapeutic treatment with alkylating drugs. *Br J Clin Pharmacol* **2012,** *74* (5), 842-853.
25. Swango, K. L.; Hudlow, W. R.; Timken, M. D.; Buoncristiani, M. R., Developmental validation of a multiplex qPCR assay for assessing the quantity and quality of nuclear DNA in forensic samples. *Forensic Sci Int* **2007,** *170* (1), 35-45.
26. Van Kan, M.; Burns, K. E.; Browett, P.; Helsby, N. A., A higher throughput assay for quantification of melphalan-induced DNA damage in peripheral blood mononuclear cells. *Sci. Rep.* **2019,** *9* (1).
27. Wang, Y.-C.; Lee, P.-J.; Shih, C.-M.; Chen, H.-Y.; Lee, C.-C.; Chang, Y.-Y.; Hsu, Y.-T.; Liang, Y.-J.; Wang, L.-Y.; Han, W.-H.; Wang, Y.-C., Damage formation and repair efficiency in the p53 gene of cell lines and blood lymphocytes assayed by multiplex long quantitative polymerase chain reaction. *Anal Biochem* **2003,** *319* (2), 206-215.
28. Zhu, S.; Coffman, J. A., Simple and fast quantification of DNA damage by real-time PCR, and its application to nuclear and mitochondrial DNA from multiple tissues of aging zebrafish. *BMC Res Notes* **2017,** *10* (1), 269.
29. Abel, G. R.; Calabrese, Z. A.; Ayco, J.; Hein, J. E.; Ye, T., Measuring and Suppressing the Oxidative Damage to DNA During Cu(I)-Catalyzed Azide–Alkyne Cycloaddition. *Bioconjug Chem* **2016,** *27* (3), 698-704.

30. Vogelstein, B.; Lane, D.; Levine, A. J., Surfing the p53 network. *Nature* **2000,** *408* (6810), 307-310.
31. Zuin Fantoni, N.; Molphy, Z.; Slator, C.; Menounou, G.; Toniolo, G.; Mitrikas, G.; McKee, V.; Chatgilialoglu, C.; Kellett, A., Polypyridyl-Based Copper Phenanthrene Complexes: A New Type of Stabilized Artificial Chemical Nuclease. *Chem. Eur. J.* **2019,** *25* (1), 221-237.
32. Zuin Fantoni, N.; McGorman, B.; Molphy, Z.; Singleton, D.; Walsh, S.; El-Sagheer, A. H.; McKee, V.; Brown, T.; Kellett, A., Development of Gene-Targeted Polypyridyl Triplex-Forming Oligonucleotide Hybrids. *Chembiochem* **2020,** *21*, 3563-3574.
33. Zuin Fantoni, N.; Molphy, Z.; O'Carroll, S.; Menounou, G.; Mitrikas, G.; Krokidis, M.; Chatgilialoglu, C.; Colleran, J.; Banasiak, A.; Clynes, M.; Roche, S.; Kelly, S.; McKee, V.; Kellett, A., Polypyridyl-Based Copper Phenanthrene Complexes: Combining Stability with Enhanced DNA Recognition. *Chem. Eur. J.* **2020**.
34. McGorman, B.; Zuin Fantoni, N.; O'Carroll, S.; Ziemele, A.; El-Sagheer, A. H.; Brown, T.; Kellett, A., Enzymatic synthesis of chemical nucelase triple-forming oligonucleotides with gene-editing applications. *Manuscript under review*.
35. Hennessy, J.; McGorman, B.; Molphy, Z.; Farrell, N. P.; Singleton, D.; Brown, T.; Kellett, A., A Click Chemistry Approach to Targeted DNA Crosslinking with cis-Platinum(II) Modified Triplex Forming Oligonucleotides. *Angew. Chem. Int. Ed.* **2021,** *60*.
36. Oleksi, A.; Blanco, A. G.; Boer, R.; Usón, I.; Aymamí, J.; Rodger, A.; Hannon, M. J.; Coll, M., Molecular Recognition of a Three-Way DNA Junction by a Metallosupramolecular Helicate. *Angew. Chem. Int. Ed.* **2006,** *45* (8), 1227-1231.
37. Gamba, I.; Rama, G.; Ortega-Carrasco, E.; Maréchal, J.-D.; Martínez-Costas, J.; Eugenio Vázquez, M.; López, M. V., Programmed stereoselective assembly of DNA-binding helical metallopeptides. *Chem. Commun.* **2014,** *50* (76), 11097-11100.

Chapter 4

Enzymatic synthesis of modified oligonucleotides

4.1 Introduction

The artificial synthesis of DNA is a requirement for many aspects of biological and chemical research, and today almost all the DNA produced outside of a cell is done so by a process known as solid-phase phosphoramidite synthesis.[1, 2] Solid-phase synthesis (SPS) is a stepwise reaction where a single phosphoramidite base is added to the growing DNA sequence with each synthetic cycle. SPS has been adapted for the inclusion of modified bases, but it is not compatible with modifications that are sensitive to oxidising agents, or that are reactive with nucleophiles.[3] Therefore, there is a desire to develop alternative methods for the production of modified oligonucleotides. Enzymatic synthesis offers an appealing alternative. The incorporation of modified nucleotide triphosphates (dNTPs) during enzymatic synthesis was first reported in 1981, when the inclusion of biotin-modified bases was reported.[4] However, the utility of enzymatic methods was limited by the inability to include modifications at specific sites. When a natural dNTP was replaced with its modified analogue, the modified dNTP was incorporated at all complementary positions. In 2013, a solution was reported.[5] Single nucleotide incorporation, followed by traditional primer extension (SNI-PEX) was developed by the Hocek group, and this methodology enabled a single modified base to be included at a specific site in the oligonucleotide sequence. However, only the incorporation of a small number of modifications has been reported,[5-7] and there is a desire to expand this technology for the synthesis of therapeutic oligonucleotides. Herein, SNI-PEX is combined with nucleic acid click chemistry to synthesise a library of triplex-forming oligonucleotides (TFOs) that are modified with artificial metallo-nucleases (AMNs).

4.2 Library preparation of modified dNTPs

A library of dNTPs bearing a variety of modifications was prepared using nucleic acid click chemistry. The copper(II)-catalysed azide-alkyne cycloaddition (CuAAC) was selected as it allowed for the rapid conjugation of azide functionalised drug molecules to alkyne tagged dNTPs. As there was no simple method available to analyse deoxyribonucleotide triphosphates (dNTPs), nucleic

acid click chemistry conditions for metallodrug complexes were optimised using short 5′-octadiynyl functionalised oligonucleotides (16 nt) (**Figure 26**), which could be analysed in-house by polyacrylamide gel electrophoresis. The concentration of alkyne-functionalised DNA, the ratio of azide to alkyne used, the reaction time, and the temperature were explored to identify optimal conditions. The copper-catalysed azide-alkyne cycloaddition (CuAAC) requires the presence of Cu(I) to form a 1,2,3-triazole and in nucleic acid click chemistry, the most common sources of Cu(I) are CuBr or by reduction of Cu(II)SO_4 using sodium-*L*-ascorbate, with the latter being employed in these reactions. The optimum solvent identified was DMSO and water (1:1).

Under anaerobic conditions the reaction components: 5′-octadiynyl DNA; $3N_3$-7-hydroxycoumarin (1-5 eq.); Na-*L*-ascorbate; and pre-mixed Cu(II)SO_4-TBTA were incubated in DMSO and water (1:1) for 3, 6, 24 or 48 hours at 25 °C and 450 RPM. At each time point one sample was removed and quenched with EDTA. The products were analysed by native PAGE (**Figure 26A**) and it was decided that 1.5 equivalents of azide to alkyne incubated for 6 hours were the optimum conditions for this click reaction. Next, the suitability of these conditions for clicking $3N_3$-7-hydroxycoumarin, $6N_3$-TPMA and $4N_3$-benzyl-DPA to C8-alkyne-dUTPs and dCTPs was investigated.

Firstly $3N_3$-7-hydroxycoumarin was clicked to C8-alkyne-dUTP. This coumarin derivative is pro-fluorogenic, which means that its fluorescent intensity increases in the presence of the triazole ring formed during the click reaction.[8] The excitation and emission of $3N_3$-7-hydroxycoumarin also changes from λ_{ex} 260 nm and λ_{em} 391 nm, to λ_{ex} 404 nm and λ_{em} 480 nm post click reaction. Therefore, a successful ‘click’ between $3N_3$-7-hydroxycoumarin and C8-alknye-dUTP can be easily visualised (**Figure 26B**), which facilitated the identification of click conditions suitable for the attachment of an azide-modified ligand to short oligonucleotides and to dNTPs. This knowledge was then applied for further nucleic acid click chemistry reactions.

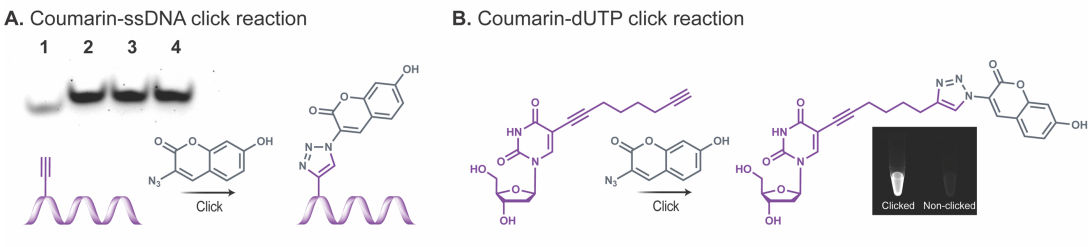


Figure 26: A. 20% native PAGE analysis of products following click reaction with a single-stranded oligonucleotide (16 bases) with $3N_3$-7-hydroxycoumarin. Lane 1: Control ssDNA where no azide was present for the click reaction, Lanes 2, 3 and 4: 3, 6 and 24 hour click reactions, respectively. The shift upwards in the gel shows there was an increase in molecular weight, which is indicative of a successful click reaction. **B.** When $3N_3$-7-hydroxycoumarin is clicked to a C8-alkyne-dUTP the fluorescence intensity significantly increases when exposed to UV light.

Artificial metallo-nucleases (AMNs) were then clicked to alkyne-modified dNTPs. Again, conditions for the attachment of $6N_3$-*tris*-(2-picolyl)amine (TPMA) and $4N_3$-benzyl-di-(2-picolyl)amine (DPA) to dNTPs were optimised on short oligonucleotides before click reactions using C8-alkyne-dUTPs and dCTPs were performed (**Figure 27**). The reactions proceeded at 25 °C and 450 RPM for 6 hours before being quenched with 500 equivalents of EDTA. The EDTA sequesters the copper thereby removing all copper from the AMN caging ligand.[9] This library of modified dNTPs is then ready for enzymatic incorporation without the need for any purification steps.

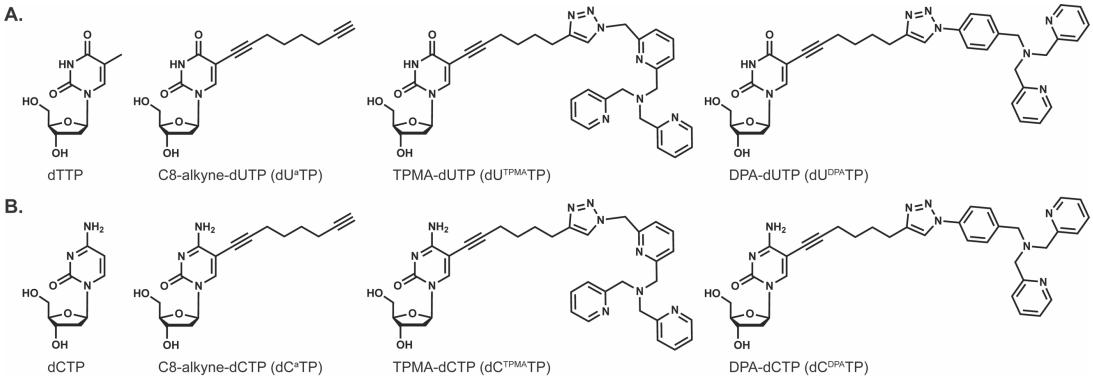


Figure 27: A. Natural thymidine base and uracil bases bearing alkyne, TPMA and DPA modifications. **B.** Library of natural and modified cytidine bases (triphosphates not shown for clarity).

4.3 Enzymatic synthesis of TFO

4.3.1 Incorporation of C8-alkyne-dNTPs

A poly-pyrimidine parallel-binding TFO was selected for this study. This TFO was designed to target a 32 base pair region of the eGFP gene (pCSanDI-HYG). This sequence contained a low number of consecutive C^+-GC triplets, as they are only stable at low pH,[10, 11] and had a minimum number of triplet inversion sites (*i.e.* G-CG), to prevent reduced triplex stability.[12] From previous analysis in the Kellett group it was shown that this unmodified TFO sequence can form a stable triplex (T_M > 45 ºC, ~pH 6).[9] Therefore, through the addition of stabilising moieties—such as a DNA intercalating agent—it was predicted that this TFO may be capable of forming a DNA triplex under physiological conditions.

Antigene oligonucleotides must be single-stranded and in this work it is desired that only a single DNA damaging agent (*i.e.* metallodrug) is present at a specific location within the oligonucleotide. Therefore the most suitable protocol for the enzymatic synthesis of the TFO is the single nucleotide incorporation-primer extension (SNI-PEX) method, followed by the use of streptavidin coated magnetic particles to isolate the TFO strand.[5] This protocol enables the synthesis of a single stranded oligonucleotide bearing a single modification at the desired position in the DNA sequence (**Figure 28**).

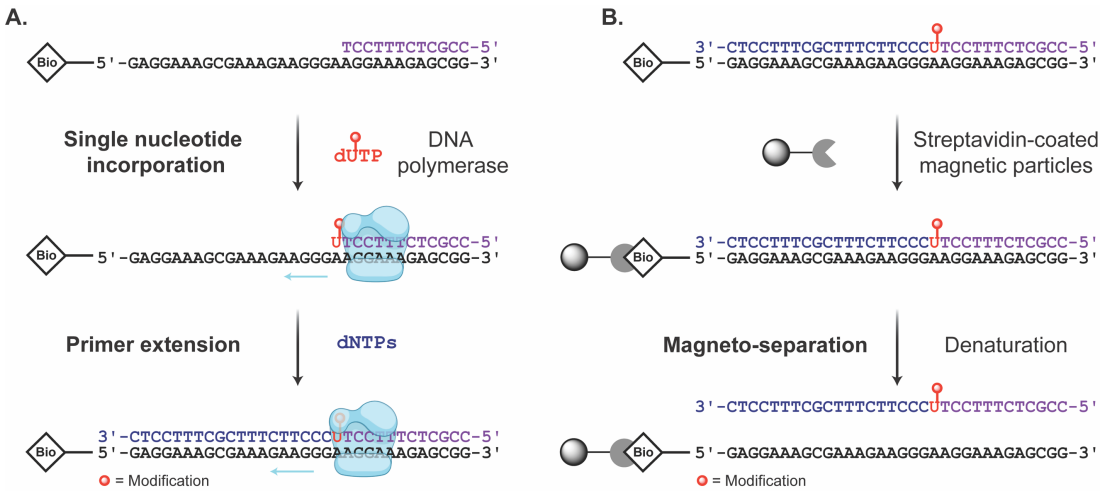


Figure 28: A. A template (black), complementary to the desired TFO sequence, and a short primer (purple), which will form the beginning of the TFO, are annealed. A modified dUTP (red) is then incorporated by a DNA polymerase (blue) immediately 3′ of the primer. The remainder of the sequence is then synthesised with natural dNTPs (dark blue). **B.** For an oligonucleotide to behave as a TFO it must be single stranded, therefore the template and newly synthesised DNA sequence must be separated. Streptavidin coated magnetic particles bind to the biotin-tag on the template, and then through the use of a magnet and a denaturation step the TFO can be isolated. DNA polymerase graphic was adapted from BioRender.

The incorporation of bases bearing large modifications can be challenging, therefore extensive optimisation of the SNI-PEX protocol was required to enable the incorporation of a single base with a variety of different modifications attached. Initially the SNI-PEX protocol was performed using the C8-alkyne-dUTPs (dU^{a}TP) to ensure they could be incorporated efficiently by a DNA polymerase. Vent (exo-) and Pwo DNA polymerases were investigated, but Vent (exo-) was found to be the most suitable due to the degradation observed when Pwo was present. Additionally, various equivalents of dUTP, polymerase concentrations, and incubation times were tested. The template and primer 1 (12 nt, **Table 2**) were incubated with 1.5 equivalents of dU^{a}TP and Vent (exo-) DNA polymerase in ThermoPol buffer at 60 °C and 450 RPM for 2.5 min. Samples were analysed by PAGE and the product was compared to positive (natural dTTP) and negative (no dNTP) controls. Full incorporation of the dU^{a}TP was observed (**Figure 29**). A similar procedure, but with a longer incubation, was followed for the incorporation of C8-alkyne-dCTPs (dC^{a}TP), 1.5 equivalents of dC^{a}TP was incubated at 60 °C and 450 RPM for 120 min.

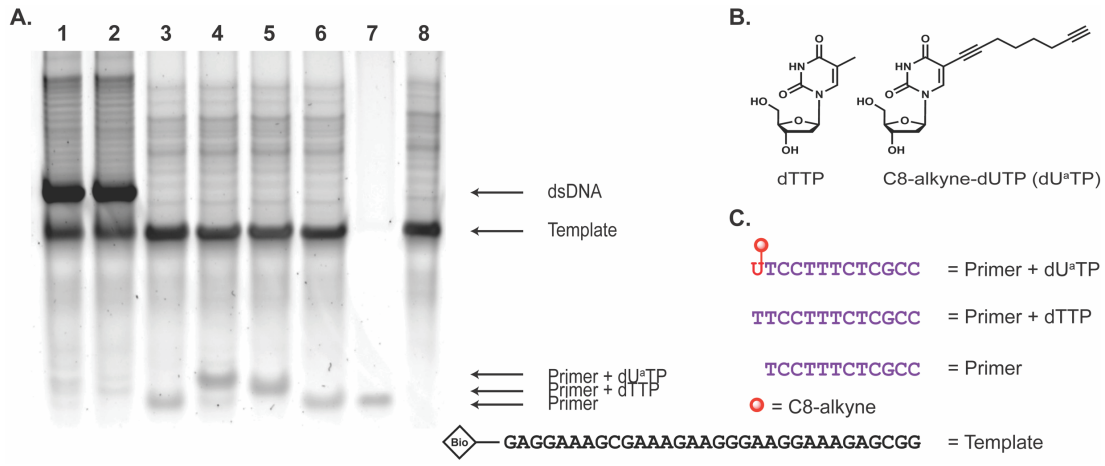


Figure 29: A. 20% denaturing PAGE: Lanes 1-3: SNI-PEX. Lane 1: Full length TFO with a single dU^{a}TP. Lane 2: positive control, TFO with all natural dNTPs. Lane 3: Negative control, SNI-PEX reaction in the absence of dTTPs and dUTPs, no full-length TFO is observed, which shows that Vent (exo-) has high base complementarity. Lanes 4-6: SNI, with no PEX. Lane 4: Primer with a single dU^{a}TP incorporated. Lane 5: Positive control, primer and single dTTP. Lane 6: Negative control, primer with no dNTP incorporated. Lane 7: Primer. Lane 8: Template. By comparing lanes 4, 5 and 6 the incorporation of a single dNTP can be visualised; as dU^{a}TPs were the only substrate available to the DNA polymerase, the increase in molecular weight visualised in lane 4 represents the addition of a single dU^{a}TP base to the primer. **B.** Structure of dTTP and C8-alkyne dUTP (dU^{a}TP) (triphosphates not shown for clarity). **C.** Sequences for DNA fragments labelled in the gel (image **A**).

4.3.2 Incorporation of dN^{TPMA}TPs

The products from the click chemistry reactions were next tested as substrates for DNA polymerases. dUTP clicked to the TPMA nuclease (dU^{TPMA}TP) (**Figure 27A**) was the first to be examined. The ability of five DNA polymerases (Vent (exo-), Therminator, Pwo, Taq and Sequenase V.2.0 DNA polymerase), to incorporate TPMA-modified dUTPs were tested. Each DNA polymerase (2.5 U) was incubated with template, primer (section 4.6.5, **Table 2**) and 1.5 equivalents of dU^{TPMA}TP in either the presence or absence of additional $MgSO_4$ (6.66 μM). $MgSO_4$ was added to ensure the EDTA present in the dU^{TPMA}TP click solution did not sequester Mg^{2+} present in the polymerase reaction buffer and thereby inhibit polymerase activity. Samples were incubated at 60 °C (excluding Sequenase, which was incubated at 37 °C) and 450 RPM for 30 min, and then analysed by denaturing PAGE (**Figure 30**). Pwo and Taq DNA polymerases (lane P and Ta) have 3′-5′ exonuclease activity, and the gel image suggests that this

proofreading ability results in DNA degradation. Therefore, both enzymes were deemed unsuitable for this SNI-PEX protocol. Vent (exo-), Therminator and Sequenase version 2.0 (hereafter Sequenase) are all capable of incorporating dU^{TPMA}TP. However, Therminator incorporates multiple non-templated nucleotides (**Figure 30**, lane Th, **Figure 31**). Further experiments with Therminator DNA polymerase were performed but under all conditions multiple dU^{TPMA}TPs were incorporated. Therefore, Vent (exo-) and Sequenase are the most suitable options. However, optimisation was required since Vent (exo-) incorporated two dU^{TPMA}TP bases, while the Sequenase samples contained unreacted primer.

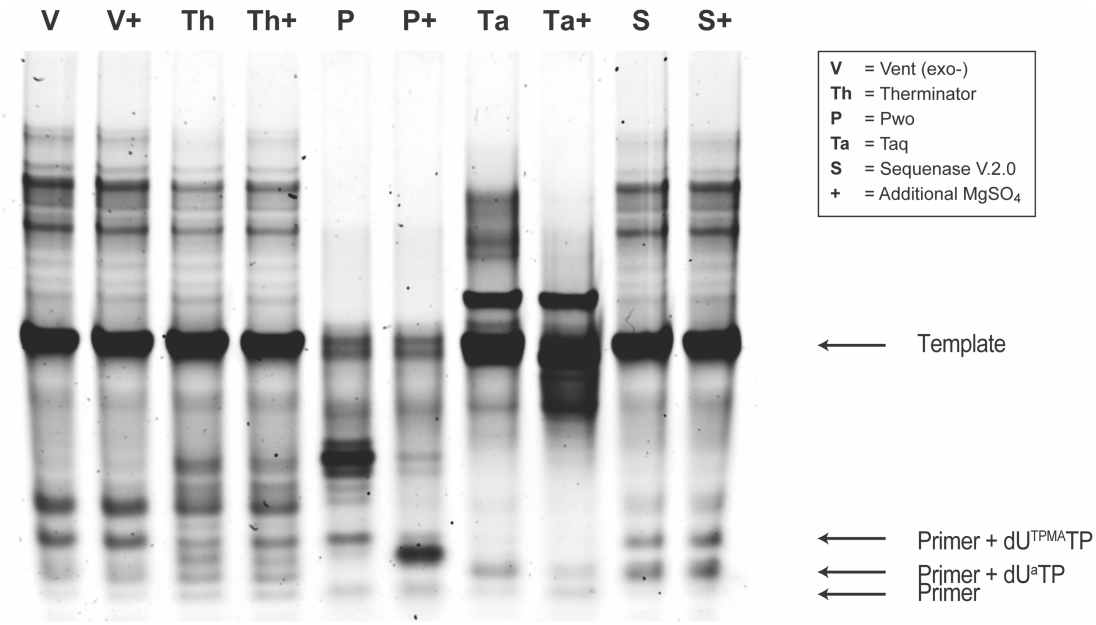


Figure 30: 20% denaturing PAGE analysis of products from SNI-PEX with five DNA polymerases. Pwo and Taq DNA polymerases are not suitable due to the degradation pattern observed. Vent (exo-), Therminator and Sequenase DNA polymerases were capable of incorporating a dU^{TPMA}TP, however Vent (exo-) and Therminator incorporated multiple bases, while excess non-reacted primer remained in the Sequenase samples.

As Sequenase did not achieve complete incorporation after 30 min, a longer incubation time (60 min) was tested. Again there was a dense band showing the unreacted primer but also a band representing incorporation of two dU^{TPMA}TPs, the second of which is non-templated (appendix, **Figure B - 1**). This

suggests that Sequenase is not suitable for this task. Further optimisation with Vent (exo-) was successful. When Vent (exo-) DNA polymerase was incubated with template, primer 1, 1.5 equivalents of $dU^{TPMA}TP$, and $MgSO_4$ in ThermoPol buffer at 60 °C and 450 RPM for 90 min, a single $dU^{TPMA}TP$ is incorporated immediately 3′ of the primer (**Figure 32**). Therefore Vent (exo-) DNA polymerase was selected for future $dN^{TPMA}TP$ incorporations. This work was included and expanded upon in Chapter 6.

4.3.3 Incorporation of $dN^{DPA}TPs$

The suitability of Sequenase, Therminator and Vent (exo-) DNA polymerases for the incorporation of DPA-modified dUTPs ($dU^{DPA}TP$) were tested using the conditions previously described. Sequenase again was inefficient at incorporating the modified dUTPs and a large concentration of unreacted primer remained after a 90 min incubation. When therminator DNA polymerase was tested, multiple non-templated $dU^{DPA}TP$ bases (**Figure 31**) were present and the major product was the primer with 3 additional bases. Vent (exo-) DNA polymerase also incorporated multiple non-templated bases but at short incubation times (5-10 min). The major products were the primer with the desired base incorporated, along with the primer with one templated and one non-templated base (appendix **Figure B - 2**). Therefore all further optimisation was performed with Vent (exo-) DNA polymerase.

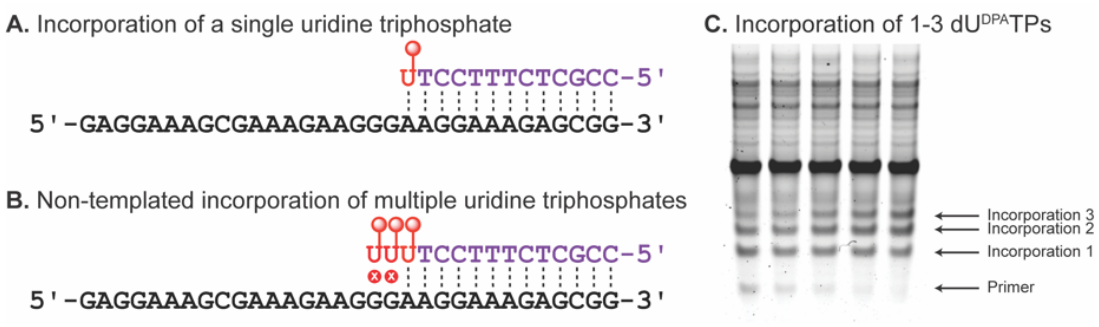


Figure 31: A. Incorporation of a single modified nucleotide at the desired position in the TFO sequence. **B.** An additional two uridine nucleotide triphosphates are incorporated. These are non-templated as they will not form Watson-Crick bonds with the guanine bases on the complementary strand. **C.** PAGE analysis showing templated (incorporation 1) and two non-templated (incorporations 2 and 3) incorporation of dU^{DPA}TP.

In an attempt to limit the incorporation of non-templated bases by Vent (exo-) DNA polymerase short incubation times (≥ 1 min), low concentrations of polymerase, and 1 equivalent of dU^{DPA}TP to primer were tested. Unfortunately no suitable products were obtained. Next, altering the reaction conditions to disfavour polymerase efficiency were considered. By lowering the incubation temperature from 60 °C to 37 °C a maximum of two dU^{DPA}TPs were incorporated (appendix **Figure B - 3**). It was therefore decided to investigate lower temperatures. A 20 °C incubation yielded excellent results with one base added to the primer when template, primer 1, Vent (exo-) DNA polymerase, and 1.5 equivalents of dU^{DPA}TP were present at 450 RPM for 90 min. These conditions were also suitable for the incorporation of dC^{DPA}TP (**Figure 32**). This led to the research presented in Chapter 5, and is included in a publication that is under review.[13]

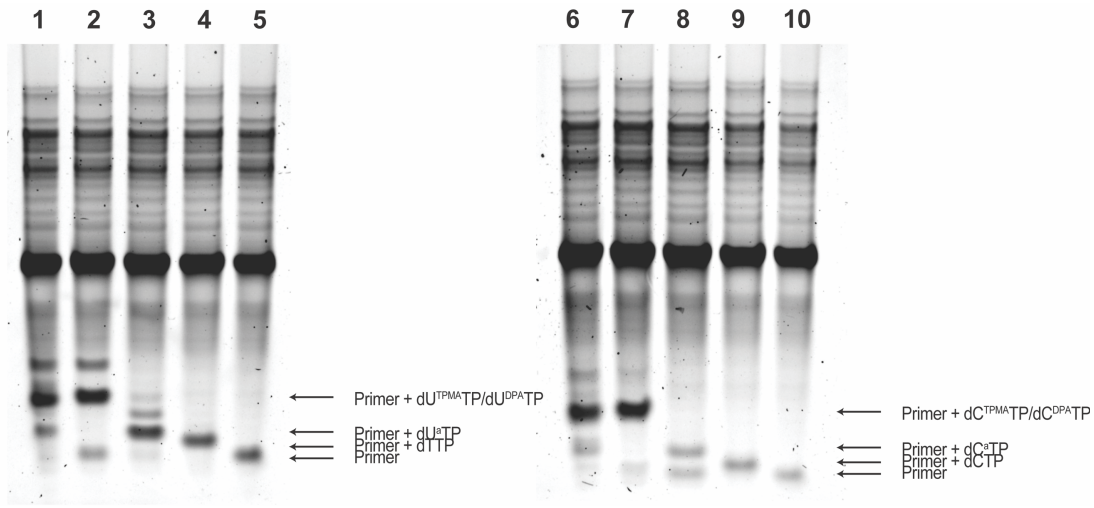


Figure 32: Denaturing PAGE (20%) analysis of SNI-PEX products. Lanes 1-5: Primer 1 (12 nt) and dUTP incorporation. Lanes 6-10: Primer 2 (10 nt) and dCTP incorporation. Lanes 1, 6: Incorporation of $dN^{TPMA}TP$. Lanes 2, 7: SNI-PEX with $dN^{DPA}TP$. Lanes 3, 8: Incorporation of $dN^{a}TP$. Lanes 4, 9: Primer with natural dTTP or dCTP. Lanes 5, 10: Negative control, no incorporation has occurred.

The internal and terminal (3′) incorporation of $dC^{TPMA}TPs$ and $dC^{DPA}TPs$ was relatively straightforward to achieve once optimisation of SNI-PEX methods with modified dUTPs was complete. Identical conditions as detailed above (1.5 equivalents, 60°C, and 450 RPM for 90 min) were suitable for the incorporation of $dC^{TPMA}TP$ at both internal and terminal sites in the TFO sequence. While the incorporation of $dC^{DPA}TP$ at an internal position was identical to dUTP conditions (1.5 equivalents, 20 °C and 450 RPM for 90 min), terminal incorporation could be performed at both 60 °C and 20 °C as no site for non-templated incorporation was available.

For TFO sequences bearing internal modifications, the remainder of the oligonucleotide was then synthesised. This was achieved by adding a high concentration of natural dNTPs (dCTP, dGTP, dTTP and dATP) to the SNI-PEX reaction mix—essentially saturating the modified base—and extending the primer-dNTP, by incubating the reaction at 60 °C and 450 RPM for 20 min. The reaction was then stopped by cooling to 4 °C.

4.4 Streptavidin Beads

For an oligonucleotide to act as an antisense or antigene therapeutic it must be single stranded. Following the SNI-PEX reaction the product is double-stranded, and therefore the strands must be separated with only newly synthesised ssDNA collected (**Figure 28B**). The biotin-streptavidin interaction can be employed for this task; the use of a biotinylated template and streptavidin coated magnetic particles enables the isolation of either strand. However, conditions which allow for the separation of the two strands of the dsDNA while maintaining the integrity of the streptavidin-biotin bond had to be identified. Methods that had been previously reported[5, 14, 15] were not suitable for this task due to the high melting temperature of the duplex (~85 °C). When the DNA solution was heated to denature the dsDNA the streptavidin-biotin bond also denatured, resulting in a high concentration of unwanted double stranded DNA being present in the product. It was reported that streptavidin-biotin bonds are easily broken in water at temperatures ≥70 °C,[16] but that the use of buffers such as Tris and salts can stabilise the bond at high temperatures. Tris buffers ranging from 10 mM to 250 mM with various NaCl and $MgCl_2$ concentrations were investigated. It was found that 100 mM Tris, 10mM $MgCl_2$, at pH 7.5 was the most suitable, but only low yields of TFO were obtained. Therefore, efforts to decrease the melting temperature of the TFO-template dsDNA, and subsequently increase the yield, were investigated. Various concentrations of NaOH (0.1-1 M), DMSO (10-70%) and formamide (50-95%) were tested to no success. As the presence of salts is known to impact the melting temperature of DNA[17-20] the use of salts was re-visited, and various less common salts were tested. Sodium pyrophosphate was found to be capable of lowering the melting temperature of the dsDNA to ~61 °C, which is below the streptavidin-biotin threshold. Therefore a denaturation step at 65 °C for 1.5 min could be performed and the TFO was successfully isolated with 50-65% yields.

4.5 Conclusion

A method that combined nucleic acid click chemistry and enzymatic synthesis has been reported for the production of modified oligonucleotides. A library of dNTPs bearing large modifications was generated through the CuAAC reaction, and SNI-PEX was chosen as the synthetic protocol as it enabled a single modified dNTP to be incorporated at a specific sequence position. The ability of five DNA polymerases to incorporate the modified nucleotides was investigated, and it was noted that DNA polymerases with exonuclease activity were not suitable for the task, as the long incubation times required resulted in DNA degradation. Vent (exo-) DNA polymerase was found to be capable of incorporating all the modified dNTPs while maintaining sequence integrity, and consequently it was utilised in the enzymatic synthesis of the modified triplex forming oligonucleotides (TFOs). Once the TFOs were synthesised there were challenges isolating them from their template and reaction components, but the high melting temperature of the TFO-template dsDNA was overcome with the use of sodium pyrophosphate. The SNI-PEX methodology reported overcomes the limitations of SPS synthesis, as theoretically any modification can be included, and the protocol can be adapted for the bench-top synthesis of any DNA sequence.

4.6 Experimental

4.6.1 General information

PAGE gels were cast using a SureCast™ gel casting system (Invitrogen) and SureCast™ acrylamide solution (Invitrogen), and run in an Invitrogen mini gel tank. A Bio-Rad basic Power Pac™ was used for PAGE gel electrophoresis. All gels were imaged using a Syngene G:Box 9 mini gel documentation system.

Raw gel images are available to download on Google drive: https://drive.google.com/drive/folders/1tu199tKFWnem-pHC3Suwn_c1pU1_YWMs?usp=sharing

4.6.2 Triplex forming oligonucleotide

A plasmid containing a green fluorescent protein (GFP) gene was chosen as the TFO target as it enables gene silencing to be easily visualised when *in cellulo* experiments are performed. The TFO sequence chosen was 32 nucleotides in length and contained two G inversion sites within the pyrimidine sequence. This TFO sequence bearing an alkyne modification has previously been studied within the Kellett research group and was found to have a melting temperature >45 °C.[9] This enables biophysical studies to be performed under physiological conditions.

4.6.3 Click chemistry with short oligonucleotides

Under inert conditions 5′-octadiynyl oligonucleotide (25 μL, 200 μM, sequence: 5′-XCCCGTTTCCTCTTCTT-3′, where X = 5′-Octadiynyl), $3N_3$-7-hydroxycoumarin/ $6N_3$-*tris*-(2-picolyl)amine ($6N_3$-TPMA)/ $4N_3$-benzyl-*di*-(2-picolyl)amine (DPA) (1-5 eq., 2 mM), Na-*L*-ascorbate (5 μL, 5 mM) and pre-mixed Cu(II)SO_4-TBTA (5 μL, 5 mM) were mixed in a total volume of 250 μL (1:1 water to DMSO). Reaction proceeded at 25 °C and 450 RPM for 3, 6, 24, or 48 hours. The 'click' reaction was stopped through the addition of EDTA (100 mM, 125 μL), which sequesters the copper. 2 μL of the product was mixed with loading dye (6X, 10 mM Tris-HCl, pH 7.6, 0.03% bromophenol blue, 0.03% xylene cyanol FF,

60% glycerol, 60 mM EDTA) and run on a 20% native polyacrylamide gel (1X TBE) at 70 V for 240 min, and post-stained with SYBR gold.

4.6.4 Click Chemistry with dNTPs

In an anaerobic environment a copper catalysed azide-alkyne cycloaddition (CuAAC) reaction mixture (5 nmol) between a C8-alkyne-dUTP/dCTP (BaseClick) and $3N_3$-7-hydroxycoumarin/$6N_3$-TPMA/$4N_3$-benzyl-DPA was prepared as described in **Table 1**, in water and DMSO (1:1) to a total volume of 250 μL. Reaction proceeded at 25 °C and 450 RPM for 6 hours, and was quenched with 500 equivalents of EDTA and stored at -20 °C.

Table 1: Concentration of azide and alkyne for CuAAC.

	Alkyne concentration	Azide concentration
$3N_3$-7-hydroxycoumarin	5 nmol	7.5 nmol
$6N_3$-TPMA	5 nmol	10 nmol
$4N_3$-benzyl-DPA	5 nmol	7.5 nmol

4.6.5 SNI-PEX for PAGE

The reaction mixture (10 μL) contained; primer (X nt, 10 μM, 1.35 μL, **Table 2**), 5′-biotinylated template (32 nt, 10 μM, 1.35 μL, **Table 2**), click-functionalised dNTP (13.3 μM, 1.52 μL), $MgSO_4$ (100 mM, 0.4 μL, NEB) and Vent (exo-) DNA polymerase (2 U/μL, 0.5 μL, NEB) in ThermoPol buffer (10 X, 1 μL, NEB). Reaction solution was incubated at 20/60 °C and 450 RPM for X min (**Table 3**). Natural dNTPs (10 mM, 1.35 μL, NEB) were added and a further 20 min incubation at 60 °C and 450 RPM was performed. Loading dye (6X, 10 mM Tris-HCl, pH 7.6, 0.03% bromophenol blue, 0.03% xylene cyanol FF, 60% glycerol, 60 mM EDTA) was added to stop the reaction and the entire solution was loaded onto a 20% denaturing PAGE gel (1 X TBE), and run at 150 V for 160 min. The gel was post-stained with SYBR gold.

Table 2: SNI-PEX primer and template sequences. Phos = phosphate, Bio = Biotin

	Length	Sequence (5'-3')
Primer 1	12 nt	CCGCTCTTTCCT
Primer 2	10 nt	CCGCTCTTTC
Template	32 nt	Bio-GAGGAAAGCGAAAGAAGGGAAGGAAAGAGCGG

Table 3: Incubation time and temperature for functionalised-dNTPs

Modified Base	Temperature	Time
Alkyne dUTP	60 °C	2.5 min
Alkyne dCTP	60 °C	120 min
TPMA-dUTP	60 °C	90 min
TPMA-dCTP	60 °C	90 min
DPA-dUTP	20 °C	90 min
DPA-dCTP	20 °C	90 min

4.6.6 SNI-PEX for TFO synthesis

The reaction mixture (200 μL) contained; primer (X nt, 10 μM, 27 μL, **Table 2**), 5′-biotinylated template (32 nt, 10 μM, 27 μL), click-functionalised dNTP (13.3 μM, 30.4 μL), $MgSO_4$ (100 mM, 8 μL, NEB) and Vent (exo-) DNA polymerase (2 U/μL, 10 μL, NEB) in ThermoPol buffer (10 x, 20 μL, NEB). The reaction mixture was incubated at 20/60 °C and 450 RPM as described in **Table 3**. Natural dNTPs (10 mM, 27 μL, NEB) were added and a further 20 min incubation at 60 °C and 450 RPM was performed, before cooling to 4 °C to stop the reaction.

4.6.7 Streptavidin-biotin magneto-separation of TFO

Streptavidin magnetic particles (100 μL, Roche) were washed three times with TEN_{100} (200 μL; 10 mM Tris, 1 mM EDTA, 100 mM NaCl, pH 7.5), and resuspended in TEN_{100} (50 μL). SNI-PEX solution (200 μL) was added and incubated at 18 °C and 1200 RPM for 20 min. Particles were collected on a magnet and solution was discarded. Particles were washed three times with TEN_{1000} (200 μL; 10 mM Tris, 1 mM EDTA, 1 M NaCl, pH 7.5), and then washed four times with elution buffer (200 μL; 100 mM sodium pyrophosphate). Particles were resuspended in elution buffer (100 μL), and double stranded DNA was denatured (65 °C for 90 sec). Particles were collected on a magnet and the solution, containing the single stranded TFO, was collected. TFO was de-salted using Sephadex™ G-25 grade gravity filtration columns (NAP-5™, Cytiva illustra™).

References

1. Caruthers, M., Gene synthesis machines: DNA chemistry and its uses. *Science* **1985,** *230* (4723), 281-285.
2. Beaucage, S. L.; Caruthers, M. H., Deoxynucleoside phosphoramidites—A new class of key intermediates for deoxypolynucleotide synthesis. *Tetrahedron Lett.* **1981,** *22* (20), 1859-1862.
3. Hocek, M., Synthesis of base-modified 2'-deoxyribonucleoside triphosphates and their use in enzymatic synthesis of modified DNA for applications in bioanalysis and chemical biology. *J. Org. Chem.* **2014,** *79* (21), 9914-21.
4. Langer, P. R.; Waldrop, A. A.; Ward, D. C., Enzymatic synthesis of biotin-labeled polynucleotides: novel nucleic acid affinity probes. *Proc. Natl. Acad. Sci.* **1981,** *78* (11), 6633-7.
5. Menova, P.; Cahova, H.; Plucnara, M.; Havran, L.; Fojta, M.; Hocek, M., Polymerase synthesis of oligonucleotides containing a single chemically modified nucleobase for site-specific redox labelling. *Chem. Comm.* **2013,** *49* (41), 4652-4.
6. Leone, D. L.; Hubálek, M.; Pohl, R.; Sýkorová, V.; Hocek, M., 1,3-Diketone-Modified Nucleotides and DNA for Cross-Linking with Arginine-Containing Peptides and Proteins. *Angew. Chem. Int. Ed.* **2021**.
7. Güixens-Gallardo, P.; Hocek, M., Acetophenyl-thienyl-aniline-Linked Nucleotide for Construction of Solvatochromic Fluorescence Light-Up DNA Probes Sensing Protein-DNA Interactions. *Chem. Eur. J.* **2021,** *27* (24), 7090-7093.
8. Seela, f.; Sirivolu, V. R.; Chittepu, P., Modification od DNA with Octadiynyl Side Chains: Synthesis, Base Pairing, and Formation of Fluorescent Coumarin Dye Conjugates of Four Nucleobases by the Alkyne-Azide “Click” Reaction. *Bioconjug. Chem.* **2008,** *19*, 211-224.
9. Zuin Fantoni, N.; McGorman, B.; Molphy, Z.; Singleton, D.; Walsh, S.; El-Sagheer, A. H.; McKee, V.; Brown, T.; Kellett, A., Development of Gene-Targeted Polypyridyl Triplex-Forming Oligonucleotide Hybrids. *Chembiochem* **2020,** *21*, 3563-3574.
10. Faria, M.; Giovannangeli, C., Triplex-forming molecules: from concepts to applications. *J. Gene Med.* **2001,** *3* (4), 299-310.
11. Fox, K. R.; Brown, T., Formation of stable DNA triplexes. *Biochem. Soc. Trans.* **2011,** *39* (2), 629-634.
12. Wang, E.; Malek, S.; Feigon, J., Structure of a G.T.A triplet in an intramolecular DNA triplex. *Biochem.* **1992,** *31*, 4838-4846.
13. McGorman, B.; Zuin Fantoni, N.; O’Carroll, S.; Ziemele, A.; El-Sagheer, A. H.; Brown, T.; Kellett, A., Enzymatic synthesis of chemical nucelase triple-forming oligonucleotides with gene-editing applications. *Manuscript under review*.
14. Matyasovsky, J.; Pohl, R.; Hocek, M., 2-Allyl- and Propargylamino-dATPs for Site-Specific Enzymatic Introduction of a Single Modification in the Minor Groove of DNA. *Chemistry* **2018,** *24* (56), 14938-14941.
15. Panattoni, A.; Pohl, R.; Hocek, M., Flexible Alkyne-Linked Thymidine Phosphoramidites and Triphosphates for Chemical or Polymerase Synthesis and Fast Postsynthetic DNA Functionalization through Copper-Catalyzed Alkyne-Azide 1,3-Dipolar Cycloaddition. *Org Lett* **2018,** *20* (13), 3962-3965.

16. Holmberg, A.; Blomstergren, A.; Nord, O.; Lukacs, M.; Lundeberg, J.; Uhlen, M., The biotin-streptavidin interaction can be reversibly broken using water at elevated temperatures. *Electrophoresis* **2005,** *26* (3), 501-10.
17. Kellett, A.; Molphy, Z.; Slator, C.; McKee, V.; Farrell, N. P., Molecular methods for assessment of non-covalent metallodrug-DNA interactions. *Chem. Soc. Rev.* **2019,** *48* (4), 971-988.
18. Tan, Z.-J.; Chen, S.-J., Nucleic Acid Helix Stability: Effects of Salt Concentration, Cation Valence and Size, and Chain Length. *Biophys. J.* **2006,** *90* (4), 1175-1190.
19. Owczarzy, R.; You, Y.; Moreira, B. G.; Manthey, J. A.; Huang, L.; Behlke, M. A.; Walder, J. A., Effects of Sodium Ions on DNA Duplex Oligomers: Improved Predictions of Melting Temperatures. *Biochem.* **2004,** *43* (12), 3537-3554.
20. Schildkraut, C.; Lifson, S., Dependence of the melting temperature of DNA on salt concentration. *Biopolymers* **1965,** *3* (2), 195-208.

Chapter 5

Enzymatic synthesis of chemical nuclease triplex-forming oligonucleotides with gene-editing applications

This chapter is written as a research article as the work enclosed within has been submitted for publication.

My contribution to this paper included; the production of DPA-dUTPs through nucleic acid click chemistry; the enzymatic synthesis of the novel DPA-TFO hybrids; and analysis of the sequence selectivity and DNA damaging properties of the DPA-hybrids. The synthesis of $4N_3$-benzyl-DPA was performed in collaboration with Dr. Nicolò Zuin Fantoni.

5.1 Abstract

Triplex forming oligonucleotides (TFOs) are short, single-stranded oligomers that hybridise to a specific sequence of duplex DNA. TFOs can block transcription and thereby inhibit protein production, which makes them highly appealing in the field of antigene therapeutics. In this work, a primer extension protocol was developed to enzymatically prepare chemically modified TFO hybrid constructs with gene-silencing applications. Click chemistry was employed to generate novel artificial metallo-nuclease (AMN)-dNTP hybrids, which were selectively incorporated into the TFO strand by a DNA polymerase. The protocol was then extended to facilitate the construction of 5-methylcytosine modified TFOs, which enabled superior target binding affinity. The utility of the AMN-TFOs was assessed through polyacrylamide gel electrophoresis, quantitative PCR, and Sanger sequencing, which revealed selective recognition and damage to a target gene of interest. To our knowledge, this is the first example of the enzymatic production of an AMN-TFO hybrid. These results indicate how chemical nuclease-TFOs may overcome limitations associated with non-molecularly targeted metallodrugs and open new avenues for artificial gene editing technology.

5.2 Introduction

There is major interest in targeting the human genome with directed nucleases for genetic engineering and knockout applications. A nuclease is an enzyme that can cleave DNA into its individual components and they have been exploited in several breakthrough technologies, such as zinc finger nucleases (ZFNs),[1] transcription activator-like effector nucleases (TALENs),[2] and clustered regularly interspaced short palindromic repeats (CRISPR),[3] with CRISPR/Cas-9 now considered the gold standard for gene editing. Synthetic chemical nucleases offer an intriguing alternative to these technologies as they provide greater flexibility and offer multiple avenues for gene silencing—including oxidative strand scission. Here, we present the first example of an enzymatically synthesised chemical nuclease-TFO hybrid and demonstrate its utility as a targeted gene knockout agent.

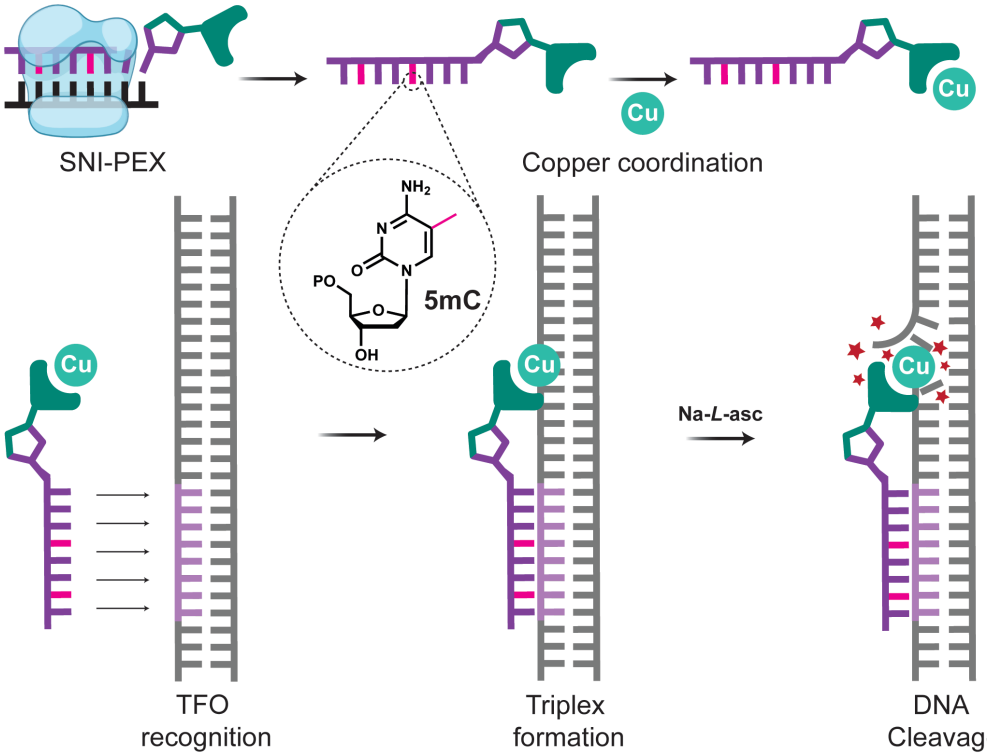


Figure 33: Enzymatic synthesis concept for the DPA-5mC-TFO hybrid and proceeding steps for targeted DNA cleavage: i.) DNA polymerase synthesises DPA-TFO; ii.) Cu(II) coordinates to the DPA ligand; iii.) Cu(II)-DPA-TFO recognises target duplex; iv.) TFO hybridises to duplex forming triple helical DNA; and v.) Na-*L*-ascorbate activates the AMN to trigger DNA cleavage.

Artificial metallo-nucleases (AMNs) were first reported by Sigman *et al.*[4] when it was found that $[Cu(1,10\text{-phenantroline})_2]^{2+}$ (Cu-Phen) could semi-intercalate and oxidise DNA from the minor groove in the presence of a reductant.[4, 5] This led to the development of a variety of AMNs including bis-chelate Cu^{2+} phenanthroline-phenazine complexes[6, 7] and, more recently, polypyridyl copper-binding AMN architectures that accommodate designer intercalators.[8-12] The copper-caging polypyridyl ligand *di*-(2-picolyl)amine (DPA) was selected for this study as it recently demonstrated superior DNA binding and cleaving activity[8] compared to the sterically crowded *tris*-(2-pyridylmethyl)amine (TPMA) caging scaffold[9]. One of the major limitations of synthetic nucleases—including Cu(II) complexes of DPA and TPMA—is their promiscuity as stand-alone compounds displaying random cleavage (or shearing) of DNA. Extensive

research has therefore been performed to direct AMNs to specific genetic elements,[13-18] including the use of DNA binding proteins, polyamides, and polynucleotides, but these technologies require laborious synthetic routes which has stunted their practicality. The advent of click chemistry[19] provided an alternative synthetic strategy and recently the attachment of metallodrugs to antigene triplex forming oligonucleotides (TFOs) has been successful.[20-23] TFOs are short single stranded oligonucleotides that can hybridise with duplex DNA and inhibit protein production at the genomic level.[24] AMN-TFO hybrids are of significant interest as they can easily be adapted to any genetic target through simple modification of the TFO sequence.

Solid-phase oligonucleotide synthesis (SPS)[25, 26] is widely used for the production of short oligonucleotides but it is not compatible with modifications that are susceptible to oxidation or that are reactive with nucleophiles.[27] This limits the functionality of SPS in the production of oxidatively active antigene therapeutics as the AMN unit must be post-synthetically attached to the TFO. Nucleic acid click chemistry[28, 29] offers a relatively simple method for this attachment but introduces an additional synthetic step and purification to isolate the desired product.[20-22]

Here, nucleic acid click chemistry was combined with a modified primer extension (PEX) protocol—known as single nucleotide incorporation-primer extension (SNI-PEX)[30]—to enzymatically synthesise a novel DPA-TFO hybrid (**Figure 33**). The enzymatic synthesis of DNA *in vitro* is not a new phenomenon and the use of polymerases to synthesise modified DNA was first reported by Langer *et al.* in 1981.[31] However, it was not until 2013 when the Hocek group reported the SNI-PEX protocol[30] that the enzymatic synthesis of AMN-TFO hybrids became a possibility. Recently, the PEX synthesis of oligonucleotides bearing crosslinking agents[32] and redox labels[33] have been reported thereby indicating the expanding possibilities of this technology. In the current work, the copper-catalysed azide-alkyne cycloaddition (CuAAC)[34, 35] was employed to generate novel DPA-modified nucleotide triphosphates, which were then incorporated into the TFO sequence using a DNA polymerase. To our knowledge this is the first example of the enzymatic synthesis of an AMN-TFO hybrid. The sequence selectivity and targeted DNA damaging capabilities of these PEX DPA-

TFO hybrids was then studied using a variety of molecular and biophysical methods, and their functionality was compared to a SPS post-synthetic click counterpart that also contains the DPA ligand. The SNI-PEX method was then extended to generate higher-order hybrids containing a heavily modified 5mC sequence with enhanced stability and target binding properties.

5.3 Results and Discussion

5.3.1 Synthesis of 4N_3-Benzyl-DPA.

A synthetic route to introduce an azide-modification into the copper binding polypyridyl DPA ligand was developed (**Figure 34A**). A synthetic strategy was designed with the aim of: i.) using canonical 'click' reaction conditions (modularity, insensitivity toward oxygen and water, regiospecificity and stereospecificity); ii.) green chemistry considerations (employment of safer solvents, chemicals, and easily removable catalysts or reactants); and iii.) enabling potential industrial up-scalability. DPA was treated with 4-nitrobenzyl bromide to form **1**. The azide group was introduced by reducing the NO_2 group to an amine followed by a diazotransfer reaction on the N-4-amminobenzyl linker of **2** (see section 5.5.2). The use of NaS_2 in the nitro- to amine-reduction provided an alternative pathway avoiding the requirement for potentially pyrophoric and oxygen sensitive conditions such as those typical of palladium on carbon hydrogenations. Similarly, the use of 2-azido-1,3-dimethylimidazolinium hexafluorophosphate (ADMP) provided a safer alternative to sodium azide, which is the common reactant in canonical azidation reactions.

5.3.2 Enzymatic synthesis of DPA-TFO hybrids.

An SNI-PEX method was developed to enable the incorporation of dNTPs bearing large modifications, such as the DPA ligand. The first step for this enzymatic synthesis was to generate the novel DPA-modified uridine triphosphates (dU^{DPA}TPs) (**Figure 34B**). The Cu(I)-catalysed azide-alkyne cycloaddition (CuAAC) reaction[34, 35] was selected for this task as it can be performed rapidly, at room temperature, and in either organic solvents or

aqueous media. This enabled the reaction between the $4N_3$-benzyl-DPA and C8-alkyne-dUTP ($dU^{a}TP$) to be performed within 6 hours without any specialised equipment and in a system that was compatible with the next step of the synthetic protocol, alleviating the need for a purification step. The click reaction was quenched with EDTA and the newly formed $dU^{DPA}TPs$ were ready to be incorporated into the TFO strand. A sample of the $dU^{DPA}TPs$ was removed, purified by HPLC, and analysed by mass spectrometry to ensure the desired product was present (appendix **Figure C - 16**).

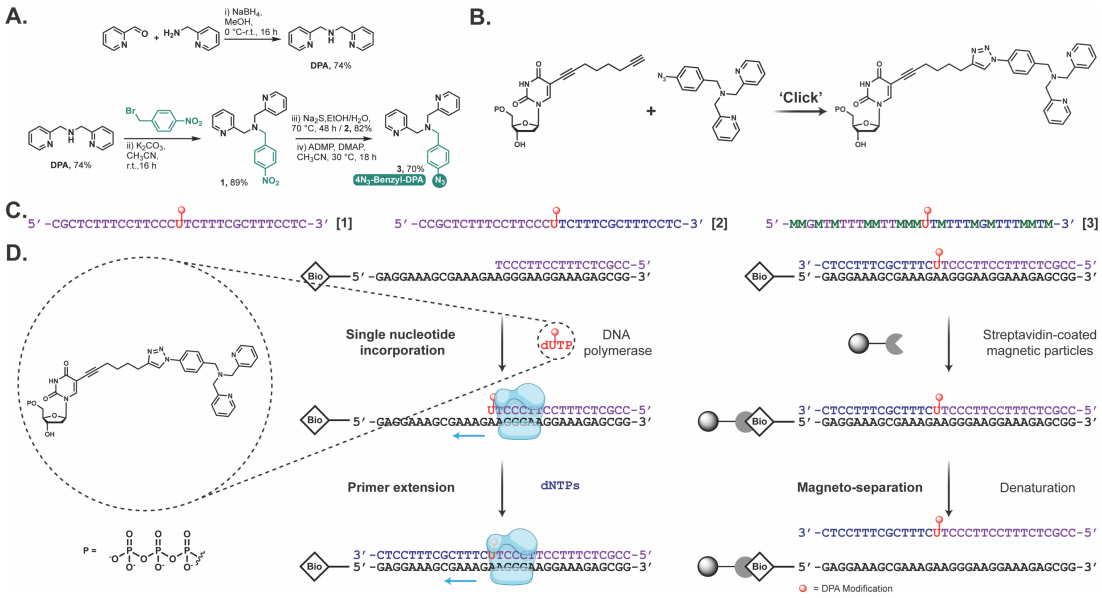


Figure 34: A. Synthesis of $4N_3$-benzyl-DPA **B.** Scheme of click reaction between C8-alkyne-dUTP and $4N_3$-benzyl-DPA to form a DPA-dUTP ($dU^{DPA}TP$). **C.** Sequence of SPS DPA-TFO1, SNI-PEX DPA-TFO2 and SNI-PEX DPA-5mC-TFO3, where M = 5mC. **D.** Template (black)—complementary to the desired TFO sequence—and a short primer (purple)—that will form the start of the TFO—are annealed. $dU^{DPA}TP$ (red) is then incorporated by a DNA polymerase (blue) immediately 3′ of the primer. The remainder of the sequence is then synthesised with natural dNTPs (dark blue). For an oligonucleotide to behave as a TFO it must be single stranded, therefore the template and newly synthesised TFO sequence must be separated. Streptavidin coated magnetic particles bind to the biotin-tag on the template, then using a magnet and a denaturation step the TFO can be isolated.

A poly-pyrimidine parallel-binding TFO was selected for this study. This TFO was designed to target a 32 base pair region of the eGFP gene (pCSanDI-HYG). The targeted region contains a low number of consecutive C^{+}-GC triplets

as they are only stable at low pH[36, 37] and contains a minimum number of triplet inversion sites (*i.e.* G-CG) to prevent reduced triplex stability (appendix **Table C - 2**).[38] In previous analysis it was shown that this unmodified TFO sequence can form a stable triple helix at ~pH 6 (T_M > 45 ºC)[20] and, in theory, this pH dependency should be overcome through the incorporation of 5mC bases in the TFO sequence.[39]

A biotinylated template strand complementary to the TFO sequence and a primer, which forms the beginning of the TFO, were required for SNI-PEX. The template and primer were annealed in the presence of a DNA polymerase, and the modified nucleotide was incorporated immediately after the primer (**Figure 34C**). However, the incorporation of a nucleotide bearing the large DPA modification required significant optimisation. The suitability of various DNA polymerases, including Sequenase V.2.0, Therminator, and Vent (exo-) was investigated. Template, primer and dU^{DPA}TP were incubated with each DNA polymerase in their recommended buffer. Sequenase V.2.0 was inefficient at incorporating the dU^{DPA}TP and a large concentration of unreacted primer remained after 90 minutes of incubation. When therminator DNA polymerase was tested, multiple non-templated dU^{DPA}TP bases were present (appendix **Figure C - 17**) and the major product was the primer with three additional bases. Vent (exo-) DNA polymerase also incorporated multiple non-templated bases but with short incubation times (5-20 min) the major products were the primer with the desired dU^{DPA}TP incorporated along with the primer with one templated and one non-templated base (appendix **Figure C - 18**). Therefore, further optimisation was performed with Vent (exo-) DNA polymerase. In an attempt to limit the incorporation of non-templated bases by Vent (exo-) short incubation times (≥ 1 min), low concentrations of polymerase, and 1 equivalent of dU^{DPA}TP to primer were tested. Unfortunately, no suitable products were obtained. Next, altering the reaction conditions to disfavour polymerase efficiency were considered. By lowering the reaction temperature from 60 °C to 37 °C a maximum of two dU^{DPA}TPs were incorporated and further optimisation at 37 °C (section 5.5.3) yielded the desired product—the primer with a single dU^{DPA}TP incorporated (**Figure 35A**). The remainder of the oligonucleotide was then synthesised by adding a high concentration of natural dNTPs (dCTP, dGTP, dTTP and dATP) to

the SNI-PEX reaction mixture—essentially saturating the modified base—and extending the primer-dU^{DPA}TP strand. This SNI-PEX protocol was then repeated for the synthesis of a methylated TFO; in this instance the natural dCTPs were replaced with 5-methyl-dCTPs (5mC) and thus every cytosine base in the sequence was methylated. Next, the newly synthesised TFOs were isolated from their template and reaction components. Streptavidin coated magnetic particles were employed for this task, but significant optimisation was required. Conditions previously reported[22, 30, 40, 41] were not suitable due to the high melting temperature of the TFO-template duplex (~85 °C) and the instability of the streptavidin-biotin interaction above 70 °C.[40] Therefore, conditions that lower the melting temperature of dsDNA, but do not impact the streptavidin-biotin bonds were required. Since the presence of salts is widely known to affect the melting temperature of DNA,[42-45] various buffers containing NaCl and $MgCl_2$, along with concentrations of NaOH, DMSO, and formamide were tested to no success. Next, the impact of several less commonly used salts was investigated. Here, sodium pyrophosphate was found to be suitable for the task, as it reduced the TFO-template dsDNA melting temperature to ~61 °C, enabling magneto-separation to be performed below the streptavidin-biotin stability threshold. DPA-TFOs were successfully isolated at yields of 57.8% and 61.5%, for TFO2 and 5mC-TFO3, respectively. Finally, the enzymatically synthesised DPA-TFO (TFO2) was analysed and compared to a DPA-functionalised TFO prepared using a combination of SPS methodology and post-synthetic click functionalisation (TFO1, yield 21.1%) (section 5.5.3). Data here (appendix **Figure C - 19**) reveals the enzymatic incorporation of DPA was successful with a small fraction of canonical triphosphate incorporation leading to non-modified TFO (appendix **Figure C - 20**).

5.3.3 Thermal melting analysis.

Fluorescence thermal melting experiments were performed to determine the stability of the DPA-TFO hybrids. Each TFO was incubated with target duplex in phosphate buffer at 37 ºC for 24 hours. SYBR green I was added, and thermal melting was performed by heating the sample to 95 ºC while recording ten fluorescence measurements per ºC. As predicted from previous analysis,[20] the

TFOs formed stable triplexes, with T_M values of 45.2 ºC, 45.5 ºC, 45.7 ºC and 46.2 ºC, for the DPA-TFO1, DPA-TFO2, copper(II) bound (section 5.5.7) Cu-DPA-TFO1 and Cu-DPA-TFO2, respectively. The introduction of methyl-cytosines further stabilised the triple helical DNA, with a T_M of 59.3 ºC recorded and enabled triplex formation at neutral pH (T_M = 44.9 ºC).

5.3.4 Targeted oxidative cleavage by DPA-TFO hybrids.

The ability of the DPA-TFOs to recognise and bind with their genomic target was investigated using polyacrylamide gel electrophoresis (PAGE). A 57 bp region of the GFP gene containing the TFO recognition site was amplified by PCR and served as the target duplex. Then, a random *off*-target 40 bp region of the pUC19 plasmid (that lacks the TFO binding sequence) was amplified by PCR. To determine the sequence specificity of the DPA-TFO hybrid, the 57 bp target and 40 bp *off*-target duplexes were incubated together with the TFO. This revealed that the TFO only formed a triplex with its target sequence, while the *off*-target remained unaltered (appendix **Figure C - 22).**

Next, the oxidative cleavage of the enzymatically synthesised copper-bound DPA-TFO was determined and compared to its SPS counterpart. Here, the Cu(II)-DPA-TFO hybrids were incubated with target and *off*-target duplexes in the presence of increasing equivalents of Na-*L*-ascorbate. DNA damage was monitored after 15 hours of continuous incubation at 37 ºC and visualised by PAGE (SNI-PEX hybrid: **Figure 35B**; SPS hybrid: appendix **Figure C - 23**). The band intensity of the triplex and target duplex decreased as the concentration of Na-*L*-ascorbate increased, while the intensity of the *off*-target duplex band remained relatively unchanged. The results between the SPS produced hybrid (TFO1) and the SNI-PEX hybrid (TFO2) are almost indistinguishable. This experiment was then repeated under identical conditions but the hybrid was replaced with free Cu(II)-DPA complex and an alkyne-modified-TFO. The products were again analysed by PAGE and no significant DNA damage was observed for either the target or *off*-target duplex (appendix **Figure C - 24**).

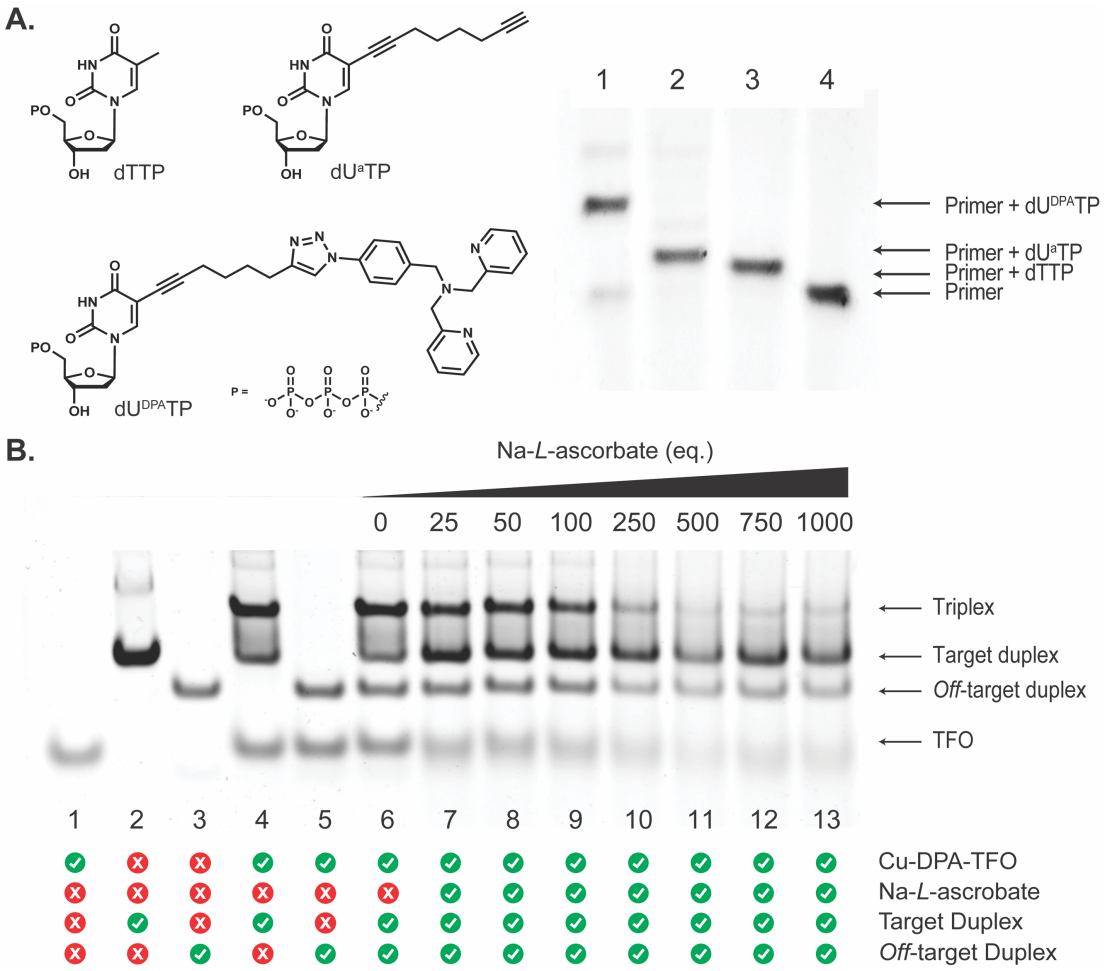


Figure 35: A. 20% denaturing PAGE analysis of SNI-PEX products, showing incorporation of Lane 1: $dU^{DPA}TP$. Lane 2: $dU^{a}TP$. Lane 3: dTTP, and Lane 4: no incorporation. **B.** 20% native PAGE showing targeted cleavage by the enzymatically synthesised Cu-DPA-TFO2. Lane 1: TFO (32 nt). Lane 2: Target duplex (57 bp). Lane 3: *Off*-target duplex (40 bp). Lane 4: TFO and target duplex hybridise to form triplex. Lane 5: TFO does not bind with *off*-target duplex. Lane 6-15: Target and *off*-target duplexes incubated with Cu-DPA-TFO2 (25 eq.) and 0-1000 eq. Na-*L*-ascorbate. TFO2 only binds with its target sequence inflicting DNA damage, while *off*-target remains relatively intact. The same cleavage profile was observed for the SPS TFO1 (appendix **Figure C - 23**).

5.3.5 Mechanistic studies

To determine the radical species involved in the Cu-DPA-TFO cleavage pathway, experiments were performed using reactive oxygen species (ROS) scavengers—L-histidine (singlet oxygen; $^1O_2$), D-mannitol (hydroxyl radical; $^{\bullet}OH$), L-methionine (hydroxyl radical; $^{\bullet}OH$, hypochlorous acid; HOCl; and hydrogen peroxide; H_2O_2,) or tiron (superoxide; $O_2^{\bullet-}$). The hybrid was incubated with the target duplex, Na-

L-ascorbate, and a ROS scavenger and the products analysed by PAGE (appendix **Figure C - 25**). In the presence of tiron no significant DNA cleavage was observed indicating damage occurs primarily through a superoxide mediated pathway, which provides a route to the formation of oxidatively active Cu-$O_2^{\bullet-}$ intermediates.[13, 46] Incubation with L-histidine and L-methionine resulted in low levels of DNA damage inhibition, while D-mannitol had no impact (appendix **Figure C - 25**). This analysis suggests that $^1O_2$, H_2O_2 and HOCl contribute only a minor role in the cleavage pathway.

5.3.6 Quantification of DNA damage by qPCR.

Although PAGE analysis revealed triplex formation and targeted cleavage activity, it could not accurately quantify DNA damage induced by the DPA-TFO hybrids. Therefore, a real-time quantitative PCR (qPCR) protocol was developed for this task. In PCR a DNA sequence of interest is amplified by a DNA polymerase through cycles of denaturation, annealing and extension, and in qPCR the concentration of DNA is monitored in real-time using a fluorescent reporter. In this assay a DNA polymerase attempted to amplify a 113 bp fragment of the GFP gene that contained the TFO recognition site. The ability of an *off*-target sequence to undergo PCR amplification was also assessed.

Similar to PAGE analysis, target and *off*-target duplexes were incubated with Cu(II)-DPA-TFO1 or the enzymatic Cu(II)-DPA-TFO2 (25 eq.) and increasing concentrations of Na-*L*-ascorbate at 37 ºC for 15 hours. The reaction was stopped through the addition of EDTA, and samples were diluted to a concentration suitable for PCR. Each sample was then subjected to two qPCR reactions: i.) amplification of the target duplex (**Figure 36A**), and ii.) amplification of the *off*-target sequence (**Figure 36B**). The resulting amplification profile for each sequence was analysed and the threshold cycle (C_T; cycle at which the fluorescent signal is 10 standard deviations above background fluorescence) was noted. In qPCR the C_T is directly proportional to the initial concentration of intact dsDNA and therefore the damage induced upon the target and *off*-target duplexes can be compared. It was found that the DPA-TFO hybrids induced significantly more damage on the target sequence when compared to the *off*-

target, with 64% versus 13%, and 57% versus 9% of the DNA being damaged in the presence of TFO1 or TFO2, respectively, and 750 equivalents of reductant (**Figure 36C**), which confirms the sequence selectivity of DPA-TFO hybrids. The experiment was then repeated using the free Cu-DPA complex and the alkyne-TFO (appendix **Figure C - 26**). In this instance no significant damage was observed for either DNA sequence (appendix **Figure C - 26**) confirming that attachment of DPA to a TFO not only allows for targeted delivery of the complex but also increases the DNA damaging propensity of the AMN. Since PAGE analysis indicated superoxide was the main ROS responsible for DNA cleavage, a scavenger experiment in the presence of tiron was repeated and analysed by qPCR. Again, no significant damage was observed (appendix **Figure C - 27**) which confirms ROS-mediated damage induced by the DPA-TFO hybrid is responsible for preventing DNA amplification.

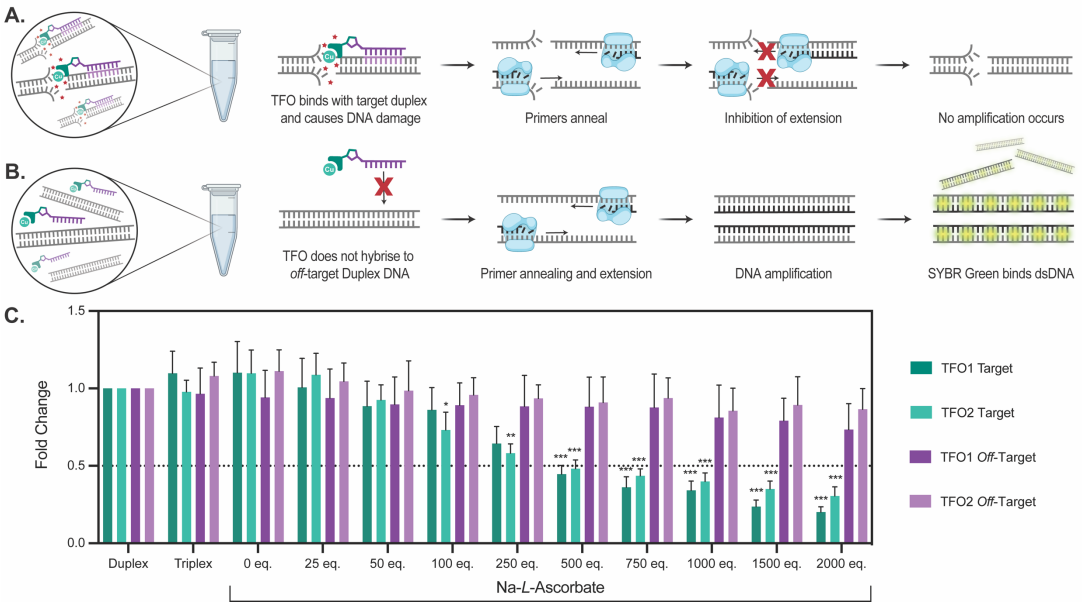


Figure 36: A. The DPA-TFO hybrid damaged its dsDNA target, therefore amplification of this sequence was inhibited. No fluorescence was detected. **B.** The *off*-target duplex was not damaged by the hybrid and thereby successful cycles of PCR were completed. SYBR green fluorescence was detected. **C.** Damage inflicted upon the target and *off*-target duplexes during incubation with SPS Cu-DPA-TFO1 (25 eq.) or SNI-PEX Cu-DPA-TFO2 (25 eq.) was analysed by comparing the threshold cycle (C_T) of experiment (15 h) and reference (0 h) samples (experiment C_T – reference C_T) to give ΔC_T. ΔC_T for each sample was normalised to a non-treated control ($\Delta\Delta C_T$) and plotted as a linear value ($2^{-\Delta\Delta CT}$) of fold change in intact DNA. A significant difference is observed between the target and *off*-target for TFO1 and 2, while no significant difference is observed between SPS TFO 1 and SNI-PEX TFO2. * = p = < 0.05, significant ** = p < 0.01, very significant. *** = p < 0.001, extremely significant.

5.3.7 Targeted damage of supercoiled plasmid DNA.

To this point, we have demonstrated how the DPA-TFO hybrids can recognise and damage a specific short DNA sequence. However, the DNA within a cell is far more complex than a simple 113 bp duplex, as it is folded, twisted and packaged into tightly wound chromatin,[47, 48] which may impede effective TFO binding. Therefore, studies involving plasmid DNA were designed to determine if the DPA-TFO hybrids could recognise and damage their target sequence in a more biologically complex environment (**Figure 37A**). Additionally, supercoiled (SC) plasmid DNA is an ideal substrate to identify oxidative damage as it can delineate single stand damage—resulting in the open-circular (OC) form—and double strand damage which produces the linear (L) form. All three conformations (SC, OC, and L) of plasmid DNA can be easily distinguished by agarose gel electrophoresis.[42]

Each DPA-TFO hybrid was incubated with a plasmid containing the target GFP gene (pCSanDI-HYG-N44) and an *off*-target pUC19 plasmid, and the resulting products were analysed by agarose gel electrophoresis (TFO1; appendix **Figure C - 28**, TFO2; **Figure 37B**, TFO3; appendix **Figure C - 29**). The DPA-TFO hybrid was observed to selectively damage the correct plasmid sequence. It was also noted that the hybrid cleaved a single strand of the GFP plasmid, resulting in relaxation of the supercoiled DNA to its OC form.

Recent investigations into the DNA cleavage affinities of copper(II) DPA complexes with a semi-intercalator, such as Phen, or designer intercalators of DPQ or DPPZ, were identified to enhance chemical nuclease activity.[8] Therefore, this study was adapted for use with the enzymatically produced DPA-TFO hybrid, whereby DPQ-Cu(II)-DPA-TFO and DPPZ-Cu(II)-DPA-TFO (25 eq.) were generated and incubated with target (GFP) and *off*-target (pUC19) plasmids, and the resulting DNA cleavage was analysed via agarose electrophoresis (appendix **Figure C - 31**). Significantly, the presence of a coordinated intercalator increases DNA binding affinity with the supercoiled target being totally transformed into its open circular form. This suggests that optimal placement of intercalating groups is key to optimising the oxidative cleavage process of this class.

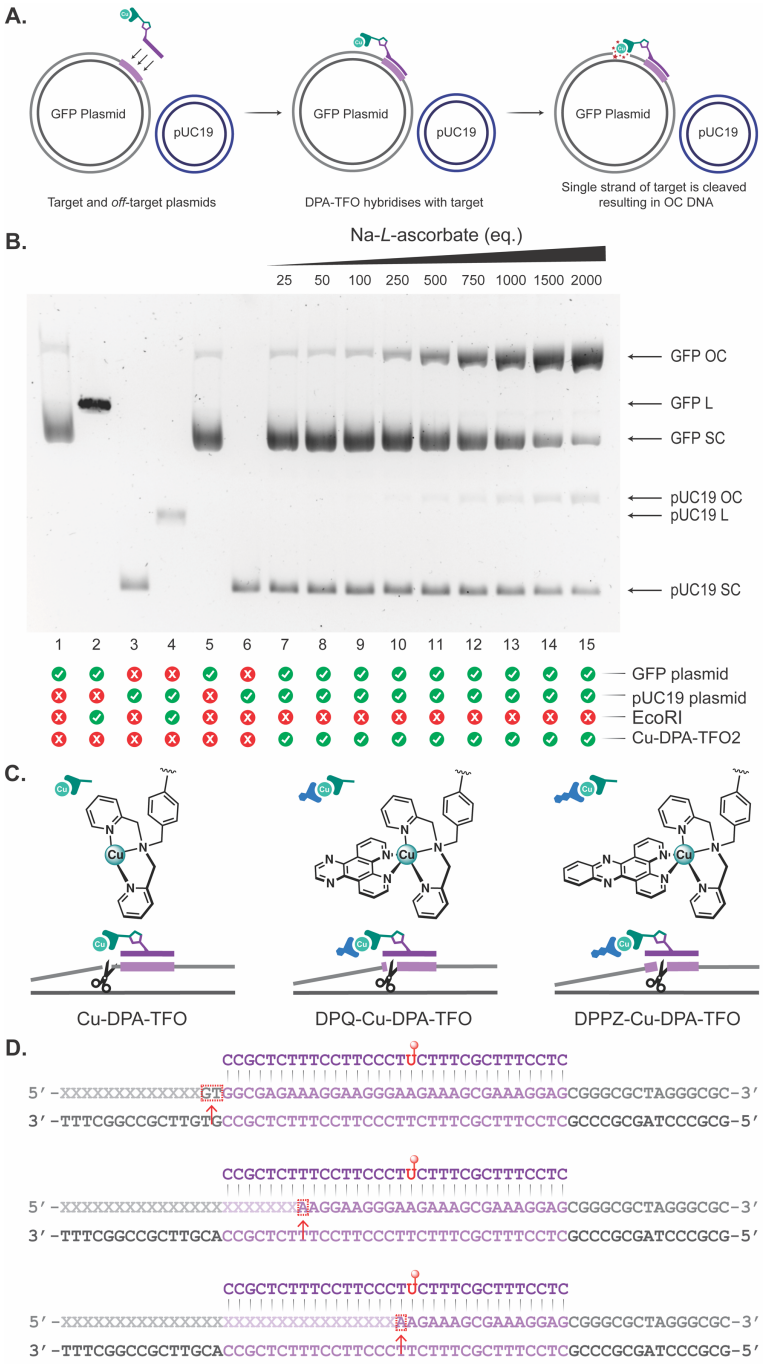


Figure 37: A. DPA-TFO hybrid incubated with target (GFP) and *off*-target (pUC19) plasmid DNA. **B.** 1% agarose gel electrophoresis. Lane 1: Supercoiled (SC) GFP (6389 bp). Lane 2: GFP linearised by EcoRI. Lane 3: Supercoiled (SC) pUC19 (2686 bp). Lane 4: pUC19 treated with EcoRI. Lane 5: SC GFP control. Lane 6: SC pUC19 control. Lane 7-15: GFP and pUC19 with 25 equivalents of Cu-DPA-TFO2 and 25-2000 equivalents of Na-*L*-ascorbate. The DPA-TFO hybrid can distinguish between the GFP and pUC19 plasmids, it cleaves a single strand of the GFP plasmid, resulting in the formation of open-circular (OC) DNA. **C.** Molecular structures of Cu-DPA (left), DPQ-Cu-DPA (middle) and DPPZ-Cu-DPA (right), along with cartoon illustration of sequencing cleavage studies involving the enzymatic DPA-TFO hybrid. **D.** Cu-DPA-TFO2 cuts a single strand of DNA target within 20 bases of the Cu-DPA modification site (top), DPQ-Cu-DPA-TFO2 nicks the target sequence < 10 bases from the modification site (middle), and DPPZ-Cu-DPA-TFO2 inflicts a single strand break < 2 bases from the modified dNTP (bottom).

5.3.8 Cleavage resolution experiments.

Sanger sequencing was next performed to determine the resolution at which the nuclease-TFO hybrids can cleave their DNA target. Here, the GFP plasmid was incubated with Cu-DPA-TFO, DPQ-Cu-DPA-TFO or DPPZ-Cu-DPA-TFO, and the resulting DNA damage was investigated by Sanger sequencing (section 5.5.13; **Figure 37C&D**). The sequencing data obtained confirmed that the DPA-TFO hybrids nick one strand of the dsDNA target. Interestingly, the pyrimidine strand remains completely intact, while the target purine strand—to which the TFO is hybridised—was damaged. Cu-DPA-TFO nicked the purine strand <20 bases downstream (3′) of the modification site at the triplex-duplex junction, while incubation with DPQ-Cu-DPA-TFO resulted in a single strand break <10 bases from the DPQ-Cu-DPA modification. Most significantly, the DPPZ-Cu-DPA-TFO nicked the GFP plasmid within 2 bases of the modification site (**Figure 37D**). This analysis reveals the presence of a designer intercalator—such as DPQ or DPPZ—increases the specificity of DNA cleavage and enables cleavage within the TFO binding region.

5.4 Conclusion

A novel DPA-TFO hybrid was successfully produced by combining click chemistry and SNI-PEX, and the viability of this method was confirmed through comparisons with a DPA-TFO prepared by SPS with post-synthetic click functionalisation. To our knowledge, this is the first report of the enzymatic synthesis of AMN-TFO hybrids. A key advantage of this approach is that targeted nucleases can now be prepared without the need for specialised equipment or complex purification, making this hybrid technology more widely accessible. Another benefit of the method is that it can be adapted for the synthesis of practically any TFO sequence, offering flexibility for the type of AMN cleaving unit and its position, thereby providing notable advantages over the existing state-of-art gene editing tools. The inclusion of 5mC bases in the DPA-TFO sequence represents one such example of this versatility. The specific incorporation of a large DPA-modification into a heavily methylated sequence demonstrates the applicability of this technology to future gene-editing systems. For example, if the

SNI-PEX could be employed for the synthesis of oligonucleotides bearing artificial backbones, such as locked nucleic acids or phosphorothioate nucleotides, this could unlock the potential of this AMN-TFO technology as a targeted therapy with increased cellular uptake and enhance stability against degradation in biological systems. The Cu-DPA-TFO hybrid was capable of distinguishing target from *off*-target DNA sequences in both short duplexes and a more complex supercoiled plasmid environment with cleavage mediated by the production of ROS. The antigene DPA-TFO developed demonstrates a high level of target discrimination, with < 2 base cleavage resolution achieved in the presence of a designer intercalator. To solidify AMN-TFOs at the forefront of gene-editing it will be important to enhance hybridisation stability—through the inclusion of modified nucleotides—and achieve codon resolution. We predicted that the reported SNI-PEX method will be invaluable in this pursuit.

5.5 Experimental

5.5.1 General information

PAGE gels were cast using a SureCast™ gel casting system (Invitrogen) and SureCast™ acrylamide solution (Invitrogen), and run in an Invitrogen mini gel tank. Agarose gel electrophoresis was performed using a Bio-Rad wide-cell mini sub system. A Bio-Rad basic Power Pac™ was used for PAGE and agarose gel electrophoresis. All gels were imaged using a Syngene G:Box 9 mini gel documentation system. PCR was performed using a Mastercycler® nexus (Eppendorf). Real-time PCR (qPCR) and fluorescence thermal melting were performed on a Roche LightCycler® 480 II using SYBR green I master mix (Roche). BioRender was used to generate the DNA polymerase graphic.

Raw gel images are available to download on Google Drive: https://drive.google.com/drive/folders/1tu199tKFWnem-pHC3Suwn_c1pU1_YWMs?usp=sharing

5.5.2 Synthesis of N-4-azidobenzyl-N-di-(2-picolyl)amine ($4N_3$-Benzyl-DPA)

Synthesis of $4N_3$-benzyl-DPA was performed in collaboration with Dr. Nicolò Zuin Fantoni.

5.5.2.1 N-4-nitrobenzyl-N-di-(2-picolyl)amine (1)

On a parallel synthesizer, ten reactions were prepared using a modification of a literature procedure reported by Du *et al*.[49] DPA (0.247 g, 1.24 mmol), K_2CO_3 (0.516 g, 3.74 mmol) and *p*-nitrobenzylbromide (0.268 g, 1.24 mmol) were mixed in CH_3CN (10 mL) and stirred overnight at room temperature. The resulting suspension was filtered and the solvent removed to yield an orange oil. The crude product was purified by column chromatography (silica gel, CH_3CN:CH_2Cl_2, gradient 0:100 to 30:70 v/v, followed by MeOH: CH_2Cl_2, gradient 5:95 to 20:80 v/v) yielding **1** as a brown solid (3.706 g, yield = 89.4%). ^{1}H-NMR (600 MHz, $CDCl_3$): δ 8.54 (dq, J = 4.9, 1.7, 0.9 Hz, 2H), 8.16 (dt, J = 8.8, 2.3 Hz, 2H), 7.67 (td, J = 7.7, 1.8 Hz, 2H), 7.58 (d, J = 8.8 Hz, 2 H), 7.52 (d, J = 7.8 Hz, 2H), 7.17 (qd, J = 7.4, 4.9, 1.1 Hz, 2H), 3.83 (s, 4H), 3.81 (s, 2H).^{13}C-NMR (151 MHz,

$CDCl_3$): δ 159.0, 149.3, 147.3, 136.7, 129.5, 123.7, 123.1, 122.4, 60.3, 57.9. ESI-MS *m/z* calcd: 357.1 $[M+Na]^+$; found: *m/z* 358.1. (appendix **Figure C - 2**, **Figure C - 3**, **Figure C - 4** and **Figure C - 5**).

5.5.2.2 N-4-amminobenzyl-N-di-(2-picolyl)amine (2)

To a solution of **1** (0.497 g, 1.49 mmol) in EtOH/H_2O (3:1; 48 mL), Na_2S (1.054 g, 13.50 mmol) was added and stirred at 70 °C for two days. The solvent was reduced and the product extracted with CH_2Cl_2 (3 x 50 mL). The combined fractions were dried over $MgSO_4$ and the solvent removed to afford **2** as an orange oil that solidifies over time (0.371 g, yield = 82.0%). ^{1}H-NMR (600 MHz, $CDCl_3$): δ 8.50 (d, J = 4.8 Hz, 2H), 7.65 (td, J = 7.9, 1.4 Hz, 2H), 7.57 (d, J = 7.8 Hz, 2H), 7.18 (d, J = 8.2 Hz, 2 H), 7.12 (q, J = 6.2, 5.1 Hz, 2H), 6.63 (d, J = 8.2 Hz, 2H), 3.77 (s, 4H), 3.55 (s, 2H).^{13}C-NMR (151 MHz, $CDCl_3$): δ 160.2, 149.0, 145.5, 136.5, 130.2, 128.9, 122.9, 122.0, 115.2, 59.9, 58.1. ESI-MS: *m/z* calcd: 372.2 $[M+Na]^+$; found: 372.1. (appendix **Figure C - 6**, **Figure C - 7, Figure C - 8** and **Figure C - 9**).

5.5.2.3 N-4-azidobenzyl-N-di-(2-picolyl)amine (3)

The diazotransfer reagent 2-azido-1,3-dimethylimidazolinium hexafluorophosphate (ADMP) used in the following synthesis was prepared according to a literature procedure previously reported by Kitamura *et al*.,[50] to a suspension of *N*-4-amminobenzyl-*N*-*di*-(2-picolyl)amine (0.159 g, 0.52 mmol) and *N,N*′-dimethyl-4-aminopyridine (DMAP; 0.076 g, 0.63 mmol) in CH_3CN (10 mL), ADMP (0.178 g, 0.63 mmol) was added and stirred overnight at 30 °C. The reaction was quenched with a saturated aqueous solution of $NaHCO_3$ and the salted-out product extracted with CH_2Cl_2 (3 x 20 mL). The combined fractions were dried over $MgSO_4$ and the solvent removed. The crude compound was purified by column chromatography (silica gel, CH_3CN:CH_2Cl_2, gradient 40:60 to 0:100 v/v, followed by MeOH:CH_2Cl_2, gradient 0:100 to 20:80 eluting the product). The combined fractions were dried *in vacuo* to afford the product **3** as a brown solid (0.121 g, yield = 70%). ^{1}H-NMR (600 MHz, $CDCl_3$): δ 8.52 (dq, J = 4.9, 1.8, 0.9 Hz, 2H), 7.66 (td, J = 7.7, 1.8 Hz, 2H), 7.55 (d, J = 7.8 Hz, 2H), 7.38 (d, J =

8.5 Hz, 2 H), 7.15 (qd, J = 7.4, 4.9, 1.1 Hz, 2H), 6.98 (dt, J = 8.5, 2.5 Hz, 2H), 3.79 (s, 4H), 3.66 (s, 2H). 13C-NMR (151 MHz, CDCl3): δ 149.2, 136.6, 130.4, 123.0, 122.2, 119.1, 60.0, 57.9. ESI-MS: *m/z* calcd: 353.1 $[M+Na]^+$; found: 353.1. (appendix **Figure C - 10**, **Figure C - 11**, **Figure C - 12** and **Figure C - 13**).

5.5.3 Solid-phase synthesis of DPA-TFO

5.5.3.1 TFO sequence

A 31 nucleotide internally modified poly-pyrimidine parallel-binding TFO was produced by solid-phase synthesis. This sequence is identical to the TPMA-TFOs previously studied.[20] It was intended that a 32 nt TFO be produced but due to an error during the synthetic process for the production of the TPMA-TFOs the 5′ cytosine was not included. It was decided to continue with this sequence to enable a direct comparison between the TPMA- and DPA-TFOs

5.5.3.2 Solid-phase synthesis of alkyne-modified TFO

TFO with an internal octadiynyl-dU (Glen Research) was synthesised by solid-phase phosphoramidite synthesis using an automated DNA synthesiser (Applied Biosystems 394) according to standard protocols. Coupling efficiencies were monitored by the trityl cation conductivity monitoring facility and were > 98%. TFO was deprotected and cleaved in standard aqueous ammonia by heating to 55 °C for 5 hours, and were purified by gradient reverse phase HPLC (C8 size exclusion column) in 0.1 M Triethylammonium acetate (TEAA) buffer with 50% CH_3CN. Gradients of 10-40% over 20 minutes were used with a 4 mL/min flow rate before desalting using Sephadex™ G-25 grade gravity filtration columns (NAP-25™, GE Healthcare). TFO was analysed by ESI-MS.

5.5.3.3 Click chemistry reaction of octadiynyl-TFO and $4N_3$-benzyl-DPA

The copper(I)-catalysed azide-alkyne cycloaddition (CuAAC) reaction to ‘click’ alkyne-modified TFO with $4N_3$-benzyl-DPA was performed according to the Lumiprobe protocol for click-chemistry labelling of oligonucleotides with minor modifications. Internal-octadiynyl-TFO (60 nmol), $4N_3$-benzyl-DPA (90 nmol) and

Na-*L*-ascorbate (1.5 μmol) were mixed in a 50:50 solution of DMSO:water. The solution was degassed with nitrogen and pre-complexed Cu-TBTA (1.5 μmol) was added. The reaction mixture was further degassed and stirred overnight, before being quenched with EDTA (30 μmol) and desalted using Sephadex™ G-25 grade gravity filtration columns (NAP-25™, GE Healthcare). The DPA-TFO was then purified by gradient (0.1 M NH_4OAc + 50% CH_3CN in NH_4OAc) reverse phase HPLC (C8 size exclusion column). DPA-TFO was analysed by ESI-MS.

5.5.4 Enzymatic synthesis of DPA-TFO

5.5.4.1 TFO sequence

A 32 nt TFO sequence, which is comparable to the SPS DPA-TFO hybrid, was chosen for enzymatic synthesis. It was intended that the SPS and SNI-PEX TFOs would have identical sequences, but it was necessary to move the modification position one base towards the 3′ end of the TFO due to the 5′ to 3′ nature of enzymatic synthesis.

5.5.4.2 Production of DPA-dUTP through click chemistry

In an anaerobic environment a copper catalysed azide-alkyne cycloaddition (CuAAC) reaction mixture (5 nmol) between a C8-alkyne-dUTP (BaseClick) and 1.5 equivalents $4N_3$-benzyl-DPA was prepared in water and DMSO (1:1) to a total volume of 250 μL. Reaction proceeded at 25 °C and 450 RPM for 6 hours, was quenched with 500 equivalents of EDTA and stored at -20 °C.

5.5.3.3 SNI-PEX & streptavidin magnetic particles

In a total volume of 200 μL a sample containing; primer (17 nt, 10 μM, 27 μL, appendix **Table C - 3**), 5′-biotinylated template (32 nt, 10 μM, 27 μL, appendix **Table C - 3**), $dU^{DPA}TP$ (13.3 μM, 30.4 μL), $MgSO_4$ (100 mM, 8 μL, NEB) and Vent (exo-) DNA polymerase (2 U/ μL, 10 μL, NEB) in ThermoPol buffer (10 x, 20 μL, NEB), was prepared. This was incubated at 37 °C and 450 RPM for 90 min. Natural dNTPs (10 mM, 27 μL, NEB) were added and a further 20 min incubation

at 60 °C and 450 RPM was performed, before cooling to 4 °C to stop the reaction. The above procedure was repeated using a primer containing 5-methyl cytosines (17nt, **Table C - 3**) and 2′-deoxy-5-methylcytidine 5′-triphosphates (27 μL, 10 mM, NEB) to synthesise a TFO containing methyl-cytosines.

Streptavidin magnetic particles (100 μL, Roche) were washed three times with TEN_{100} (200 μL; 10 mM Tris, 1 mM EDTA, 100 mM NaCl, pH 7.5), and resuspended in TEN_{100} (50 μL). SNI-PEX solution (200 μL) was added and incubated at 18 °C and 1200 RPM for 20 min. Particles were collected on a magnet and solution was discarded. Particles were washed three times with TEN_{1000} (200 μL; 10 mM Tris, 1 mM EDTA, 1 M NaCl, pH 7.5), and then washed four times with elution buffer (200 μL, 100 mM sodium pyrophosphate). Particles were resuspended in elution buffer (100 μL), and double stranded DNA was denatured (65 °C for 90 sec). Particles were collected on a magnet and the solution, containing the single stranded TFO, was collected. TFO was de-salted using Sephadex™ G-25 grade gravity filtration columns (NAP-5™, Cytiva illustra™).

5.5.5 Denaturing PAGE to visualise single nucleotide incorporation

20% denaturing polyacrylamide gels (1x TBE buffer, 7M urea) were cast. Denaturing loading buffer (95% formamide, 18 mM EDTA, 0.025% SDS, xylene cyanol, bromophenol blue, Invitrogen) was added to SNI-PEX samples (10 μL) and heated to 95 °C for 4 min. Samples were loaded directly onto the gel and run at 150 V for 160 min, before being post-stained with SYBR gold.

5.5.6 Amplification of TFO target and *off*-target

A 57 bp amplicon containing the TFO recognition sequence (pCSanDI-HYG; forward: 5′-AAGCCGGCGAACGTGGCGG-3′ and reverse: 5′-CCTAGCGCCCGCTCCTTTCG -3′), and a 40 bp amplicon lacking the TFO target sequence (pUC19, NEB; forward: 5′-TGACTCCCCGTCGTGTAGAT-3′ and reverse: 5′-AGCCCTCCCGTATCGTAGTT-3′) were generated by PCR (MyTaq

Red DNA polymerase, Bioline) and purified into 6 μL of nuclease-free water using membrane spin columns (Monarch PCR & DNA clean-up kit, NEB). These are the 57 bp target and 40 bp *off*-target duplexes.

5.5.7 Fluorescent thermal melting

Prior to T_M analysis $Cu(ClO_4)_2$ was incubated with DPA-TFO (1:1) for 15 min at room temperature to allow for coordination of Cu(II) with DPA ligand for copper-bound samples. TFO (25 pmol) and 57 bp target duplex (5 pmol) were incubated in phosphate buffer (10 mM PO_4^{3-}, 150 mM NaCl, 2 mM $MgCl_2$, pH 6.1) at 37 ºC for 15 hours. SYBR green I (1 μL, Roche) was added to each sample and the melting profile for the triplex was analysed on a LightCycler® 480 II (Roche). Samples were heated to 99 ºC with 10 fluorescence measurements recorded per ºC. A plot of sample fluorescence versus temperature is obtained and the first negative derivative of the sample is calculated, resulting in the melting temperature being displayed as a peak.

5.5.8 Triplex formation

Target (57 bp, 1 pmol) and *off*-target (40 bp, 1 pmol) duplexes were incubated with 10, 25 and 50 equivalents of TFO (32 nt) in phosphate buffer (10 mM PO_4^{3-}, 150 mM NaCl, 2 mM $MgCl_2$, pH 6.1) at 37 ºC for 24 hours. 6X loading dye (10 mM Tris-HCl, pH 7.6, 0.03% bromophenol blue, 0.03% xylene cyanol FF, 60% glycerol, 60 mM EDTA, Invitrogen) was added, and the entire solution was loaded onto a 20% native PAGE gel (50 mM Tris-acetate, 75 mM NaCl, 5 mM $MgCl_2$, pH 6.1). Gel was run at 70 V for 240 min and was post-stained with SYBR gold.

5.5.9 DPA-TFO hybrids PAGE

A DPA-TFO hybrid (15.625 pmol) was incubated with 1 equivalent of $Cu(ClO_4)_2$ for 15 min at room temperature, to allow Cu(II) to coordinate with DPA. This copper-bound hybrid (15.625 pmol), and increasing concentrations of Na-*L*-ascorbate (0-2000 eq.), was then incubated with a duplex containing the TFO recognition site (57 bp fragment of GFP, 0.625 pmol) and *off*-target duplex (40

bp fragment of pUC19, 0.625 pmol) in phosphate buffer (10 mM PO_4^{3-}, 150 mM NaCl, 2 mM $MgCl_2$, pH 6.1) at 37 °C for 15 hours, the reaction was quenched with 6X loading dye (10 mM Tris-HCl, pH 7.6, 0.03% bromophenol blue, 0.03% xylene cyanol FF, 60% glycerol, 60 mM EDTA, Invitrogen). The entire solution was loaded onto a 20% native PAGE gel (50 mM Tris-acetate, 75 mM NaCl, 5 mM $MgCl_2$, pH 6.1) and was run at 70 V for 240 min. The gel was post-stained with SYBR gold.

5.5.10 ROS scavengers

Samples for PAGE were prepared as described above, however the *off*-target sequence was excluded and a reactive oxygen species (ROS) scavenger (50 nmol) was added prior to incubation at 37 °C. The DNA damage inflicted was analysed by PAGE.

5.5.11 qPCR analysis of catalytic activity with target and off-target

qPCR was performed using SYBR green I fluorescence. A 113 bp amplicon containing the TFO recognition sequence (pCSanDI-HYG; forward: 5′-AAAGGGAGCCCCCGATTTAG-3′ and reverse: 5′-GTGACCGCTACACTTGCCA-3′), and a 116 bp amplicon lacking the TFO target sequence (pUC19, NEB; forward: 5′-TCCGGTCCCAACGATCAAG-3′ and reverse: 5′-AGTGATAACACTGCGGCCAA-3′) were generated by PCR (MyTaq Red DNA polymerase, Bioline) and purified using membrane spin columns (Monarch PCR & DNA clean-up kit, NEB). In a total volume of 12 μL (10 mM PO_4^{3-}, 150 mM NaCl, 2 mM $MgCl_2$, pH 6), the target duplex (113 bp, 1.25 pmol) and *off*-target sequence (116 bp, 1.25 pmol) were exposed to Cu-DPA-TFO or a 1:1 mixture of free Cu-DPA and free TFO (31.25 pmol) in the presence of increasing equivalents of Na-*L*-ascorbate (0-2000 eq.). At t = 0 hours, 6 μL of each reaction volume was quenched with EDTA (60 nmol) and kept as the reference samples. The remaining 6 μL was incubated at 37 °C for t = 15 hours (experiment) prior to addition of EDTA. Diluted ($1:40^5$) reference and experiment samples were analysed by qPCR over 45 PCR cycles. The changes in C_T (threshold cycle) between experiment and reference samples

(experiment C_T – reference C_T) were calculated (ΔC_T). ΔC_T was then normalised to a non-treated control (ΔC_T sample - ΔC_T control = $\Delta\Delta C_T$), and this was plotted as a linear value $2^{-\Delta\Delta CT}$. 2way ANOVA with Tukey's multiple comparisons was performed, using GraphPad Prism, to determine the significance of the $2^{-\Delta\Delta CT}$ values obtained. * = p = < 0.05, significant ** = p < 0.01, very significant. *** = p < 0.001, extremely significant.

5.5.12 Plasmid Studies

A plasmid containing the GFP gene (400 ng, pCSanDI-HYG-N44) and the pUC19 plasmid (400 ng, NEB) were incubated with 25 equivalents of (DPQ/DPPZ)Cu(II)-DPA-TFO (2.5 pmol) and increasing concentrations of Na-*L*-ascorbate (25-2000 eq., 62.5 – 5000 pmol) in phosphate buffer (10 mM PO_4^{3-}, 150 mM NaCl, 2 mM $MgCl_2$, pH 6.1) at 37 ºC for 15 hours. The reaction was quenched with 6X loading dye (10 mM Tris-HCl, pH 7.6, 0.03% bromophenol blue, 0.03% xylene cyanol FF, 60% glycerol, 60 mM EDTA, Invitrogen) and loaded onto a 1% agarose gel containing SYBR safe (1X, Invitrogen). The gel was run at 50 V for 270 min, and then imaged using UV fluorescence.

5.5.13 Sequencing

The GFP plasmid (2.25 mg, pCSanDI-HYG-N44) was incubated with 25 equivalents of (DPQ/DPPZ)Cu(II)-DPA-TFO (14 pmol) and Na-*L*-ascorbate (2000 eq., 28 nmol) in phosphate buffer (10 mM PO_4^{3-}, 150 mM NaCl, 2 mM $MgCl_2$, pH 6.1) at 37 ºC for 15 hours. The reaction was quenched with EDTA (500 eq., 7 nmol) and purified into 15 μL of nuclease-free water using membrane spin columns (Monarch PCR & DNA clean-up kit, NEB). Samples were subjected to Sanger sequencing (Eurofins) with forward (`5′-CGGTGGATGTGGAATGTGTG-3′`) and reverse primers (`5′-CTGAGTAGGTGTCATTCTATTCTG-3′`), and data was analysed using SnapGene. It is important to note that the sequencing information obtained is complementary to the DNA strand read during Sanger sequencing. Thus, the undefined "X" region read on the extended reverse primer (*i.e.*

pyrimidine-rich sequence) indicates damage on the complementary (*i.e.* poly-purine) sequence of the plasmid that is cleaved by the DPA-TFO hybrids.

References

1. Kim, Y. G.; Cha, J.; Chandrasegaran, S., Hybrid restriction enzymes: zinc finger fusions to Fok I cleavage domain. *Proc. Natl. Acad. Sci.* **1996,** *93* (3), 1156-1160.
2. Zhang, F.; Cong, L.; Lodato, S.; Kosuri, S.; Church, G. M.; Arlotta, P., Efficient construction of sequence-specific TAL effectors for modulating mammalian transcription. *Nat. Biotech.* **2011,** *29* (2), 149-153.
3. Jinek, M.; Chylinski, K.; Fonfara, I.; Hauer, M.; Doudna, J. A.; Charpentier, E., A Programmable Dual-RNA-Guided DNA Endonuclease in Adaptive Bacterial Immunity. *Science* **2012,** *337* (6096), 816-821.
4. Sigman, D. S.; Graham, D. R.; D'Aurora, V.; Stern, A. M., Oxygen dependent cleavage of DNA by the 1,10-Phenanthroline cuprous complex. *J. Biol. Chem.* **1979,** *254*, 12269-12272.
5. Sigman, D. S., Nuclease activity of 1,10-phenanthroline-copper ion. *Acc. Chem. Res.* **1986,** *19* (6), 180-186.
6. Molphy, Z.; Prisecaru, A.; Slator, C.; Barron, N.; McCann, M.; Colleran, J.; Chandran, D.; Gathergood, N.; Kellett, A., Copper phenanthrene oxidative chemical nucleases. *Inorg. Chem.* **2014,** *53* (10), 5392-404.
7. Molphy, Z.; Slator, C.; Chatgilialoglu, C.; Kellett, A., DNA oxidation profiles of copper phenanthrene chemical nucleases. *Front. Chem.* **2015,** *3*, 28.
8. Zuin Fantoni, N.; Molphy, Z.; O'Carroll, S.; Menounou, G.; Mitrikas, G.; Krokidis, M.; Chatgilialoglu, C.; Colleran, J.; Banasiak, A.; Clynes, M.; Roche, S.; Kelly, S.; McKee, V.; Kellett, A., Polypyridyl-Based Copper Phenanthrene Complexes: Combining Stability with Enhanced DNA Recognition. *Chem. Eur. J.* **2020**.
9. Zuin Fantoni, N.; Molphy, Z.; Slator, C.; Menounou, G.; Toniolo, G.; Mitrikas, G.; McKee, V.; Chatgilialoglu, C.; Kellett, A., Polypyridyl-Based Copper Phenanthrene Complexes: A New Type of Stabilized Artificial Chemical Nuclease. *Chem. Eur. J.* **2019,** *25* (1), 221-237.
10. Thyagarajan, S.; Murthy, N. N.; Narducci Sarjeant, A. A.; Karlin, K. D.; Rokita, S. E., Selective DNA Strand Scission with Binuclear Copper Complexes: Implications for an Active Cu2−O2 Species. *J. Am. Chem. Soc.* **2006,** *128* (21), 7003-7008.
11. Humphreys, K. J.; Karlin, K. D.; Rokita, S. E., Targeted Strand Scission of DNA Substrates by a Tricopper(II) Coordination Complex. *J. Am. Chem. Soc.* **2002,** *124* (27), 8055-8066.
12. Humphreys, K. J.; Karlin, K. D.; Rokita, S. E., Efficient and Specific Strand Scission of DNA by a Dinuclear Copper Complex: Comparative Reactivity of Complexes with Linked Tris(2-pyridylmethyl)amine Moieties. *J. Am. Chem. Soc.* **2002,** *124* (21), 6009-6019.
13. Bales, B. C.; Kodama, T.; Weledji, Y. N.; Pitie, M.; Meunier, B.; Greenberg, M. M., Mechanistic studies on DNA damage by minor groove binding copper-phenanthroline conjugates. *Nucleic Acids Res.* **2005,** *33* (16), 5371-9.
14. Pitie, M.; Burrows, C. J.; Meunier, B., Mechanisms of DNA cleavage by copper complexes of 3-clip-phen and of its conjugate with a distamycin analogue. *Nucleic Acids Res.* **2000,** *28* (24), 4856-64.
15. Pitié, M.; Van Horn, J. D.; Brion, D.; Burrows, C. J.; Meunier, B., Targeting the DNA Cleavage Activity of Copper Phenanthroline and Clip-Phen to

A·T Tracts via Linkage to a Poly-N-methylpyrrole. *Bioconjug. Chem.* **2000,** *11* (6), 892-900.
16. Sigman, D. S.; Bruice, T. W.; Mazumder, A.; Sutton, C. L., Targeted chemical nucleases. *Acc. Chem. Res.* **1993,** *26* (3), 98-104.
17. Francois, J. C.; Saison-Behmoaras, T.; Barbier, C.; Chassignol, M.; Thuong, N. T.; Helene, C., Sequence-specific recognition and cleavage of duplex DNA via triple-helix formation by oligonucleotides covalently linked to a phenanthroline-copper chelate. *Proc. Natl. Acad. Sci.* **1989,** *86* (24), 9702-9706.
18. Kane, S. A.; Hecht, S. M.; Sun, J.-S.; Garestier, T.; Helene, C., Specific cleavage of a DNA triple helix by FeII.bleomycin. *Biochem.* **1995,** *34* (51), 16715-16724.
19. Kolb, H. C.; Finn, M. G.; Sharpless, K. B., Click Chemistry: Diverse Chemical Function from a Few Good Reactions. *Angew. Chem. Int. Ed.* **2001,** *40*, 2004-2021.
20. Zuin Fantoni, N.; McGorman, B.; Molphy, Z.; Singleton, D.; Walsh, S.; El-Sagheer, A. H.; McKee, V.; Brown, T.; Kellett, A., Development of Gene-Targeted Polypyridyl Triplex-Forming Oligonucleotide Hybrids. *ChemBioChem* **2020,** *21* (24), 3563-3574.
21. Lauria, T.; Slator, C.; McKee, V.; Müller, M.; Stazzoni, S.; Crisp, A. L.; Carell, T.; Kellett, A., A Click Chemistry Approach to Developing Molecularly Targeted DNA Scissors. *Chem. Eur. J.* **2020**.
22. Panattoni, A.; El-Sagheer, A. H.; Brown, T.; Kellett, A.; Hocek, M., Oxidative DNA Cleavage with Clip-Phenanthroline Triplex-Forming Oligonucleotide Hybrids. *ChemBioChem* **2020,** *21* (7), 991-1000.
23. Hennessy, J.; McGorman, B.; Molphy, Z.; Farrell, N. P.; Singleton, D.; Brown, T.; Kellett, A., A Click Chemistry Approach to Targeted DNA Crosslinking with cis-Platinum(II) Modified Triplex Forming Oligonucleotides. *Angew. Chem. Int. Ed.* **2021,** *60*.
24. Felsenfeld, G.; Davies, D.; Rich, A., Formation of a three stranded polynucleotide molecule-annotated. *J. Am. Chem. Soc.* **1957,** *79* (8), 2023-2024.
25. Beaucage, S. L.; Caruthers, M. H., Deoxynucleoside phosphoramidites—A new class of key intermediates for deoxypolynucleotide synthesis. *Tetrahedron Lett.* **1981,** *22* (20), 1859-1862.
26. Caruthers, M., Gene synthesis machines: DNA chemistry and its uses. *Science* **1985,** *230* (4723), 281-285.
27. Hocek, M., Synthesis of base-modified 2'-deoxyribonucleoside triphosphates and their use in enzymatic synthesis of modified DNA for applications in bioanalysis and chemical biology. *J. Org. Chem.* **2014,** *79* (21), 9914-21.
28. Zuin Fantoni, N.; Brown, T.; Kellett, A., DNA-targeted metallodrugs: an untapped source of artificial gene editing technology. *ChemBioChem* **2021**.
29. Zuin Fantoni, N.; El-Sagheer, A. H.; Brown, T., A Hitchhiker's Guide to Click-Chemistry with Nucleic Acids. *Chem. Rev.* **2021**.
30. Menova, P.; Cahova, H.; Plucnara, M.; Havran, L.; Fojta, M.; Hocek, M., Polymerase synthesis of oligonucleotides containing a single chemically modified nucleobase for site-specific redox labelling. *Chem. Comm.* **2013,** *49* (41), 4652-4.
31. Langer, P. R.; Waldrop, A. A.; Ward, D. C., Enzymatic synthesis of biotin-labeled polynucleotides: novel nucleic acid affinity probes. *Proc. Natl. Acad. Sci.* **1981,** *78* (11), 6633-7.

32. Leone, D. L.; Hubálek, M.; Pohl, R.; Sýkorová, V.; Hocek, M., 1,3-Diketone-Modified Nucleotides and DNA for Cross-Linking with Arginine-Containing Peptides and Proteins. *Angew. Chem. Int. Ed.* **2021**.
33. Simonova, A.; Magrina, I.; Sykorova, V.; Pohl, R.; Ortiz, M.; Havran, L.; Fojta, M.; O'Sullivan, C. K.; Hocek, M., Tuning of Oxidation Potential of Ferrocene for Ratiometric Redox Labeling and Coding of Nucleotides and DNA. *Chem. Eur. J.* **2020,** *26* (6), 1286-1291.
34. Rostovtsev, V. V.; Green, L. G.; Fokin, V. V.; Sharpless, K. B., A stepwise Huisgen cycloaddition process: Copper (I)-catalysed regioselective "ligation" of azides and terminal alkynes. *Angew. Chem. Int. Ed.* **2002,** *41* (14).
35. Tornøe, C. W.; Christensen, C.; Meldal, M., Peptidotriazoles on Solid Phase: [1,2,3]-Triazoles by Regiospecific Copper(I)-Catalyzed 1,3-Dipolar Cycloadditions of Terminal Alkynes to Azides. *J. Org. Chem.* **2002,** *67* (9), 3057-3064.
36. Faria, M.; Giovannangeli, C., Triplex-forming molecules: from concepts to applications. *J. Gene Med.* **2001,** *3* (4), 299-310.
37. Fox, K. R.; Brown, T., Formation of stable DNA triplexes. *Biochem. Soc. Trans.* **2011,** *39* (2), 629-634.
38. Wang, E.; Malek, S.; Feigon, J., Structure of a G.T.A triplet in an intramolecular DNA triplex. *Biochem.* **1992,** *31*, 4838-4846.
39. Fox, K. R.; Brown, T.; Rusling, D. A., Chapter 1. DNA Recognition by Parallel Triplex Formation. In *DNA - targeting molecules as therapeutic agents*, Waring, M. J., Ed. Royal Society of Chemistry: 2018; pp 1-32.
40. Holmberg, A.; Blomstergren, A.; Nord, O.; Lukacs, M.; Lundeberg, J.; Uhlen, M., The biotin-streptavidin interaction can be reversibly broken using water at elevated temperatures. *Electrophoresis* **2005,** *26* (3), 501-10.
41. Matyasovsky, J.; Pohl, R.; Hocek, M., 2-Allyl- and Propargylamino-dATPs for Site-Specific Enzymatic Introduction of a Single Modification in the Minor Groove of DNA. *Chemistry-a European Journal* **2018,** *24* (56), 14938-14941.
42. Kellett, A.; Molphy, Z.; Slator, C.; McKee, V.; Farrell, N. P., Molecular methods for assessment of non-covalent metallodrug-DNA interactions. *Chem. Soc. Rev.* **2019,** *48* (4), 971-988.
43. Schildkraut, C.; Lifson, S., Dependence of the melting temperature of DNA on salt concentration. *Biopolymers* **1965,** *3* (2), 195-208.
44. Owczarzy, R.; You, Y.; Moreira, B. G.; Manthey, J. A.; Huang, L.; Behlke, M. A.; Walder, J. A., Effects of Sodium Ions on DNA Duplex Oligomers: Improved Predictions of Melting Temperatures. *Biochem.* **2004,** *43* (12), 3537-3554.
45. Tan, Z.-J.; Chen, S.-J., Nucleic Acid Helix Stability: Effects of Salt Concentration, Cation Valence and Size, and Chain Length. *Biophys. J.* **2006,** *90* (4), 1175-1190.
46. Pitié, M.; Pratviel, G., Activation of DNA Carbon−Hydrogen Bonds by Metal Complexes. *Chem. Rev.* **2010,** *110* (2), 1018-1059.
47. Noll, M., Subunit structure of chromatin. *Nature* **1974,** *251*, 249-251.
48. Kornberg, R. D., Chromatin Struture: A repeating unit of histones and DNA. *Science* **1974,** *184 (4139)*, 868-871.
49. Du, P.; Lippard, S. J., A Highly Selective Turn-On Colorimetric, Red Fluorescent Sensor for Detecting Mobile Zinc in Living Cells. *Inorg. Chem.* **2010,** *49* (23), 10753-10755.

50. Kitamura, M.; Kato, S.; Yano, M.; Tashiro, N.; Shiratake, Y.; Sando, M.; Okauchi, T., A reagent for safe and efficient diazo-transfer to primary amines: 2-azido-1,3-dimethylimidazolinium hexafluorophosphate. *Organic & Biomolecular Chemistry* **2014,** *12* (25), 4397.

Chapter 6

Multiple nucleotide incorporation-primer extension: A method for the enzymatic synthesis of therapeutic oligonucleotides

Chapter 6 is written as a research article as a publication containing this research has been prepared and will be submitted for publication.

My contribution to this paper included; the production of novel modified nucleotide triphosphates through nucleic acid click chemistry; design and optimisation of the novel MNI-PEX protocol; and the enzymatic synthesis of a TPMA-TO-TFO hybrid.

6.1 Abstract

The synthesis of modified oligonucleotides is complex, inefficient and incompatible with various modifications. Consequently, there is growing interest in the development of alternative protocols for the synthesis of modified DNA. Enzymatic synthesis is an appealing choice, as it is compatible with a wide-range of modifications, and has been adapted for the incorporation of a single modified nucleotide at a specific sequence position (SNI-PEX). However, no enzymatic methodology has been reported for the synthesis of an oligonucleotide bearing multiple modifications at distinct sequence positions. Therefore, in this work, a new enzymatic method to incorporate multiple modifications is reported. The method is called multiple nucleotide incorporation-primer extension (MNI-PEX), and allows multiple different modified-nucleotides to be incorporated at specific sequence positions. The method is examined here as a means for enzymatically synthesising a triplex forming oligonucleotide (TFO), bearing an artificial metallo-nuclease (AMN) and a fluorescent intercalator, for enhanced cleavage resolution. However, the principle of MNI-PEX will be of broad interest to the field of nucleic acid therapeutics, as there is a demand for incorporating tailored modifications with diverse applications.

6.2 Introduction

The artificial synthesis of DNA is not a new phenomenon. It has been exploited within biological research for many decades, and today almost all DNA produced outside of a cell is generated by solid-phase phosphoramidite synthesis.[1, 2] However, phosphoramidite synthesis has its limitations as it is not efficient at synthesising long DNA sequences (> 200 nt), it produces hazardous waste products, and it requires the use of specialised equipment and complex purification steps. Additionally, the demand for modified oligonucleotides is increasing, and phosphoramidite synthesis is not compatible with modifications that are susceptible to oxidation, or that are reactive with nucleophiles.[3] Therefore, there is an increasing desire to develop alternative methods for the synthesis of DNA, specifically DNA bearing modifications.

Enzymatic synthesis is an appealing choice as it is a natural phenomenon that occurs within all organisms during DNA replication and repair, and thus does not require specialised equipment or produce hazardous waste. The use of enzymes, known as DNA polymerases, for the synthesis of modified DNA was first reported in 1981, when biotin-labelled polynucleotides were reported.[4] Since then, the enzymatic synthesis of modified DNA has expanded, and nucleotide triphosphates (dNTPs) bearing modifications are now commercially available. However, the synthesis of DNA with modifications at specific sequence positions is still limited. In 2013, the Hocek group reported SNI-PEX (single nucleotide incorporation, followed by primer extension), which was the first example of methodology that enabled the synthesis of an oligonucleotide with a modification at one specific site.[5] SNI-PEX has since been applied for the synthesis of DNA bearing larger modifications—including AMNs,[6] peptides crosslinking agents[7] and fluorophores[8] (appendix **Figure D - 1**)—but it is limited to the inclusion of a single modified nucleotide.

Herein, a novel method of enzymatic synthesis is reported. It expands upon SNI-PEX and can incorporate multiple different modifications at distinct sequence positions. This multiple nucleotide incorporation–primer extension (MNI-PEX) protocol has the potential to greatly expand the utility of enzymatic synthesis and enable the production of heavily modified DNA sequences. The overarching goal of this methodology is to increase the accessibility of modified DNA, and to accelerate research in the field of therapeutic oligonucleotides.

6.3 Design of MNI-PEX

MNI-PEX was designed to enable the incorporation of two different modifications at specific positions in an oligonucleotide sequence. Significant planning and optimisation was necessary for the development of MNI-PEX, with many different factors requiring consideration. The first objective was to develop the protocol for production of the modified nucleotide triphosphates. The selected method must be compatible with a variety of modifications, simple to perform, and ideally not require any specialised equipment or complex purification. Nucleic acid click chemistry[9] satisfied these criteria, and consequently was employed for this task.

Alkyne-modified nucleotide triphosphates are commercially available, and azide-functionalised metallo-drugs have previously been synthesised.[6, 10-14] Therefore, the copper-catalysed azide-alkyne cycloaddition (CuAAC) was performed to 'click' azide-functionalised metallo-drugs to C8-alkyne-dNTPs (dN^{a}TPs). Each CuAAC reaction was performed in a solvent system (50% DMSO/DMF: 50% water) compatible with enzymatic synthesis, alleviating the need for a purification step. Therefore, the library of dNTPs generated by click chemistry (**Figure 38**) was ready to be incorporated into an oligonucleotide sequence.

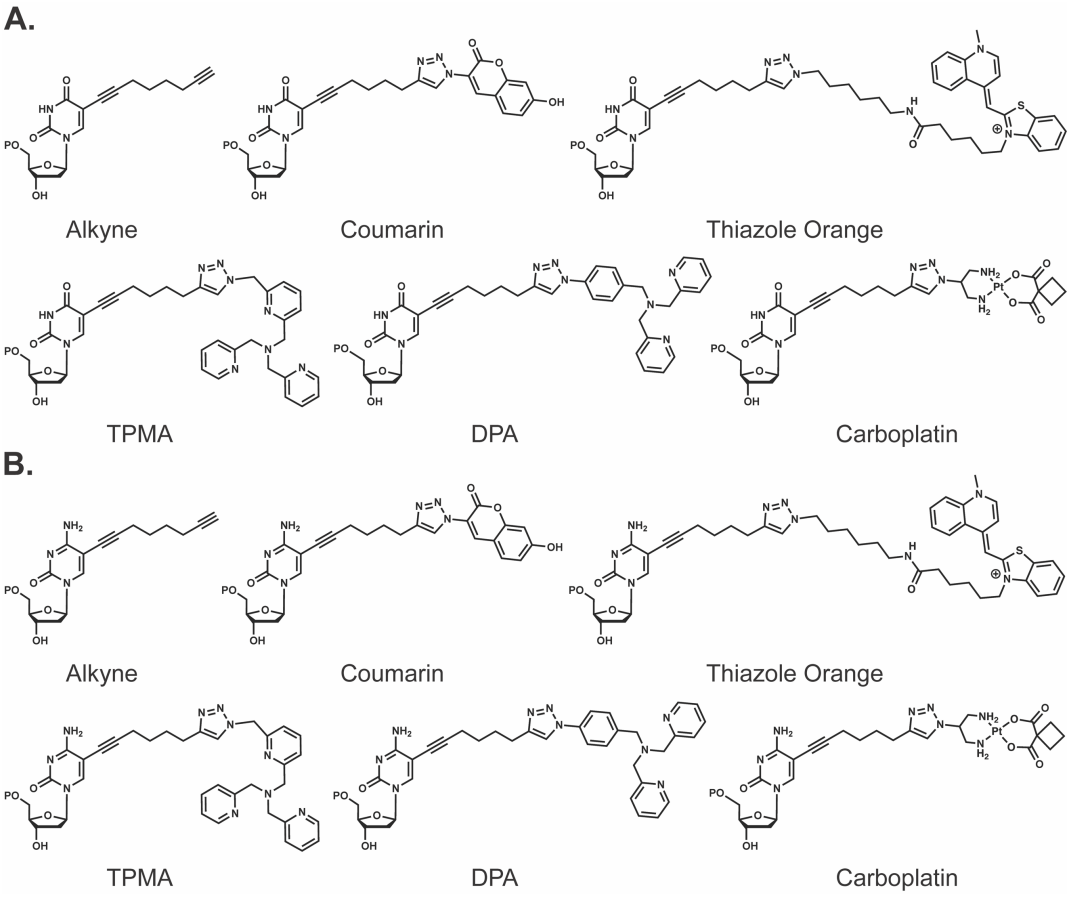


Figure 38: Library of modified dUTPs (**A.**) and dCTPs (**B.**) that could be generated by nucleic acid click chemistry.

However, the method by which these modified dNTPs would be incorporated had to be considered. Single nucleotide incorporation-primer extension (SNI-PEX) has previously been reported as a suitable method for the incorporation of a single modified dNTP at a specific sequence position,[5-7] but it

is limited to the incorporation of a single modified base, and no method for the inclusion of multiple modifications at specific positions exists. Therefore, a new protocol that expands upon SNI-PEX was derived. This protocol required two, or three, primers for the incorporation of two, or three, modified dNTPs (**Figure 39**). These primers required meticulous design such that: i.) each primer must anneal to the template, but not to each other; ii.) the primers require an annealing temperature compatible with the chosen DNA polymerase; iii.) each primer must allow for incorporation of a different nucleotide (*i.e.* the base in the 3′ position following the primer must be different); and iv.) the primers act as a spacer between the modified bases, so it was important to ensure each primer was of sufficient length to prevent interaction between the modifications. Once the primers were identified, optimisation of the enzymatic synthetic protocol began.

In a manner similar to SNI-PEX,[5] a short primer (primer A) and biotinylated template were annealed. Then, a DNA polymerase incorporates a single modified dNTP at the 3′ end of the primer (**Figure 39A**). Next a second round of SNI occurred; primer B was annealed to the template immediately 3′ of the previous incorporation site, and a different dNTP was then incorporated following primer B (**Figure 39B**). The remainder of the TFO sequence was then synthesised by traditional PEX with natural dNTPs (**Figure 39C**). However, the newly synthesised DNA strand was not ready to be isolated from its template. Effectively there was a 'nick' between the modified dNTP incorporated at position A and primer B, as the DNA polymerase did not extend past the incorporation site, instead the new primer was annealed. This 'nick' was ligated by a DNA ligase. T4 DNA ligase was selected for this task as it is a sequence independent ligase that catalyses the formation of a phosphodiester bond between juxtaposed 5′ phosphate and 3′ hydroxyl termini in duplex DNA. This attached the modified dNTP to primer B, and thereby completed synthesis of an oligonucleotide bearing two different modifications at specific sequence positions (**Figure 39D**). It was important that a sequence independent ligase was chosen for this step, as it enables MNI-PEX to be adapted for the synthesis of any DNA sequence. At this stage, the newly synthesised oligonucleotide, bearing the modifications, was still annealed to its template and must be isolated. Streptavidin-coated magnetic particles were employed for this task. The biotin-tag on the template binds with

streptavidin magnetic particles, and through a magneto-denaturation step, the newly synthesised DNA strand was isolated (**Figure 39E**).

6.4 Application of MNI-PEX for the synthesis of TPMA-TO-TFO

The novel MNI-PEX protocol was then applied for the synthesis of a triplex forming oligonucleotide (TFO) with two modifications; a DNA damaging chemical nuclease, and an intercalating triplex stabilisation agent. The polypyridyl copper binding artificial metallo-nuclease (AMN), *tris*-(2-pyridylmethyl)amine (TPMA) was selected as the DNA-damaging agent for this study (**Figure 38A**). TPMA[15] derivatives have previously been attached to TFOs,[11] and the ability of those hybrids to selectively damage a target DNA sequence was reported. Therefore, the attachment of $6N_3$-TPMA to C8-alkyne dUTPs (dU^{a}TPs) was the first step in this MNI-PEX protocol. Under anaerobic conditions dU^{a}TPs, $6N_3$-TPMA, pre-complexed Cu(II)-TBTA and Na-*L*-ascorbate were incubated in 50% DMSO at 25 °C for 6 hours, before being quenched with EDTA. The TPMA-dUTPs (dU^{TPMA}TPs) were then ready to be incorporated into the TFO sequence without any purification.

Thiazole orange (TO) was chosen as the fluorogenic intercalator as it has been shown to stabilise triplex formation,[11, 16] and not impede DNA cleavage by AMNs.[11] As TPMA was attached to dUTPs, N_3-thiazole orange (N_3-TO) was tethered to C8-alkyne dCTPs (**Figure 38B**), to enable incorporation at distinct sequence positions. In this instance 5 equivalents of N_3-TO was mixed with dC^{a}TPs, Cu(II)-TBTA and Na-*L*-ascorbate in DMSO and water (50:50), before being incubated at 25 °C for 24 hours. Again, the reaction was quenched, and no purification was required.

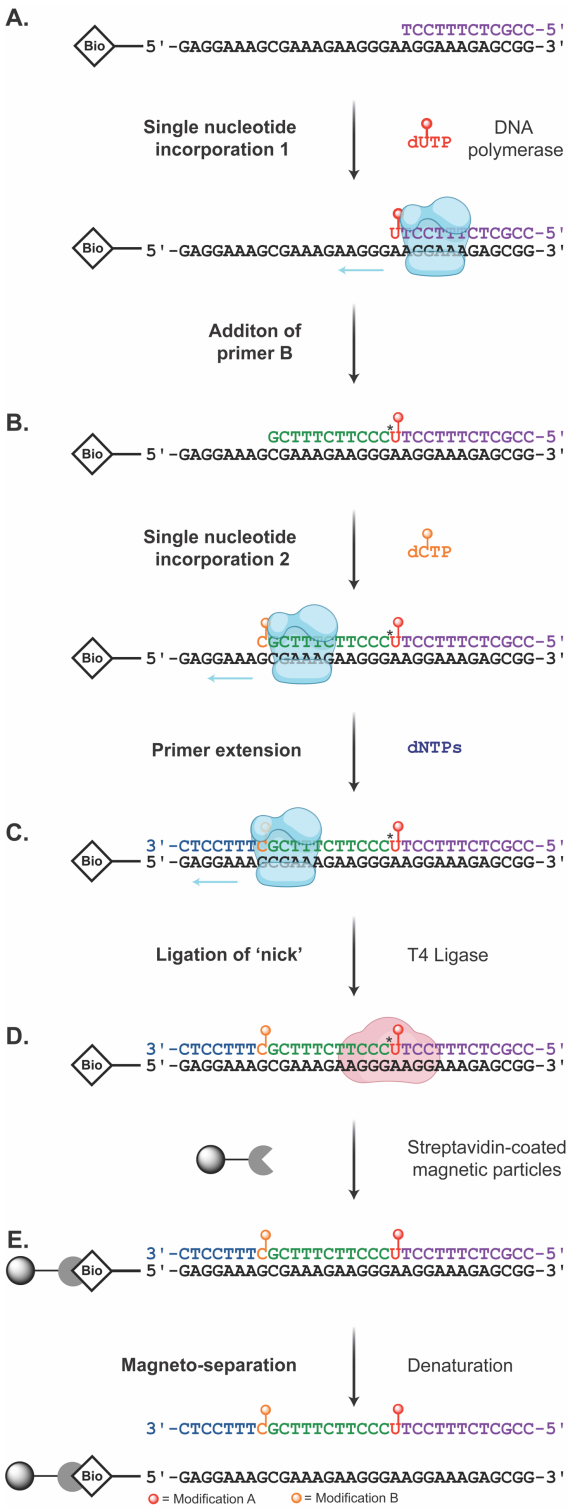


Figure 39: MNI-PEX is performed without any wash/purification steps. All reaction components are sequentially added to the same solution. **A.** Primer A (purple) was annealed to the biotinylated template (black) and a dUTP bearing modification A (red) was incorporated immediately 3′ of primer A. **B.** Primer B (green) was added and a dCTP bearing modification B (orange) was incorporated. **C.** The remainder of the TFO sequence was synthesised with natural dNTPs (blue). **D.** The 'nick' (*) between the dUTP (red) and primer B (green) was ligated using T4 ligase (pink). **E.** The newly synthesised DNA strand was then isolated using streptavidin magnetic particles and a magneto-denaturation step.

A 32-nucleotide poly-pyrimidine parallel-binding TFO, that targets a specific sequence of the eGFP gene (pCSanDI-HYG) was chosen for this study. This TFO sequence has previously been studied, and is capable of selectively hybridising with its target sequence and forming stable triple helical DNA (T_M > 45 °C).[6, 11] MNI-PEX began when a biotinylated template, complementary to this TFO sequence, and primer A were annealed in the presence of a thermostable DNA polymerase, and the dU^{TPMA}TP was incorporated immediately 3′ of the primer. However, the incorporation of dU^{TPMA}TPs required significant optimisation. The ability of five DNA polymerases to incorporate the dU^{TPMA}TPs was investigated: Vent (exo-), Therminator, Pwo, Taq and Sequenase V.2.0 (from here on Sequenase) DNA polymerases (**Figure 40**). Pwo and Taq DNA polymerases were immediately eliminated as their exonuclease activity resulted in DNA degradation. Vent (exo-), Therminator and Sequenase DNA polymerases were all capable of incorporating the dU^{TPMA}TPs to varying extents. However, upon further optimisation it was noticed that incubations with Therminator DNA polymerase yielded no suitable products. Sequenase DNA polymerase was the next to be eliminated, as it always resulted in the presence of unreacted primer and/or the incorporation of multiple non-templated bases. Vent (exo-) was found to be the most suitable, it was capable of the full incorporation of a single dU^{TPMA}TP at the 3′ position of primer A (**Figure 42**), and consequently was used for synthesis of the modified TFO.

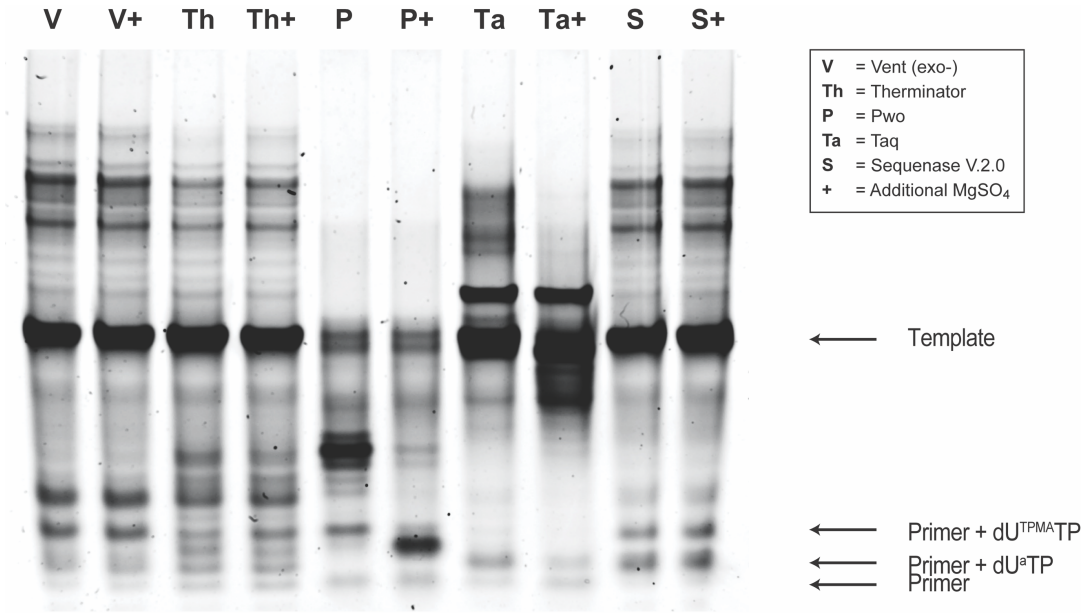


Figure 40: 20% denaturing polyacrylamide gel electrophoresis (PAGE) showing the incorporation of $dU^{TPMA}TPs$ by five DNA polymerases.

Next, primer B was annealed to the template immediately 3′ of the $dU^{TPMA}TP$, and a TO-dCTP ($dC^{TO}TP$) was incorporated after primer B. Again, this required considerable optimisation. As Vent (exo-) DNA polymerase was already in the reaction mixture it was the obvious choice for this second incorporation step. However, the incorporation of $dC^{TO}TPs$ was challenging. Various incubation times, temperatures and equivalents of $dC^{TO}TP$ were investigated, but none yielded full incorporation (*i.e.* there was unreacted primer remained in the sample). As TO is a fluorophore its position in a gel could be visualised without a DNA stain, so products from the incorporation reactions were analysed by denaturing PAGE, and visualised prior to staining with SYBR gold—to enable visualisation of TO (**Figure 41**). It was observed that a high concentration of TO was present with DNA that had not been denatured and it was realised that the TO was intercalating with dsDNA (primer annealed to template) rather than being incorporated by the DNA polymerase. Therefore, steps were taken to discourage intercalation. Acidic conditions and various salts, including NaCl, $MgCl_2$ and $MgSO_4$, were tested and it was found that NaCl (~66 mM) was sufficient at preventing intercalation, and enabled incorporation of a single $dC^{TO}TP$ at position

B (**Figure 42**). The remainder of the sequence was then synthesised with natural dNTPs.

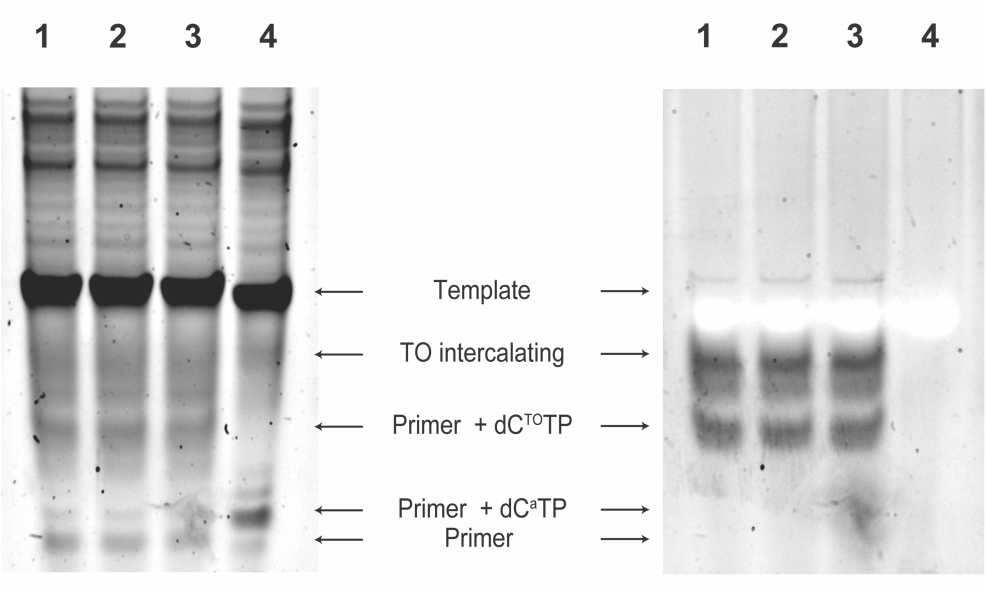


Figure 41: 20% denaturing PAGE analysis of SNI-PEX with $dC^{TO}TPs$. Left: DNA stained with SYBR gold and visualised by UV fluorescence. Right: Thiazole orange fluorescence visualised under UV fluorescence prior to staining with SYBR gold. Lane 1: 30 min. Lane 2: 45 min. Lane 3: 60 min. Lane 4: $dU^{a}TP$ control. There is a large concentration of unreacted primer remaining in lanes 1, 2 and 3, due to the TO intercalating with the primer-template dsDNA rather than being incorporated by Vent (exo-) DNA polymerase.

However, as previously mentioned there is effectively a 'nick' between the $dU^{TPMA}TP$ and primer B. T4 ligase was added to ligate this 'nick', but it was noticed that under the recommended incubation times T4 ligase was incapable of complete ligation. It was hypothesised that this was due to the large TPMA modification attached to the 5′ base, as ligation between natural and C8-alkyne modified dNTPs was successful and full length TFO products were obtained. Longer incubation times and a higher concentration of T4 ligase was found to overcome this issue, and the TPMA-TO-TFO was isolated using streptavidin coated magnetic particles and a magneto-denaturation step. The TPMA-TO-TFO was then ready (**Figure 43**, lane 1) for biophysical analysis without further purification.

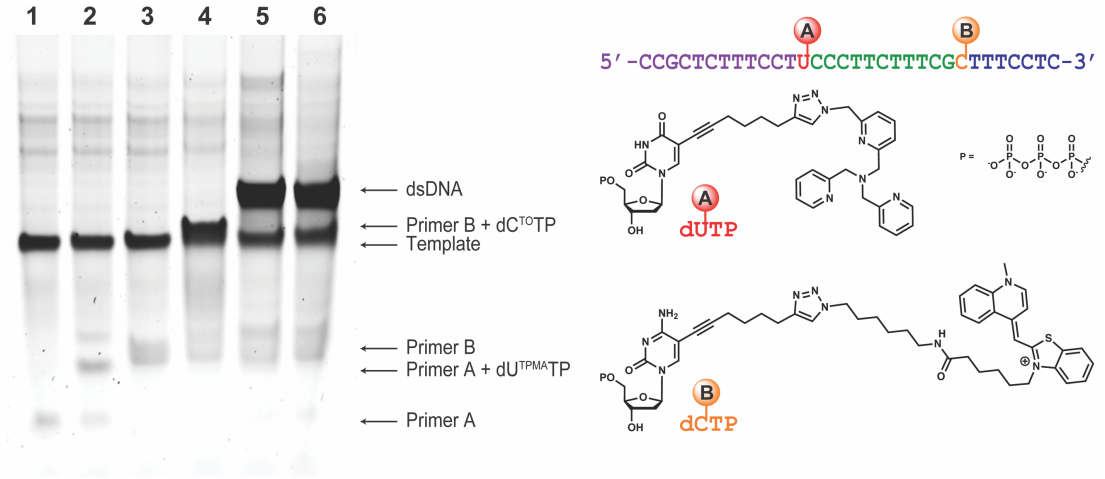


Figure 42: 20% denaturing PAGE showing incorporation of modified dNTPs during MNI-PEX. Each lane contains template DNA. Lane 1: Primer A. Lane 2: Primer A + dU^{TPMA}TP. Lane 3: Primer B. Lane 4: Primer B + dC^{TO}TP. Lane 5: Primer A + dU^{TPMA}TP + primer B. Lane 6: Primer A + dU^{TPMA}TP + primer B + dC^{TO}TP. The presence of TO can be visualised prior to staining with SYBR gold (appendix **Figure D - 2**).

Finally, the ability of the newly synthesised TPMA-TO-TFO hybrid to recognise and bind with its target DNA sequence was investigated. The TPMA-TO-TFO was incubated with a 57 bp duplex, containing the TFO recognition sequence, at 37 °C for 15 hours, before being analysed by native PAGE (**Figure 43**). It was observed that the TPMA-TO-TFO was capable of forming triple helical DNA with its target duplex, thereby confirming MNI-PEX as a viable method for the synthesis of modified antigene oligonucleotides.

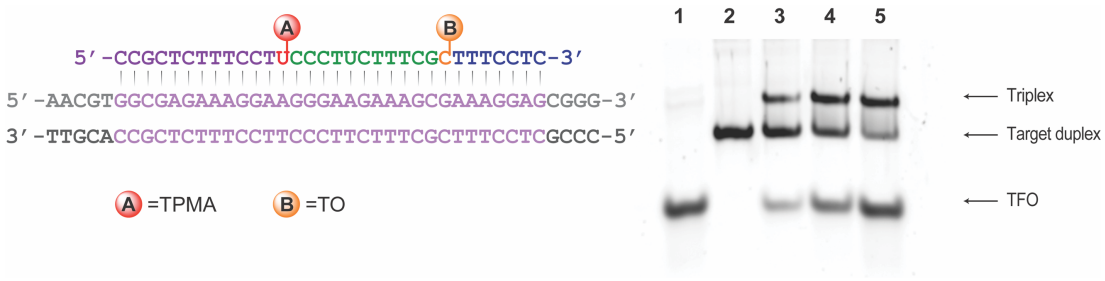


Figure 43: 20% native PAGE showing the ability of the TPMA-TO-TFO to hybridise with its genetic target. Lane 1: TPMA-TO-TFO. Lane 2: 57 bp target duplex. Lane 3-5: TPMA-TO-TFO (10, 25 and 50 eq., respectively) forming triplex DNA with a target duplex.

6.5 Conclusion

MNI-PEX is the first enzymatic protocol for the synthesis of oligonucleotides bearing multiple different modifications at distinct sequence positions. This bench-top methodology could revolutionise the production of modified-DNA, as it overcomes the environmental concerns, compatibility issues and equipment requirements of solid-phase phosphoramidite DNA synthesis. The utility of MNI-PEX was demonstrated through the production of an antigene therapeutic, bearing both a chemical nuclease and a triplex stabilising fluorophore. This technology can be further expanded for the synthesis of methyl-cytosine modified DNA, the production of RNA-DNA hybrid molecules, and the inclusion of modified backbones, such as phosphorothioate bases and locked nucleic acids. Therefore, MNI-PEX will increase the accessibility of modified oligonucleotides and help progress research into therapeutic oligonucleotides.

6.6 Experimental

6.6.1 General information

PAGE gels were cast using a SureCast™ gel casting system (Invitrogen) and SureCast™ acrylamide solution (Invitrogen), and run in an Invitrogen mini gel tank. A Bio-Rad basic Power Pac™ was used for PAGE gel electrophoresis. All gels were imaged using a Syngene G:Box 9 mini gel documentation system. PCR was performed using a Mastercycler® nexus (Eppendorf). BioRender was used to generate the DNA polymerase and T4 ligase graphics.

Raw gel images are available to download on Goggle Drive: https://drive.google.com/drive/folders/1tu199tKFWnem-pHC3Suwn_c1pU1_YWMs?usp=sharing

6.6.2 Click chemistry for the production of modified dNTPs

In an anaerobic environment a copper catalysed azide-alkyne cycloaddition (CuAAC) reaction mixture (5 nmol) between a C8-alkyne-dUTP/dCTP (BaseClick) and 6N_3-TPMA/N_3-TO was prepared (**Table 4**), in water and DMSO (1:1) to a total volume of 250 μL. Reaction proceeded at 25 °C and 450 RPM for 6 hours, and was quenched with 500 equivalents of EDTA and stored at -20 °C.

Table 4: Concentration of azide and alkyne for CuAAC.

	Alkyne concentration	Azide concentration
6N_3-TPMA	5 nmol	10 nmol
N_3-TO	5 nmol	25 nmol

6.6.3 MNI-PEX for PAGE analysis

A 10 μL MNI-PEX reaction solution was prepared; primer A (12 nt, 10 μM, 1.35 μL, appendix **Table D - 1**), 5′-biotinylated template (32 nt, 10 μM, 1.35 μL),

$dU^{TPMA}TPs$ (13.3 μM, 1.52 μL), $MgSO_4$ (100 mM, 0.4 μL, NEB) and Vent (exo-) DNA polymerase (2 U/ μL, 0.5 μL, NEB) in ThermoPol buffer (10 x, 1 μL, NEB) and incubated at 60 °C and 450 RPM for 90 min. Next primer 1 B (18 nt, 10 μM, 1.35 μL, appendix **Table D - 1**) and $dC^{TO}TPs$ (13.3 μM, 2.026 μL) were added and sample was incubated at 60 °C and 450 RPM for 30 min. Sample was cooled to 4 °C to stop the reaction. MNI-PEX sample was added to pre-mixed T4 DNA ligase (1 μL, NEB) and T4 ligase buffer (10X, 1.5 μL, NEB) and incubated at room temperature for 180 min, before the enzyme was deactivated by heating to 60 °C.

6.6.4 Denaturing PAGE

20% denaturing polyacrylamide gels (1x TBE buffer, 7M urea) were cast. Denaturing loading buffer (2X, 95% formamide, 18 mM EDTA, 0.025% SDS, xylene cyanol, bromophenol blue, Invitrogen) was added to MNI-PEX samples (10 μL) and heated to 95 °C for 4 min. Samples were loaded directly onto the gel and run at 150 V for 160 min. Gel was post-stained with SYBR gold and visualised under UV fluorescence.

6.6.5 MNI-PEX for synthesis of TPMA-TO-TFO

A 300 μL MNI-PEX reaction solution was prepared; primer A (12 nt, 10 μM, 40.5 μL, appendix **Table D - 1**), 5′-biotinylated template (32 nt, 10 μM, 40.5 μL), $dU^{TPMA}TPs$ (13.3 μM, 45.6 μL), $MgSO_4$ (100 mM, 12 μL, NEB) and Vent (exo-) DNA polymerase (2 U/ μL, 15 uL, NEB) in ThermoPol buffer (10 x, 30 μL, NEB) and incubated at 60 °C and 450 RPM for 90 min. Next primer 1 B (18 nt, 10 μM, 40.5 μL, appendix **Table D - 1**) and $dC^{TO}TPs$ (13.3 μM, 60.78 μL) were added and sample was incubated at 60 °C and 450 RPM for 30 min. Sample was cooled to 4 °C to stop the reaction. MNI-PEX sample was added to pre-mixed T4 DNA ligase (20 μL, NEB) and T4 ligase buffer (10X, 60 μL, NEB) and incubated at room temperature for 180 min, before the enzyme was deactivated by heating to 60 °C.

6.6.6 Streptavidin bead isolation of TPMA-TO-TFO

Streptavidin magnetic particles (150 μL, Roche) were washed three times with TEN_{100} (300 μL; 10 mM Tris, 1 mM EDTA, 100 mM NaCl, pH 7.5), and resuspended in TEN_{100} (150 μL). MNI-PEX solution (300 μL) was added and incubated at 18 °C and 1200 RPM for 20 min. Particles were collected on a magnet and solution was discarded. Particles were washed three times with TEN_{1000} (300 μL; 10 mM Tris, 1 mM EDTA, 1 M NaCl, pH 7.5), and then washed four times with elution buffer (300 μL, 100 mM sodium pyrophosphate). Particles were resuspended in elution buffer (150 μL), and double stranded DNA was denatured (65 °C for 90 sec). Particles were collected on a magnet and the solution, containing the single stranded TFO, was collected. TFO was de-salted using Sephadex™ G-25 grade gravity filtration columns (NAP-5™, Cytiva illustra™).

6.6.7 Analysis of TPMA-TO-TFO

6.6.7.1 Amplification of TFO target

A 57 bp amplicon containing the TFO recognition sequence (pCSanDI-HYG; forward: 5′-AAGCCGGCGAACGTGGCGG-3′ and reverse: 5′-CCTAGCGCCCGCTCCTTTCG -3′) was generated by PCR (MyTaq Red DNA polymerase, Bioline) and purified into 6 μL of nuclease-free water using membrane spin columns (Monarch PCR & DNA clean-up kit, NEB).

6.6.7.2 Triplex PAGE

Target (57 bp, 1 pmol) and *off*-target (40 bp, 1 pmol) duplexes were incubated with 10, 25 and 50 equivalents of TPMA-TO-TFO (32 nt) in phosphate buffer (10 mM PO_4^{3-}, 150 mM NaCl, 2 mM $MgCl_2$, pH 6.1) at 37 ºC for 24 hours. 6X loading dye (10 mM Tris-HCl, pH 7.6, 0.03% bromophenol blue, 0.03% xylene cyanol FF, 60% glycerol, 60 mM EDTA, Invitrogen) was added, and the entire solution was loaded onto a 20% native PAGE gel (50 mM Tris-acetate, 75 mM NaCl, 5 mM $MgCl_2$, pH 6.1). Gel was run at 70 V for 240 min, before being post-stained with SYBR gold.

References

1. Caruthers, M., Gene synthesis machines: DNA chemistry and its uses. *Science* **1985,** *230* (4723), 281-285.
2. Beaucage, S. L.; Caruthers, M. H., Deoxynucleoside phosphoramidites—A new class of key intermediates for deoxypolynucleotide synthesis. *Tetrahedron Lett.* **1981,** *22* (20), 1859-1862.
3. Hocek, M., Synthesis of base-modified 2'-deoxyribonucleoside triphosphates and their use in enzymatic synthesis of modified DNA for applications in bioanalysis and chemical biology. *J. Org. Chem.* **2014,** *79* (21), 9914-21.
4. Langer, P. R.; Waldrop, A. A.; Ward, D. C., Enzymatic synthesis of biotin-labeled polynucleotides: novel nucleic acid affinity probes. *Proc. Natl. Acad. Sci.* **1981,** *78* (11), 6633-7.
5. Menova, P.; Cahova, H.; Plucnara, M.; Havran, L.; Fojta, M.; Hocek, M., Polymerase synthesis of oligonucleotides containing a single chemically modified nucleobase for site-specific redox labelling. *Chem. Comm.* **2013,** *49* (41), 4652-4.
6. McGorman, B.; Zuin Fantoni, N.; O'Carroll, S.; Ziemele, A.; El-Sagheer, A. H.; Brown, T.; Kellett, A., Enzymatic synthesis of chemical nucelase triple-forming oligonucleotides with gene-editing applications. *Manuscript under review*.
7. Leone, D. L.; Hubálek, M.; Pohl, R.; Sýkorová, V.; Hocek, M., 1,3-Diketone-Modified Nucleotides and DNA for Cross-Linking with Arginine-Containing Peptides and Proteins. *Angew. Chem. Int. Ed.* **2021**.
8. Güixens-Gallardo, P.; Hocek, M., Acetophenyl-thienyl-aniline-Linked Nucleotide for Construction of Solvatochromic Fluorescence Light-Up DNA Probes Sensing Protein-DNA Interactions. *Chem. Eur. J.* **2021,** *27* (24), 7090-7093.
9. Kolb, H. C.; Finn, M. G.; Sharpless, K. B., Click Chemistry: Diverse Chemical Function from a Few Good Reactions. *Angew. Chem. Int. Ed.* **2001,** *40*, 2004-2021.
10. Hennessy, J.; McGorman, B.; Molphy, Z.; Farrell, N. P.; Singleton, D.; Brown, T.; Kellett, A., A Click Chemistry Approach to Targeted DNA Crosslinking with cis-Platinum(II) Modified Triplex Forming Oligonucleotides. *Angew. Chem. Int. Ed.* **2021,** *60*.
11. Zuin Fantoni, N.; McGorman, B.; Molphy, Z.; Singleton, D.; Walsh, S.; El-Sagheer, A. H.; McKee, V.; Brown, T.; Kellett, A., Development of Gene-Targeted Polypyridyl Triplex-Forming Oligonucleotide Hybrids. *ChemBioChem* **2020,** *21* (24), 3563-3574.
12. Lauria, T.; Slator, C.; McKee, V.; Müller, M.; Stazzoni, S.; Crisp, A. L.; Carell, T.; Kellett, A., A Click Chemistry Approach to Developing Molecularly Targeted DNA Scissors. *Chem. Eur. J.* **2020**.
13. McStay, N.; Slator, C.; Singh, V.; Gibney, A.; Westerlund, F.; Kellett, A., Click and Cut: a click chemistry approach to developing oxidative DNA damaging agents. *Nucleic Acids Res.* **2021**.
14. Panattoni, A.; El-Sagheer, A. H.; Brown, T.; Kellett, A.; Hocek, M., Oxidative DNA Cleavage with Clip-Phenanthroline Triplex-Forming Oligonucleotide Hybrids. *ChemBioChem* **2020,** *21* (7), 991-1000.

15. Zuin Fantoni, N.; Molphy, Z.; Slator, C.; Menounou, G.; Toniolo, G.; Mitrikas, G.; McKee, V.; Chatgilialoglu, C.; Kellett, A., Polypyridyl-Based Copper Phenanthrene Complexes: A New Type of Stabilized Artificial Chemical Nuclease. *Chem. Eur. J.* **2019,** *25* (1), 221-237.
16. Walsh, S.; El-Sagheer, A. H.; Brown, T., Fluorogenic thiazole orange TOTFO probes stabilise parallel DNA triplexes at pH 7 and above. *Chem Sci* **2018,** *9* (39), 7681-7687.

Chapter 7

Conclusion and Future Work

7.1 Conclusion

The objectives of this project were to: 1) Develop a series of molecular methods for the analysis of gene-targeted metallodrug hybrids; 2) devise and optimise a protocol for the enzymatic synthesis of oligonucleotides bearing large modifications; 3) enzymatically synthesise a chemical nuclease-TFO hybrid and compare its functionality to its solid-phase synthesis counterpart; and 4) design a novel method for the enzymatic synthesis of complex oligonucleotides containing multiple different modifications at distinct sequence positions.

Metallodrug-TFO hybrids are capable of damaging a specific DNA target, and therefore techniques for the analysis of this damage were required. Gel electrophoresis protocols that enable visualisation of sequence selective triplex formation and the resulting DNA damage were developed. These Tris-acetate polyacrylamide gels allow for distinct TFO, target duplex, *off*-target duplex and triple helical DNA bands to be visualised, and sequence selective DNA damage to be observed. Fluorescence thermal melting was optimised to determine the stability of the TFO hybrids, and changes in T_M were observed between modified and non-modified sequences. A real-time qPCR protocol was designed to quantify the DNA damage that these metallodrug-TFO hybrids inflict upon target and *off*-target sequences. This qPCR method calculates the relative concentration of intact DNA duplex, and thereby determines the extent of DNA damage that has inflicted upon target and *off*-target dsDNA. These PAGE, T_M and qPCR methods are applicable to the analysis of a wide range of sequence selective DNA damaging agents, including AMN-TFO hybrids, Pt(II)-TFOs and three-way-junction binding helicates.

An enzymatic method for the production of modified oligonucleotides was developed for the synthesis of AMN-TFO hybrids. This began with the generation of a library of click-functionalised nucleotide triphosphates that could be incorporated into an oligonucleotide sequence by a thermostable DNA polymerase. SNI-PEX was chosen as the most suitable protocol for the synthesis of modified DNA, and this methodology was optimised for the incorporation of AMN-dNTPs at a specific sequence position. However, the isolation of the AMN-TFO hybrids proved a significant challenge, as the melting temperature of the

TFO-template dsDNA was above the streptavidin-biotin threshold. This was overcome through the addition of sodium pyrophosphate, and the AMN-TFO was successfully isolated.

The molecular methods for the analysis of targeted genetic damage and the enzymatic protocol for the production of metallodrug-TFOs were then combined for the synthesis and analysis of a DPA-TFO hybrid. The DPA-TFO was produced through nucleic acid click chemistry and SNI-PEX, and its sequence selective activity was compared to its SPS and post-synthetic functionalisation counterpart. The results obtained confirmed that the SNI-PEX methodology was suitable for the synthesis of modified antigene therapeutics.

However, SNI-PEX was only capable of incorporating a single modified dNTP at a specific position, which limited its functionality in the production of therapeutic oligonucleotides. Therefore, a novel protocol that expands upon SNI-PEX, and enables the synthesis of oligonucleotides bearing multiple different modifications was developed. MNI-PEX (multiple nucleotide incorporation-primer extension) was carefully designed and optimised for the production of a TFO with a chemical nuclease (TPMA) and a fluorogenic intercalator (TO) at distinct sequence positions, and the ability of this TPMA-TO-TFO hybrid to bind with its genetic target was reported. This MNI-PEX technology can be expanded for the synthesis of a wide range of oligonucleotides, giving it the potential to expand enzymatic synthesis and increase the accessibility of modified oligonucleotides.

7.2 Future work

7.2.1 MNI-PEX

In Chapter 6, a novel MNI-PEX protocol was developed, and the extensive planning and optimisation was reported. A TPMA-TO-TFO was successfully synthesised by MNI-PEX, and its ability to form triple helical DNA was visualised by PAGE. However, there are many opportunities for the expansion within the MNI-PEX methodology: i.) The use of additional primers would allow more modified bases to be included at specific sequence positions; ii.) the library of modified-dNTPs can be expanded to include DNA crosslinking agents, alternative chemical nucleases and fluorescent reporters; iii.) through the use of modified

primers, oligonucleotides containing artificial backbones can be synthesised, this may include phosphorothioates or locked nucleic acids (LNA)[1]; and iv.) RNA-DNA hybrid molecules can be synthesised, which will expand the genetic targeting possibilities of the therapeutic oligonucleotides produced (**Figure 44**).

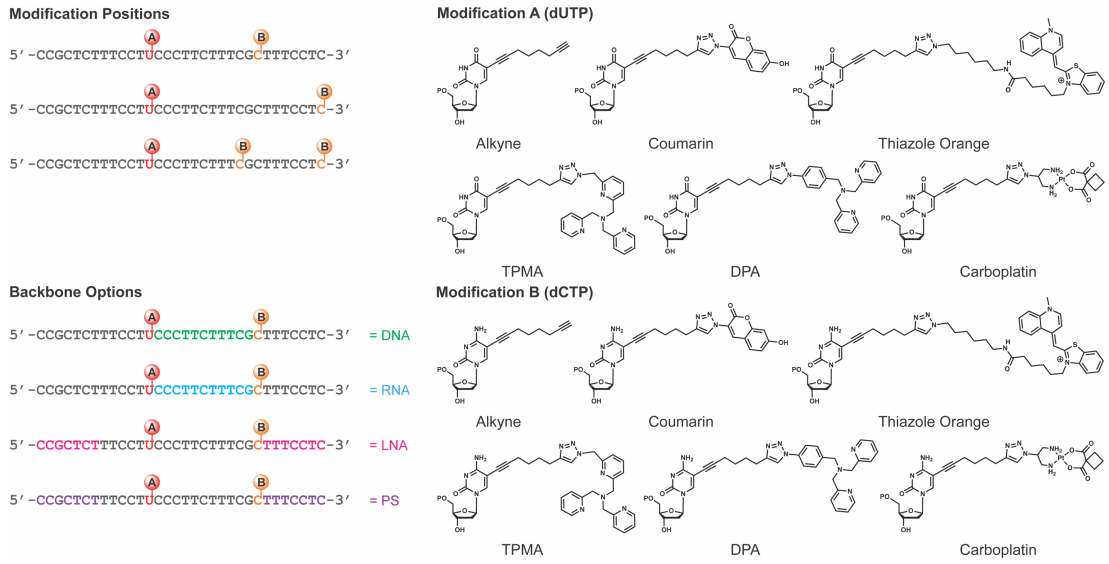


Figure 44: Possible expansions of the MNI-PEX protocol, includes alternative backbones and a wider variety of modifications. LNA = locked nucleic acid. PS = phosphorothioate.

7.2.2 NEAR for primer synthesis

When primer extension is used as a method of enzymatic synthesis the primer forms a significant portion of the resulting oligonucleotide. This is further increased in the MNI-PEX protocol as it requires the use multiple primers. Typically, these primers are non-modified sequences, purchased from commercial suppliers, and therefore do not aid in triplex stabilisation or DNA binding. The nicking enzyme amplification reaction (NEAR)[2, 3] offers a method for the enzymatic synthesis of DNA primers, which enables modified dNTPs, such as 5-methyl-cytosines or phosphorothioates,[1] to be included in the primer sequence. Therefore, a NEAR protocol for the synthesis of modified primers, for use in SNI-PEX and MNI-PEX, would expand the applications of the oligonucleotides produced. There will be challenges involved with using modified nucleotides in the NEAR protocol as a nicking enzyme, such as Nt. BstNBI, must

recognise and cleave the DNA at the correct site, but through optimisation of the protocol these challenges can be overcome.

7.2.3 Analysis of TFO hybrids within a cellular system

The TFO hybrids produced in this project were not tested in a cellular context, but this will be an important step towards the development of a successful antigene therapeutic. However, before cell experiments are performed it will be necessary to synthesise TFO hybrids with modified backbones (section 7.2.1), such as phosphorothioates or LNAs, as these modifications increase the stability of an oligonucleotide in biological systems by reducing its sensitivity to DNases.[4] It will also be important to perform analysis, such as ESI-MS and HPLC, to ensure sample purity before performing cell culture experiments. There may also be challenges regarding the delivery of antigene TFOs to their biological target. These will be overcome through the use of a carefully designed delivery mechanism. Lipid nanoparticles are an attractive technology for this task. They can be designed to ensure stability within the blood stream and the efficient delivery of oligonucleotides to biological targets. Lipid nanoparticles have successfully been utilised in the delivery system of the SARS-CoV-2 mRNA vaccines (Pfizer BioNTech and Moderna),[5] and therefore are an attractive choice for the delivery of antigene oligonucleotides. Additionally, the inclusion of phosphorothioates in an oligonucleotide backbone confers nuclease resistance[4] and promotes binding with proteins, including nucleolin, that aid delivery of oligonucleotides to the nucleus.[6] Therefore, by combining a lipid nanoparticle delivery system with a phosphorothioate backbone it is hypothesised that TFOs can be successfully studied in a cellular context.

7.2.4 Alternative genetic targets

In the work to date the metallo-drug-TFO hybrids produced have been designed to target the GFP gene. While this is a useful target during the developmental stages it does not represent a clinical application. Therefore, the production of antigene oligonucleotides with therapeutic applications is an important next step for this research. In collaboration with Dr. Thomas Frischmuth, the CEO of

BaseClick GmbH, there are plans to expand the MNI-PEX technology for the development of a COVID-19 therapeutic. The BaseClick team have identified a region of looped RNA that is conserved between all variants of SARS-CoV-2 offering a potential target sequence for an antigene therapeutic. The MNI-PEX methodology will be combined with Tri-Click ligands,[7] developed in the Kellett research group, in the hope of achieving this ambitious goal.

References

1. Flamme, M.; Hanlon, S.; Iding, H.; Puentener, K.; Sladojevich, F.; Hollenstein, M., Towards the enzymatic synthesis of phosphorothioate containing LNA oligonucleotides. *Bioorg. Med. Chem. Lett.* **2021,** *48*, 128242.
2. Hocek, M., Synthesis of base-modified 2'-deoxyribonucleoside triphosphates and their use in enzymatic synthesis of modified DNA for applications in bioanalysis and chemical biology. *J. Org. Chem.* **2014,** *79* (21), 9914-21.
3. Ménová, P.; Raindlová, V.; Hocek, M., Scope and Limitations of the Nicking Enzyme Amplification Reaction for the Synthesis of Base-Modified Oligonucleotides and Primers for PCR. *Bioconjug. Chem.* **2013,** *24* (6), 1081-1093.
4. Spitzer, S.; Eckstein, F., Inhibition of deoxyribonucleases by phosphorothioate groups in oligodeoxyribonucleotides. *Nucleic Acids Res.* **1988,** *16* (24), 11691-11704.
5. Tenchov, R.; Bird, R.; Curtze, A. E.; Zhou, Q., Lipid Nanoparticles─From Liposomes to mRNA Vaccine Delivery, a Landscape of Research Diversity and Advancement. *ACS Nano* **2021,** *15* (11), 16982-17015.
6. Roberts, T. C.; Langer, R.; Wood, M. J. A., Advances in oligonucleotide drug delivery. *Nature Reviews Drug Discovery* **2020,** *19* (10), 673-694.
7. McStay, N.; Slator, C.; Singh, V.; Gibney, A.; Westerlund, F.; Kellett, A., Click and Cut: a click chemistry approach to developing oxidative DNA damaging agents. *Nucleic Acids Res.* **2021**.

Appendix A

A.1 PAGE analysis

A.1.1 Triplex PAGE

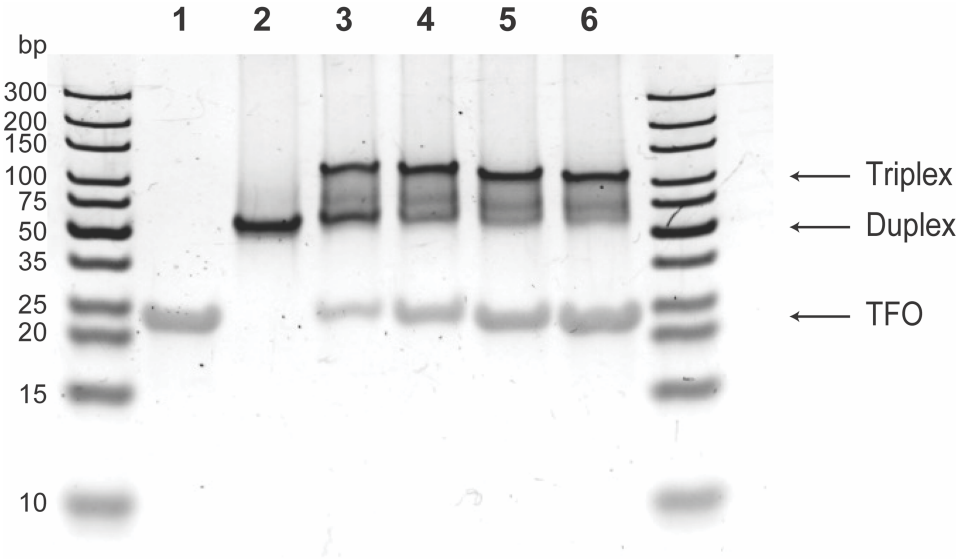


Figure A - 1: 20% native Tris-acetate PAGE analysis of triplex formation. Lane 1: TFO (32 nt). Lane 2: Target duplex (57 bp). Lane 3-6: Triplex formation; TFO incubated with target duplex at 10, 25, 50 and 100 equivalents to duplex, respectively. Ultra-low molecular weight double-stranded DNA ladder shown in outside lanes.

A.1.2 AMN-TFO hybrids

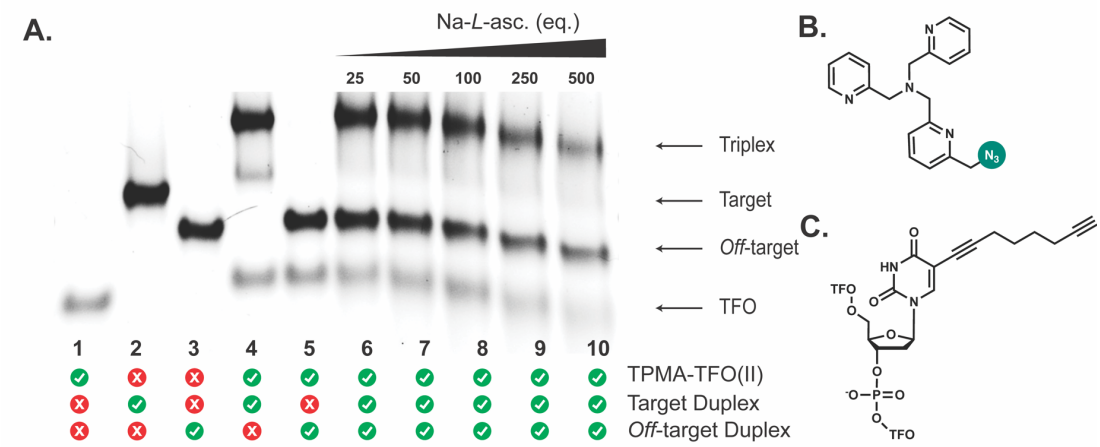


Figure A - 2: A. 20% native PAGE showing the DNA damage resulting from incubation with TPMA-TFO(II). Lane 1: TPMA-TFO(II). Lane 2: 57 bp target duplex. Lane 3: *Off*-target duplex (40 bp). Lane 4: TPMA-TFO hybridised with target duplex to form triplex DNA. Lane 5: TFO does not bind with *off*-target duplex. Lanes 6-10: TPMA-TFO(II) incubated with target and *off*-target duplexes and increasing concentrations of Na-*L*-ascorbate (25-500 eq.). **B.** 6N_3-TPMA. **C.** Octadiynyl-dU modification included in TFO sequence.

A.1.3 Pt(II)-TFO hybrids

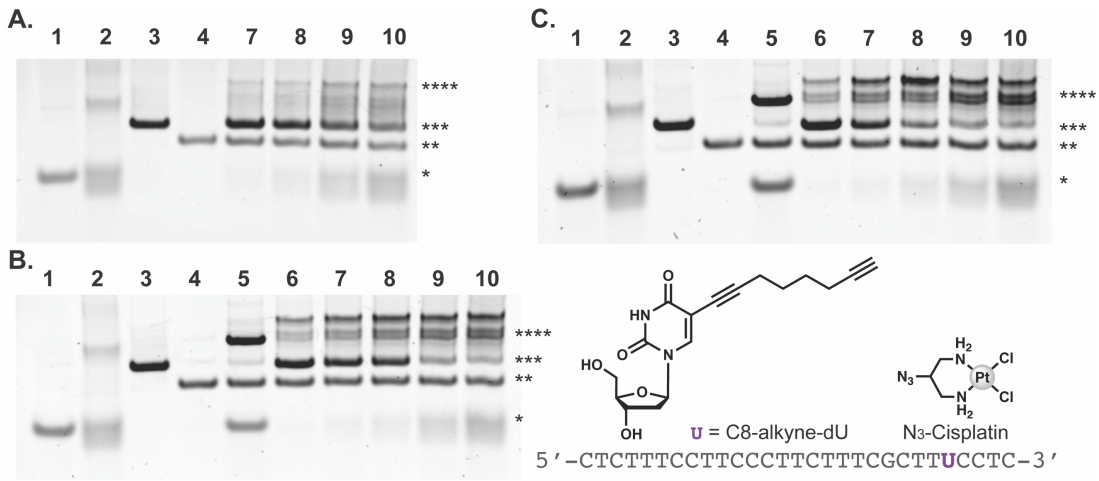


Figure A - 3: 20% native Tris-acetate PAGE analysis of cisplatin-TFO3 hybrid. Lane 1: Alkyne TFO. Lane 2: Pt-TFO. Lane 3: Target duplex. Lane 4: *Off*-target duplex. Lane 5: Alkyne TFO and duplexes. Lanes 6-10: 2.5, 5, 10, 25 and 50 equivalents of Pt-TFO to duplex. TFO was incubated with duplex for 2 (**A.**), 24 (**B.**) or 48 (**C.**) hours. * = TFO, ** = *Off*-target duplex, *** = Target duplex, **** = Triplex.

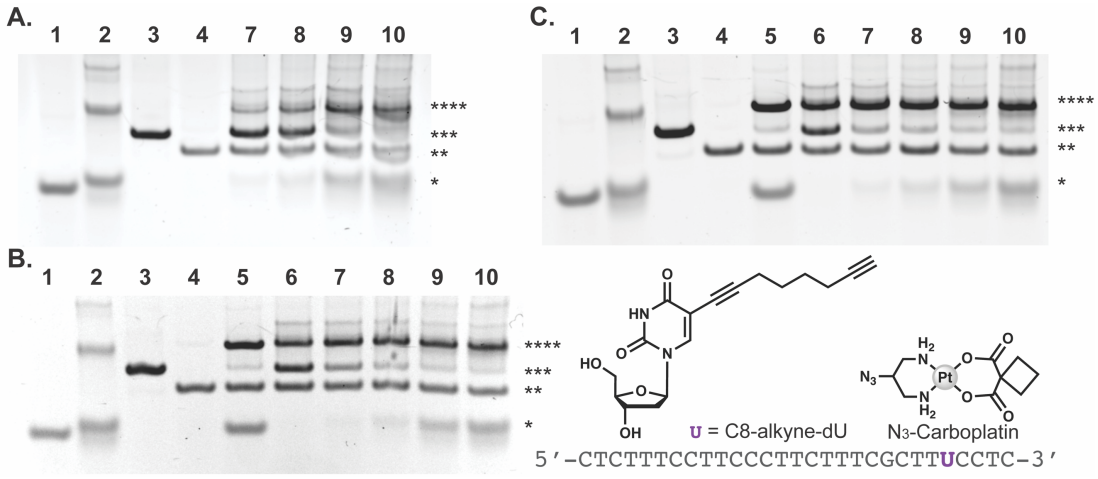


Figure A - 4: Native PAGE (20%) analysis of carboplatin-TFO3 hybrid. Lane 1: Alkyne TFO. Lane 2: Pt-TFO. Lane 3: Target duplex. Lane 4: *Off*-target duplex. Lane 5: Alkyne TFO and duplexes. Lanes 6-10: 2.5, 5, 10, 25 and 50 equivalents of Pt-TFO to duplex. TFO was incubated with duplex for 2 (**A.**), 24 (**B.**) or 48 (**C.**) hours. * = TFO, ** = *Off*-target duplex, *** = Target duplex, **** = Triplex.

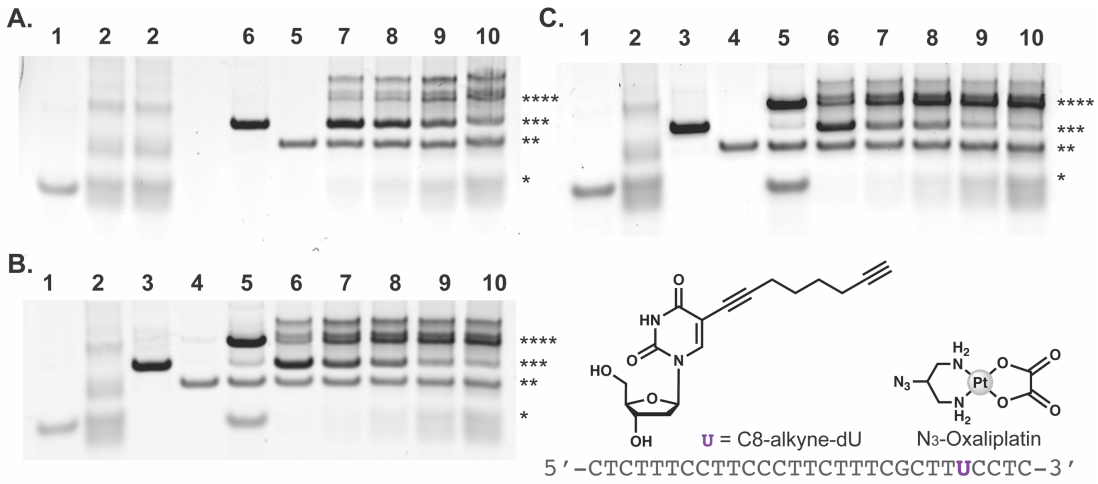


Figure A - 5: 20% Tris-acetate PAGE analysis of oxaliplatin-TFO3 hybrid. Lane 1: Alkyne TFO. Lane 2: Pt-TFO. Lane 3: Target duplex. Lane 4: *Off*-target duplex. Lane 5: Alkyne TFO and duplexes. Lanes 6-10: 2.5, 5, 10, 25 and 50 equivalents of Pt-TFO to duplex. TFO was incubated with duplex for 2 (**A.**), 24 (**B.**) or 48 (**C.**) hours. * = TFO, ** = *Off*-target duplex, *** = Target duplex, **** = Triplex.

A.2 qPCR controls

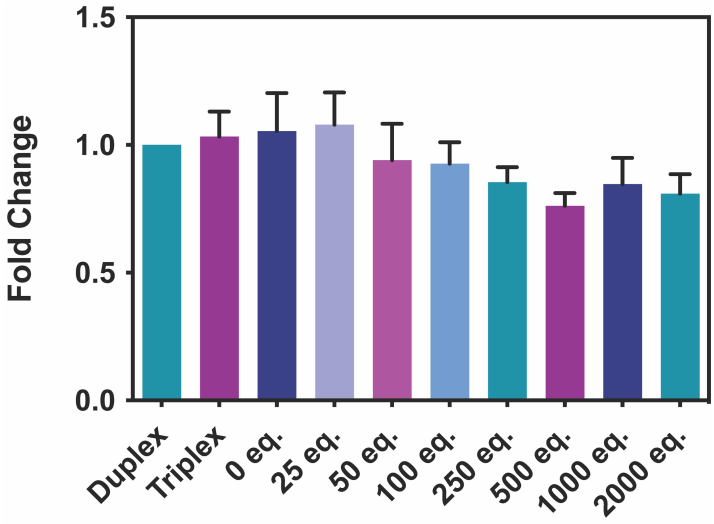


Figure A - 6: Control qPCR experiment performed with 25 equivalents of $Cu(ClO_4)_2$ to duplex DNA and increasing equivalents of Na-*L*-ascorbate. No significant DNA damage was observed.

Appendix B

B.1 Incorporation of modified dNTPs

B.1.1 SNI-PEX – dN^{TPMA}TPs

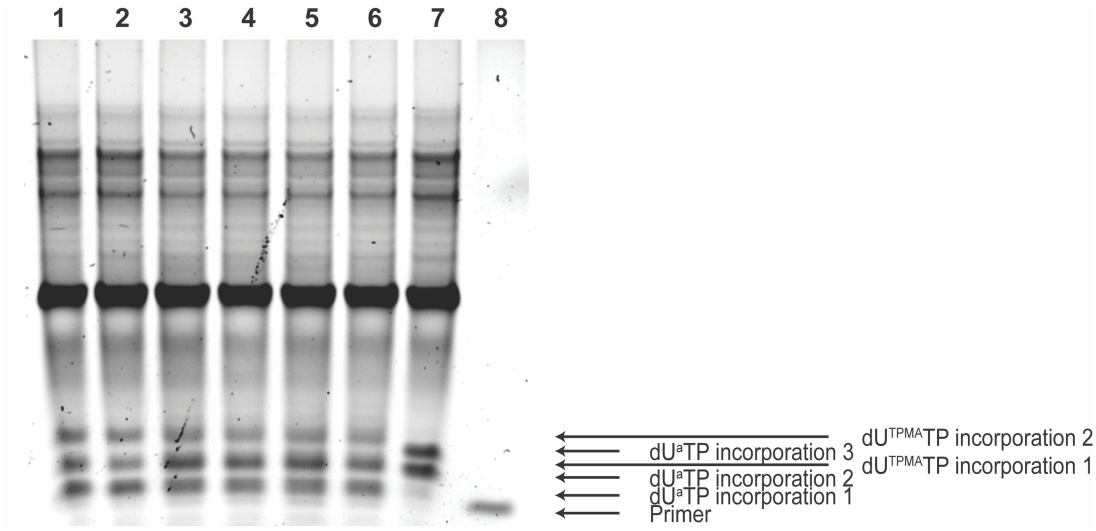


Figure B - 1: Incorporation of dU^{TPMA}TP with various concentration of Sequenase DNA polymerase, incubated at 37 ºC for 60 min. Lane 1: 2.5 U sequenase. Lane 2: 2.5 U sequenase + $MgSO_4$. Lane 3: 5 U sequenase. Lane 4: 5 U sequenase + $MgSO_4$. Lane 5: 7.5 U sequenase. Lane 6: 7.5 U sequenase + $MgSO_4$. Lane 7: Incorporation of dU^{a}TP with 2.5 U sequenase. Lane 8: Primer control. In all lanes sequenase DNA polymerase incorporated multiple dUTPs, the second (and third) of which are non-templated. Therefore sequenase DNA polymerase was not suitable for the incorporation of dU^{TPMA}TPs.

B.1.2 SNI-PEX - dN^{DPA}TPs

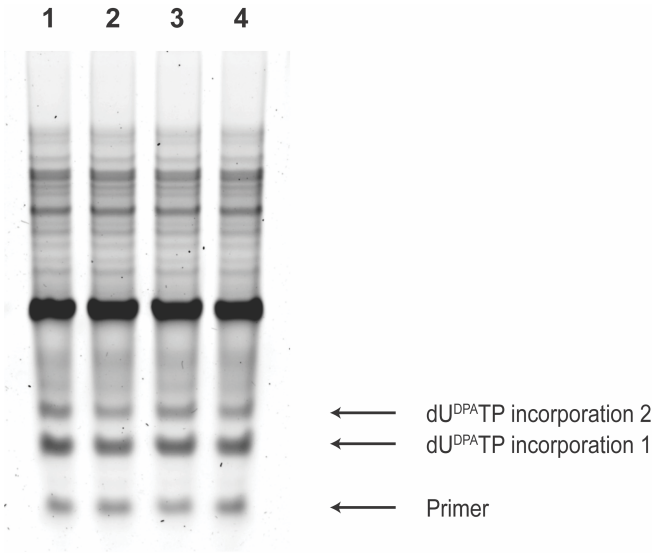


Figure B - 2: Vent (exo-) DNA polymerase incorporation of dU^{DPA}TP. Lane 1: 2 U Vent (exo-) DNA polymerase incubated for 5 min. Lane 2: 2 U Vent (exo-) DNA polymerase and $MgSO_4$ incubated for 5 min. Lane 3: 1 U Vent (exo-) DNA polymerase incubated for 5 min. Lane 4: 1 U Vent (exo-) DNA polymerase and $MgSO_4$ incubated for 5 min. A second (non-templated) dU^{DPA}TP is incorporated by Vent (exo-) DNA polymerase but after 5 min of incubation no incorporation of a third dU^{DPA}TP is observed.

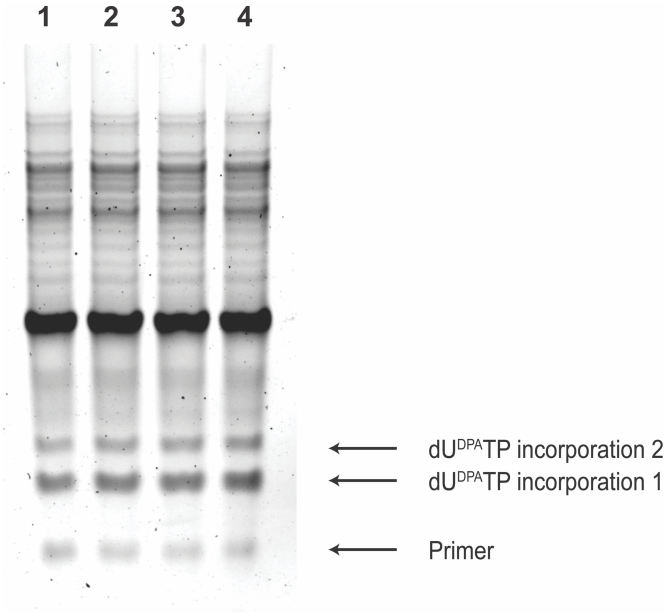


Figure B - 3: Incorporation of dU^{DPA}TP by Vent (exo-) DNA polymerase at 37 ºC. Lane 1-4: Incubation time of 5, 15, 30 and 60 min, respectively. A maximum of two dU^{DPA}TPs (the first templated and the second non-templated) are incorporated at 37 ºC.

Appendix C

C.1 Synthesis of 4N$_3$-benzyl-DPA

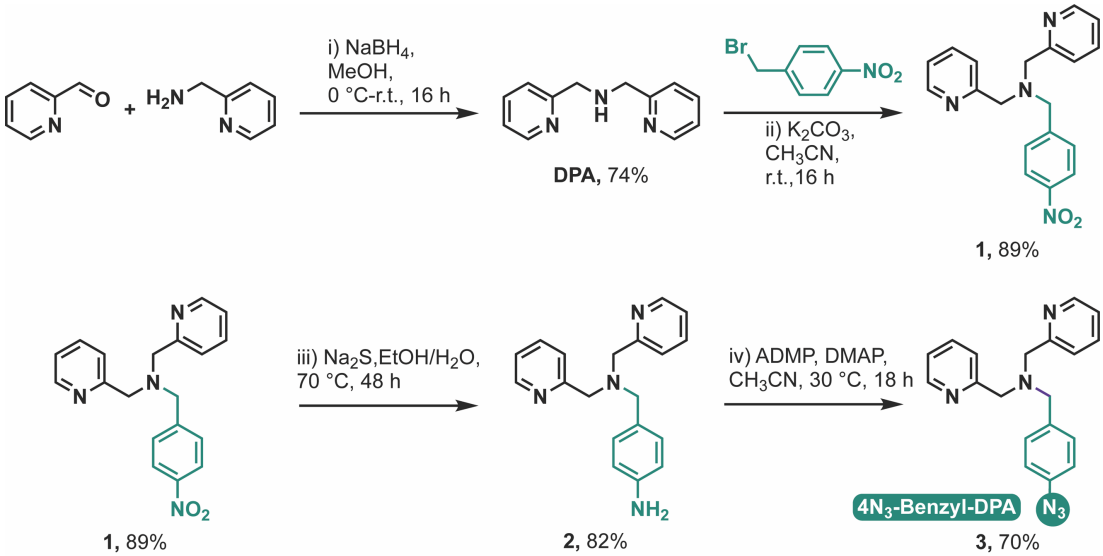


Figure C - 1: Schematic for the synthesis of 4N$_3$-benzyl-DPA.

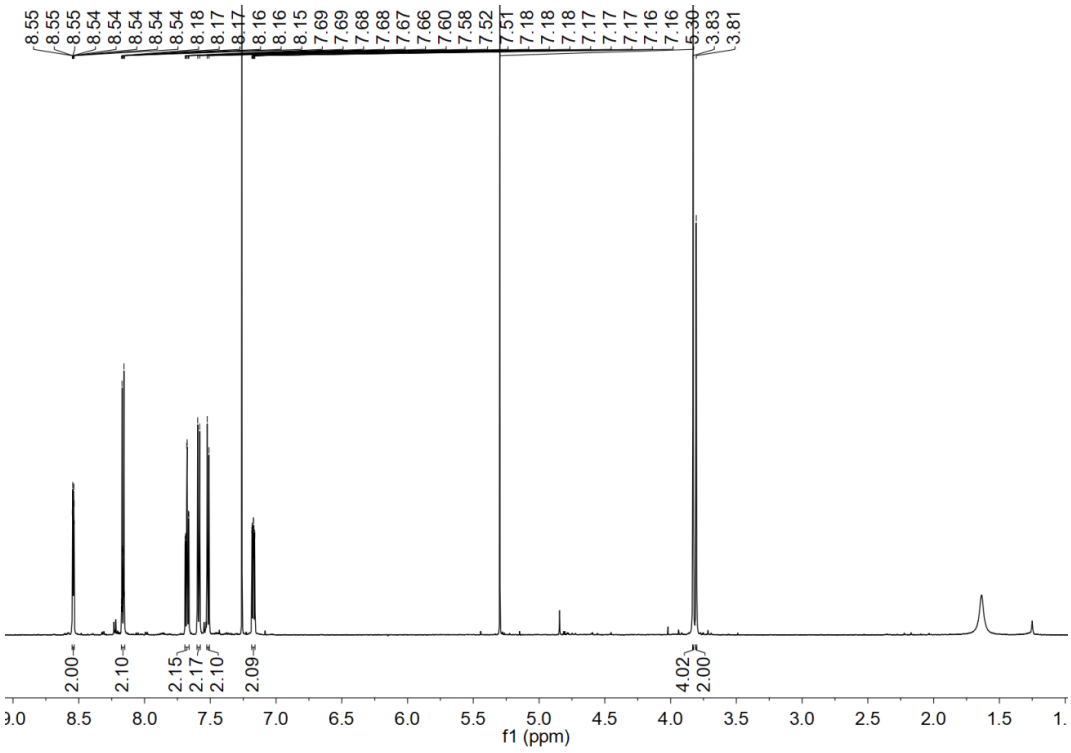


Figure C - 2: ^{1}H-NMR spectrum of N-4-nitrobenzyl-N-di-(2-picolyl)amine (1).

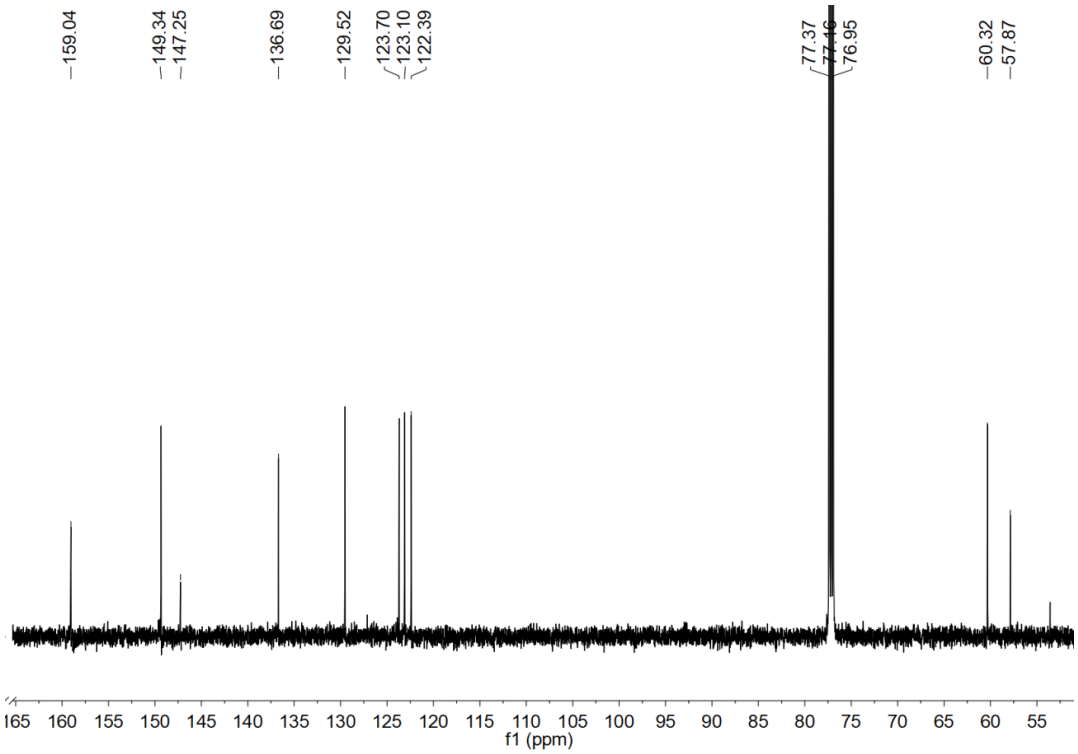


Figure C - 3: ^{13}C-NMR spectrum of *N*-4-nitrobenzyl-*N*-*di*-(2-picolyl)amine (1).

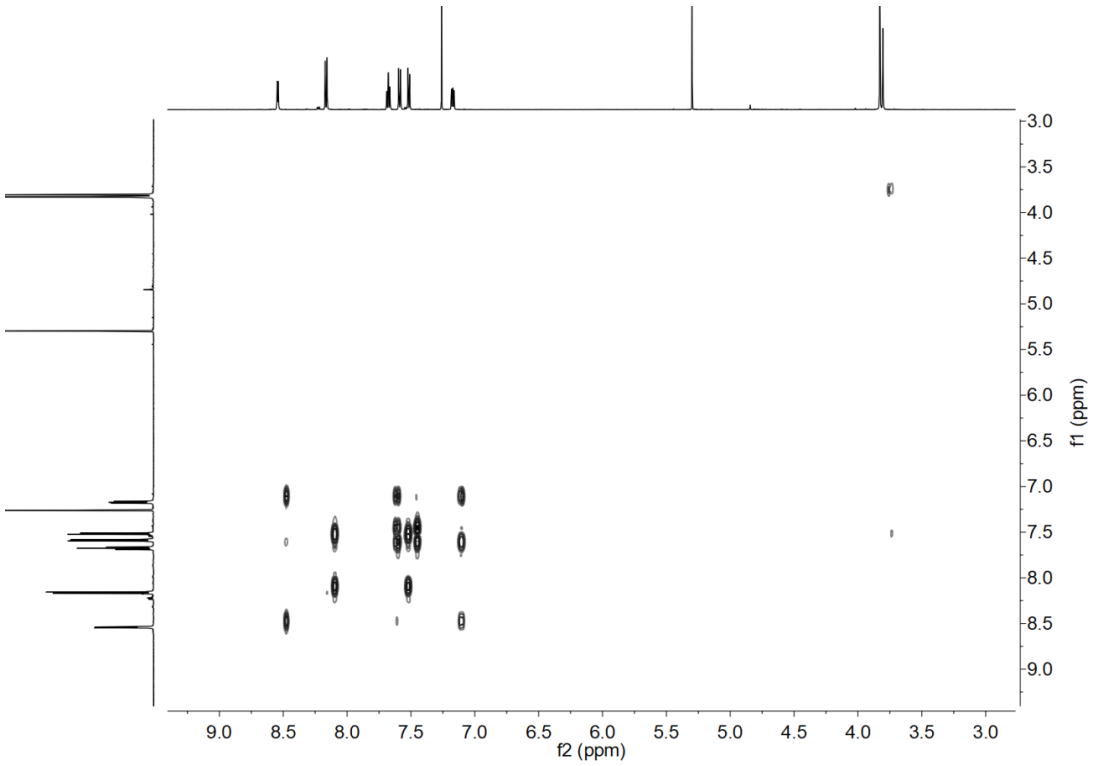


Figure C - 4: ^{1}H-^{1}H COSY spectrum of N-4-nitrobenzyl-N-di-(2-picolyl)amine (1).

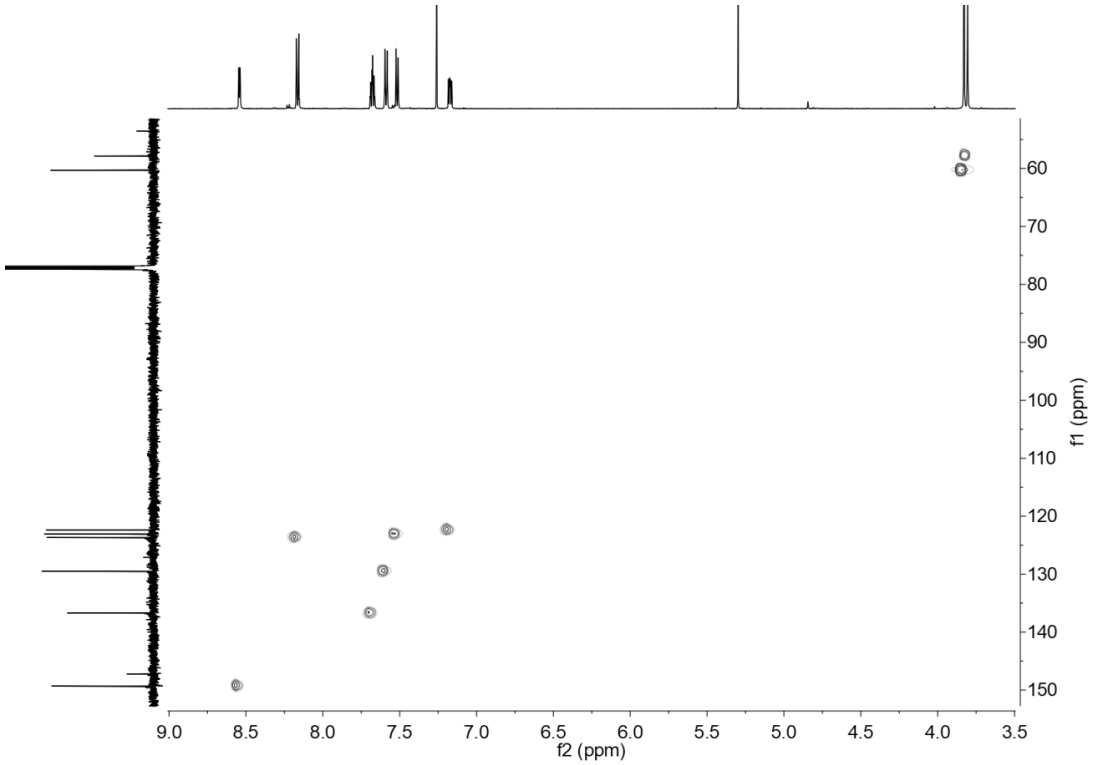


Figure C - 5: ^{1}H-13C HSQC spectrum of N-4-nitrobenzyl-N-di-(2-picolyl)amine (1).

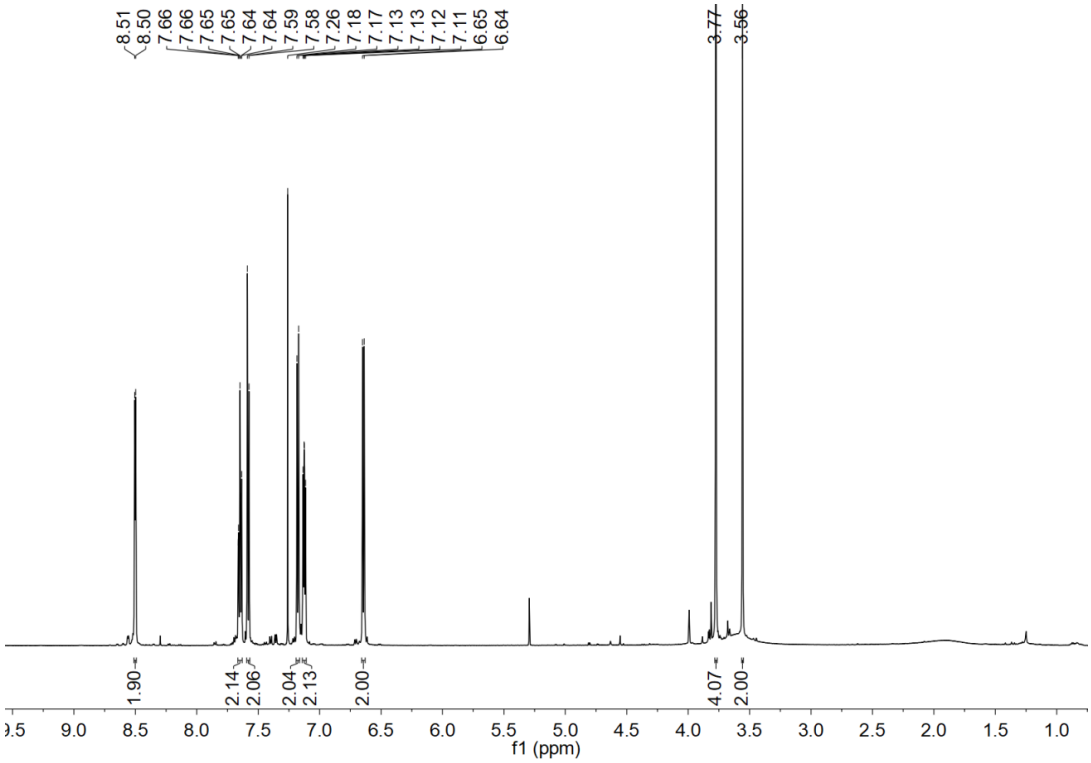


Figure C - 6: ^{1}H-NMR spectrum of N-4-amminobenzyl-N-di-(2-picolyl)amine (2).

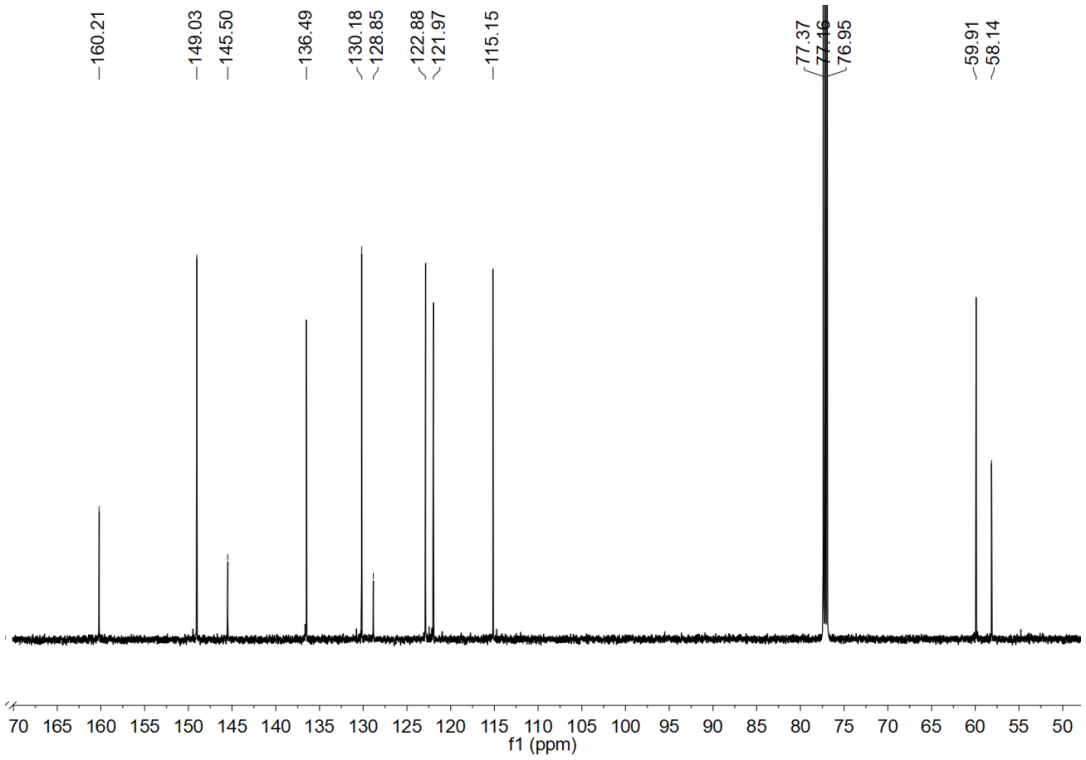


Figure C - 7: ^{13}C-NMR spectrum of N-4-amminobenzyl-N-di-(2-picolyl)amine (2).

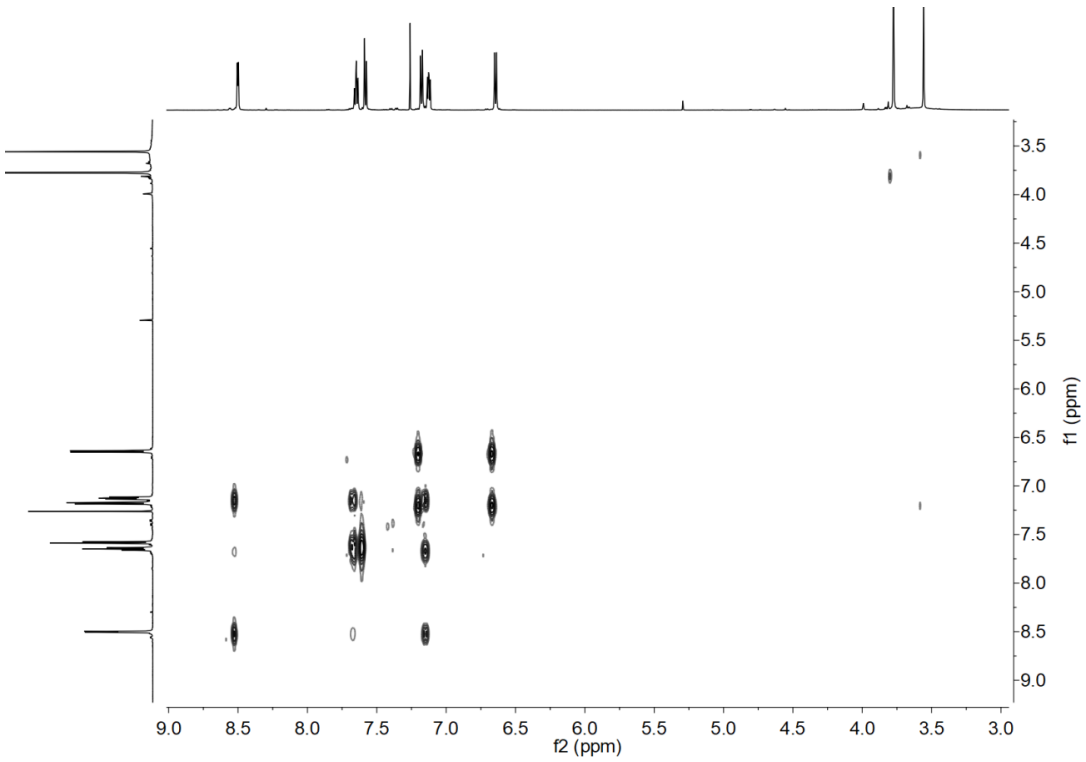


Figure C - 8: ^{1}H-^{1}H COSY spectrum of *N*-4-amminobenzyl-*N-di*-(2-picolyl)amine (2).

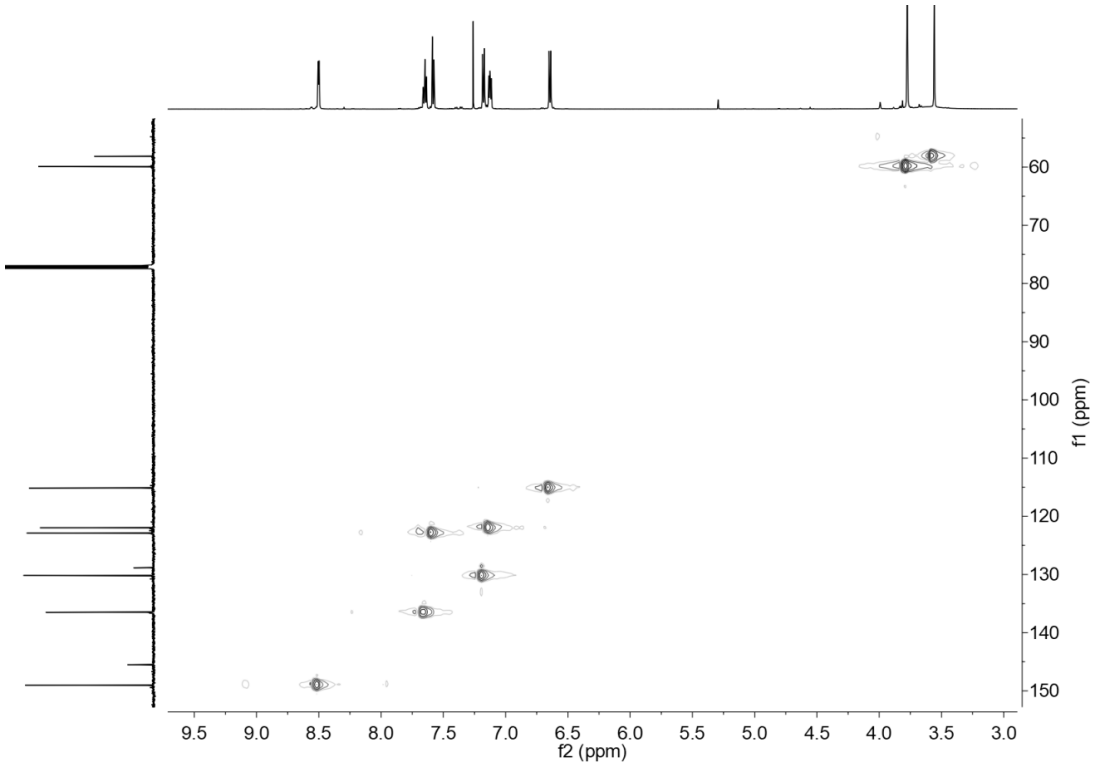


Figure C - 9: ^{1}H-1^{3}C HSQC spectrum of N-4-amminobenzyl-N-di-(2-picolyl)amine (2).

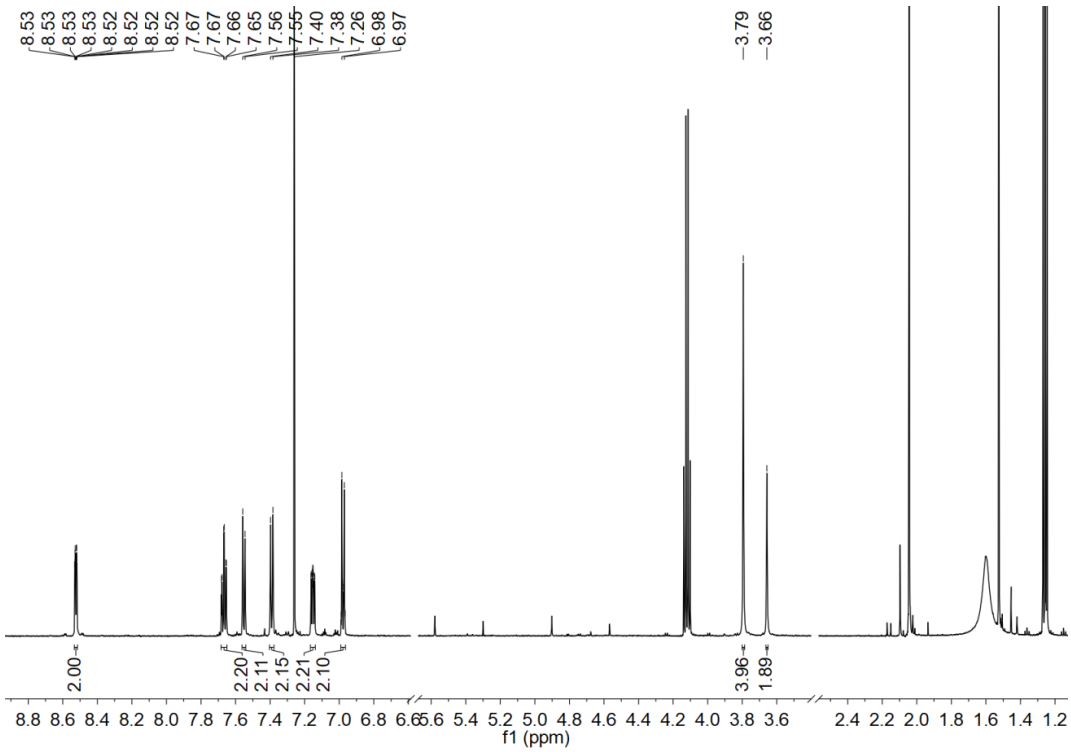


Figure C - 10: ^{1}H-NMR spectrum of *N*-4-azidobenzyl-*N*-*di*-(2-picolyl)amine (3).

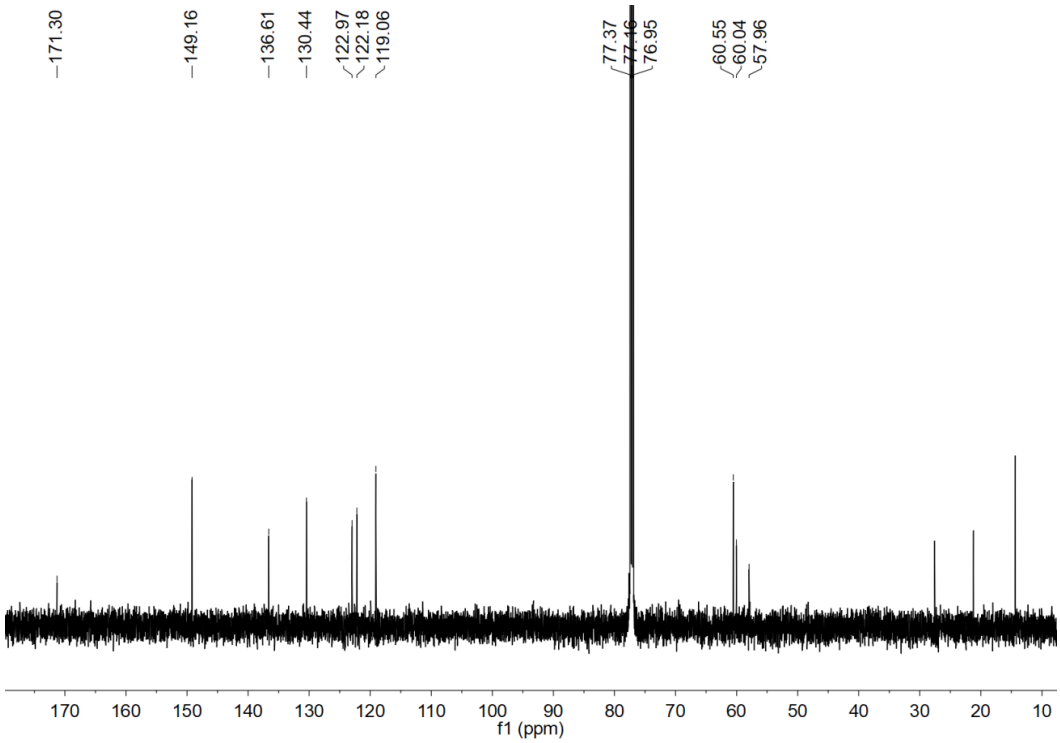


Figure C - 11: ^{13}C-NMR spectrum of *N*-4-azidobenzyl-*N*-*di*-(2-picolyl)amine (3).

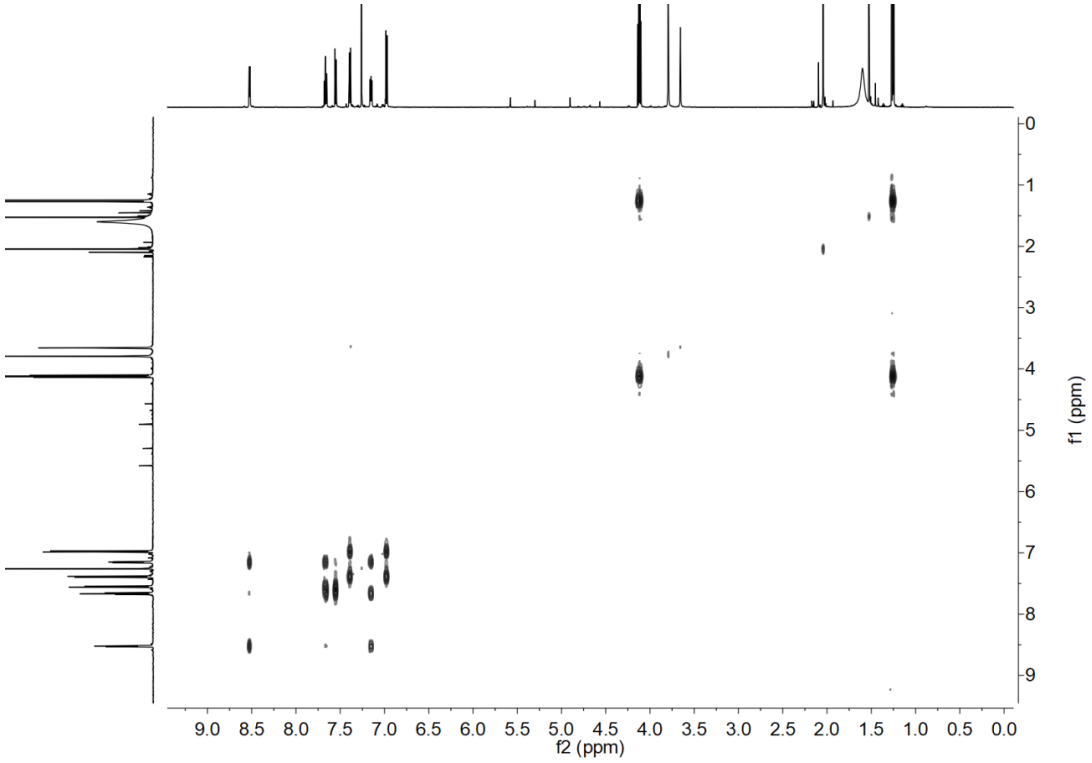


Figure C - 12: ^{1}H-^{1}H COSY spectrum of N-4-azidobenzyl-N-di-(2-picolyl)amine (3).

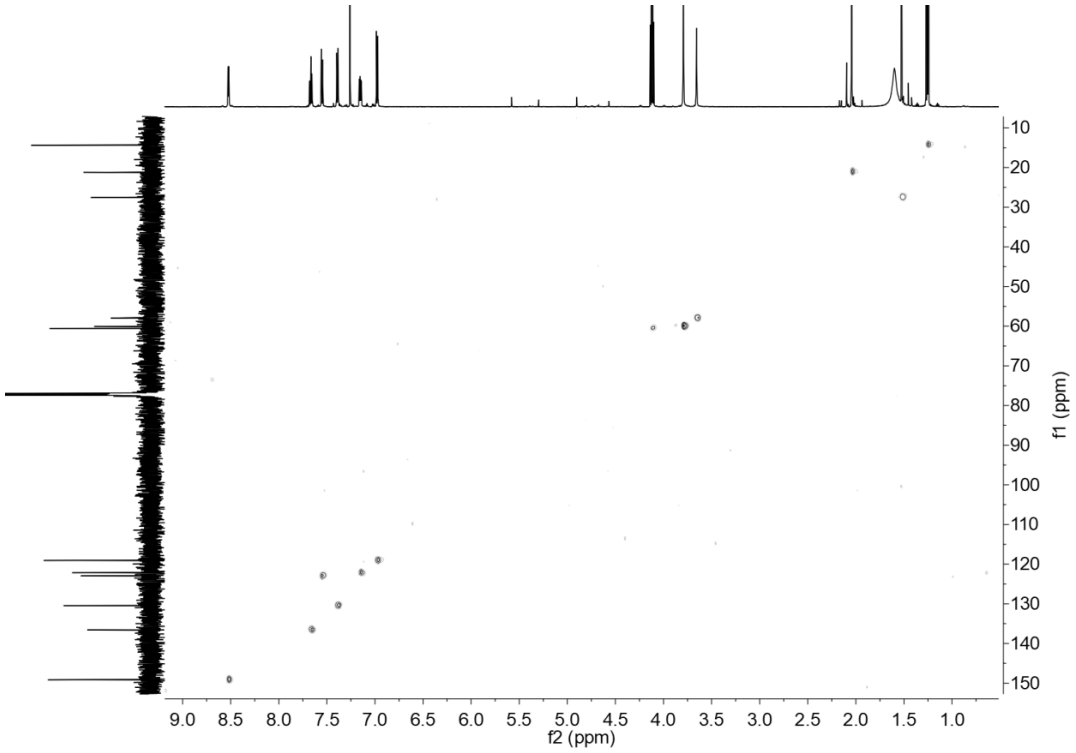


Figure C - 13: ^{1}H-^{13}C HSQC spectrum of N-4-azidobenzyl-N-di-(2-picolyl)amine (3

C.2 'Click' reaction yields

Table C - 1: Experimental yields of DPA-TFO1 after 'click' reaction, desalting and HPLC purification; int-dU[a] = internal-octadiynyl-deoxyuridine; $4N_3$-DPA = *N*-4-azidobenzyl-*N*-*di*-(2-picolyl)amine.

Oligo	Sequence	Modification	Yield (%)
TFO1	5′ – CGC TCT TTC CTT CCC UTC TTT CGC TTT CCT C – 3′	int-dU[a]-$4N_3$-DPA	21.1

C.3 Mass Spectrometry Data of the Oligonucleotides

Table C - 2: Oligonucleotide sequences, modifications and dC content. Calculated and found m/z; (a) = + 63 m/z caused by the ligand scavenging Cu(II) from the UPLC column in the analysis. int-dU[a] = internal-octadiynyl-deoxyuridine; $4N_3$-DPA = *N*-4-azidobenzyl-*N*-*di*-(2-picolyl)amine.

Oligo name	Sequence	Modification	Calcd. Mass	Found Mass
Alkyne-TFO	5′ – CGC TCT TTC CTT CCC UTC TTT CGC TTT CCT C – 3′	int-dU[a]	9298	9297.7
DPA-TFO1	5′ – CGC TCT TTC CTT CCC UTC TTT CGC TTT CCT C – 3′	int-dU[a]-$4N_3$-DPA	9628.4	9690.8[a]

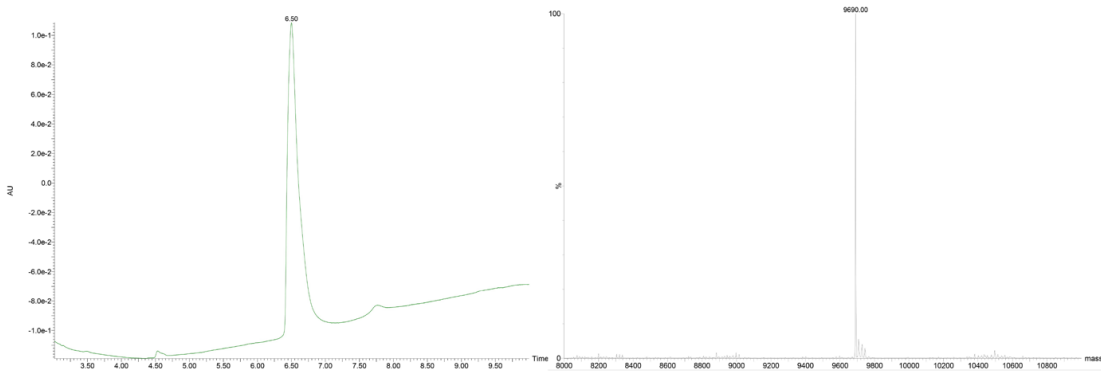


Figure C - 14: A. UPLC-MS chromatograms of pure DPA-TFO. SPS DPA-TFO1 was produced in yields according to **Table C - 1** and mass was confirmed according to **Table C - 2** UPLC x-axis = time (min) and y-axis = UV absorbance at 260nm. **B.** Deconvoluted (MaxEnt) mass spectrum of SPS DPA-TFO1.

C.4 Mass Spectrometry Data of the DPA-dU^{DPA} triphosphate

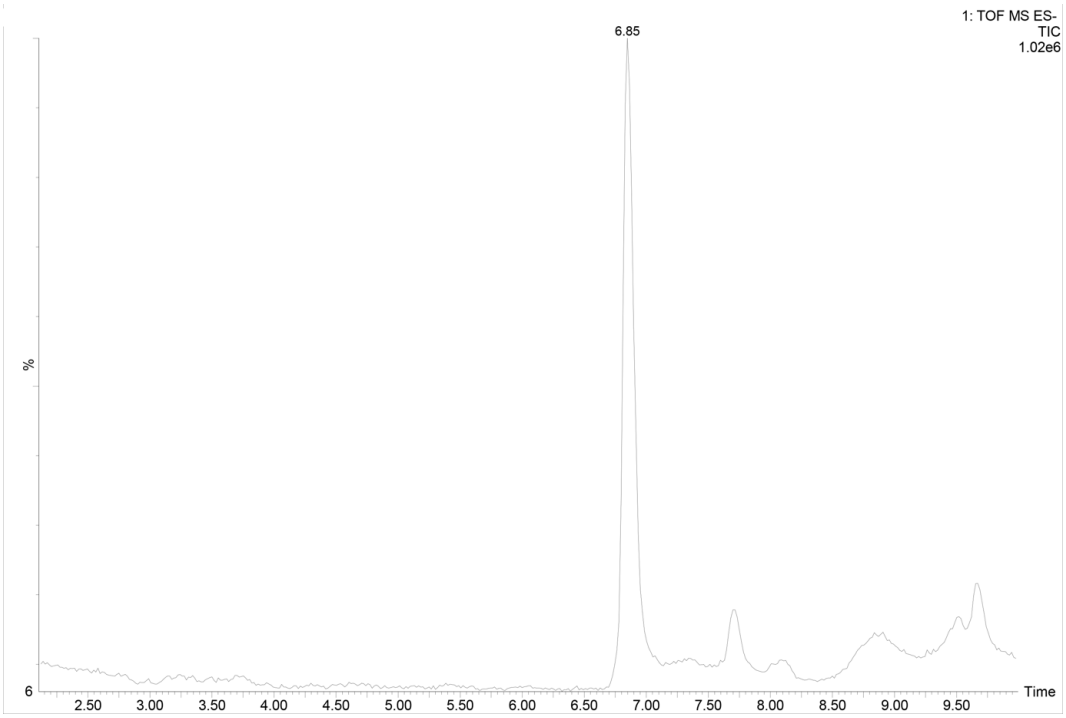


Figure C - 15: UPLC-MS chromatograms of dU^{DPA}TP.



Figure C - 16: ESI-mass spectrum of DPA-dU^{DPA}TP [M+Cu^{2+}]$^{-}$.

C.5 Enzymatic synthesis of DPA-TFO

Table C - 3: Sequence of SNI-PEX primers, template and TFOs. M = 5-methyl-cytosine.

	Length	Sequence (5'-3')
Primer	17 nt	CCGCTCTTTCCTTCCCT
Me-C Primer	17 nt	MMGMTMTTTMMTTMMMT
Template	32 nt	Bio-GAGGAAAGCGAAAGAAGGGAAGGAAAGAGCGG
TFO2	32 nt	CCGCTCTTTCCTTCCCTUCTTTCGCTTTCCTC
5mC-TFO3	32 nt	MMGMTMTTTMMTTMMMTUMTTTMGMTTTMMTM

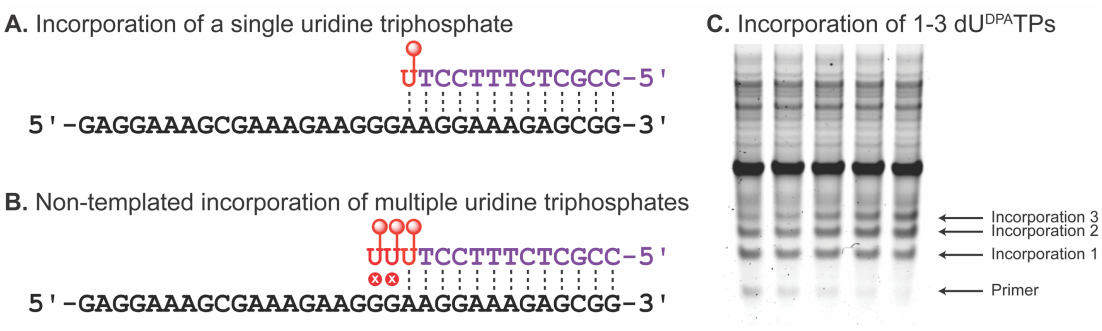


Figure C - 17: A. Incorporation of a single modified nucleotide at the desired position in the TFO sequence. **B.** An additional two uridine nucleotide triphosphates are incorporated. These are non-templated as they will not form Watson-Crick bonds with the guanine bases on the complementary strand. **C.** 20% denaturing PAGE analysis of incorporation by Therminator DNA polymerase. There is one templated (incorporation 1) and two non-templated (incorporation 2 and 3) incorporations of $dU^{DPA}TP$.

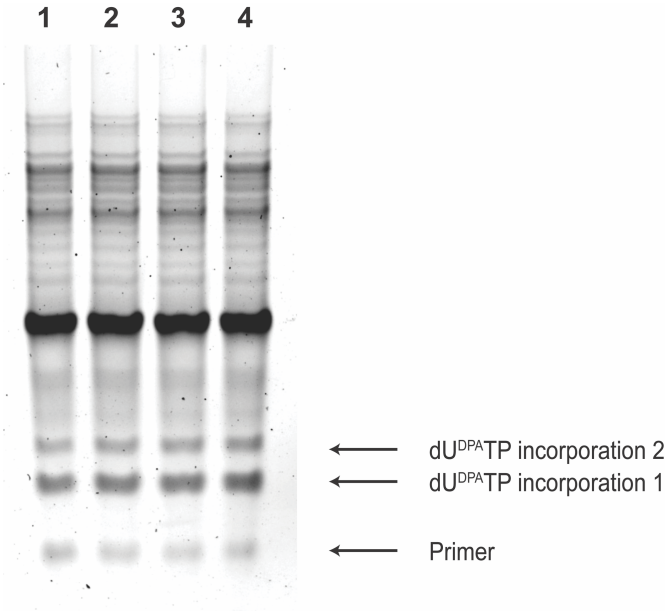


Figure C - 18: 20% denaturing PAGE showing the incorporation of $dU^{DPA}TP$ by Vent (exo-) DNA polymerase. Lane 1-4: Incubation time 5, 10, 15 and 20 min, respectively. A maximum of two $dU^{DPA}TPs$ (the first templated and the second non-templated) are incorporated.

Table C - 4: Yield for enzymatically synthesised DPA-TFO hybrids. M = 5-methyl-cytosine.

Oligo name	Sequence	Modification	Yield (%)
TFO2	5′ – CCG CTC TTT CCT TCC CT**U** CTT TCG CTT TCC TC – 3′	dU^{DPA}TP	57.8%
5mC-TFO3	5′ – MMG MTM TTT MMT TMM MT**U** MTT TMG MTT TMM TM – 3′	dU^{DPA}TP	61.5%

Table C - 5: Oligonucleotide sequence and modifications. Calculated and found m/z; (a) = + 63 m/z caused by the ligand scavenging Cu(II) from the UPLC column in the analysis. M = 5-methyl-cytosine

Oligo name	Sequence	Modification	Calcd. Mass	Found Mass
TFO2	5′ – CCG CTC TTT CCT TCC CT**U** CTT TCG CTT TCC TC – 3′	dU^{DPA}TP	9917.5	9980$_a$
5mC-TFO3	5′ – MMG MTM TTT MMT TMM MT**U** MTT TMG MTT TMM TM – 3′	dU^{DPA}TP	10,127.5	10,191$_a$

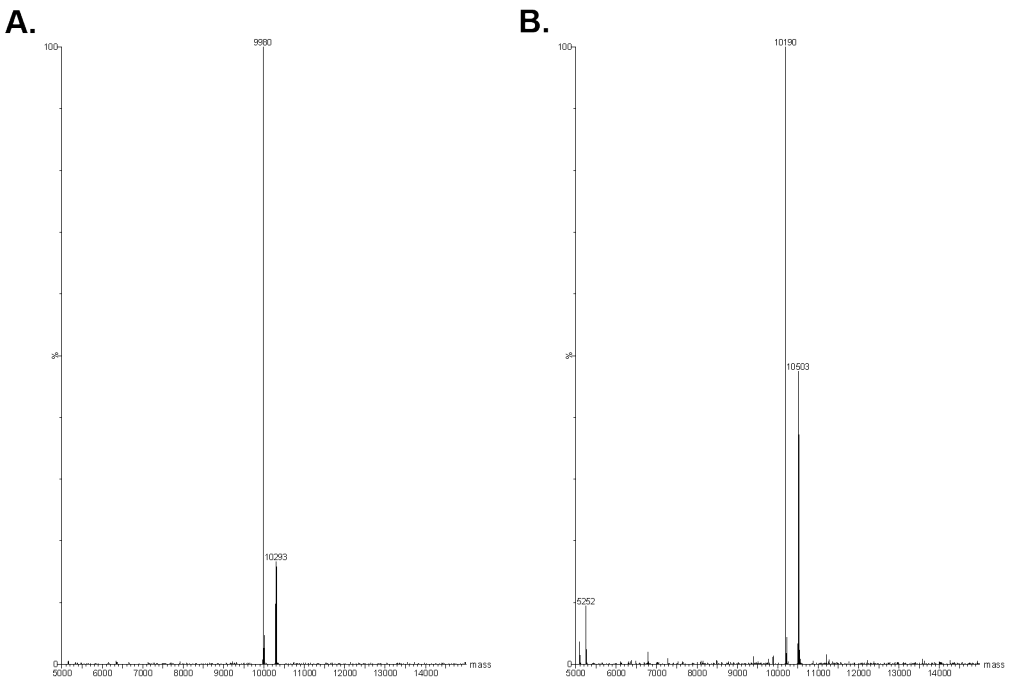


Figure C - 19: A. ESI-mass spectrum of DPA-TFO2 [M + Cu^{2+}], **B.** ESI-mass spectrum of DPA-5mC-TFO3 [M + Cu^{2+}].

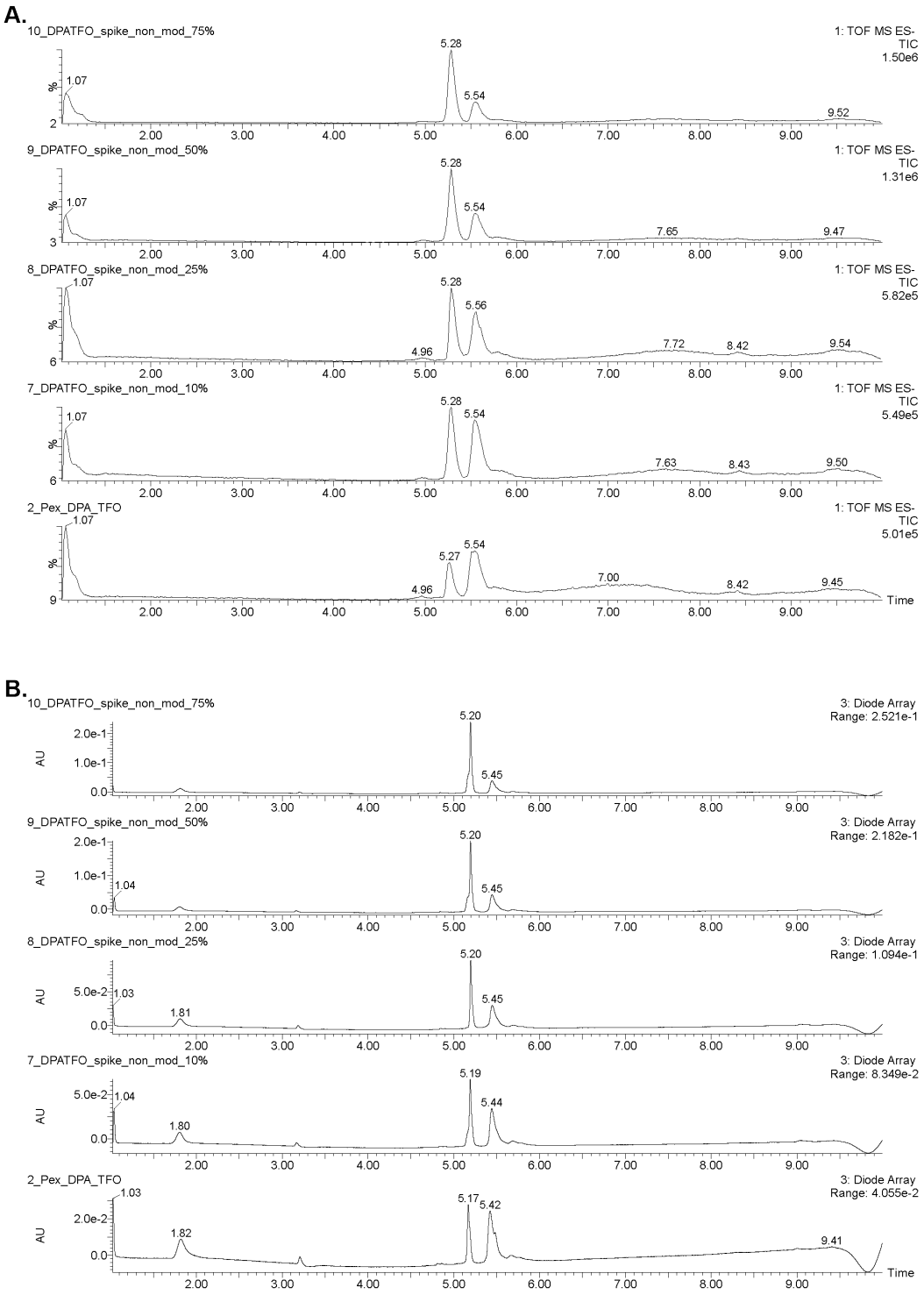


Figure C - 20: Mass spectroscopy (**A.**) and HPLC (**B.**) trace of PEX DPA-TFO2 spiked with non-modified TFO. DPA-TFO2 was spiked with 0, 10, 25, 50 or 75% non-modified TFO to determine the amount of non-modified TFO present in the PEX DPA-TFO2 sample. **A.** 5.27/5.28 = non-modified TFO. 5.54 = DPA-TFO. **B.** 5.17/5.19/5.20 = non-modified TFO. 5.42/5.44/5.45 = DPA-TFO.

C.6 Analysis of DPA-TFO

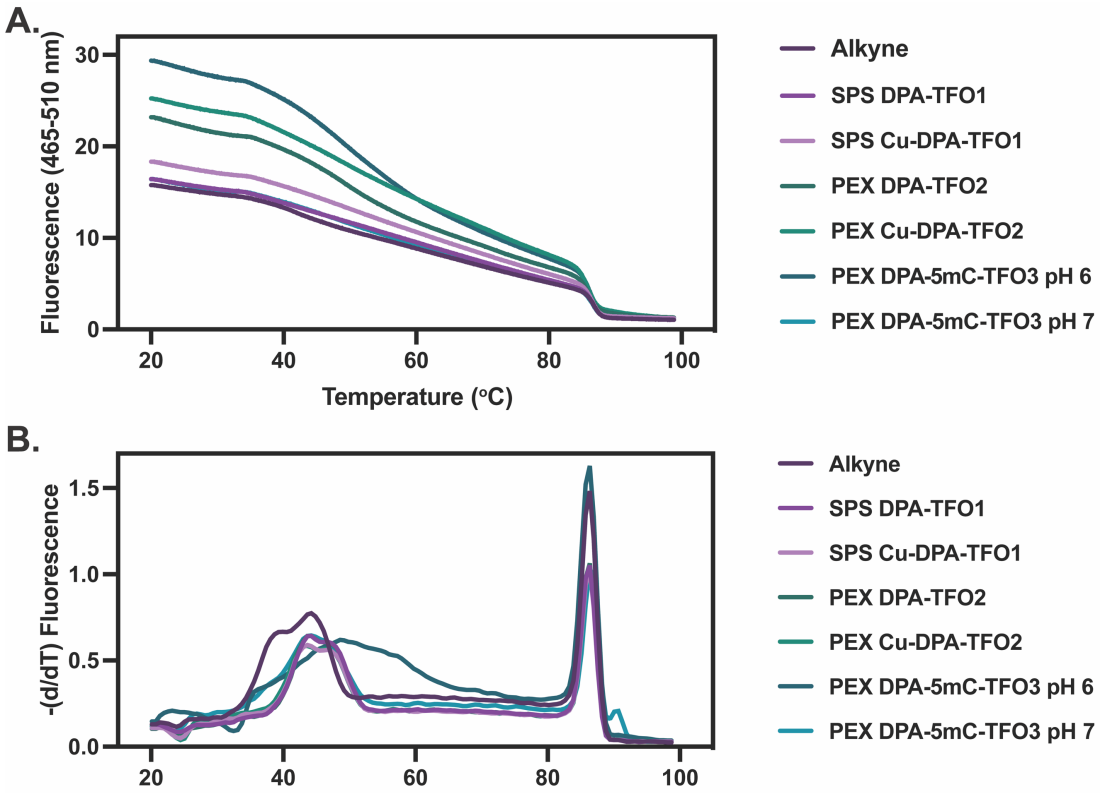


Figure C - 21: A. Plot of fluorescence readings taken during thermal melting. **B.** First negative derivative

Table C - 6: Triplex melting temperature for TFO1, TFO 2 and TFO3.

Oligo name	Sequence	T_M (°C)
Alkyne TFO	5′ – CGC TCT TTC CTT CCC T**U**C TTT CGC TTT CCT C – 3′	44.0
SPS DPA-TFO1	5′ – CGC TCT TTC CTT CCC T**U**C TTT CGC TTT CCT C – 3′	45.2
SPS Cu-DPA-TFO1	5′ – CGC TCT TTC CTT CCC T**U**C TTT CGC TTT CCT C – 3′	45.7
PEX DPA-TFO2	5′ – CCG CTC TTT CCT TCC CT**U** CTT TCG CTT TCC TC – 3′	45.5
PEX Cu-DPA-TFO2	5′ – CCG CTC TTT CCT TCC CT**U** CTT TCG CTT TCC TC – 3′	46.2
DPA-5mC-TFO3 pH 6	5′ – MMG MTM TTT MMT TMM MT**U** MTT TMG MTT TMM TM – 3′	59.3
DPA-5mC-TFO3 pH 7	5′ – MMG MTM TTT MMT TMM MT**U** MTT TMG MTT TMM TM – 3′	44.9

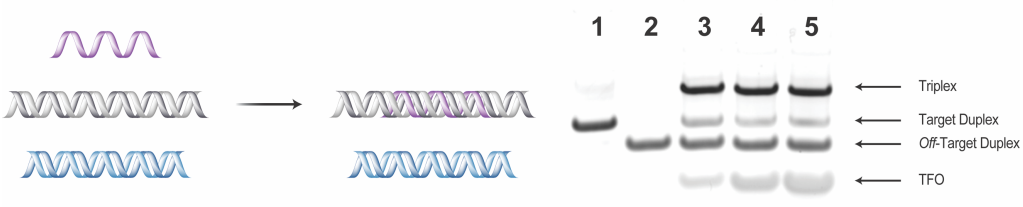


Figure C - 22: TFO (purple) hybridises with target duplex (grey) to form triplex, while *off*-target (blue) remains in duplex state. Lane 1: 57 bp target duplex. Lane 2: *Off*-target duplex. Lanes 3-5: Triplex with 10, 25 and 50 equivalents of TFO to duplex.

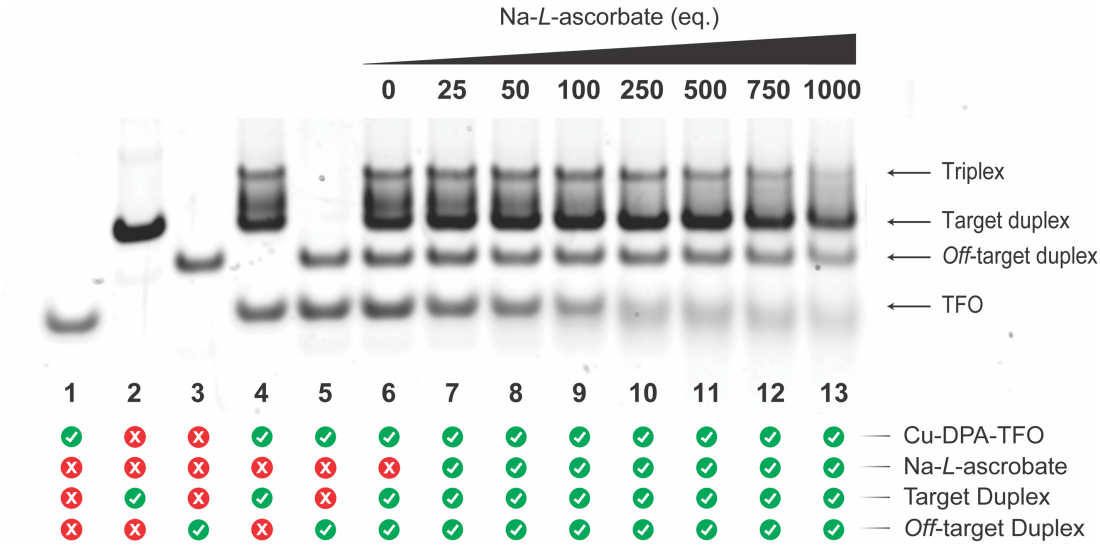


Figure C - 23: 20% native PAGE showing the targeted DNA damage inflicted by SPS Cu-DPA-TFO1. Lane 1: TFO (32 nt). Lane 2: Target duplex (57 bp). Lane 3: *Off*-target duplex (40 bp). Lane 4: TFO and target duplex hybridise to form triplex. Lane 5: TFO does not bind with *off*-target duplex. Lane 6-15: Target and *off*-target duplexes incubated with Cu-DPA-TFO (25 eq.) and 0-1000 equivalents of Na-*L*-ascorbate. TFO only binds with its target sequence inflicting DNA damage, while *off*-target remains relatively intact.

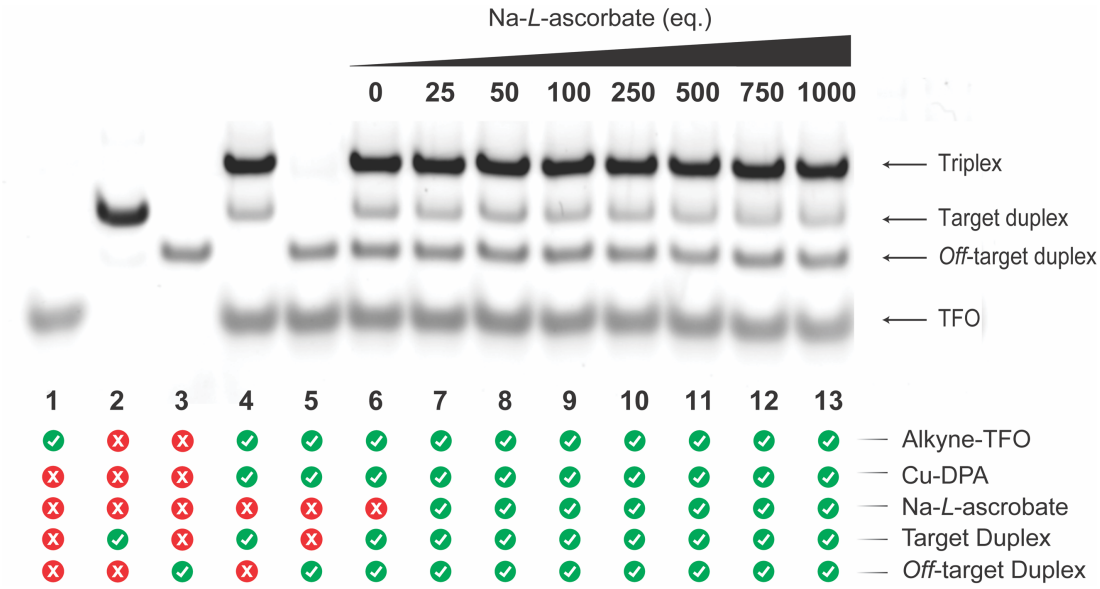


Figure C - 24: 20% native PAGE displaying DNA damage caused by free Cu-DPA and free-alkyne-TFO. Lane 1: Alkyne TFO (32 nt). Lane 2: Target duplex (57 bp). Lane 3: *Off*-target duplex (40 bp). Lane 4: Alkyne-TFO and target duplex hybridise to form triplex. Lane 5: Alkyne-TFO does not bind with *off*-target duplex. Lane 6-15: Target and *off*-target duplexes incubated with free Cu(II)-DPA and free alkyne-TFO (25 eq.) and 0-1000 equivalents of Na-*L*-ascorbate. No significant DNA damage is observed for either DNA duplex.

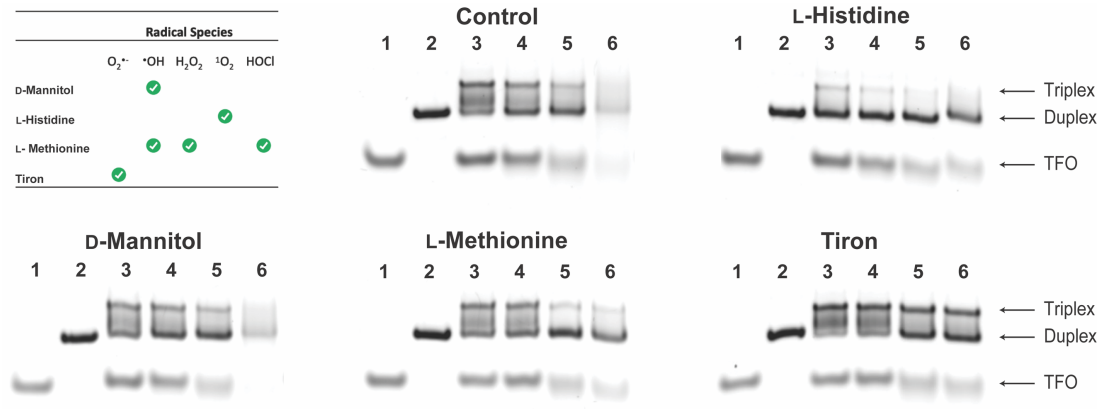


Figure C - 25: 20% native PAGE showing impact ROS have on activity of Cu-DPA-TFO. Lane 1: TFO. Lane 2: Target duplex. Lane 3-6: Cu-DPA-TFO incubated with target duplex and ROS scavenger and 0, 50, 500 or 2000 equivalents of Na-*L*-ascorbate. Control contains no scavenger species.

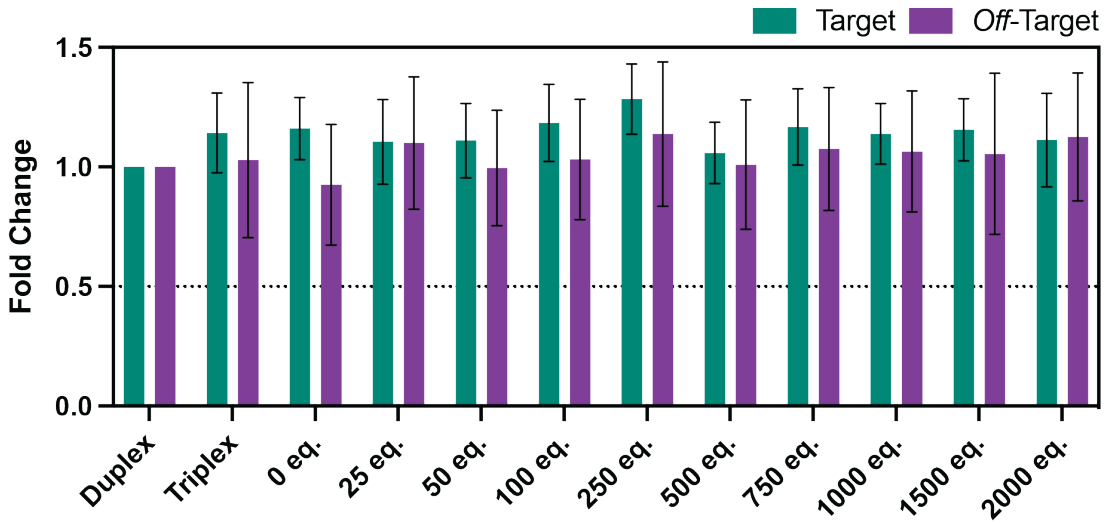


Figure C - 26: Target and *off*-target DNA duplexes were incubated with free Cu-DPA and free alkyne-modified TFO. The fold change in intact DNA concentration was plotted. No significant damage has occurred to either DNA duplex.

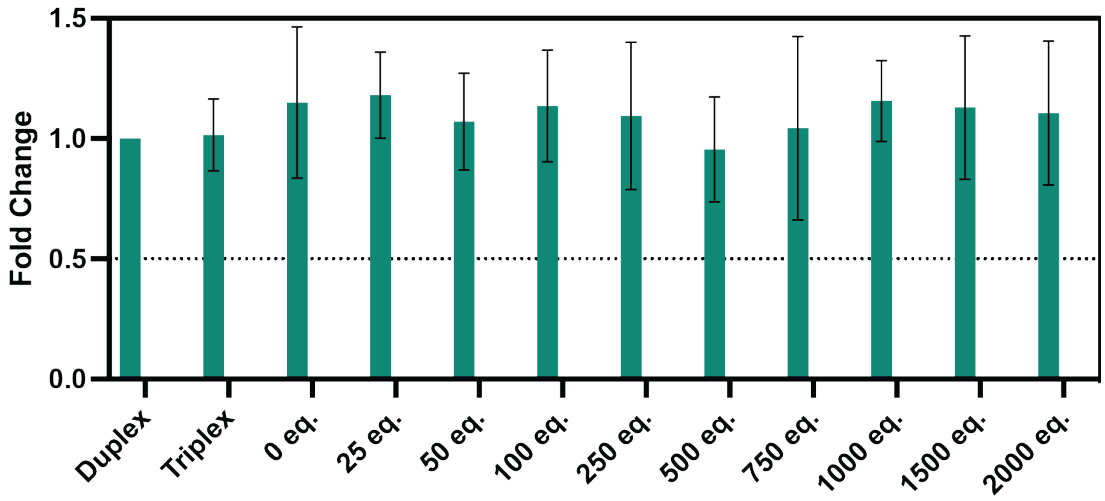


Figure C - 27: qPCR was performed to quantify the DNA damage that occurred to the target duplex in the presence of Cu-DPA-TFO and the ROS species tiron. No significant damage was observed. This confirms that the DNA damage inflicted by the DPA-TFO hybrid is responsible for inhibiting DNA amplification during PCR.

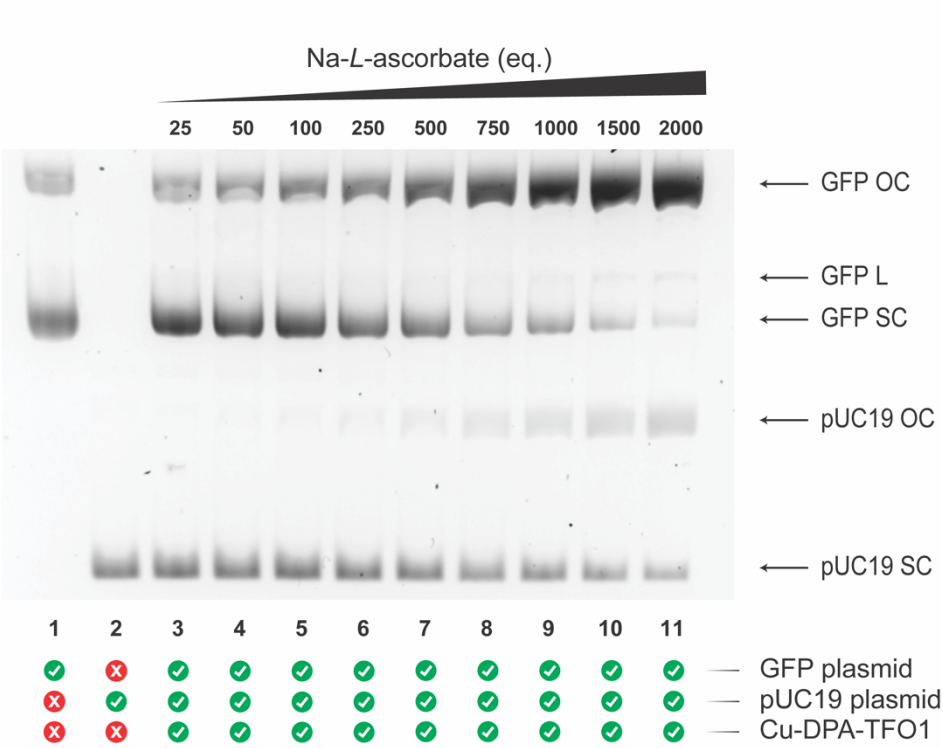


Figure C - 28: Agarose (1%) gel electrophoretic analysis of the damage inflicted upon target and *off*-target supercoiled DNA plasmids by SPS Cu-DPA-TFO1. Lane 1: Supercoiled (SC) GFP (6389 bp). Lane 2: Supercoiled (SC) pUC19 (2686 bp). Lane 3-11: GFP and pUC19 with 25 equivalents of Cu-DPA-TFO1 and 25-2000 equivalents of Na-*L*-ascorbate.

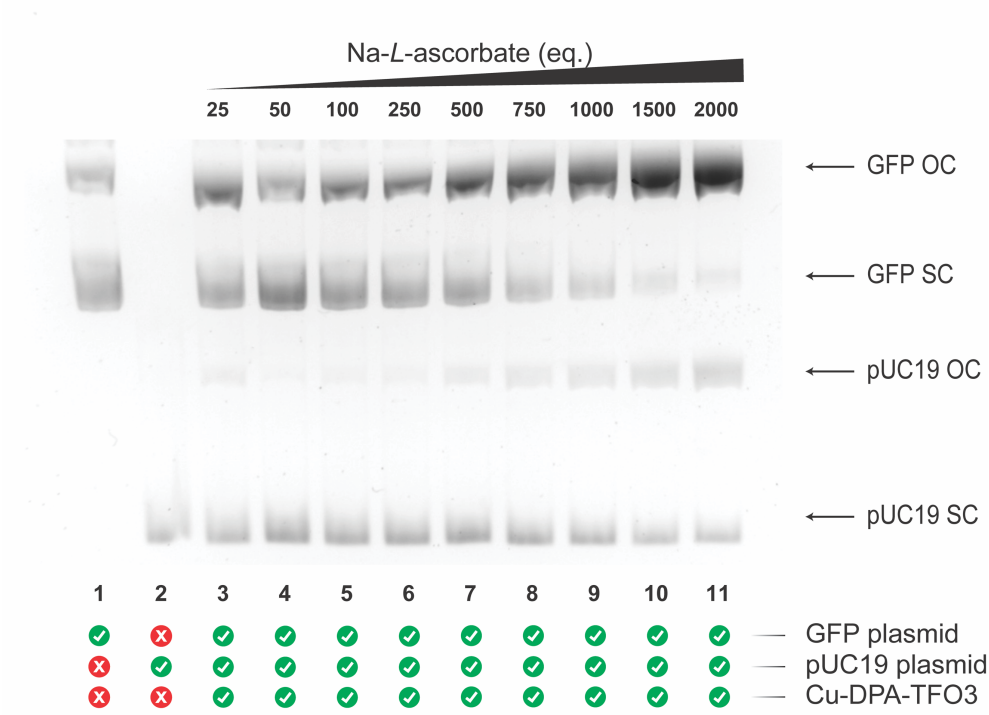


Figure C - 29: 1% agarose gel analysis of enzymatically synthesised TFO3. Lane 1: Supercoiled (SC) GFP (6389 bp). Lane 2: Supercoiled (SC) pUC19 (2686 bp). Lane 3-11: GFP and pUC19 with 25 equivalents of Cu-DPA-5mC-TFO3 and 25-2000 equivalents of Na-*L*-ascorbate.

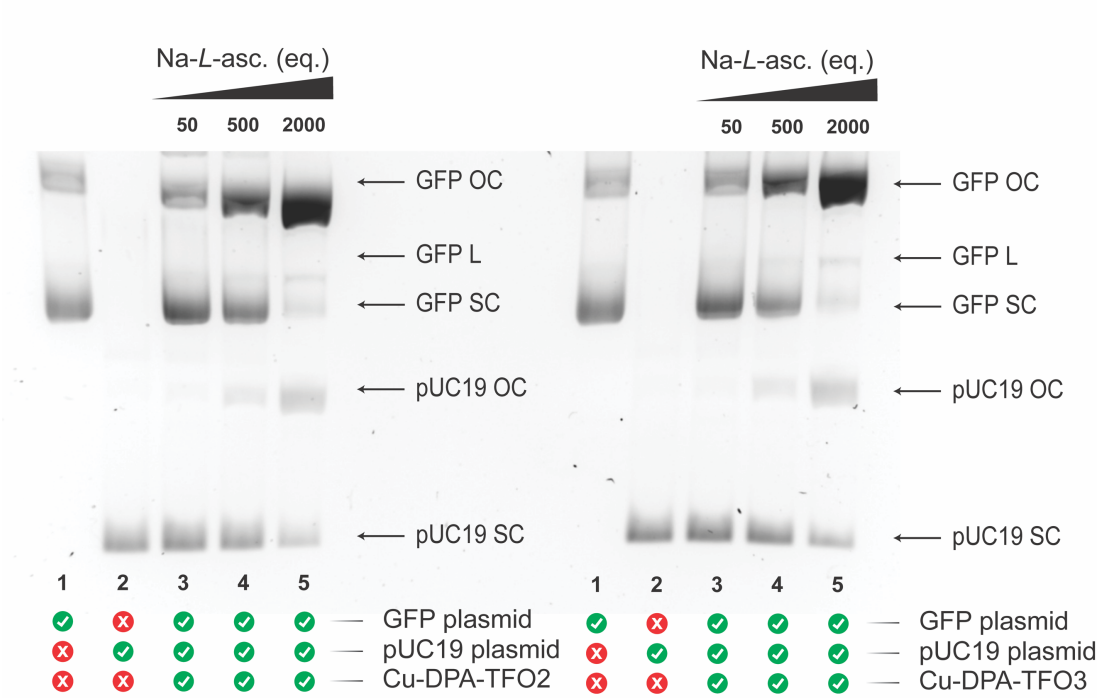


Figure C - 30: 1% agarose gel displaying the sequence specific damage inflicted by the enzymatically synthesised Cu-DPA-TFO2 and Cu-DPA-5mC-TFO3. Left: Lane 1: Supercoiled (SC) GFP (6389 bp). Lane 2: Supercoiled (SC) pUC19 (2686 bp). Lane 3-5: GFP and pUC19 with 25 equivalents of Cu-DPA-TFO2 and 50, 500 or 2000 equivalents of Na-*L*-ascorbate. Right: Lane 1: Supercoiled (SC) GFP (6389 bp). Lane 2: Supercoiled (SC) pUC19 (2686 bp). Lane 3-5: GFP and pUC19 with 25 equivalents of Cu-DPA-TFO2 and 50, 500 or 2000 equivalents of Na-*L*-ascorbate.

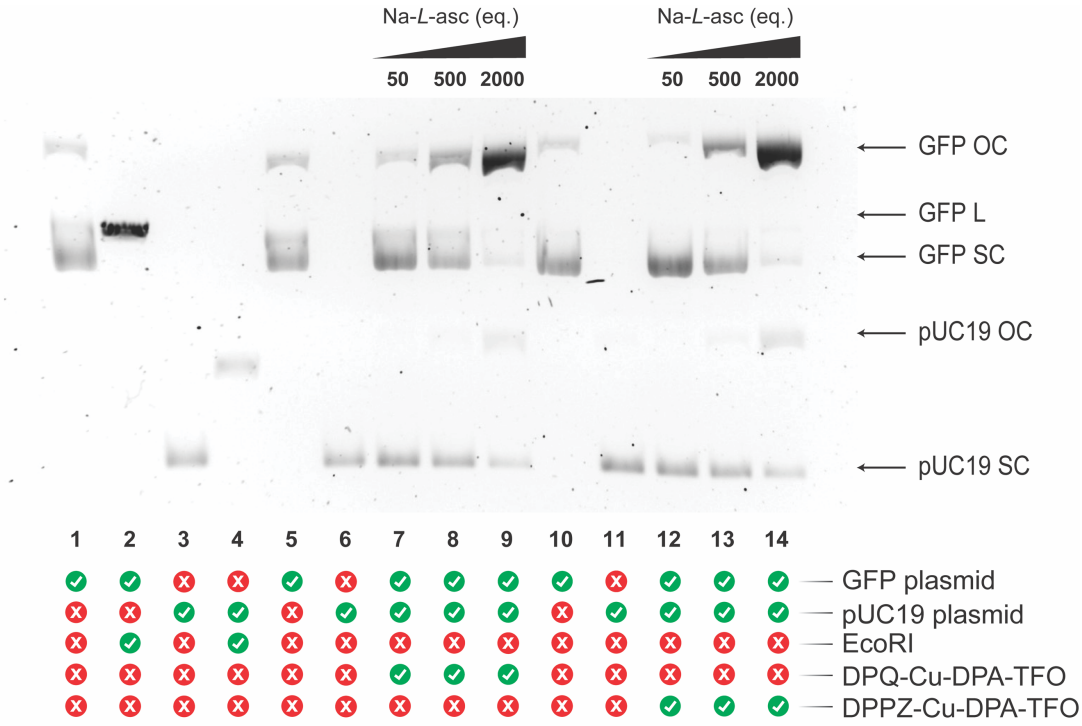
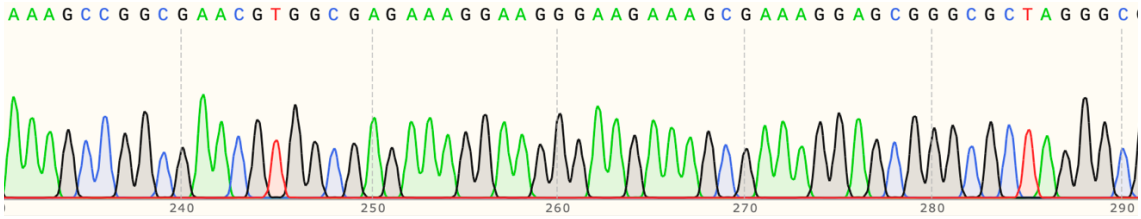


Figure C - 31: 1% agarose gel showing targeted DNA cleavage for Cu-DPA-TFO with designer intercalators, DPQ and DPPZ. Lane 1: Supercoiled (SC) GFP (6389 bp). Lane 2: GFP linearised (L) with EcoRI. Lane 3: Supercoiled (SC) pUC19 (2686 bp). Lane 4: pUC19 linearised (L) with EcoRI. Lane 5: GFP control. Lane 6: pUC19 control. Lane 7-9: GFP and pUC19 with 25 equivalents of DPQ-Cu-DPA-TFO and 50, 500 or 2000 equivalents of Na-*L*-ascorbate. Lane 10: GFP control. Lane 11: pUC19 control. Lanes 12-14: GFP and pUC19 with 25 eq. DPPZ-Cu-DPA-TFO and 50,500 or 2000 equivalents of Na-*L*-ascorbate.

C.7 Sequencing data

C.7.1 Control Forward

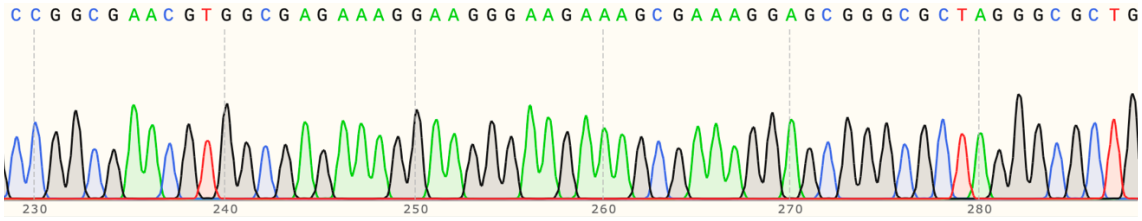
TCCCAGCCTTGTTGTAGCGCCAAGTGCCCAGCGGGGCTGCTAAAGCGCATGCTCCAGA
CTGCCTTGGGAAAAGCGCCTCCCCTACCCGGTATCTAGAGAATAGGAACTTCGGAATA
GGAACTTCTAGGTACGTGAACCATCACCCTAATCAAGTTTTTTGGGGTCGAGGTGCCG
TAAAGCACTAAATCGGAACCCTAAAGGGAGCCCCCGATTTAGAGCTTGACGGGGAAAG
CCGGCGAACGTGGCGAGAAAGGAAGGGAAGAAAGCGAAAGGAGCGGGCGCTAGGGCGC
TGGCAAGTGTAGCGGTCACGCTGCGCGTAACCACCACACCCGCCGCGCTTAATGCGCC
GCTACAGGGCGCGTGGGGATACCCCCTAGAGCCCCAGCTGGTTCTTTCCGCCTCAGAA
GCCATAGAGCCCACCGCATCCCCAGCATGCCTGCTATTGTCTTCCCAATCCTCCCCCT
TGCTGTCCTGCCCCACCCCACCCCCCAGAATAGAATGACACCTACTCAGACAATGCGA
TGCAATTTCCTCATTTTATTAGGAAAGGACAGTGGGAGTGGCACCTTCCAGGGTCAAG
GAAGGCACGGGGGAGGGGCAAACAACAGATGGCTGGCAACTAGAAGGCACAGTCGAGG
CATGCATCGAGAATTCCGATGGGACCCTAGACTCGAGCGGCCGCCTACACATTGATCC
TAGCAGAAGCACAGGCTGCAGGGTGACGGTCCATCCCGCTCTCCTGGGCACAAGACAT
GGGCAGCGTGCCATCATCCTGCTCCTCCACCTCCGGCGGGAAGCCATGGCTAAGCTTC
TTGTACAGCTCGTCCATGCCGAGAGTGATCCCGGCGGCGGTCACGAACTCCAGCAGGA
CCATGTGATCGCGCTTCTCGTTGGGGTCTTTGCTCAGGGCGGACTGGGTGCTCAGGTA
GTGGTTGTCGGGCAGCAGCACGGGGCCGTCGCCGATGGGGGTGTTCTGCTGGTAGTGG
TCGGCGAGCTGCACGCTGCCGTCCTCGATGTTGTGGCGGATCTTGAAGTTCACCTTGA
TGCCGTTCTTCTGCTTGTCGGCATGATATAGACGTTGTGGCTGTTGTAATTGTACTCC
AGCTTGTGCCCCAGAATGTTGCCGTCCTCCTTGAAATCGATGCCCTTCACCTCAAGCG
GTTCCCAGGGTGTCGCCCCCAAATTTCCCCCGGGCGGGGCTTGGAATTTCCTCGCCCT
TAGAAAAAAAGGGCGCCCCGGAATAACCTTCGGGAGGCGGAATTAAAAAAAAAGGTGT
TTCTTGGGCGGGGGAAGGCTAAAACTCACCCCCCAAGTCAGGGTGTCCAAGGTGGGCA
GGCCGGGAACTTTCCGGGGGGGGAAAAAATTAAGGAAATTTGCAAAGGGATCACCCCC
CCCCCCCCCACCAAATTAGGTTTTTTTTTCCCTTTCACAAGAACCCCGAAACCCCCCT
CCCGGGGGGGGGGGGGGCGTTTAAAAATTGCCCTTTTTTTTTATAATTTTAATTAAAC
CACCCCCCCCCGCGCGGTGGTTGGAGAGGGGTGAGGGGGGGGGGGGAAAAGTCTAGAA
AATAAAGATATCTAAGTATAAATATATATAATGATTCAGCATTTTGATTATATCAATA
GTAATATATCGTGATATATATTAATATGAGATTATTA



C.7.2 Cu-DPA Forward

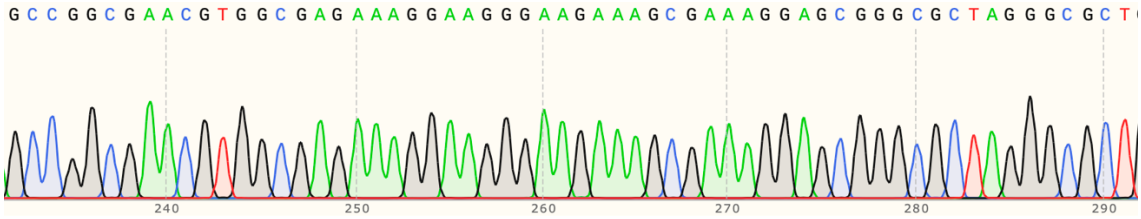
CTTGTGTAGCGCCAAGTGCCCAGCGGGGCTGCTAAAGCGCATGCTCCAGACTGCCTTG
GGAAAAGCGCCTCCCCTACCCGGTATCTAGAGAATAGGAACTTCGGAATAGGAACTTC
TAGGTACGTGAACCATCACCCTAATCAAGTTTTTTGGGGTCGAGGTGCCGTAAAGCAC
TAAATCGGAACCCTAAAGGGAGCCCCCGATTTAGAGCTTGACGGGGAAAGCCGGCGAA
CGTGGCGAGAAAGGAAGGGAAGAAAGCGAAAGGAGCGGGCGCTAGGGCGCTGGCAAGT

GTAGCGGTCACGCTGCGCGTAACCACCACACCCGCCGCGCTTAATGCGCCGCTACAGG
GCGCGTGGGGATACCCCCTAGAGCCCCAGCTGGTTCTTTCCGCCTCAGAAGCCATAGA
GCCCACCGCATCCCCAGCATGCCTGCTATTGTCTTCCCAATCCTCCCCCTTGCTGTCC
TGCCCCACCCCACCCCCCAGAATAGAATGACACCTACTCAGACAATGCGATGCAATTT
CCTCATTTTATTAGGAAAGGACAGTGGGAGTGGCACCTTCCAGGGTCAAGGAAGGCAC
GGGGGAGGGGCAAACAACAGATGGCTGGCAACTAGAAGGCACAGTCGAGGCATGCATC
GAGAATTCCGATGGGACCCTAGACTCGAGCGGCCGCCTACACATTGATCCTAGCAGAA
GCACAGGCTGCAGGGTGACGGTCCATCCCGCTCTCCTGGGCACAAGACATGGGCAGCG
TGCCATCATCCTGCTCCTCCACCTCCGGCGGGAAGCCATGGCTAAGCTTCTTGTACAG
CTCGTCCATGCCGAGAGTGATCCCGGCGGCGGTCACGAACTCCAGCAGGACCATGTGA
TCGCGCTTCTCGTTGGGGTCTTTGCTCAGGGCGGACTGGGTGCTCAGGTAGTGGTTGT
CGGGCAGCAGCACGGGGCCGTCGCCGATGGGGGTGTTCTGCTGGTAGTGGTCGGCGAG
CTGCACGCTGCCGTCCTCGATGTTGTGGCGGATCTTGAAGTTCACCTTGATGCCGTTC
TTCTGCTTGTCGGCATGATATAGACGTTGTGGCTGTTGTAGTTGTACTCCAGCTTGTG
CCCAGGATGTTGCCGTCCTCCTTGAAATCAAG



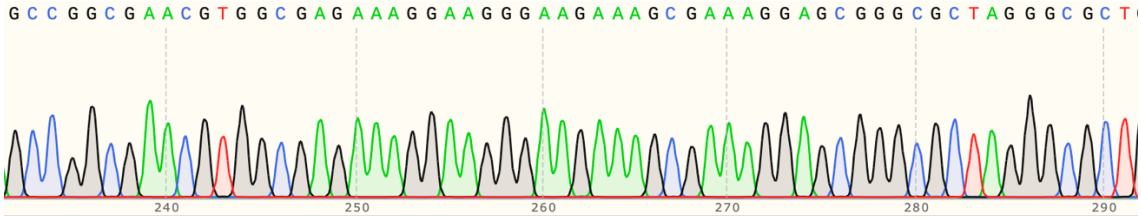
C.7.3 DPQ-Cu-DPA-TFO

TCCGAGCCTTGTGTGCGCCAAGTGCCCAGCGGGGCTGCTAAAGCGCATGCTCCAGACT
GCCTTGGGAAAAGCGCCTCCCCTACCCGGTATCTAGAGAATAGGAACTTCGGAATAGG
AACTTCTAGGTACGTGAACCATCACCCTAATCAAGTTTTTTGGGGTCGAGGTGCCGTA
AAGCACTAAATCGGAACCCTAAAGGGAGCCCCCGATTTAGAGCTTGACGGGGAAAGCC
GGCGAACGTGGCGAGAAAGGAAGGGAAGAAAGCGAAAGGAGCGGGCGCTAGGGCGCTG
GCAAGTGTAGCGGTCACGCTGCGCGTAACCACCACACCCGTCGCGCTTAAAGCTCCGC
TACAGGGCGCGTGGGGATCCCCCCTACTTTTTTAACCGGTACTTTCGCCTCCTTCATA
CTTGCAGTGTCCTTTCAGACCAGGTATTCAAGAAATGCTTGCACCTCTCACGGTTTCA
GCGTCAGGCCGCAAGTCGCACCTATCTACAATATCTTCTTATAATGAAGATTTGAAAG
ATTTCCAGGAAGCAGAGCCGATACGACCAGGTGAAGAGTAATATTGTTTAGTACTTAA
AGCCATTTAGGAACCTCTTAGCATCGCCCAGGTGTTAGGAGTGTTACTCCACCGGATA
GTGCACGACCCTTTCACGTGCGGAGCCAATCTGAATTCTGAGGACCGGCTGACTTGGA
GCATACCTGAAATCACGGCTGACATTGTTCGGACAAGCAGTCACAAGTTGCTGTCAAA
GTTCAGGACCGCACTCGAACACCCCCACTTGTGTATAAACTATCATAAGTGACTCGAT
GTTCACACCTTCACACATTTTAGAGAGGTACAGCCAGAAGACCGTAAGACAGTCATCA
CTCTGCTGAGGATATCCATAACCTGTCGGGTGTCCAAACAATCATCGTCAGAGGATCA
CTTCTACAAAGCTGCTGTGAGATGCGAGAACAAGGCGGCTCTTGCGTAAGTCCTCCTT
GGTCGATAACTTACTTGCTACTACCGGCATGGGACGAACGCCCCGATGACAAGATCCT
GACCCGGGGGTCCCAAA



C.7.4 DPPZ-Cu-DPA-TFO Forward

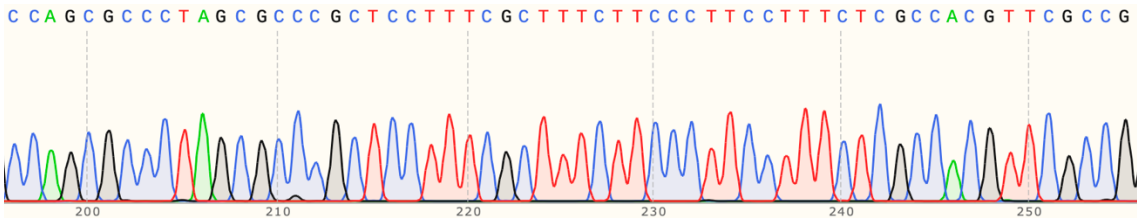
GTTGTAGCGCCAAGTGCCCAGCGGGGCTGCTAAAGCGCATGCTCCAGACTGCCTTGGG
AAAAGCGCCTCCCCTACCCGGTATCTAGAGAATAGGAACTTCGGAATAGGAACTTCTA
GGTACGTGAACCATCACCCTAATCAAGTTTTTTGGGGTCGAGGTGCCGTAAAGCACTA
AATCGGAACCCTAAAGGGAGCCCCCGATTTAGAGCTTGACGGGGAAAGCCGGCGAACG
TGGCGAGAAAGGAAGGGAAGAAAGCGAAAGGAGCGGGCGCTAGGGCGCTGGCAAGTGT
AGCGGTCACGCTGCGCGTAACCACCACACCCGCCGCGCTTAATGCGCCGCTACAGGGC
GCGTGGGGATACCCCCTAGAGCCCCAGCTGGTTCTTTCCGCCTCAGAAGCCATAGAGC
CCACCGCATCCCCAGCATGCCTGCTATTGTCTTCCCAATCCTCCCCCTTGCTGTCCTG
CCCCACCCCACCCCCCAGAATAGAATGACACCTACTCAGACAATGCGATGCAATTTCC
TCATTTTATTAGGAAAGGACAGTGGGAGTGGCACCTTCCAGGGTCAAGGAAGGCACGG
GGGAGGGGCAAACAACAGATGGCTGGCAACTAGAAGGCACAGTCGAGGCATGCATCGA
GAATTCCGATGGGACCCTAGACTCGAGCGGCCGCCTACACATTGATCCTAGCAGAAGC
ACAGGCTGCAGGGTGACGGTCCATCCCGCTCTCCTGGGCACAAGACATGGGCAGCGTG
CCATCATCCTGCTCCTCCACCTCCGGCGGGAAGCCATGGCTAAGCTTCTTGTACAGCT
CGTCCATGCCGAGAGTGATCCCGGCGGCGGTCACGAACTCCAGCAGGACCATGTGATC
GCGCTTCTCGTTGGGGTCTTTGCTCAGGGCGGACTGGGTGCTCAGGTAGTGGTTGTCG
GGCAGCAGCACGGGGCCGTCGCCGATGGGGGTGTTCTGCTGGTAGTGGTCGGCGAGCT
GCACGCTGCCGTCCTCGATGTTGTGGCGGATCTTGAAGTTCACCTTGATGCCGTTCTT
CTGCTTGTCGGCATGATATAGACGTTGTGGCTGTTGTAATTGTACTCCAGCTTGTGCC
CCAGAATGTTGCCGTCCTCCTTGAAATCGATGCCCTTCACC



C.7.5 Control Reverse

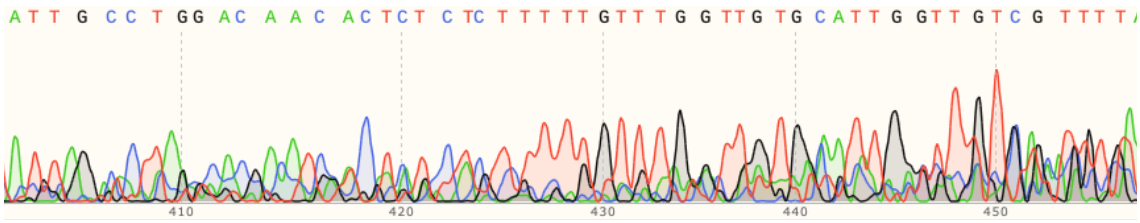
CAGGAAAGCAAGGGGGAGGATTGGGAAGACAATAGCAGGCATGCTGGGGATGCGGTGG
GCTCTATGGCTTCTGAGGCGGAAAGAACCAGCTGGGGCTCTAGGGGGTATCCCCACGC
GCCCTGTAGCGGCGCATTAAGCGCGGCGGGTGTGGTGGTTACGCGCAGCGTGACCGCT
ACACTTGCCAGCGCCCTAGCGCCCGCTCCTTTCGCTTTCTTCCCTTCCTTTCTCGCCA
CGTTCGCCGGCTTTCCCCGTCAAGCTCTAAATCGGGGGCTCCCTTTAGGGTTCCGATT
TAGTGCTTTACGGCACCTCGACCCCAAAAAACTTGATTAGGGTGATGGTTCACGTACC
TAGAAGTTCCTATTCCGAAGTTCCTATTCTCTAGATACCGGGTAGGGGAGGCGCTTTT
CCCAAGGCAGTCTGGAGCATGCGCTTTAGCAGCCCCGCTGGGCACTTGGCGCTACACA

AGTGGCCTCTGGCCTCGCACACATTCCACATCCACCGGTAGGCGCCAACCGGCTCCGT
TCTTTGGTGGCCCCTTCGCGCCACCTTCTACTCCTCCCCTAGTCAGGAAGTTCCCCCC
CGCCCCGCAGCTCGCGTCGTGCAGGACGTGACAAATGGAAGTAGCACGTCTCACTAGT
CTCGTGCAGATGGACAGCACCGCTGAGCAATGGAAGCGGGTAGGCCTTTGGGGCAGCG
GCCAATAGCAGCTTTGCTCCTTCGCTTTCTGGGCTCAGAGGCTGGGAAGGGGTGGGTC
CGGGGGCGGGCTCAGGGGCGGGCTCAGGGGCGGGGCGGGCGCCCGAAGGTCCTCCGGA
GGCCCGGCATTCTGCACGCTTCAAAAGCGCACGTCTGCCGCGCTGTTCTCCTCTTCCT
CATCTCCGGGCCTTTCGACCGATCCAGCCGCCACCATGAAAAAGCCTGAACTCACCGC
GACGTCTGTCGAGAAGTTTCTGATCGAAAAGTTCGACAGCGTCTCCGACCTGATGCAG
CTCTCGGAGGGCGAAGAATCTCGTGCTTTCAGCTTCGATGTAGGAGGGCGTGGATATG
TCCTGCGGGTAAATAGCTGCGCCGATGGTTTCTACAAAGATCGTTATGTTTATCGGCA
CTTTGCATCGGCCGCGCTCCCGATTCCGGAAATGCTTGAAATTGGGGAATTCA



C.7.6 Cu-DPA-TFO Reverse

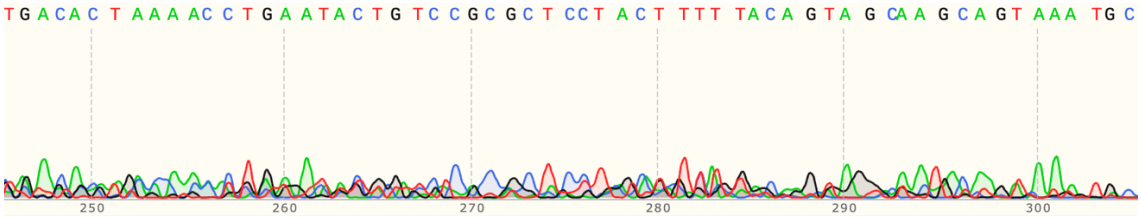
CGTCCCCCACAACAACAAACATTCGCTGGCCTAACATAAGCAGGGAACAATCTTCTTT
CTCATCCTCGGCCACTGTTATTTATGGACGAGTTGCGGGCGGGGTCGTGGTTCCGGGA
CCCCTCATGTTCGGTGTGGATTTTGGGTGCTCATGGTCACCGGAGAGTCTAATTCGCC
TGGTGACCCTGCTACCCTGCCGTGCGGAGGGCAGATATGCCTTAACCATGGGCAGTAT
CGGTGGGTGACGTCAGTTTTGAACCCAACAGGTTGAAACACCTGCCGACTAACCACCT
GATGACACTCCTGGCCATATCAGCCCCCTACCCTATGTTCGTGTAATTGTGATCGAAC
TCCCATGAGAGATTATCTGTCTTTAGTGGACAACTGCGACCTTGCGTTTTGGATATTG
CCTGGACAACACTCTCTCTTTTTGTTTGGTTGTGCATTGGTTGTCGTTTTATGGAGAA
TATCTAATGGTCCCGCAGTTTGTTGTTTG



C.7.7 DPQ-Cu-DPA-TFO Reverse

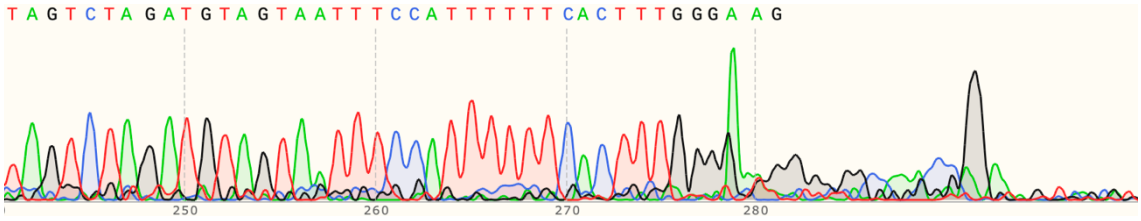
CCACTTAAAAAAAAAAACCTAGCCTGTCTCATGATCTTCAGTATTTGGGTATGTTTGA
ATTTGTCAATAATAGTAAAGATTGTCACTCTTTTACAGGAGGCAATAACAGATGGCTT
GGAAATTGTGGTTTCACCTACAAGTCTACACAGTGAATTAATGTGCCCATGTTGTTTG
GATATGTGAATCCAAACGATGGCTACAATCGAGTGTGCACGGATTGTTTTCTCGGATC
CCTTAATCATGGGCCTGTTGGATTGGTTTATTACTCTATCTTTATACTACATCCTAAC
ACTGCTGTCTGGAACCGAACTCAGAAGTATGATAACATGTAAGACTTATAAAATTCTT

CGACTCCCCGTCCTTAATCCCTACATAAAGAAGACGGCGGTCAACACCAGCACACATC
CCCGCGTTACTTTGACAAAACCCGCCCACCCTCTAACTATTTGTTTGAAGTACCCCTG
TTTTCGCTGCACTGCACTTAAATAACGTTTCTAATTTCGTTGA



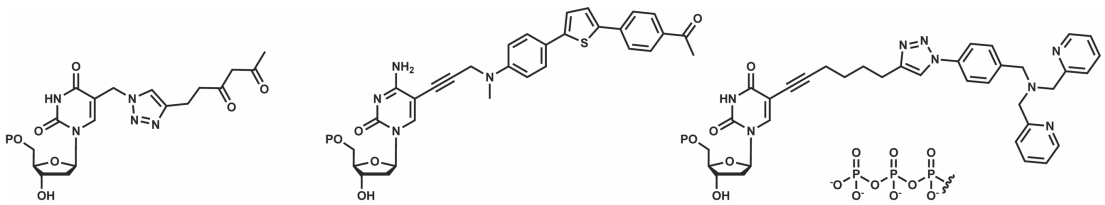
C.7.8 DPPZ-Cu-DPA-TFO Reverse

AAACAAAACCCAGGCCAAGCAAAGGTCCAGATACATCCTCACTAAACGAATCCTGCTG
GAAGCGAGCGGGACCCGTAGAAACCTGGGAGAAGTGGTGAGACTGGGAATTTTCTGCC
CAGACTGTCGGCATCCTGGCCGGCAGCCGATGATGCGCCGGGGGACTGCCCCTGTACC
CCATAACTGCCAGTTCGCCCTTGAATAACCTTGGGTGAGAGATTCGATCAGGCGGGAT
TTCCGCGCGTGAAGGTATCCTGACGAGCAAGGCGGTCAGCATTGACGGGCATGGCCGG
CATGTGCCCGTGCTGGATCACCTCTCCCAATGGCACCACTTTGCCGGTTTCTACAGCG
TCAGCCGGGAAAGGCTCTCCTGCTATCTCATGATTTTGGGGATACGATTGGTCGAAAC
TCCTCGCTGCCGACACGCTGTAGACGGGCGCGGCAAGACTGCCCGGGGCCTGCGGCAT
TGAGTAGGTCCGCCCCACTTGACGGTGTGGCCTTAACTTACACTAAAGTGATAGCAGA
TGATCCCTAGCCCAACAAGATGACACAATGCAGGACCAGTTCGGCAGCAACAGCTCCG
AGTTGCCTGAAGCAATCATGTAGTGATGCACTTCATGCGAGCCCTTCTGCCATCGTTA
ATTGGGGTTCGTCCTATTCGGAAAAAA



Appendix D

D.1 Previous modified-dNTPs incorporated during SNI-PEX



Hocek *et al.* (2021) Hocek *et al*. (2021) Kellett *et al.* (under review)

Figure D - 1: Modified dNTPs previously incorporated by a DNA polymerase during SNI-PEX. Left: Peptide crosslinking agent. Middle: Fluorophore: Right: Artificial metallo-nuclease.

D.2 MNI-PEX of TFO with TPMA and TO modifications

Table D - 1: Sequence of primers and template for MNI-PEX. `Phos` = 5′ Phosphate. `Bio` = Biotin tag

	Length	Sequence (5'-3')
Primer A	12 nt	`CCGCTCTTTCCT`
Primer B 1	18 nt	`Phos-CCCTTCTTTCGCTTTCCT`
Primer B 2	10 nt	`Phos-CCCTTCTTTCG`
Template	32 nt	`Bio-GAGGAAAGCGAAAGAAGGGAAGGAAAGAGCGG`

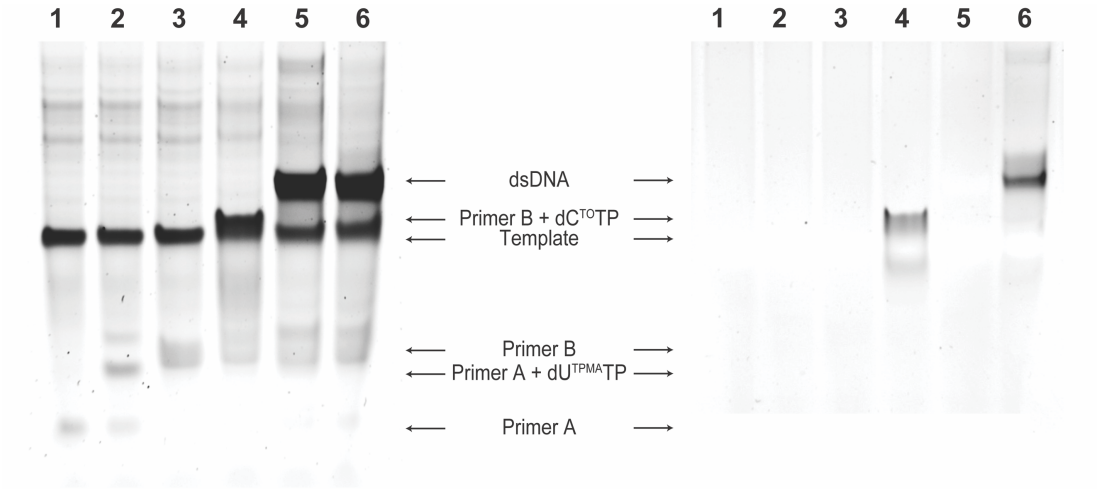


Figure D - 2: 20% denaturing PAGE analysis of MNI-PEX products. Left: SYBR gold stain. Right: Thiazole orange fluorescence. A single $d^{UTPMA}TP$ and a $dC^{TO}TP$ have been incorporated at the desired sequence positions.